Networked Haptic Cooperation with Remote Dynamic Proxies

by

Zhi Li
B.Sc., University of China Agricultural University, 2006

A Thesis Submitted in Partial Fulfillment of the
Requirements for the Degree of

MASTER OF APPLIED SCIENCE

in the Department of Mechanical Engineering

Networked Haptic Cooperation with Remote Dynamic Proxies

by

Zhi Li
B.Sc., University of China Agricultural University, 2006

Supervisory Committee

Dr. Daniela Constantinescu, Supervisor
(Department of Mechanical Engineering)

Dr. Afzal Suleman, Departmental Member
(Department of Mechanical Engineering)

Dr. Brad Buckham, Outside Member
(Department of Mechanical Engineering)

Supervisory Committee

Dr. Daniela Constantinescu, Supervisor
(Department of Mechanical Engineering)

Dr. Afzal Suleman, Departmental Member
(Department of Mechanical Engineering)

Dr. Brad Buckham, Outside Member
(Department of Mechanical Engineering)

ABSTRACT

Networked haptic cooperation entails direct interactions among the networked users in addition to joint manipulations of shared virtual objects. For example, therapists may want to feel and guide the motions of their remote patients directly rather than via an intervening virtual object during tele-rehabilitation sessions. To support direct user-to-user haptic interaction over a network, this dissertation introduces the concept of remote dynamic proxies and integrates it into two distributed control architectures. The remote dynamic proxies are avatars of users at the sites of their distant peers. They have second order dynamics and their motion is coordinated to the remote user whom they represent either via virtual coupling or via wave-based control. The remote dynamic proxies render smooth motion of the distant peers regardless of the infrequent and delayed information received over the network. Therefore, the integration of remote dynamic proxies into distributed networked haptic cooperation allows stiffer contacts to be rendered to users and improves position coherency in the presence of longer constant network delays.

The thesis investigates the advantages and limitations of the remote dynamic proxies for two distributed haptic architectures. These architectures coordinate the peer users and their virtual environments via:

1. virtual coupling control. For virtual coupling-based networked haptics with remote dynamic proxies, stability is analyzed within a multi-rate state space framework and the analysis is validated through experiments involving both cooperative manipulations and direct user-to-user interactions. The results show

that the remote dynamic proxies maintain high coherency between the distributed virtual environments and enable users to see and feel their peers moving smoothly. They also increase the stiffness of direct user-to-user contact in the presence of larger constant network delay. However, the remote dynamic proxies do not lessen users' perception of a predominantly viscous virtual environment in the presence of network delay.

2. wave-based control. To enable users to feel other dynamics in addition to viscosity during networked haptic cooperation, this dissertation further develops a wave-based distributed coordination approach for the remote dynamic proxies. The performance of the proposed approach is investigated via experiments involving both cooperative manipulations and direct user-to-user interactions. The results demonstrate that the remote dynamic proxies mitigate the poor coherency typical to wave-based coordination architectures and enable users to touch their peers. Furthermore, the remote dynamic proxies improve users' perception of inertia in the presence of network delay.

Contents

List of Tables

List of Figures

ACKNOWLEDGEMENTS

I would like to thank:

My supervisor, Dr. Daniela Constantinescu for mentoring, caring, and encouraging me with patience.

My friend Nisular Fu for supporting me in the low monments.

My dear grandparents for sheltering and nurturing me with their warm heart.

My dear mother for everything and everyday.

There is a time for everything, and a season for every activity under heaven:
a time to be born and a time to die, a time to plant and a time to uproot,
a time to kill and a time to heal, a time to tear down and a time to build,
a time to weep and a time to laugh, a time to mourn and a time to dance,
a time to scatter stones and a time to gather them, a time to embrace and a time to refrain,
a time to search and a time to give up, a time to keep and a time to throw away,
a time to tear and a time to mend, a time to be silent and a time to speak,
a time to love and a time to hate, a time for war and a time for peace.

DEDICATION

For my dear supervisor Dr Daniela Constantinuescu, who leads me to the way of academic research. Thank you for all the unconditional love, guidance, and support that you have always given me, helping me to succeed and instilling in me the confidence that I am capable of doing anything I put my mind to. Thank you, my dear supervisor.

For my mother Ms Ying Su, who have raised me to be the person I am today. You have been with me every step of the way, through good times and bad. Thank you for everything. I love you!

For my grandparents, Mr Xingchun Su and Mrs Zhimin Xie. Although in the heaven, I believe you are watching and still taking care of me. I believe you see me, and what I have done. I am setting up for a new trip. Bless me.

Chapter 1

Introduction

1.1 Networked Haptic Cooperation

Computer haptics, or haptics, enables human users to interactively touch and manipulate virtual environments [3]. Generally, the haptics adds perception to traditional visual and/or audio applications and have wide and promising use in various areas such as military training [4], industrial design and maintenance [5], remote surgery [6, 7], creative painting [8] and sculpting [9], etc. To be specific, haptics is involved in surgery training, teaching of palpatory diagnosis (detection of medical problems via touch) [10] and so on. For entertainment, haptics adds the perception and manipulation of virtual objects to video games [11]. In a virtual art exhibition, haptics enables human users to play virtual musical instruments as well as touch and feel the haptic attributes of the displays.

In networked haptics, the virtual environment is shared by multiple users distributed over networks. According to the ways that the users interact with each other as well as touch and feel the virtual environments, networked haptics can be categorized into three groups: (1) haptic interaction with static shared virtual environments, (2) haptic collaboration and (3) haptic cooperation [12].

- **Haptic interaction with a static shared virtual environment**: users touch and feel a fixed virtual environment.

  In the haptic interaction with static shared virtual environments, users passively explore the shared virtual environment and experience corresponding visual, audio and haptic feedback. Users are not enabled to manipulate or modify the shared virtual environment. The shared virtual environment has fixed geometric

attributes (such as the shape, texture, etc.), kinematic attributes (position, velocity, etc.), dynamic attributes (such as mass, damping, etc.) and so on. Therefore, its implementation is largely simplified. In haptic interaction with a static shared virtual environment, users usually visit a central database in client-server fashion to touch and feel the shared virtual environment, which is managed by a centralized server. At the same time, a user can access the information of the other users in the same shared virtual environment in two ways: (a) via contacting a centralized server which keeps the most recent status of the other users; or (b) via directly contacting the other users for their updated state.

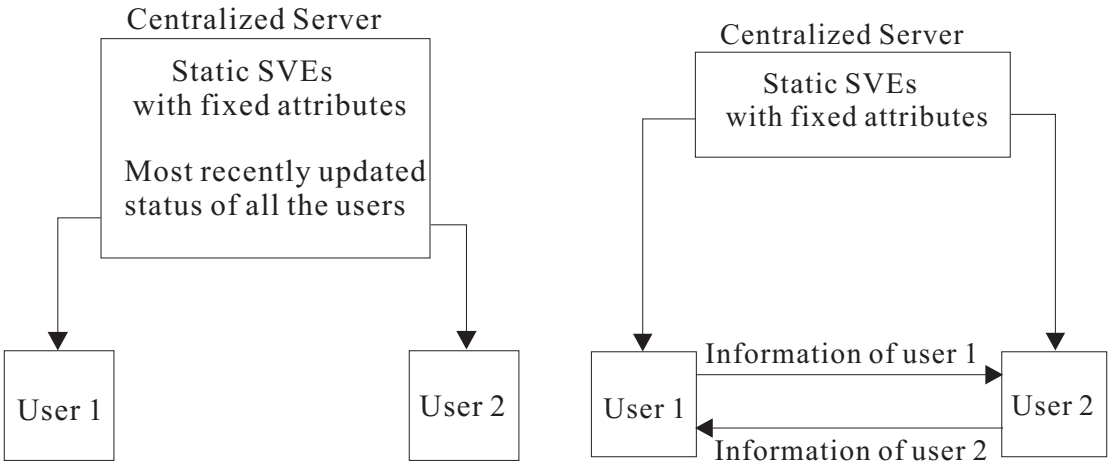

(a) Users contact a centralized server for the update status of the other users.

(b) Users contact other users directly for their updated state.

Figure 1.1: Haptic interaction with a static shared virtual environment (SVEs).

- **Haptic collaboration**: users take turns at touching and feeling the shared virtual environment.

  In haptic collaboration, users are enabled to manipulate and modify the shared virtual environment with the restriction of "one user at a time". Two kinds of approaches are available to synchronize the networked haptic cooperation, respectively for: (1) client-server topology; and (2) peer-to-peer topology.

  During networked haptic collaboration with users connected in client-server fashion, while being modified by one of the users, the information of the shared virtual environment can be locked by a central server which keeps its only "official" copy. As illustrated in Figure 1.2, User 1 and User 2 are connected

to a centralized server. When being modified by User 1, the shared virtual environment is locked by User 1 (i.e. User 2 can only touch and feel the shared virtual environment passively).

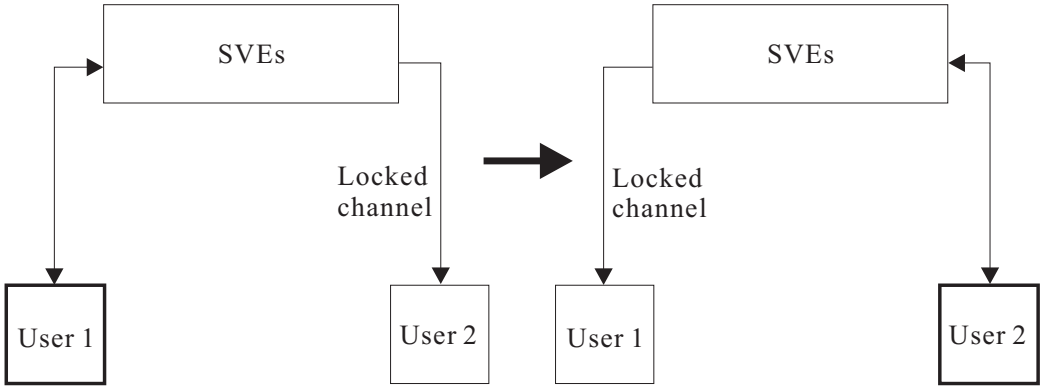

Figure 1.2: Synchronization of haptic collaboration in a shared virtual environment (SVE) via client-server synchronization.

For networked haptic collaboration with users connected in peer-to-peer fashion, the official copy of the shared virtual environment is managed by each user in turn via a token ring scheme. While one of the users is authorized to modify the official copy of shared virtual object, other users in the networked haptic collaboration can only touch and feel it passively (Figure 1.3). Peer-to-Peer topology demonstrates effective synchronization performance via the token ring implementation. In the token ring implementation, a token will be circulated among the interconnected users. The user who gets the token has the right to modify the shared virtual environment, while the other users without token could only passively touch and feel the shared virtual environment. However, due to the complexity of connection and the large load of network traffic, this synchronization scheme does not scale well as the number of users increases.

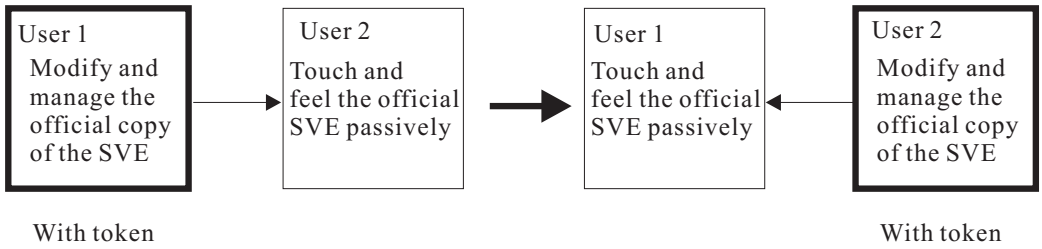

Figure 1.3: Peer-to-peer haptic collaboration in a shared virtual environment (SVE) with token ring synchronization.

- **Haptic cooperation**: users touch and modify the shared virtual environment simultaneously.

  It is only in haptic cooperation that multiple users can simultaneously manipulate and modify the same shared virtual object in a shared virtual environment (Figure 1.4).

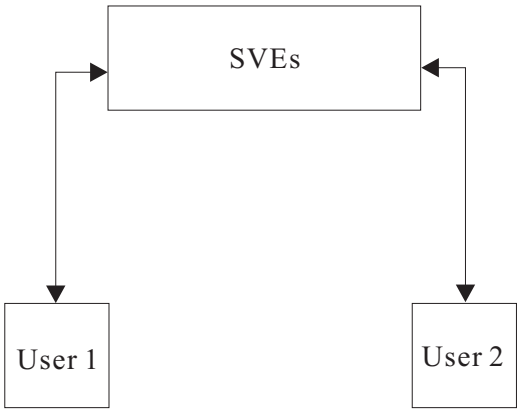

Figure 1.4: Haptic cooperation.

As the restriction of "one user at a time" is removed, task performance in the shared virtual environment is largely improved. It has been experimentally demonstrated in [13] that, when the task of haptically passing a virtual object is performed by two people working together, the error rate for exchanging objects is diminished without increasing the time to move the object. The physical realism is also enhanced in haptic cooperation since users are allowed to feel and push each other directly or indirectly while moving the shared virtual object. For example, users involved in networked haptic cooperation interact with each other via a shared virtual cube in [14].

The "Transatlantic Touch" [15] is the first published implementation of networked haptic cooperation over long distance. Since that, networked haptic cooperation has been implemented in various practical applications. Some applications have emerged in the industrial area. For instance, designers located in different cities or even different countries may need to haptically cooperate on the same project in a shared virtual environment. An example is the CAD assembly task cooperatively carried out between the University of Manchester in UK and the University of North California at Chapel Hill in the USA [16].

The designed system provided effective transatlantic cooperative haptic manipulation of objects whose motion was computed using a physically-based model. Although the network latencies have been of the order of 120ms, the performance achieved over the Internet is comparable to that on a local area network (LAN). Other applications of networked haptic cooperation are in medicine. For example, the Jerusalem TeleRehabilitation System [17] is a low-cost and easy-to-use rehabilitation system which allows the therapist and the patient cooperatively perform a rehabilitation procedure.

1.2 Challenges in Networked Haptic Cooperation

Networked haptic cooperation faces challenges due to the network attributes. As the number of users and user groups increases, the synchronization will also be a problem. This section briefly overviews how the network attributes and the synchronization issues affect the performance of networked haptic cooperation. A more detailed discussion will be presented in Chapter 2.

1.2.1 Network Challenges

The performance of a network is limited by the following network attributes:

- **Network Delay**

  The network delay, or latency, is the delay experienced by a packet within the network. In a IP network, the network delay consists four parts: (1) processing delay, i.e., the time that routers need for processing the packet header; (2) queuing delay, i.e., the time that the packet remains in routing queues; (3) transmission delay, i.e., the time for pushing the packet's bits onto the network link; and (4) propagation delay, i.e., the time for propagating the signal over the medium it is being transmitted through. The network delay has various negative impacts on networked haptic cooperation. By introducing latency between the human action and the force feedback, it leads to instability. The network delay may affect the networked haptic cooperation to various extent depending on the nature of the task. Generally speaking, the negative effects become more severe as the delay increases.

- **Network Delay Jitter**

The network delay jitter is the variation of the network delay. The network jitter has the largest impact on networked haptic cooperation in the presence of long network delay. It is notable that the adverse effect of network jitter is comparable to that of long constant network delay. This is because data transmission buffer schemes can transform network jitter into constant long network delay.

- **Packet Loss**

  Packet loss refers to the situation in which one or more packets of data transmitted over networks fail to reach their destination. Packet loss may be due to unavoidable data loss in transmission or to intentional network traffic reduction. For example, many networked haptic cooperation schemes employ the User Datagram Protocol (UDP) transmission protocol, which emphasizes on communication efficiency at the expense of transmission reliability. To reduce the network traffic, other implementations either selectively transmit update packets [18, 19] or employ a network transmission rate that is lower than the rate of local haptic rendering [2].

- **Network Bandwidth**

  Network bandwidth refers to the data rate supported by a network connection or interface and represents the capacity of the network connection. The greater the capacity of the network connection, the more likely it is that the data transmission will achieve better performance. Network bandwidth limitations may aggravate other adverse network effects, such as network delay and jitter, and packet loss. Especially in the presence of heavy network traffic and large number of users, network bandwidth may limit the performance of networked haptic cooperation.

  Heavy network traffic may be required by haptic applications that need to exchange video and audio data across the network in addition to update messages that control users' motion and interaction. In addition, the real-time synchronization that is critical in networked haptic cooperation makes network traffic load an outstanding problem. Therefore, a heavy network traffic load over limited network bandwidth may impose stringent constraints on the number of users that can be included in the networked haptic cooperation and may aggregate adverse network effects such as the network latency, jitter and packet

loss.

A large number of users involved in networked haptic cooperation may also have communication needs that exceed the network bandwidth. For instance, many users interconnected in peer-to-peer fashion require large network bandwidth because each pair of cooperative participants needs to exchange various information. In this case, the network bandwidth will limit the number of users that can be involved in networked haptic cooperation.

These network attributes may adversely impact (1) the stability and (2) the physical realism of the networked haptic cooperation:

- **Impact of network attributes on the stability of haptic cooperation**

  Networked haptic cooperation can become unstable because of network delay and jitter. The work in [20] demonstrated through experiments that the virtual coupler [21] connecting the copies of the shared virtual objects need to become more compliant as the network delay increases. The theoretical analysis in [2] showed that the stability region shrank as the delay increased regardless whether centralized or distributed control architectures connected the networked users.

  Network delay, jitter, and packet loss also lead to network update rates that are usually much lower than the typical haptic rendering rate of 1 KHz. The low network update rates lead to a multi-rate force feedback loop which presents additional stability challenges. These challenges are detailed in Chapter 2.

- **Impact of network attributes on the realism of haptic cooperation**

  Physical realism is important in many networked haptic cooperation applications, including tele-rehabilitation and tele-training for surgical procedures. Yet realism may need to be traded off for stability in networked haptic cooperation. For example, typical haptic applications increase damping to maintain stability in the presence of network communication delays. However, the damping injected through control may overwhelm users' perception of the virtual environment dynamics, in particular of the dynamics of the shared virtual object [2].

  When users are represented in the virtual environments of their remote peers directly from the network updates, their motion will be sampled at varying, relatively large intervals (tens to hundreds of ms compared to ms) due to the characteristics of the network traffic. Hence, the motion of remote peers will

appear discontinuous, jumping from one position to the next, instead of evolving smoothly in time.

1.2.2 Synchronization Among Users and User Groups

Multi-user computer games and on-line art expositions with haptic feedback are examples of networked haptic cooperation applications that strive to involve as many cooperating participants as possible in the virtual environment. This intention brings about the challenge of haptically synchronizing cooperative users and user groups. The synchronization comprises the synchronization of the shared virtual objects, as well as the synchronization of member status. The complexity of the synchronization increases significantly as the number of users grows larger.

- **Synchronization of Shared Virtual Objects**

  As a real-time network application, networked haptic cooperation requires the synchronization of the shared virtual objects. In other words, each participant must perceive the properties of the shared virtual objects in a manner consistent with the other participants. For example, position coherency requires all the distributed copies of the shared virtual object to be at the same location. However, due to the interaction controller and/or the imperfect network data transmission among users, position differences always exist among the distributed copies of the shared objects (Figure 1.5).

- **Synchronization of Member Status**

  The synchronization of member status aims to maintain the network connection among all users involved in the networked haptic cooperation, and to inform all participants about the most recent status of all other users. Via synchronization of member status, participants are informed when other participants join in and leave the networked haptic cooperation; the network information such as the IP addresses of other users are disseminated to participants in order to build up suitable network connections; participants learn the geometric (shape, texture) and dynamic (mass, stiffness, damping) attributes, as well as dynamic status (position, velocity) of the other participants.

- **Synchronization of Users and User Groups**

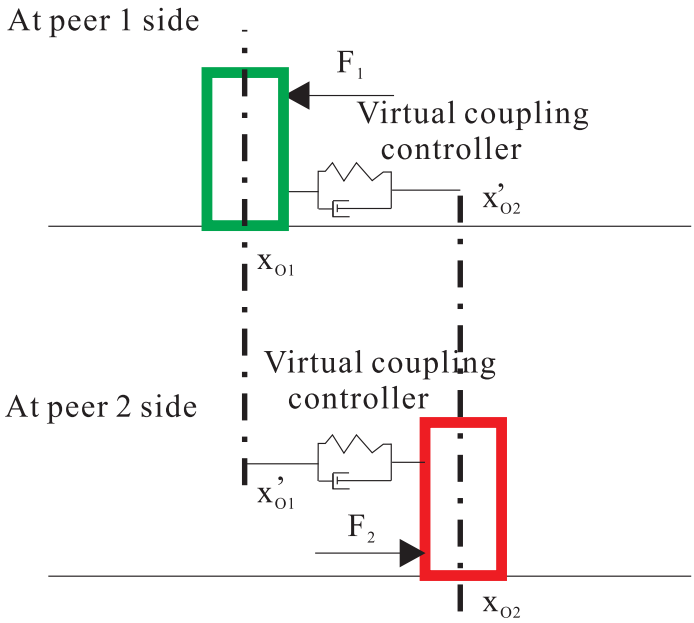

Figure 1.5: Position difference among the distributed copies of the shared virtual object (SVO). F_1 and F_2 are the forces applied by Peer 1 and Peer 2 on their respective copies of the shared virtual object.

Scalability is a major challenge in networked haptic cooperation with large number of participants. Scalable networked haptic cooperation should be able to handle a growing amount of network traffic gracefully, as well as be easily enlarged. When expanding the hierarchical structure of networked haptic cooperation, a balanced hierarchical tree of communication is desirable. In an unbalanced hierarchical tree, many participants connect to the same synchronization reference node as clients and the acknowledgements of receiving synchronization packets may overwhelm the node through acknowledgement implosion.

1.3 Objective of the Thesis

This dissertation aims to provide a framework for distributed networked haptic cooperation that enables direct user-to-user interaction in addition to cooperative manipulation of a shared virtual object. The framework will focus on two-users haptic cooperation in the presence of low network update rate and constant network delay. Therefore, synchronization will be assumed to have negligible impact on both the stability and the performance of the interaction. The performance will be evaluated via: (1) the position coherency among the distributed copies of the shared virtual

object during cooperative manipulations; (2) the contact stiffness that the users can perceive; and (3) the range of network delays for which the networked haptic cooperation is stable. Potential applications of the framework proposed in this dissertation include tele-rehabilitation and multi-user computer games.

To achieve its aims, this thesis will: develop a methodology for distributing peer users across the network that is based on the new concept of remote dynamic proxies; integrate the remote dynamic proxies into peer-to-peer haptic control architectures with virtual coupling control and with wave-based control; derive stability margins for peer-to-peer networked haptic cooperation via remote dynamic proxies with virtual coupling coordination; and validate through experiments the performance of the remote dynamic proxies.

1.4 Structure of the Thesis

The thesis is organized as follows:

Chapter 2 reviews existing research on networked haptic cooperation emphasizing work that focuses on the adverse network effects and on improving performance.

Chapter 3 introduces the concept of remote dynamic proxies and integrates them into two peer-to-peer networked haptics architectures: (1) the distributed control architecture with remote dynamic proxies and virtual coupling coordination; and (2) the distributed control architecture with remote dynamic proxies and wave-based coordination.

Chapter 4 develops the stability analysis for two-users networked haptic cooperation rendered via RDP-s with virtual coupling coordination. The analysis formulates the state space representation of the multi-rate haptic feedback system under constant network delays, both for cooperative manipulation of a shared virtual object and for direct user-to-user interaction.

Chapter 5 compares through experiments the remote dynamic proxies with virtual coupling and with wave-based coordination to three recent peer-to-peer controllers. It also validates the analysis in Chapter 4.

Chapter 6 summarizes the conclusions of this dissertation and discusses directions for future work.

Appendix A details the derivations required for the stability analysis in Chapter 4, both for distributed cooperative manipulation and for direct user-to-user interaction. It also presents the procedure for setting up the experiments presented in Chapter 5.

Chapter 2

Literature Review

This chapter reviews the research history of networked haptic cooperation. After addressing the influence of the adverse network effects (i.e. the limited bandwidth, the network delay, jitter and packet loss), the chapter presents the state of art to achieve the ideal networked haptic cooperation from three perspectives: (1) the network-based approaches to improve the performance of networked haptic cooperation, (2) design of control architectures with various controllers, and (3) representation of human users with proxies of higher order dynamics.

2.1 The Influence of the Adverse Network Effect

The performance of a network is limited by adverse network effects such as: (1) network delay, (2) network delay jitter, (3) packet loss, (4) limited network bandwidth. This section will address to detail the influence of the above adverse network effects on networked haptic cooperation according to the existing researches.

2.1.1 Network Delay

The network delay, namely the network latency, has various negative impacts on the networked haptic cooperation. The network delay not only causes the response latency between human operation and the force feedback, but also leads to instability perceived by human users as rebound and/or vibration of the haptic devices.

In [22] experimental study on the effects of constant network delay in cooperative shared haptic virtual environment (CSHVE), task performance in CSHVEs have been evaluated from three perspectives: (1) force perception, (2) consistency of the

haptic-visual feedback, and (3) the system stability of networked haptic cooperation. In this experimental study, human users are connected to the shared virtual environments in Client-Server way. In objective assessment, although the increasing network delay does not affect the force feedback significantly, the task performance measured via Task Completion Time (TCT) decreased. Especially when the delay goes to 1800ms, the performance decreased by 50%. In the subjective assessment, the task performance is evaluated via contact stiffness, as well as the physical-intuition, i.e. how realistic and comfortable the experienced perceptions are and whether these perceptions are comparable to those in real-life situation. It is described by human users that there existed "discontinuity" in the force perception for large delay. For each user, the other users in the same shared virtual environment move slower as the delay increases. In [23] the adverse effect of constant network delay is examined quantitatively. In the haptically cooperative task, human users first reached forward to touch each other, then moved to a target without losing contact. The network delay between 0 ms to 400 ms is graded into 10 levels. It is experimentally demonstrated that as the delay increases, in the cooperation exists more movement errors of aiming (i.e. users can not properly aim each other), penetration (i.e. users penetrate into each other while contacting) and separation (i.e. users can not persist the contact while moving to the targets). The error rates increases rapidly as delay rises from 0 ms to 100 ms, but slowly when delay is over 100 ms.

In conclusion, the adverse effects of network delay affect the networked haptic cooperation to different extent according to the nature of the task, yet generally speaking, their negative effects become severe as the delay increases. [22].

2.1.2 Network Delay Jitter

The network delay jitter is the variation of network delay. The network jitter has the greatest adverse effect on networked haptic cooperations when combined with long network delay. In [24, 25] cooperative tasks are conducted in the presence 10 ms network delay and 200 ms delay with and without jitter. It is demonstrated that the task completion time significantly correlated to both the network delay and the delay jitter.

While increasing the task completion time, the network delay jitter also affects human users' perception of the shared virtual objects. It is described in [26] that due to the fact that it is after the transmission delay (single-trip-time for Peer-to-Peer

connection and round-trip-time for Client-Sever connection) that the shared virtual object can respond to human users' manipulations, as the delay varies, participants in networked haptic cooperation will try to push the shared virtual objects with larger or smaller force, which is equivalent to the mass variation of the shared virtual objects.

It is notable that the adverse effect of network delay jitter is comparable to that of constant long network delay. With buffer schemes in data transmission, network jitter may transformed to constant long network delay. [27] suggested that 10 ms delay with jitter resulted adverse effect equivalent to 200 constant network delay without jitter. Although experimentally generated in networked haptic collaboration, this result may also be referred to by researches on networked haptic cooperations.

2.1.3 Packet Loss

The packet loss may come from either the unavoidable data loss in transmission or the intentionally network traffic reduction. For example, many networked haptic cooperations employ UDP as transmission protocol, which emphasizes on the communication efficiency at the expense of transmission reliability [28, 29, 15, 30, 31]. To reduce the network traffic loads, other implementations of networked haptic cooperation either selectively transmit update packets [18, 19] or employ a lower network transmission rate than the rate of local haptic rendering [2]. In [2] The intentionally decreased network update rate results in a control system with multiple sampling rates and further affects the control stability of the networked haptic cooperation.

2.1.4 Limited Network Bandwidth

One challenge in networked haptic cooperation is the heavy traffic load over limited network bandwidth. The limitation of bandwidth becomes severer especially when including large number of users and user groups in a networked haptic cooperation. The heavy network traffic may impose stringent constraints on the system layout and the aggregate other adverse network effects such as the network latency, jitter and packet loss [12].

[32] categorized data existing in networked haptic collaboration into five columns. They are:

- real-time audio and video data;
- data describing objects/scences in shared virtual environments;

- data representing traditional 2D collaborative data such as whiteboards;
- data used by the system to perform tasks such as consistency control, management, etc. (i.e. data for control);
- data for updates.

[32] explained that based on the received control data and update data, user can simulate at his/her own side the real-time audio and video, as well as the background of shared virtual environments which is seldom changed during the networked haptic collaboration. Therefore, messages containing the control data and update data are most frequently transmitted and consequently become the main focus of synchronization.

During the period that participants exist in a networked haptic cooperation environment, they exchange status information with the networked haptic cooperation system that they are involved in. Specifically, the participants need to receive occasional and/or periodic information related to:

- permission to join the cooperative task;
- synchronization with the shared virtual environment, including the background and audio and video information;
- current static and dynamic status of the shared virtual environment;
- current static and dynamic status of other participants in the cooperative task;
- current static and dynamic status of other participants passing by (optional);
- other participants joining in and leaving the cooperative task;
- other participants joining in and leaving the shared virtual environment (optional);
- current network traffic load (optional).

At the same time, they are required to send own information related to:

- the intention of joining in and leaving the shared virtual environment;
- the intention of joining in and leaving the cooperative task;

- their static and dynamic status.

As described in [32], messages transmitted in networked haptic collaborations have different requirements of reliability. So it is with networked haptic cooperation. For example, messages containing the control data insist reliable transmission since without reliably receiving control messages such as IP address of new members, the connections among participants will not be built up and expanded correctly. In comparison, messages for updating the positions and velocities emphasize on the transmission efficiency instead of reliability in order to render smooth motion for the representations of remote users. Limited by the network bandwidth, networked haptic cooperation aim at a tradeoff the reliability and efficiency of data transmission.

2.2 State of the Art

According to the challenges described in the Chapter 1, existing researches focus on improving the performance of networked haptic cooperation from three perspectives. (1) From the perspective of network, research to date has mitigated the adverse network effects such as network delay, jitter, packet loss and has synchronized large number of users & user groups via the implementing advanced protocols. Especially, various buffer schemes and prediction & interpolation are implemented to smooth the network delay jitter and make up for the packet loss. (2) From the perspective of control stability, centralized and distributed control architectures with various controllers are designed to improve the performance of networked haptic cooperation. (3) From the perspective of physically-intuitive virtual reality, proxies of different orders of dynamics (i.e. proxies with zero order, first order or second order dynamics) are implemented to represent the users' motion in the shared virtual environments. Furthermore, controllers are designed to help the shared virtual objects with maintaining their dynamic properties.

2.2.1 Network-based Approaches to Improve the Performance of Networked Haptic Cooperation

Protocols for Networked Haptic Cooperation

Traditionally, networked haptic cooperation employ TCP (Transmission Control Protocol) and/or UDP (User Datagram Protocol) as communication protocol over net-

work. These two commonly used network protocol have different emphasis on transmission performance. The TCP is a reliable transmission protocols so that it persists sending a packet until acknowledgement of this packet is received from the destination side. Therefore, the transmission reliability is ensured at the expense of relatively lower transmission efficiency. On the contrary, the UDP only transmits the packets with best effort without any requirement for acknowledgement. In most situation, users in the networked haptic cooperation prefer frequent updates from the remote side rather than reliable transmission of any specific update. Therefore, the UDP is much more commonly implemented in networked haptic cooperation.

As previously described, updates of networked haptic cooperation have various transmission requirements, which could not be satisfied by protocols that solitarily emphasizes on either the transmission reliability or efficiency. [33] solve this problem by opening multiple communication channels for updates with different transmission requirement. In their implementation, three transmission channels are built up between each of the two client users and the server that manages the official copy of the shared virtual environment. Users' positions relevant to the collision detections with the shared virtual object are reliably transmitted with TCP while UDP is used to transmit positions of users when they are idling around. The position of the shared virtual object can be transmitted either by TCP or UDP. Their experiments demonstrated that combination of TCP and UDP can achieve higher performance of cooperation than only using either the TCP or the UDP.

Instead of the combination of multiple protocols, some other researches have solved this problem by employing a single protocol with adaptive transmission reliability and efficiency, or even suggested designing network protocol particularly for networked haptic cooperation [34]. Recently, the SCTP (Synchronous Collaborative Transmission Protocol) and the S-SCTP (Smoothed SCTP) have been implemented in networked haptic cooperations, both of which distinguishes the key updates from regular updates and set different transmission reliability for them respectively.

Synchronization Among Users and User Groups

Applications of networked haptic cooperations such as computer games and haptic art exposition intend to simultaneously involve as many participants as possible. This intention leads to challenge of synchronizing among haptically cooperative users and user groups. This synchronization consists (1) the synchronization of the shared

virtual objects, as well as (2) the synchronization of member status. Complexity of the synchronization becomes increasingly significant as the user number grows larger.

- Two Approaches for the Synchronization of Shared Virtual Objects

  Synchronization of the shared virtual objects can be achieved either via (1) controllers connecting copies of the shared virtual objects [14, 2, 35] or via (2) update packet for synchronization [19, 28, 31, 36]. For the synchronization with controller, the potential challenges are maintaining the control stability as well as minimizing the position difference among the distributed copies of the shared virtual objects. For example in [14], the virtual couplers are used to generate the inter-connection control forces which maintain the position coherency of the distributed copies of the shared virtual objects. The control stability for long network delay is ensured at the expense of less stiff virtual couplers which leads to worse position consistency of the distributed copies of the shared virtual objects. [2] demonstrated that for the distributed multi-rate control architecture with delay steps of $n = 1$, $n = 2$ and $n = 3$, the remote contact stiffness is inversely proportional to the stiffness of coordinating virtual coupler in the presence of a fixed local contact stiffness. According to this theoretical analysis, the rendered contact stiffness also bounds the stiffness of the virtual couplers connecting the copies of the shared virtual objects, which affects further on the position coherency of the shared virtual objects.

  When synchronizing the shared virtual objects with inter-connecting controllers, the generated control forces are reciprocal that copies of the shared virtual objects are synchronized with reference to each other. However, synchronization with update packets entails choosing the **synchronization reference node** and expending the synchronization architecture based on leveled **authorization of synchronization**. For instance, for a networked haptic cooperation with two users, two nodes exist in the networked haptic cooperation and one of them can be chosen as the synchronization reference node, which maintains an official copy of the shared virtual objects. If using an extra centralized server to maintain the official copy of shared virtual objects, there will be three nodes included in this networked haptic cooperation. The node of the extra centralized server will be selected as the synchronization reference node with both the two users connecting to it in Client-Server way. In both the above two situations, the synchronization reference node has higher level of synchronization authorization

comparing to the other node(s).

As the networked haptic cooperation involving larger number of users, more cooperative participants and/or centralized servers can be selected as the synchronization reference nodes for the sake of scalability. Consequently, the synchronization authorizations of these cooperative users/centralized servers have to be graded to multiple levels, ensuring that only one official copy exists in the networked haptic cooperation. As the nodes with different level of synchronization authorization inter-connect and expand, users and user groups form an hierarchical structure in the networked haptic cooperation.

It is notable that some special cases of networked haptic cooperation require synchronization of temporal coordinate system. In [16], this temporal coordinate system is defined as virtual time, which is the abstraction of real time and implemented via a system of logical clock. This synchronization ensures the consistent state across all participants connected via high latency network, preparing for implementation of interpolation and/or prediction to smooth the rendering of shared virtual environments as well as the motions of remote participants.

- Acknowledgement Strategy

  Basically, two acknowledge mechanisms are available to ensure update transmission reliability. The positive acknowledgement based (ACK-based)approach is sender-initiated while the negative acknowledgement based (NACK-based) approach is a receiver-initiated one. Efficient acknowledgement suppression mechanism is necessary for both of them to reduce network traffic load and avoid acknowledgement implosion.

  For the ACK-based approach, updates with strong reliability requirement must be acknowledged immediately. The sender can realize a packet loss either by timeout scheme or duplicated acknowledges for previous update messages. The expense for this prompt response is the sender's danger of acknowledgement implosion. As the user number grows, the adverse effect of acknowledgement implosion becomes severe.

  Proposed suppression scheme for those ACK-based approach is to build up a temporary hierarchical tree in synchronization topology. The sender periodically picks some representatives from a group of receivers. The acknowledge-

ment from a representative is considered as a symbol of successful transmission for the whole group area. If an acknowledgement from the representative is received, the sender will consider the whole group gets the new update message. Otherwise, the update message is resent and another representative for this local group will be selected. All users except the previous representative in this group will send out acknowledgement based on a acknowledgement suppression algorithm. The sender will then choose a new representative to take the place of the old one. With this approach it is still possible for some users to be kicked out. However, the acknowledgement implosion is suppressed in large area.

The NACK-based approach works on the assumption that any practical network will deliver successfully many more packets than it drops. Thus, the congestion caused by acknowledge packets are largely reduced. This NACK-based approach is preferred by many multi-cast protocols. Negative acknowledgement can only be sent out when the receiver realizes some packet loss. Acknowledgement implosion is avoid at the expense of lossen the sender's control over the receivers.

NACK-based approach demonstrates low performance when the network jitter is available. Update packets are not received at fixed interval, which may confuse the receiver. Available solution is to have the receivers send the "heart beat" message to the sender periodically. These messages keep the sender informed with the receiver's state and response accordingly.

Generally speaking, the NACK-based approaches have the wider popularity than the ACK-based approaches for their consuming less bandwidth. Sometimes, Automatic Repeat Request (ARQ) and Forward Error Correction (FEC) are combined to the NACK-based approaches to achieve higher performances. The ARQ mechanism can only response to packet loss when it receives a new update message with a larger time stamp or sequence number. If the new update is sent very late, it is possible for the delayed user to be kicked out of the collaboration for a while. Even worse, if the new updates never comes, the collaboration will be a total failure. Some paper proposed to integrate the FEC technique with the NACK approaches. It puts many adjacent packets in a block and tails the repair packets for the whole block at the end. However, networked haptic communication pays attention to key update at interval rather than the integrity of adjacent packets. Therefore, the use of FEC is almost a waste.

Buffer Schemes

As described previously, the jitter of network delay introduces worse effect than contant network delay. Therefore, it is preferred to smooth this jitter even at the expense of introducing additional delay of the update packets. To smooth the jitter of network delay, buffers with fixed or adaptive size have been either embedded in transmission protocol or additionally implemented at the receiving sides of updates. The implementations of buffer schemes may further rearrange the receive the update packets according to their time stamps and make up for the lost packet with proper interpolation, which smoothes the update flow and improves the system control stability.

Available networked haptic cooperation with fixed buffer scheme lies in [30], which employs the S-SCTP as transmission protocol. Fixed buffer embedded in the S-SCTP results in less time to successfully complete the networked haptic cooperation in the presence of network delay and jitter, comparing to that of using transmission protocols of UDP and SCTP. Furthermore, [36] implemented adaptive buffer for haptic media synchronization and the adaptable buffer size is determined by the expected network delay, which is calculated via a single-input adaptive transversal filter structure of adaptive signal processing. This implementation of adaptive buffer demonstrated higher performance in preventing overall packet loss comparing to the fixed buffer scheme, especially for longer network delay and severe jitter. Another implementation of adaptive buffer in [37] proposed a priority-based buffer scheme with low processing delay. The buffer time adaptively varies for updates of different importance. This method effectively reduced the additional delay that the buffer schemes introduced when smoothing the received updates.

Network Decorators

[23] thoroughly examined the human user's behavior in the presence of different network delay. It is experimentally demonstrated that users adaptively adjust their manipulation in an "impact-perceive-adapt" way to achieve successful networked haptic cooperation based on their feeling of network condition. Users become aware of delay at 50 ms, before which people don't perceive any difficulties caused by network delay. As network delay increases, people intentionally slow their movement to avoid unsuccessful manipulation. However, although users are aware of delay affecting their performance, it is less than 100 ms they fail to slow their movements enough to stop an increase in errors. Consequently, there are three delay thresholds at which users

intentionally change their manipulation.

- Impact threshold of 25 ms, at which errors of manipulations increase significantly and users become aware of delay.
- Perception threshold of 50 ms, at which users clearly perceive network delay and start to adjust their manipulation. However, as the movements of the remote user still appears smooth, the delay is not disruptive enough to slow users' movement sufficiently to halt the rise in error rate.
- Adaptation threshold of 100 ms, at which network delay is significant to cause a breakdown in the force perception so that the remote user's movement appears jerky and disjointed. From this point onwards, users slow down their movement proportionally to delay to stop the increasingly more error manipulations.

Successful networked haptic cooperation can be achieved by offering users the information of network condition, which results in S. Shirmohammadi's serial researches on decorators. The decorators initially proposed in [38] are graphical queues used to virtually inform the user in networked haptic cooperation about the current network condition, e.g. the network delay and jitter. Based on the evaluation of network condition, the decorator varies its color to indicate the network is "ok", "so-so" and "not ok". [39] further enriched the color scheme for the decorator and [40] categorized the decorators into 3 groups: (1)jitter decorator to reveal the delay variation, (2) direction decorator to indicate the direction of movement and (3) trajectory decorator to predict the future state of a shared virtual object according to previous movement, which visualizes more complicated network condition.

Instead of solitary implementation of decorator, [41] adds to networked haptic cooperation with decorators a prediction algorithm that predicts the current behavior of the shared virtual object based on interpolations from a history buffer. This prediction algorithm works similar to dead reckoning, using a short-interval prediction to improve the cooperation performance. [28] conducted comprehensive implementation consisting the network transmission protocols of SCTP and UDP, decorators and prediction algorithms. The performance of networked haptic cooperation is examined in the presence of complicated network condition. It was experimentally demonstrated that to achieve higher performance of networked haptic cooperation, decorator, prediction and effective network transmission protocols are supposed to be combined together.

Prediction and Interpolation

Predictions in networked haptic cooperation reduce the network traffic load as well as smooth the updates by making up for the delayed and/or lost packets. The prediction algorithm can be either a simple interpolation based on history update record [41] or a advanced prediction algorithm such as dead-reckoning. The dead-reckoning algorithm selectively transmits updates according to the evaluation of the difference between the realistic update generated at local user side and the predicted one at remote user side. When this difference goes beyond a setup threshold, the generated update will be sent out. Although [42] indicated that the dead-reckoning algorithm does not performed well in highly synchronous closely-coupled task, [40] suggests that re-examination of this prediction algorithm leads to positive results [43], [44].

[37] implemented a dead reckoning algorithms based compensation scheme to make up for the delayed or lost updates. At the receiver's side, a predictor checks whether there is a haptic event in the buffer for the current time. If it returns false, the application uses the predicted haptic event to update the position and rotation of the virtual object. The prediction algorithm is the third order predictive algorithm and it shows high performance before the delay increases to about 80 ms. Furthermore, [25] conducts similar experiment to evaluate the adverse effect of network jitter when dead reckoning involved. It is suggested that without the dead reckoning, the average delay affects more than jitter in the networked haptic cooperation. However, as soon as the dead reckoning joins in, the adverse effect of jitter overwhelms that of delay.

2.2.2 Control Architectures with Various Controllers

Control architecture is the blueprint of the implementation of networked haptic cooperations. It embeds the haptic devices, the representations of users in the shared virtual environment, the shared virtual objects and the communication channels. It also defines their relationship in control and topology over network.

Previous research on designs of control architectures of networked haptic cooperation can be categorized into two groups: (1) the centralized (i.e. Client-Sever) control architectures [2, 20] and (2) the distributed (i.e. Peer-to-Peer) control architectures [45, 46, 15, 16, 20, 1]. Generally speaking, the centralized control architectures have the advantage of simplicity for synchronizing among users and expanding topology, while the distributed control architectures outperform in the inherent control stability. The centralized control architectures usually manage on the centralized

server the shared virtual environments as well as the official status of each client user, which avoids the synchronization of multiple copies of the shared virtual environments. Users newly joining in a networked haptic cooperation directly connect to the centralized server instead of building connection to each other user respectively, which simplifies the topology among users and reduces the network traffic load. However, the centralized control architectures have worse inherent control stability than the distributed control architectures, which is due to the longer delay of updates from the remote sides. In the centralized control architectures, updates from remote sides are delayed for round-trip-time, which is double of the delay in the distributed control architectures. Larger inherent delay for updates may result in worse inherent control stability and cooperative performance.

Most of the previous designs of control architectures focus on the cooperative manipulation of the shared virtual objects. However, participants in networked haptic cooperations also intend to directly interact with each other in addition to jointly manipulating the shared virtual objects. In addition to connecting the local copies of the shared virtual object through virtual coupling, the distributed control architecture in [2] provided the position and velocity of a user at its peer site. Although not developed for this purpose specifically, that architecture can render direct peer-to-peer interaction in addition to cooperative manipulation.

For haptic interaction with given haptic device and sampling rate, there is limitation of stiffness K and damping B that the shared virtual environment can render. Although high stiffness of the virtual spring is preferred, in practical implementation, a stiffness K as high as 2000-8000 N/m is sufficient to render a feeling of rigidity. The damping B of the rigid virtual wall exists to prevent prevent noticeable oscillation when users contact the wall, yet high damping B results in a high frequency oscillation.

To improve the contact stiffness of haptic interaction without losing control stability, various controllers are integrated in to control architectures. Additional controllers can be implemented between distributed copies of the shared virtual objects to combat the network adverse effects.

Virtual Coupling Controller

The concept of the virtual coupling controller, or virtual coupler, was presented for the first time in [47] to achieve passivity in the haptic interaction at the expense of

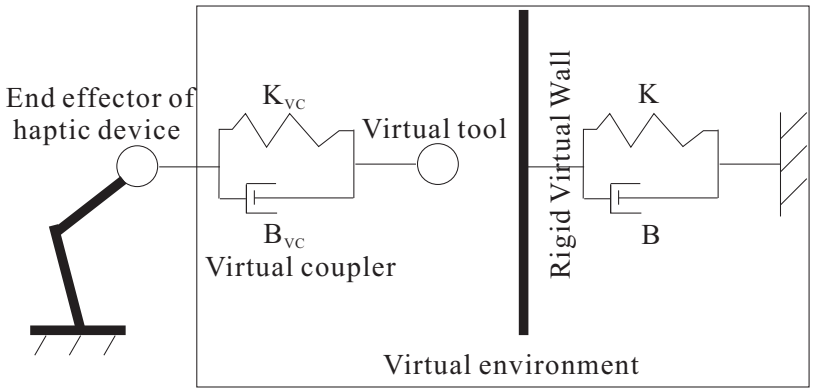

Figure 2.1: Human user contacts the virtual environment via the virtual tool, which is controlled by the haptic device it represents via the virtual coupler.

limiting the impedance the haptic devices can exhibit. Instead of directly contacting the virtual environment, human user contacts the virtual environment via the virtual tool, which is controlled by the haptic device via virtual coupler. Therefore, the stiffness that human users can feel depends on the stiffness K_{VC} and damping B_{VC} of the virtual coupling controller, instead of the real stiffness K and damping B of the virtual environment (Figure 2.1). Introducing a virtual coupling into haptic interaction separated the dynamics of virtual environment from dynamics of haptic devices, which allows independent design of each of them.

Various control architectures with virtual coupling coordination has been developed for networked haptic cooperation. In these designs virtual couplers render the contact in cooperation as well as coordinate the distributed copies of the shared virtual objects. [14] introduced three virtual coupling schemes for two haptically cooperative users either in Peer-to-Peer connection or in Client-Sever connection. These three schemes are experimentally compared by their performance in maintaining position coherency. [2] designed the distributed control architecture and the centralized control architecture, as well as theoretically derived their control stability in the presence of constant network delay and multiple sampling rate. In [1], the virtual couplers are combined with passivity control and wave-based control to improve the control stability in the presence of network delay.

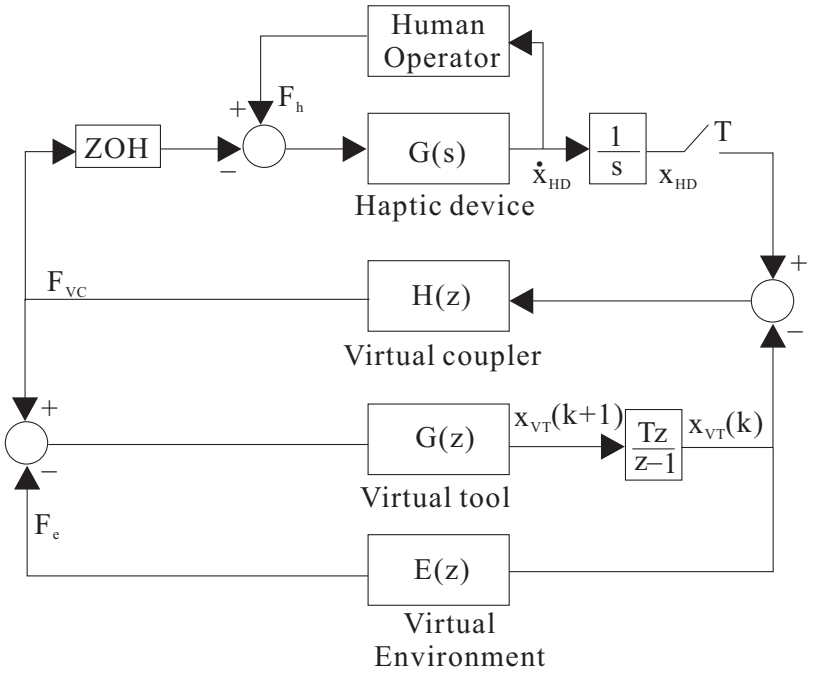

Figure 2.2: Model of a one-degree-freedom haptic interaction with virtual coupler.

Passivity Observer and Controller

A passivity observer and controller (POC) [48] ensures the system passivity in real time by adjusting power flow according to the observed energy calculated by passivity observer(PO). For a one-port system with zero initial energy storage and sampling period T, the energy observer can be implemented according to Equation 2.1

$$E_{obsv}(n) = T \sum_{k=0}^{n} f(k)v(k) \tag{2.1}$$

Similarly, for an M-port network with zero initial energy storage and sampling period T the observed energy follows Equation 2.2

$$E_{obsv}(n) = T \sum_{k=0}^{n} \left(f_1(k)v_1(k) + \cdots + f_M(k)v_M(k)\right) \tag{2.2}$$

in which $f_i(k)$ and $v_i(k)$ are the admissible force and velocity to the port i of the M-port network.

For both the above two energy observers, if $E_{obsv(n)} \geq 0$ for every time step n, the system dissipates energy. If there is any instance that $E_{obsv} < 0$, the system generates

energy and the amount of generated energy is $-E_{obsv}(n)$.

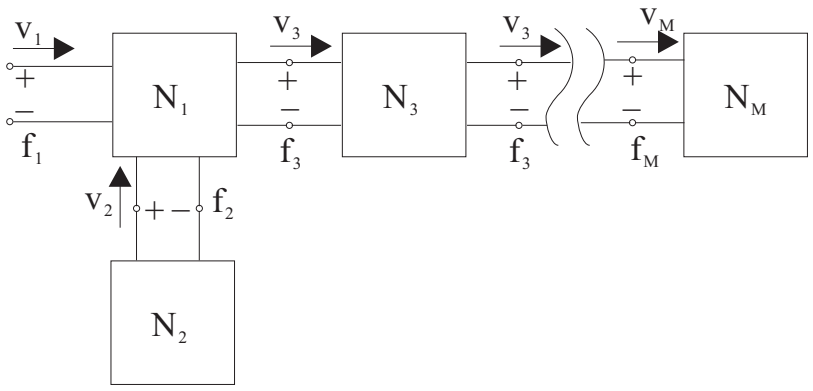

Figure 2.3: A network of inter-connected elements with one open port.

For a system including multiple interconnected elements, energy observers can be implemented to either monitor any of the element or a group of elements, even the system as a whole. Given a network of inter-connected elements with one open port as Figure 2.3, energy observer is implemented at each element. Assuming the initial energy of each elements is zero, the observed energy at each element will follow Equation 2.3 to Equation 2.6

$$E_{\mathrm{N1}}(n) = T\sum_{k=0}^{n}\left[f_1(k)v_1(k) + f_2(k)v_2(k) - f_M(k)v_M(k)\right] \tag{2.3}$$

$$E_{\mathrm{N2}}(n) = T\sum_{k=0}^{n} -f_2(k)v_2(k) \tag{2.4}$$

$$E_{\mathrm{N3}}(n) = T\sum_{k=0}^{n}\left[f_3(k)v_3(k) - f_4(k)v_4(k)\right] \tag{2.5}$$

$$E_{\mathrm{N}M}(n) = T\sum_{k=0}^{n} f_M(k)v_M(k) \tag{2.6}$$

The total energy of these inter-connected elements is: (Equation 2.7)

$$E_{\mathrm{obsv}}(n) = E_{\mathrm{N2}}(n) + E_{\mathrm{N2}}(n) + \cdots + E_{\mathrm{N}M}(n) \tag{2.7}$$

Which determines the passivity of the entire network of inter-connected elements. It is notable that the total observed energy is equivalent to the observed energy at

the open port (Equation 2.8)

$$E_{\text{obsv}}(n) = T \sum_{k=0}^{n} f_1(k) v_1(k) \tag{2.8}$$

According to the observed energy, passivity controller compensates the negative energy to dissipate an otherwise active system. The the passivity controller may be arranged either in series connection or in parallel connection. Given a observed and controlled element with admissible force f_2 and velocity v_2, as well as the passivity controller with admissible force f_1 and velocity v_1. For passivity controller in series

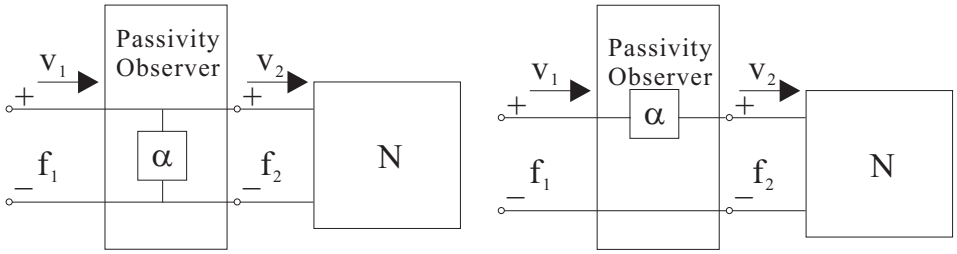

Figure 2.4: Series (left) and parallel (right) configuration of passivity controllers for one-port networks.

connection (Figure 2.4), at time step n

$$f_1(n) = f_2(n) + \alpha(n-1) v_2(n) \tag{2.9}$$

The α is the adjustable damping element, which is computed in real-time as:

$$\alpha(n) = \begin{cases} -E_{obsv}(n)/T(v_2(n))^2 & \text{if } E_{obsv}(n) < 0 \\ 0 & \text{otherwise} \end{cases} \tag{2.10}$$

In Equation 2.10, the $E_{obsv}(n)$ is the observed energy at the n step, which is computed as: (Equation 2.11)

$$E_{obsv}(n) = E_{obsv}(n-1) + [f_2(n) v_2(n) + \alpha(n-1)(v_2(n-1))^2 T \tag{2.11}$$

Note that $F_{ad} = \alpha(n-1) v_2(n-1)$ is the additional force for energy compensation.

It is notable that T can be canceled from Equation 2.10 and 2.11, which simplifies the computation. Therefore, the passivity observer can be also expressed as

$$W(n) = \sum_{k=0}^{n} f_2(k)v_2(k) + \sum_{k=0}^{n-1} \alpha(k)(v_2(k))^2 \tag{2.12}$$

Where

$$W(n) = \frac{1}{T} E_{obsv}(n) \tag{2.13}$$

Consequently, the observed and controlled element achieves system passivity if for arbitrary step n

$$\begin{aligned} \sum_{k=0}^{n} f_1(k)v_1(k) &= \sum_{k=0}^{n} f_2(k)v_2(k) + \sum_{k=0}^{n} \alpha(k)(v_2(k))^2 \\ &= \sum_{k=0}^{n} f_2(k)v_2(k) + \sum_{k=0}^{n-1} \alpha(k)(v_2(k))^2 + \alpha(n)(v_2(n))^2 \\ &= W(n) + \alpha(n)(v_2(n))^2 \geq 0 \end{aligned} \tag{2.14}$$

The passivity controller in series connection has two potential problems. First of all, the force required for energy dissipation may exceed the largest force that the actuator can generate, which becomes more obvious for smaller v_2. To avoid this situation, some implementations of passivity controllers set time-varying energy reference instead of a fixed threshold for energy compensation. Therefore, the negative energy will be compensated during multiple time steps rather than in one time step.

Another potential problem comes from the notorious difficulty of rendering velocity signal without noise. In passivity controller in series connection, the noise of velocity will be easily magnified by the adjustable damping parameter α. In this case, a upper boundary of α is necessary and the excess energy will be dissipated during the following one or several steps.

For passivity controller in parallel connection,

$$v_2(n) = v_1(n) - \frac{f_1}{\alpha(n-1)} \tag{2.15}$$

$$\frac{1}{\alpha(n)} = \begin{cases} -E_{obsv}(n)/[T \cdot f_2(n)] & \text{if } E_{obsv}(n) < 0 \\ 0 & \text{otherwise} \end{cases} \tag{2.16}$$

where

$$E_{obsv}(n) = E_{obsv}(n-1) + [f_2(n)v_2(n) + \frac{1}{\alpha(n-1)}(f_2(n-1))^2]T \tag{2.17}$$

Similarly, the above computation can be simplified as:

$$W(n) = \sum_{k=0}^{n} f_2(k)v_2(k) + \sum_{k=0}^{n-1} \frac{1}{\alpha(k)}(f_2(k))^2 \tag{2.18}$$

Where

$$W(n) = \frac{1}{T}E_{obsv}(n) \tag{2.19}$$

For system is passive if for arbitrary step n

$$\begin{aligned} \sum_{k=0}^{n} f_1(k)v_1(k) &= \sum_{k=0}^{n} f_2(k)v_2(k) + \sum_{k=0}^{n} \frac{1}{\alpha(k)}(f_2(k))^2 \\ &= \sum_{k=0}^{n} f_2(k)v_2(k) + \sum_{k=0}^{n-1} \frac{1}{\alpha(k)}(f_2(k))^2 + \frac{1}{\alpha(n)}(f_2(n))^2 \\ &= W(n) + \frac{1}{\alpha(n)}(v_2(n))^2 \geq 0 \end{aligned} \tag{2.20}$$

It is notable that some implementations of passivity controllers can adjust the observed energy flow according to a varying energy reference. This approach can eliminate the potential transient unstable behavior due to dissipating excess energy at one time step [49]. The reference energy behavior is designed according to the dynamic model information of the system. For the virtual environments with (approximatively) linear dynamic behavior, it is possible to design a passive reference energy behavior by calculating the stored energy $S(t)$ and the dissipated energy $D(t)$ of the system. For a continuous and energy lossless one-port network system, the net energy input to the system $E(t)$ is supposed to equal to sum of the stored energy and dissipated energy as Equation 2.21

$$E_t(n) = \int_0^t f(\tau)\dot{x}(\tau)d\tau = S(t) + D(t) \tag{2.21}$$

in which $S(t) + D(t)$ could be the reference energy behavior.

With the reference energy behavior, a passivity controller in serial connection as Figure 2.5 could be implemented in a one-port network via algorithm as the following steps:

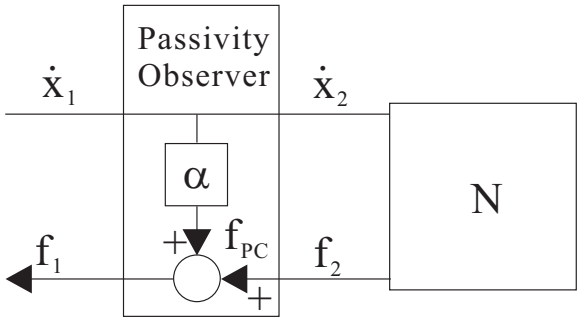

Figure 2.5: Passivity Observer and Controller with Energy Reference Flow.

- the input is

$$x_2(k) = x_1(k) \tag{2.22}$$

from which

$$\Delta x(k) = x_1(k) - x_1(k-1) \tag{2.23}$$

- the accurate energy at the step k is

$$E_{obsv}(k) = \int_{j=0}^{k} f_1(j-1)\Delta x(j) \tag{2.24}$$

- with $S(k)$ and $D(k)$ as the amount of stored energy and the dissipated energy of the virtual environment at step k, the control force of the passivity controller followed the reference energy which is calculated as:

$$f_{PC} = \begin{cases} -[E_{obsv}(k) - S(k) - D(k)]/\Delta x(k) & \text{if } W(k) < 0 \\ 0 & \text{else} \end{cases} \tag{2.25}$$

Where

$$W(k) = E_{obsv}(k) - S(k) - D(k) \tag{2.26}$$

- with the output of the one port system$f_2(k)$, the controlled output $f_1(k)$

$$f_1(k) = F_{PC}(k) + f_2 k \tag{2.27}$$

For the virtual environments without the dynamic model information of the system, maintaining the system passivity requires a hypothetical reference energy behav-

ior of the virtual environment, which simulate the continuous time energy behavior of the virtual environment. For example, the numerical integration of the power flow in to the virtual environment (the product of displacement and the resulting force output) can be used as reference energy behavior (Equation 2.28).

$$E_{ref}(t_k) = \int_{j=0}^{k} f(x(t_j), x(t_j - 1), \cdots, x(t_0))(x(t_j) - x(t_j - 1)) \tag{2.28}$$

Where the $f(x(t_j), x(t_j - 1), \cdots, x(t_0))$ is the computed force output of virtual environment for the input position displacement $(x(t_j) - x(t_j - 1))$.

[49] is experimentally demonstrated that the passivity observer and controller with energy reference renders smoother control output and removes the sudden impulsive control force which may destabilize a system. As the design energy reference is based on the dynamic behavior of the system, negative reference energy is allowed that it is possible to display an intentionally active behavior of the virtual environment, such as a virtual object is taken down from a virtual shelf.

Wave-based Controller

The wave-based control is originally designed to implement a passive communication channel for teleoperation [50]. In the wave based control, the standard power variables (i.e. the forces F and velocities $\dot{x}$) are encoded into wave variables (i.e. the forward wave variable u and the backward wave variable v) before being transmitted across the communication channel and decoded via the opposite algorithm after the transmission. The transformation between the standard power variables and the wave variables leads to the redefinition of the power flow P according to Equation 2.29.

$$P = \dot{x}^T F = \frac{1}{2} u^T u - \frac{1}{2} v^T v \tag{2.29}$$

Note that the standard power variables can be any other effort and flow pair instead of the force and velocity.

The wave variables is computed from the standard power variables as the transformation of Equation 2.30. This transformation is unique and invertible.

$$u = \frac{b\dot{x} + F}{\sqrt{2b}} \qquad v = \frac{b\dot{x} - F}{\sqrt{2b}} \tag{2.30}$$

Where the wave impedance b is the scaling coefficient relating the standard power

variables and the wave variables.

Actually, the wave transformation could determine any combination of the power and wave variables. Any two of the four variables can be selected as input or output (Figure 2.6).

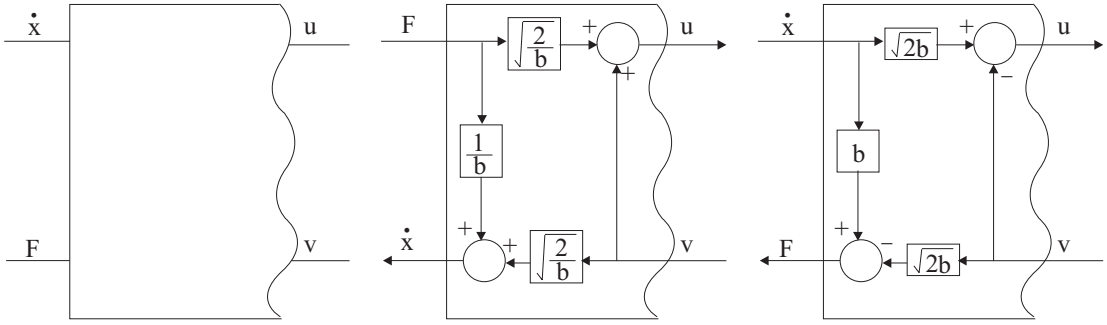

Figure 2.6: Wave transformation between standard power and wave variables.

The wave-based communication channel in continuous time maintains passivity in the presence of arbitrary communication delay [50]. Furthermore, [51] demonstrated that an equivalence can be obtained between the continuous time and discrete time energy flows and therefore proved that with the equivalence the discrete communication channel is lossless since the constant delay is passive for time-varying delay and packet loss. With the ensured passivity of the communication channel, the system stability of the networked haptic cooperation can be largely improved.

As the coordination between copies of the shared virtual objects, wave-based controller helps to render more accurate dynamic properties of the shared virtual objects in addition to maintain passivity of the communication channel in networked haptic cooperation, which outperforms the virtual coupler. Consider a shared virtual object with virtual coupling coordination among its distributed copies. As the network delay increases, it takes longer for the remote copy of the shared virtual object to response the manipulation to the local copy of the shared virtual object. This latency in response makes the users feel that the shared virtual object is increasingly difficult to move, which leads to the feeling that the shared virtual object is increasingly heavier. As in [35], networked haptic cooperation with wave-based communication channel demonstrated higher performance in maintaining force perception of the same cooperative manipulation to the same shared virtual object in the presence of different network delay.

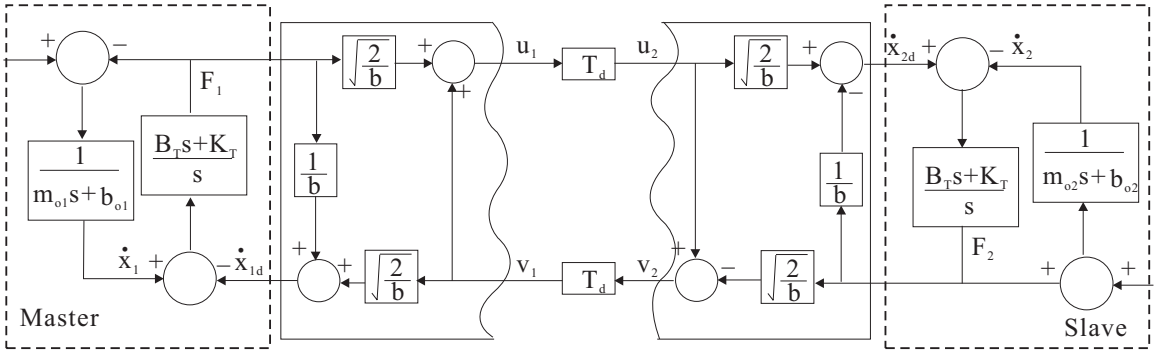

Figure 2.7: Teleoperation with traditional wave-based communication channel.

Although wave-based communication channel perform highly in maintaining control stability in the presence of adverse network effects, two disadvantages prevent it prevailing as the coordination among distributed copies of the shared virtual object. As in [1], wave-based coordination demonstrated much worse position coherency comparing to the virtual coupling coordination. Although the wave-based coordination may improve its performance in minimizing position difference by increasing the wave impedance b, an larger wave impedance b will result in large damping effect that users feel their manipulations become viscous in a supposed free space [50].

Another disadvantage of the wave-based coordination is that it inherently distinguishes the master from the slave among the users it coordinates. Traditionally, users in teleoperation have inequivalent statuses in control that the user as slave has to follow to the user as master. This inequality of status embedded in control through distinguishing forward moving (from master to slave) and returning (from slave to master) waves. The two sides maintain distinct roles even when they communicate using the symmetric configuration [50]. However in a networked haptic cooperation with an exactly Peet-to-Peer connection, users are expected to have equal status in control. The distributed copies of the same shared virtual object expect being coordinated with equivalently reciprocal forces, instead of being commanded by any of the copy. Therefore, networked haptic cooperation also look forwards to an wave-based communication with which users can achieve Peer-to-Peer status in control.

2.2.3 Representing Human Users with Proxies of Higher Order of Dynamics

In currently existing networked haptic cooperation, human users are commonly represented with zero order dynamics in the virtual environments of its remote peers' sides [2]. As described previously, representing users in virtual environments with higher order dynamics result in motions of users in virtual environments with better physical realismTherefore, researches on proxies with first and second order dynamics can server as proper reference, although some of these researches are not particularly designed for representing users in the remote virtual environments.

The concept of proxies are initially introduced for improving the accuracy of collision detection in the virtual environments. The first proxy-like design of the god object [52] has its motion fully controlled to prevent any penetration into the virtual object. In free space, the god object coincides with the position input from the haptic device. When the haptic device moves into an virtual object, the god-object persists to stay on the surface and its location is computed to be a point on the currently contacted surface so that its distance from the real position of haptic device is minimized. Therefore, the implementation of god-object visually renders haptic contact with infinite stiffness. [53] inherits the design of surface-persisting proxy and possesses only the zero order dynamics. This simplification achieves efficient collision detection with geometrically complicated virtual object at the expense of losing physically realistic motion of the users.

[54] proposed the design of proxies with first order dynamics and the geometric constraints in virtual environments are converted into equivalent velocity constrains for the sake of collision detection. This approach is extended to rigid-body collision detections between multiple independent proxies, such as two virtual tools in interaction. Proxies with second order dynamics have been proposed in [55]. For single user interaction with a slow virtual environment, the second order dynamic proxies have mitigated the effect of computational delay on the stability of the interaction and on user's perception of rigid contact.

2.3 Summary

This chapter reviewed the research history of networked haptic cooperation. After addressing the influence of the adverse network effects (i.e. the limited bandwidth,

the network delay, jitter and packet loss), the chapter presented the state of art in networked haptic cooperation from three perspectives. 1) From the perspective of network, available research mitigates the adverse network effects and synchronize large number of users and user groups via the implementing advanced protocols. Especially, various buffer schemes and prediction & interpolation are implemented to smooth the network delay jitter and to make up for the packet loss. (2) From the perspective of control stability, centralized and distributed control architectures with various controllers are designed to improve the performance of networked haptic cooperation. (3) From the perspective of physically-intuitive virtual reality, proxies of different orders of dynamics are implemented to represent the users' motion in the shared virtual environment. Furthermore, controllers are designed to help the shared virtual objects with maintaining their dynamic properties.

Chapter 3

Remote Dynamic Proxies for Distributed Control of Networked Haptic Cooperation

This chapter introduces the concept of remote dynamic proxies and integrates it into two distributed control architectures. The two architectures coordinate the peer networked sites via virtual coupling and via wave variable control, respectively. The remote dynamic proxies are integrated into distributed rather than centralized control architectures because centralized architectures have been shown to be able to render only limited contact stiffness to the client users [2]. The continuous time dynamics of haptic cooperation between two users controlled via the two architectures are also presented in this chapter, both for cooperative manipulation of a shared virtual object and for direct user-to-user interaction.

3.1 Remote Dynamic Proxies

This section introduces the remote dynamic proxies for networked haptic interaction between two users. The extension to networked haptic cooperation among more users will be pursued in future work. This extension requires advanced scheme for synchronization among large number of users and user groups in the networked haptic cooperation, in addition to the computational complexity resulted from rendering large number of remote dynamic proxies in the shared virtual environment.

The motivation for proposing remote dynamic proxies is to enable far away users

to directly touch and feel each other in the presence of network update rates that are much lower than the haptic feedback rate, and in the presence of constant network delays. Direct interactions between distant users are expected to benefit physical therapists assisting remote patients.

A remote dynamic proxy is an avatar of a user in the virtual environment of their peer (see Figure 3.1 and Figure 3.2, where RDP_{12} denotes the remote dynamic proxy of Peer 1 in the virtual environment of Peer 2). The remote dynamic proxy inherits the inertial and damping properties from the haptic device of the user whom it represents. Its position and velocity are computed using physics-based simulation rather than being updated from network packets. In Figure 3.1 and Figure 3.2, T_d is the network delay, m_{HD} is the mass of the haptic device of the peer whom the remote dynamic proxy represents, and the controllers commanding the motion of the remote dynamic proxies to follow the motion of their respective user are schematically represented via the spring K_{RDP} and damper B_{RDP} connection in the peer's virtual environment. This compliant connection allows the networked users to perceive the motion of distant peers smoothly in the presence of update discontinuities due to network characteristics (e.g., limited bandwidth, delay, jitter, packet loss, etc.). Note that, while the haptic device imposes a controlling force on the remote dynamic proxy, it receives no force feedback from this remote dynamic proxy.

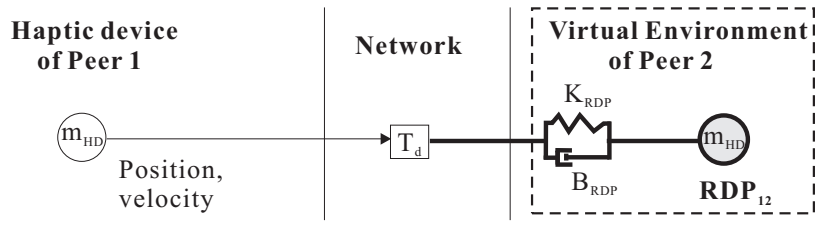

Figure 3.1: Remote dynamic proxy (RDP) with motion commanded via virtual coupling control.

Via the remote dynamic proxies, the motion of the cooperative users is updated at the haptic rate in the virtual environment of their peer. As a result, all participants to the interaction (i.e., both cooperative users and the shared virtual objects) are rendered at the speed of the haptic loop at each peer site. Therefore, the adverse effect of the low network update rate on stability is limited. To some extent, the remote dynamic proxies separate the design of the virtual environment with high rendering rate from the design of the coordination controller with low network update rate. Furthermore, the remote dynamic proxies allow cooperation between remote sites

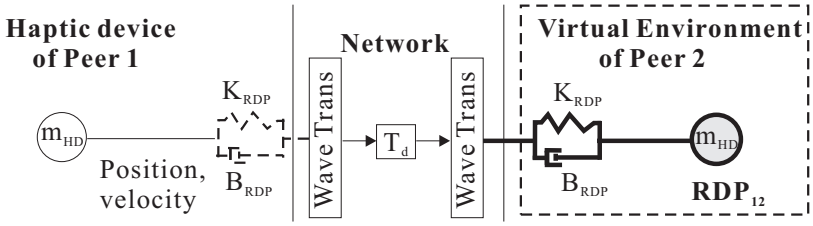

Figure 3.2: Remote dynamic proxy (RDP) with motion commanded via wave-based control.

with different rendering rates in their local virtual environments.

As avatars of remote peers in the virtual environment of each user, the remote dynamic proxies require: (1) larger communication bandwidth to accommodate the additional information that peers need to exchange; and (2) a more time consuming simulation that includes the remote dynamic proxies of all peer sites in the collision detection and the dynamic response algorithms. While they may limit the number of users simultaneously present in a shared virtual environment, these requirements are typical for networked haptic cooperation approaches that provide users with avatars of their remote peers. Furthermore, the additional communication bandwidth and simulation overhead are minimal in the case of cooperation between two users, which is the focus of this thesis.

The integration of the remote dynamic proxies into a distributed architecture with virtual coupling coordination between the distant peers is presented in the next section, while their integration into a distributed architecture with wave-based coordination follows in Section 3.3. Note that with the proposed control architecture involving the remote dynamic proxies with wave-based coordination have passive communication channel to be passive and therefore enable the proposed distributed control architecture to sustain longer network delay.

3.2 Distributed Control Architecture with Virtual Coupling Coordination

The proposed distributed control architecture is shown in Figure 3.3 for cooperative manipulation of a shared virtual object by two networked users. For simplicity, the two haptic devices are assumed similar. In Figure 3.3, notation is used as follows: m_{HD} and b_{HD} are the mass and the damping of the haptic interfaces; $m_{\mathrm{O}i}$ and $b_{\mathrm{O}i}$

are the mass and the damping of Peer i's copy of the shared virtual object; $K_{\mathrm{VC}i}$ and $B_{\mathrm{VC}i}$ are the stiffness and the damping of the **local contact**, i.e. the contact between Peer i and its copy of the virtual object; $F_{\mathrm{VC}i}$ is the interaction force between Peer i and its copy of the virtual object; $K_{\mathrm{VC}ij}$ and $B_{\mathrm{VC}ij}$ are the stiffness and the damping of **remote contact**, i.e. the contact between Peer i's remote dynamic proxy in Peer j's virtual environment and Peer j's copy of the virtual object; $F_{\mathrm{VC}ij}$ is the interaction force between Peer i's remote dynamic proxy and Peer j-th copy of the virtual object; K_{T} and B_{T} are the stiffness and the damping of virtual coupling coordination among the distributed copies of the shared virtual object; $F_{\mathrm{T}i}$ is the coordinating force applied on each copy; K_{RDP} and B_{RDP} are the stiffness and the damping of virtual coupler controlling the RDP-s ; $F_{\mathrm{RDP}ij}$ is the controlling force applied on the remote proxy of Peer i in the virtual environment of Peer j; x_i and $\dot{x}_i$ are the position and the velocity of the i-th haptic device; $x_{\mathrm{O}i}$ and $\dot{x}_{\mathrm{O}i}$ are the position and the velocity of Peer i's copy of the virtual object; x_{ij} and $\dot{x}_{ij}$ are the position and the velocity of the remote proxy of Peer i in the virtual environment of Peer j; x_{i_n} and $\dot{x}_{i_n}$ are the position and the velocity commands sent by the i-th haptic device to their peers; $x_{\mathrm{O}i_n}$ and $\dot{x}_{\mathrm{O}i_n}$ are the position and velocity commands sent by Peer i's copy of the virtual object to the peer users; lastly, $F_{\mathrm{h}i}$ is the force applied by the i-th user to their device. Since $F_{\mathrm{VC}i}$ and $F_{\mathrm{VC}ij}$ represent contacts, they are unilateral forces activated by collision detection.

Note that, in the proposed architecture, the virtual environment of Peer i comprises:

1. a copy of the virtual object jointly manipulated by the users.

2. the remote dynamic proxy RDP_{ji} of Peer j.

The mass of the shared virtual object m_{O} is equally divided between its two copies as $m_{\mathrm{O}i} = \frac{m_{\mathrm{O}}}{2}$. The damping b_{O} is assigned to each copy, $b_{\mathrm{O}i} = b_{\mathrm{O}}$.

The dynamics of the networked haptic cooperation rendered via the distributed control architecture with remote dynamic proxies shown in Figure 3.3 are:

- for the haptic devices:

$$m_{\mathrm{HD1}}\ddot{x}_1 + b_{\mathrm{HD1}}\dot{x}_1 = F_{\mathrm{h1}} - F_{\mathrm{VC1}} \tag{3.1}$$

$$m_{\mathrm{HD2}}\ddot{x}_2 + b_{\mathrm{HD2}}\dot{x}_2 = F_{\mathrm{h2}} - F_{\mathrm{VC2}} \tag{3.2}$$

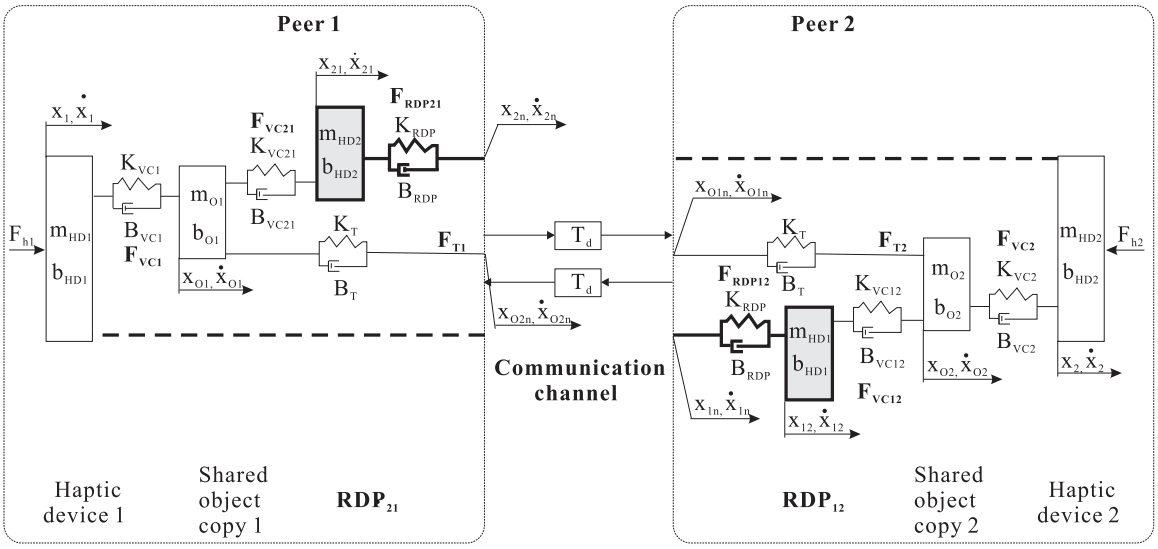

Figure 3.3: Distributed control architecture with remote dynamic proxies (RPDs) and virtual coupling coordination of two users involved in cooperative manipulation of a shared virtual object. The remote dynamic proxies are shaded, and their connection to the corresponding haptic device is bolded.

- for the remote dynamic proxies:

$$m_{\mathrm{HD1}}\ddot{x}_{12} + b_{\mathrm{HD1}}\dot{x}_{12} = F_{\mathrm{RDP12}} - F_{\mathrm{VC12}} \tag{3.3}$$

$$m_{\mathrm{HD2}}\ddot{x}_{21} + b_{\mathrm{HD2}}\dot{x}_{21} = F_{\mathrm{RDP21}} - F_{\mathrm{VC21}} \tag{3.4}$$

- for the copies of the shared virtual object:

$$m_{\mathrm{O1}}\ddot{x}_{\mathrm{O1}} + b_{\mathrm{O1}}\dot{x}_{\mathrm{O1}} = F_{\mathrm{VC1}} + F_{\mathrm{VC21}} + F_{\mathrm{T1}} \tag{3.5}$$

$$m_{\mathrm{O2}}\ddot{x}_{\mathrm{O2}} + b_{\mathrm{O2}}\dot{x}_{\mathrm{O12}} = F_{\mathrm{VC2}} + F_{\mathrm{VC12}} + F_{\mathrm{T2}} \tag{3.6}$$

where:

$$F_{\mathrm{VC1}} = K_{\mathrm{VC1}}(x_1 - x_{\mathrm{O1}}) + B_{\mathrm{VC1}}(\dot{x}_1 - \dot{x}_{\mathrm{O1}}) \tag{3.7}$$

$$F_{\mathrm{VC2}} = K_{\mathrm{VC1}}(x_2 - x_{\mathrm{O2}}) + B_{\mathrm{VC1}}(\dot{x}_2 - \dot{x}_{\mathrm{O2}}) \tag{3.8}$$

$$F_{\mathrm{VC12}} = K_{\mathrm{VC12}}(x_{12} - x_{\mathrm{O2}}) + B_{\mathrm{VC12}}(\dot{x}_{12} - \dot{x}_{\mathrm{O2}}) \tag{3.9}$$

$$F_{\mathrm{VC21}} = K_{\mathrm{VC21}}(x_{21} - x_{\mathrm{O1}}) + B_{\mathrm{VC21}}(\dot{x}_{21} - \dot{x}_{\mathrm{O1}}) \tag{3.10}$$

$$
\begin{aligned}
F_{\mathrm{T1}} &= K_{\mathrm{T}}(x_{\mathrm{O2}_n} - x_{\mathrm{O1}}) + B_{\mathrm{T}}(\dot{x}_{\mathrm{O2}_n} - \dot{x}_{\mathrm{O1}}) \\
&= K_{\mathrm{T}} x_{\mathrm{O2}_n} + B_{\mathrm{T}} \dot{x}_{\mathrm{O2}_n} + (-K_{\mathrm{T}} x_{\mathrm{O1}} - B_{\mathrm{T}} \dot{x}_{\mathrm{O1}}) \\
&= F_{\mathrm{T1}_n} + F_{\mathrm{T1}_c} \qquad (3.11) \\
F_{\mathrm{T2}} &= K_{\mathrm{T}}(x_{\mathrm{O1}_n} - x_{\mathrm{O2}}) + B_{\mathrm{T}}(\dot{x}_{\mathrm{O1}_n} - \dot{x}_{\mathrm{O2}}) \\
&= K_{\mathrm{T}} x_{\mathrm{O1}_n} + B_{\mathrm{T}} \dot{x}_{\mathrm{O1}_n} + (-K_{\mathrm{T}} x_{\mathrm{O2}} - B_{\mathrm{T}} \dot{x}_{\mathrm{O2}}) \\
&= F_{\mathrm{T2}_n} + F_{\mathrm{T2}_c} \qquad (3.12)
\end{aligned}
$$

$$
\begin{aligned}
F_{\mathrm{RDP21}} &= K_{\mathrm{RDP}}(x_{2_n} - x_{21}) + B_{\mathrm{RDP}}(\dot{x}_{2_n} - \dot{x}_{21}) \\
&= K_{\mathrm{RDP}} x_{2_n} + B_{\mathrm{RDP}} \dot{x}_{2_n} + (-K_{\mathrm{RDP}} x_{21} - B_{\mathrm{RDP}} \dot{x}_{21}) \\
&= F_{\mathrm{RDP21}_n} + F_{\mathrm{RDP21}_c} \qquad (3.13) \\
F_{\mathrm{RDP12}} &= K_{\mathrm{RDP}}(x_{1_n} - x_{12}) + B_{\mathrm{RDP}}(\dot{x}_{1_n} - \dot{x}_{12}) \\
&= K_{\mathrm{RDP}} x_{1_n} + B_{\mathrm{RDP}} \dot{x}_{1_n} + (-K_{\mathrm{RDP}} x_{12} - B_{\mathrm{RDP}} \dot{x}_{12}) \\
&= F_{\mathrm{RDP12}_n} + F_{\mathrm{RDP12}_c} \qquad (3.14)
\end{aligned}
$$

For direct interaction between two networked users, the distributed control architecture with remote dynamic proxies and virtual coupling coordination is shown in Figure 3.4.

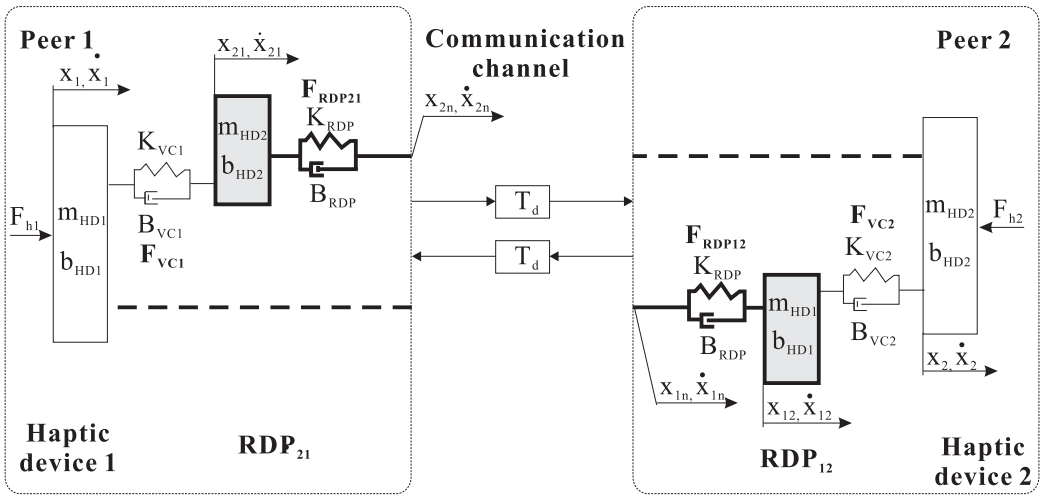

Figure 3.4: Distributed control architecture with remote dynamic proxies (RPD) and virtual coupling coordination of two users in direct interaction with each other. The remote dynamic proxies are shaded, and their connection to the corresponding haptic device is bolded.

In this case, the dynamics of the interaction are:

- for the peer haptic devices:

$$m_{\mathrm{HD1}}\ddot{x}_1 + b_{\mathrm{HD1}}\dot{x}_1 = F_{\mathrm{h1}} - F_{\mathrm{VC1}} \tag{3.15}$$
$$m_{\mathrm{HD2}}\ddot{x}_2 + b_{\mathrm{HD2}}\dot{x}_2 = F_{\mathrm{h2}} - F_{\mathrm{VC2}} \tag{3.16}$$

- for the remote dynamic proxies:

$$m_{\mathrm{HD1}}\ddot{x}_{12} + b_{\mathrm{HD1}}\dot{x}_{12} = F_{\mathrm{RDP12}} + F_{\mathrm{VC2}} \tag{3.17}$$
$$m_{\mathrm{HD2}}\ddot{x}_{21} + b_{\mathrm{HD2}}\dot{x}_{21} = F_{\mathrm{RDP21}} + F_{\mathrm{VC1}} \tag{3.18}$$

where:

$$\begin{aligned} F_{\mathrm{VC1}} &= K_{\mathrm{VC1}}(x_1 - x_{21}) + B_{\mathrm{VC1}}(\dot{x}_1 - \dot{x}_{21}) && (3.19)\\ F_{\mathrm{VC2}} &= K_{\mathrm{VC1}}(x_2 - x_{12}) + B_{\mathrm{VC1}}(\dot{x}_2 - \dot{x}_{12}) && (3.20) \end{aligned}$$

$$\begin{aligned} F_{\mathrm{RDP21}} &= K_{\mathrm{RDP}}(x_{2_n} - x_{21}) + B_{\mathrm{RDP}}(\dot{x}_{2_n} - \dot{x}_{21}) \\ &= K_{\mathrm{RDP}}x_{2_n} + B_{\mathrm{RDP}}\dot{x}_{2_n} + (-K_{\mathrm{RDP}}x_{21} - B_{\mathrm{RDP}}\dot{x}_{21}) \\ &= F_{\mathrm{RDP21}_n} + F_{\mathrm{RDP21}_c} && (3.21)\\ F_{\mathrm{RDP12}} &= K_{\mathrm{RDP}}(x_{1_n} - x_{12}) + B_{\mathrm{RDP}}(\dot{x}_{1_n} - \dot{x}_{12}) \\ &= K_{\mathrm{RDP}}x_{1_n} + B_{\mathrm{RDP}}\dot{x}_{1_n} + (-K_{\mathrm{RDP}}x_{12} - B_{\mathrm{RDP}}\dot{x}_{12}) \\ &= F_{\mathrm{RDP12}_n} + F_{\mathrm{RDP12}_c} && (3.22) \end{aligned}$$

Based on the dynamics in Equations (3.1) to (3.6) and in Equations (3.15) to (3.18), Chapter 4 will derive the state space representation of the multi-rate haptic cooperation system, as well as its stability region in the presence of several constant network delays.

3.3 Distributed Control Architecture with Wave-based Controller

3.3.1 Traditional symmetric wave variable control

Wave (or scattering)-based communications have been introduced in teleoperation [56, 57] to render the communication line passive in the presence of communication delay. In teleoperation, the master and the slave robots play different roles. Their dissimilar functions have been embedded in control through distinguishing forward moving (from master to slave) and returning (from slave to master) waves. The two sides maintain distinct roles even when they communicate using the symmetric configuration [50][1].

Peer-to-peer haptic cooperation between two users via the symmetric configuration and the traditional wave transformation [50] has been implemented in [1], as shown Figure 3.5. The figure details only the power-to-wave transformations and the proportional derivative (PD) controllers coordinating the two peer copies of the shared virtual object. The PD control forces due to the interaction of each user with their local copy of this object provide the inputs in Figure 3.5. In this figure, notation is used as follows: indices 1 and 2 identify the two peers; T_{d} is the communication delay; b is the wave impedance; u and v are the forward and returning waves, respectively; K_{T} and B_{T} are the gains of the coordinating controllers at the two remote sites; F_i are the control forces on the copy of the shared object of Peer i; $m_{\mathrm{O}i}$ and $b_{\mathrm{O}i}$ are the inertia and the damping of those copies; x_i and $\dot{x}_i$ are their simulated position and velocity; and $\dot{x}_{id}$ is their commanded velocity.

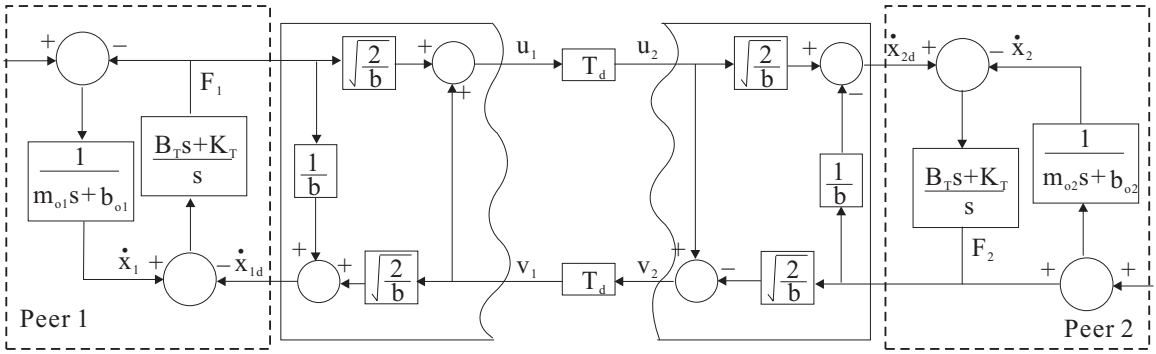

Figure 3.5: Traditional symmetric wave variable control of the shared virtual object [1].

[1]In the symmetric configuration, forces are encoded into, and velocities are decoded from, wave signals at both sides.

In the symmetric wave transformation shown in Figure 3.5, the control force on the copy of the shared virtual object of Peer 1 is:

$$F_1 = -B_{\mathrm{T}}(\dot{x}_{1_d} - \dot{x}_1) - K_{\mathrm{T}}(x_{1_d} - x_1), \tag{3.23}$$

while the forward moving wave and the desired velocity are computed via:

$$u_1 = \frac{b\dot{x}_{1_d} + F_1}{\sqrt{2b}} = v_1 + F_1\sqrt{\frac{2}{b}}. \tag{3.24}$$

and:

$$\dot{x}_{1_d} = \frac{v_1\sqrt{2b} + F_1}{b}, \tag{3.25}$$

After unwrapping the algebraic loop created by the PD controller (proportional-derivative controller) and the wave transformation, the desired velocity no longer depends on the control force (i.e., F_1):

$$\dot{x}_{1_d} = \frac{v_1\sqrt{2b} + B_{\mathrm{T}}\dot{x}_1 + K_{\mathrm{T}}(x_1 - x_{1_d})}{b + B_{\mathrm{T}}} \tag{3.26}$$

At the Peer 2 side, the control force, the returning wave and the desired velocity (after unwrapping the algebraic loop) are calculated using:

$$F_2 = -B_{\mathrm{T}}(\dot{x}_2 - \dot{x}_{2_d}) - K_{\mathrm{T}}(x_2 - x_{2_d}), \tag{3.27}$$

$$v_2 = \frac{b\dot{x}_{2_d} - F_2}{\sqrt{2b}} = u_2 - F_2\sqrt{\frac{2}{b}}, \tag{3.28}$$

$$\dot{x}_{2_d} = \frac{u_2\sqrt{2b} + B_{\mathrm{T}}\dot{x}_2 + K_{\mathrm{T}}(x_2 - x_{2_d})}{b + B_{\mathrm{T}}}. \tag{3.29}$$

Note that the asymmetric roles of the two peer sites are reflected in the control forces F_1 and F_2. Because of this asymmetry, it is not straightforward to employ the traditional taxonomy in distributed architectures that support cooperation among multiple users. With a view to the future extension of the current framework to cooperation among multiple users, the following section proposes a peer-based classification of wave signals.

3.3.2 Peer-to-peer symmetric wave variable control

The peer-based view of the haptic cooperation adopted in this work:

1. distinguishes outgoing (i.e., leaving a site) and incoming (i.e., arriving at a site) waves. Accordingly, $u_{\text{out}i}$ and $u_{\text{in}i}$ will hereafter identify the outgoing and incoming wave signals at Peer i, respectively (see Figure 3.6).

2. regards the haptic interfaces of all interacting users as similar to the master robot in teleoperation. Control forces at all peer sites provide feedback to users in interaction with their local copies of the shared virtual object. Therefore, they are defined via:

$$F_i = -B_{\text{T}}(\dot{x}_{i_d} - \dot{x}_i) - K_{\text{T}}(x_{i_d} - x_i). \tag{3.30}$$

Figure 3.6 illustrates the peer-to-peer symmetric wave variable control of the shared virtual object for haptic collaboration between two users.

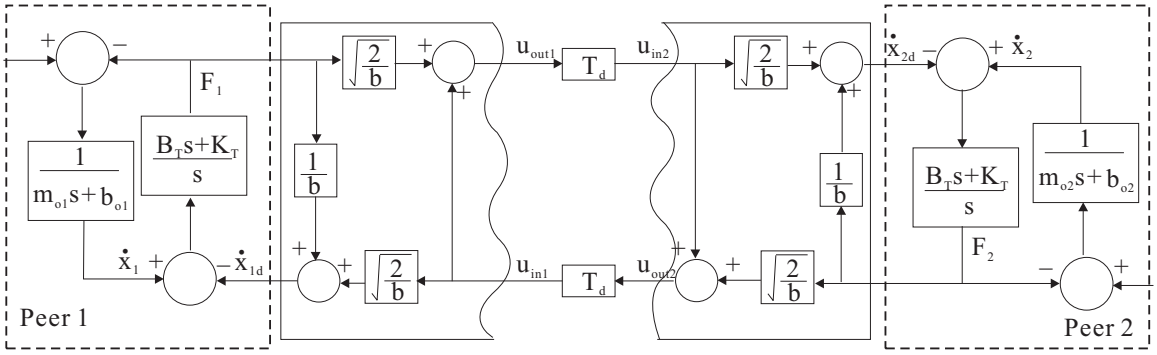

Figure 3.6: Peer-to-peer symmetric wave variable control of the shared virtual object.

Given the definition in Equation (3.30), the outgoing wave at Peer i becomes:

$$u_{\text{out}i} = u_{\text{in}i} + F_i\sqrt{\frac{2}{b}}, \tag{3.31}$$

while the desired (reference) velocity of the local copy of the shared virtual object at Peer i is computed via:

$$\dot{x}_{i_d} = \frac{u_{\text{in}i}\sqrt{2b} + B_{\text{T}}\dot{x}_i + K_{\text{T}}(x_i - x_{i_d})}{b + B_{\text{T}}}. \tag{3.32}$$

To avoid drift of x_{i_d} in Equation (3.32) (due to sampling, numerical integration, data loss, etc.), the communications are augmented to include wave integrals [58]. Then, the outgoing wave integral is computed via:

$$U_{\text{out}i} = U_{\text{in}i} + p_i\sqrt{\frac{2}{b}}, \tag{3.33}$$

and the desired position is decoded using:

$$x_{i_d} = U_{\text{in}i}\sqrt{\frac{2}{b}} + \frac{1}{b}p_i. \tag{3.34}$$

Notation in (3.33) and (3.34) follows [58], i.e., U denotes wave integrals and p is momentum (i.e., the integral of the control force):

$$p_i = \int_0^t F_i dt. \tag{3.35}$$

3.3.3 Distributed Control Architecture with Wave-based Controller

The proposed distributed control architecture is shown in Figure 3.7 for two users engaged in cooperative manipulation of a shared virtual object. As in the previous section, the two haptic devices are assumed similar. In Figure 3.7, notation is used as follows: m_{HD} and b_{HD} are the mass and the damping of the haptic interfaces; $m_{\text{O}i}$ and $b_{\text{O}i}$ are the mass and the damping of Peer i's copy of the shared virtual object; $K_{\text{VC}i}$ and $B_{\text{VC}i}$ are the stiffness and the damping of the contact between Peer i and its copy of the shared virtual object; $F_{\text{VC}i}$ is the interaction force between Peer i and its copy of the shared virtual object; $K_{\text{VC}ij}$ and $B_{\text{VC}ij}$ are the stiffness and the damping of the contact between Peer i's remote dynamic proxy in Peer j's virtual environment and Peer j's copy of the shared virtual object; $F_{\text{VC}ij}$ is the interaction force between Peer i's remote dynamic proxy and Peer j-th copy of the shared virtual object; x_i and $\dot{x}_i$ are the position and the velocity of the i-th haptic device; $x_{\text{O}i}$ and $\dot{x}_{\text{O}i}$ are the position and the velocity of Peer i's copy of the virtual object; x_{ij} and $\dot{x}_{ij}$ are the position and the velocity of the remote proxy of Peer i in the virtual environment of Peer j; x_{id} and $\dot{x}_{id}$ are the position and the velocity commands received by the i-th haptic device from their peers via wave signals; $x_{\text{O}id}$ and $\dot{x}_{\text{O}id}$ are the position and velocity commands received by Peer i's copy of the virtual object from the peer users;

lastly, $F_{\mathrm{h}i}$ is the force applied by the i-th user to their device. Since $F_{\mathrm{VC}i}$ and $F_{\mathrm{VC}ij}$ represent contacts, they are unilateral forces activated by collision detection.

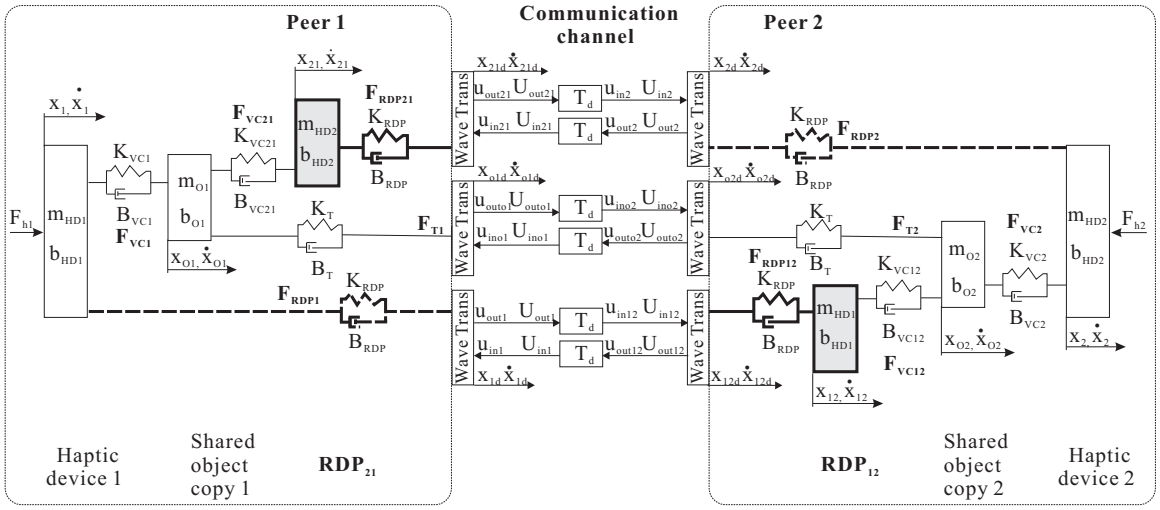

Figure 3.7: Distributed control architecture with remote dynamic proxies (RPDs) and wave-based coordination of two users involved in cooperative manipulation of a shared virtual object. The remote dynamic proxies are shaded, and their connection to the corresponding haptic device is bolded.

Note that, as in the distributed architecture with RDP-s and virtual coupling coordination, the virtual environment of Peer i comprises:

1. a copy of the virtual object jointly manipulated by the users.
2. the remote dynamic proxy RDP_{ji} of Peer j.

The designed mass of the shared virtual object m_{O} is equally divided between its two copies as $m_{\mathrm{O}i} = \frac{m_{\mathrm{O}}}{2}$. the damping b_{O} is assigned to each copy, $b_{\mathrm{O}i} = b_{\mathrm{O}}$.

The dynamics of the networked haptic cooperation rendered via the distributed control architecture with remote dynamic proxies shown in Figure 3.7 are:

- for the peer haptic devices (device motion and virtual contact forces balanced by the user force $F_{\mathrm{h}i}$):

$$m_{\mathrm{HD1}}\ddot{x}_1 + b_{\mathrm{HD1}}\dot{x}_1 = F_{\mathrm{h1}} - F_{\mathrm{VC1}} \tag{3.36}$$

$$m_{\mathrm{HD2}}\ddot{x}_2 + b_{\mathrm{HD2}}\dot{x}_2 = F_{\mathrm{h2}} - F_{\mathrm{VC2}} \tag{3.37}$$

- for the remote dynamic proxies (remote dynamic proxy motion and virtual contact forces balanced by the force due to the remote user $F_{\mathrm{T}ij}$):

$$m_{\mathrm{HD1}}\ddot{x}_{12} + b_{\mathrm{HD1}}\dot{x}_{12} = F_{\mathrm{RDP12}} - F_{\mathrm{VC12}} \tag{3.38}$$

$$m_{\mathrm{HD2}}\ddot{x}_{21} + b_{\mathrm{HD2}}\dot{x}_{21} = F_{\mathrm{RDP21}} - F_{\mathrm{VC21}} \tag{3.39}$$

- for the shared virtual object (shared virtual object motion caused by forces from the local user, the remote dynamic proxy and the remote copy of the shared virtual object):

$$m_{\mathrm{O1}}\ddot{x}_{\mathrm{O1}} + b_{\mathrm{O1}}\dot{x}_{\mathrm{O1}} = F_{\mathrm{VC1}} + F_{\mathrm{VC21}} + F_{\mathrm{T1}} \tag{3.40}$$

$$m_{\mathrm{O2}}\ddot{x}_{\mathrm{O2}} + b_{\mathrm{O2}}\dot{x}_{\mathrm{O12}} = F_{\mathrm{VC2}} + F_{\mathrm{VC12}} + F_{\mathrm{T2}} \tag{3.41}$$

where:

$$\begin{aligned}
F_{\mathrm{VC1}} &= K_{\mathrm{VC1}}(x_1 - x_{\mathrm{O1}}) + B_{\mathrm{VC1}}(\dot{x}_1 - \dot{x}_{\mathrm{O1}}) && (3.42)\\
F_{\mathrm{VC2}} &= K_{\mathrm{VC1}}(x_2 - x_{\mathrm{O2}}) + B_{\mathrm{VC1}}(\dot{x}_2 - \dot{x}_{\mathrm{O2}}) && (3.43)\\
F_{\mathrm{VC12}} &= K_{\mathrm{VC12}}(x_{12} - x_{\mathrm{O2}}) + B_{\mathrm{VC12}}(\dot{x}_{12} - \dot{x}_{\mathrm{O2}}) && (3.44)\\
F_{\mathrm{VC21}} &= K_{\mathrm{VC21}}(x_{21} - x_{\mathrm{O1}}) + B_{\mathrm{VC21}}(\dot{x}_{21} - \dot{x}_{\mathrm{O1}}) && (3.45)\\
F_{\mathrm{T1}} &= K_{\mathrm{T}}(x_{\mathrm{O1}} - x_{\mathrm{O1}_d}) + B_{\mathrm{T}}(\dot{x}_{\mathrm{O1}} - \dot{x}_{\mathrm{O1}_d}) && (3.46)\\
F_{\mathrm{T2}} &= K_{\mathrm{T}}(x_{\mathrm{O2}} - x_{\mathrm{O2}_d}) + B_{\mathrm{T}}(\dot{x}_{\mathrm{O2}} - \dot{x}_{\mathrm{O2}_d}) && (3.47)\\
F_{\mathrm{RDP1}} &= K_{\mathrm{RDP}}(x_1 - x_{1_d}) + B_{\mathrm{RDP}}(\dot{x}_1 - \dot{x}_{1_d}) && (3.48)\\
F_{\mathrm{RDP2}} &= K_{\mathrm{RDP}}(x_2 - x_{2_d}) + B_{\mathrm{RDP}}(\dot{x}_2 - \dot{x}_{2_d}) && (3.49)\\
F_{\mathrm{RDP21}} &= K_{\mathrm{RDP}}(x_{21} - x_{21_d}) + B_{\mathrm{RDP}}(\dot{x}_{21} - \dot{x}_{21_d}) && (3.50)\\
F_{\mathrm{RDP12}} &= K_{\mathrm{RDP}}(x_{12} - x_{12_d}) + B_{\mathrm{RDP}}(\dot{x}_{12} - \dot{x}_{12_d}) && (3.51)
\end{aligned}$$

If the wave transformation has wave impedance b, then:

$$\dot{x}_{\mathrm{o1}_d} = \frac{u_{\mathrm{in}o_1}\sqrt{2b} + B_{\mathrm{T}}\dot{x}_{\mathrm{o1}} + K_{\mathrm{T}}(x_{\mathrm{o1}} - x_{\mathrm{o1}_d})}{b + B_{\mathrm{T}}} \tag{3.52}$$

$$\dot{x}_{\mathrm{o2}_d} = \frac{u_{\mathrm{in}o_2}\sqrt{2b} + B_{\mathrm{T}}\dot{x}_{\mathrm{o2}} + K_{\mathrm{T}}(x_{\mathrm{o2}} - x_{\mathrm{o2}_d})}{b + B_{\mathrm{T}}} \tag{3.53}$$

$$\dot{x}_{1_d} = \frac{u_{\mathrm{in}_1}\sqrt{2b} + B_{\mathrm{RDP}}\dot{x}_1 + K_{\mathrm{RDP}}(x_1 - x_{1_d})}{b + B_{\mathrm{RDP}}} \tag{3.54}$$

$$\dot{x}_{2_d} = \frac{u_{\mathrm{in}_2}\sqrt{2b} + B_{\mathrm{RDP}}\dot{x}_2 + K_{\mathrm{RDP}}(x_2 - x_{2_d})}{b + B_{\mathrm{RDP}}} \tag{3.55}$$

$$\dot{x}_{12_d} = \frac{u_{\mathrm{in}_{12}}\sqrt{2b} + B_{\mathrm{RDP}}\dot{x}_{12} + K_{\mathrm{RDP}}(x_{12} - x_{12_d})}{b + B_{\mathrm{RDP}}} \tag{3.56}$$

$$\dot{x}_{21_d} = \frac{u_{\mathrm{in}_{21}}\sqrt{2b} + B_{\mathrm{RDP}}\dot{x}_{21} + K_{\mathrm{RDP}}(x_{21} - x_{21_d})}{b + B_{\mathrm{RDP}}} \tag{3.57}$$

The wave outputs are computed as:

$$u_{\mathrm{out}_1} = u_{\mathrm{in}_1} + F_{\mathrm{RDP1}}\sqrt{\frac{2}{b}}, \quad u_{\mathrm{out}_2} = u_{\mathrm{in}_2} + F_{\mathrm{RDP2}}\sqrt{\frac{2}{b}} \tag{3.58}$$

$$u_{\mathrm{out}_{12}} = u_{\mathrm{in}_{12}} + F_{\mathrm{RDP12}}\sqrt{\frac{2}{b}}, \quad u_{\mathrm{out}_{21}} = u_{\mathrm{in}_{21}} + F_{\mathrm{RDP21}}\sqrt{\frac{2}{b}} \tag{3.59}$$

$$u_{\mathrm{out}O_1} = u_{\mathrm{in}O_1} + F_{\mathrm{T1}}\sqrt{\frac{2}{b}}, \quad u_{\mathrm{out}O_2} = u_{\mathrm{in}O_2} + F_{\mathrm{T2}}\sqrt{\frac{2}{b}} \tag{3.60}$$

Furthermore, if the communication channel has a delay T_d, the following relations hold between the input and the output wave signals:

$$u_{\mathrm{in}o_1} = u_{\mathrm{out}o_2}(t - T), \quad u_{\mathrm{in}o_2} = u_{\mathrm{out}o_1}(t - T) \tag{3.61}$$

$$u_{\mathrm{in}_{21}} = u_{\mathrm{out}_2}(t - T), \quad u_{\mathrm{in}_{12}} = u_{\mathrm{out}_1}(t - T) \tag{3.62}$$

$$u_{\mathrm{in}_1} = u_{\mathrm{out}_{12}}(t - T), \quad u_{\mathrm{in}_2} = u_{\mathrm{out}_{21}}(t - T) \tag{3.63}$$

For direct interaction between two networked users, the distributed control architecture with remote dynamic proxies and wave-based coordination is shown in Figure 3.8

In this case, the dynamics of the interaction are:

- for the peer haptic devices (device motion and virtual contact forces balanced

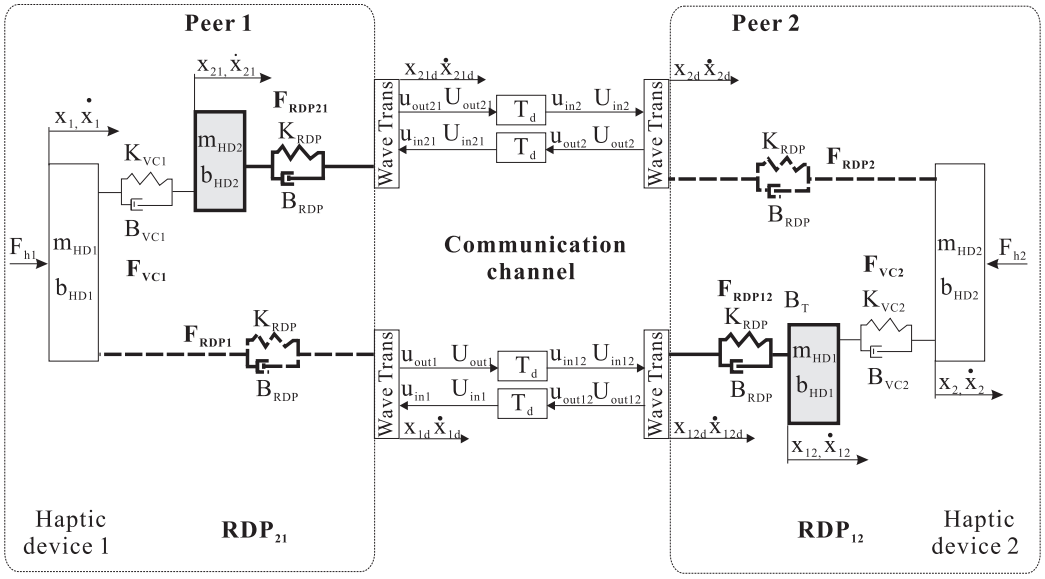

Figure 3.8: Distributed control architecture with remote dynamic proxies (RPD) and wave-based coordination of two users in direct interaction with each other. The remote dynamic proxies are shaded, and their connection to the corresponding haptic device is bolded.

by the user force $F_{\mathrm{h}i}$):

$$m_{\mathrm{HD1}}\ddot{x}_1 + b_{\mathrm{HD1}}\dot{x}_1 = F_{\mathrm{h1}} - F_{\mathrm{VC1}} \tag{3.64}$$

$$m_{\mathrm{HD2}}\ddot{x}_2 + b_{\mathrm{HD2}}\dot{x}_2 = F_{\mathrm{h2}} - F_{\mathrm{VC2}} \tag{3.65}$$

- for the remote dynamic proxies (remote dynamic proxy motion and virtual contact forces balanced by the force due to the remote user $F_{\mathrm{T}ij}$):

$$m_{\mathrm{HD1}}\ddot{x}_{12} + b_{\mathrm{HD1}}\dot{x}_{12} = F_{\mathrm{RDP12}} - F_{\mathrm{VC2}} \tag{3.66}$$

$$m_{\mathrm{HD2}}\ddot{x}_{21} + b_{\mathrm{HD2}}\dot{x}_{21} = F_{\mathrm{RDP21}} - F_{\mathrm{VC1}} \tag{3.67}$$

where:

$$F_{\text{VC1}} = K_{\text{VC1}}(x_1 - x_{21}) + B_{\text{VC1}}(\dot{x}_1 - \dot{x}_{21}) \quad (3.68)$$

$$F_{\text{VC2}} = K_{\text{VC1}}(x_2 - x_{12}) + B_{\text{VC1}}(\dot{x}_2 - \dot{x}_{12}) \quad (3.69)$$

$$F_{\text{RDP1}} = K_{\text{RDP}}(x_1 - x_{1_d}) + B_{\text{RDP}}(\dot{x}_1 - \dot{x}_{1_d}) \quad (3.70)$$

$$F_{\text{RDP2}} = K_{\text{RDP}}(x_2 - x_{2_d}) + B_{\text{RDP}}(\dot{x}_2 - \dot{x}_{2_d}) \quad (3.71)$$

$$F_{\text{RDP21}} = K_{\text{RDP}}(x_{21} - x_{21_d}) + B_{\text{RDP}}(\dot{x}_{21} - \dot{x}_{21_d}) \quad (3.72)$$

$$F_{\text{RDP12}} = K_{\text{RDP}}(x_{12} - x_{12_d}) + B_{\text{RDP}}(\dot{x}_{12} - \dot{x}_{12_d}) \quad (3.73)$$

Given the wave transformation has wave impedance b, then:

$$\dot{x}_{1_d} = \frac{u_{\text{in}_1}\sqrt{2b} + B_{\text{RDP}}\dot{x}_1 + K_{\text{RDP}}(x_1 - x_{1_d})}{b + B_{\text{RDP}}} \quad (3.74)$$

$$\dot{x}_{2_d} = \frac{u_{\text{in}_2}\sqrt{2b} + B_{\text{RDP}}\dot{x}_2 + K_{\text{RDP}}(x_2 - x_{2_d})}{b + B_{\text{RDP}}} \quad (3.75)$$

$$\dot{x}_{12_d} = \frac{u_{\text{in}_{12}}\sqrt{2b} + B_{\text{RDP}}\dot{x}_{12} + K_{\text{RDP}}(x_{12} - x_{12_d})}{b + B_{\text{RDP}}} \quad (3.76)$$

$$\dot{x}_{21_d} = \frac{u_{\text{in}_{21}}\sqrt{2b} + B_{\text{RDP}}\dot{x}_{21} + K_{\text{RDP}}(x_{21} - x_{21_d})}{b + B_{\text{RDP}}} \quad (3.77)$$

The wave outputs are computed as:

$$u_{\text{out}_1} = u_{\text{in}_1} + F_{\text{RDP1}}\sqrt{\frac{2}{b}}, \quad u_{\text{out}_2} = u_{\text{in}_2} + F_{\text{RDP2}}\sqrt{\frac{2}{b}} \quad (3.78)$$

$$u_{\text{out}_{12}} = u_{\text{in}_{12}} + F_{\text{RDP12}}\sqrt{\frac{2}{b}}, \quad u_{\text{out}_{21}} = u_{\text{in}_{21}} + F_{\text{RDP21}}\sqrt{\frac{2}{b}} \quad (3.79)$$

Furthermore, if the communication channel has a delay T_d, the following relations hold between the input and the output wave signals:

$$u_{\text{in}_{21}} = u_{\text{out}_2}(t - T), \quad u_{\text{in}_{12}} = u_{\text{out}_1}(t - T) \quad (3.80)$$

$$u_{\text{in}_1} = u_{\text{out}_{12}}(t - T), \quad u_{\text{in}_2} = u_{\text{out}_{21}}(t - T) \quad (3.81)$$

3.4 Summary

Motivated by the need to support direct interaction between distant users, this chapter has proposed to distribute the users across the network via avatars with second

order dynamics called remote dynamic proxies. It has also integrated the remote dynamic proxies into two distributed control architectures that coordinate the networked sites via virtual coupling and via wave-based control, respectively. The continuous time dynamics of networked haptic cooperation between two uses rendered through the two architectures have been derived both for cooperative manipulation of a shared virtual object and for direct user-to-user interaction. These dynamics provide the starting point of the stability analysis of networked haptic cooperation with remote dynamic proxies and virtual coupling coordination in Chapter 4. Furthermore, they are implemented in the setup employed in the experimental validation of the two distributed architectures with remote dynamic proxies in Chapter 5.

Chapter 4

Stability of Networked Haptic Cooperation with Remote Dynamic Proxies and Distributed Virtual Coupling Coordination

This chapter investigates the stability of networked haptic cooperation between two users when rendered via remote dynamic proxies and virtual coupling coordination. The users can interact across an Ethernet-based Local Area Network (LAN) or a high-speed Metropolitan Area Network (MAN). In this context, the network delay can be assumed to be jitter-less and of the order of one to three transmission sample times, and the packet loss can be assumed negligible [2]. Although restrictive, these assumptions are valid in many applications because LAN- and MAN-based networks can cover several buildings and even large cities and thus, make tele-rehabilitation and multi-user on-line computer games feasible for users within the same city.

The key challenge involved in haptic cooperation over a LAN or a high-speed MAN is the low network update rate typical to communications implemented via network protocols like UDP and TCP/IP. This rate is generally equal to 128 Hz [2], and is well below the 1 KHz force feedback rate required for high fidelity haptic rendering. Therefore, the network update rate can severely limit the realism of the cooperation. However, by adopting the multi-rate control strategy introduced in [59] and applied to haptic cooperation in [2], the force control loops at each cooperating user can be executed at a much higher rate than that of data transmission over the network.

Within the multi-rate framework proposed in [59], this chapter develops the mathematical model for the distributed control of haptic cooperation with remote dynamic proxies and virtual coupling coordination, over a LAN or high-speed MAN. It then investigates the stability of cooperation between two users connected via this controller, for cooperative manipulation of a shared virtual object and for direct user-to-user contact. Network delays up to three transmission sample times are considered in the analysis. Compared to the distributed controllers with virtual coupling coordination in [2] and [1], the architecture with remote dynamic proxies maintains similar stiffness for the local contact and for the coordinating virtual coupler, and achieves much higher stiffness for the remote contact[1] during cooperative manipulation of a shared virtual object. In turn, the high stiffness of the remote contact improves the position coherency for the shared virtual object. For direct user-to-user interaction, the proposed architecture renders higher contact stiffness in the presence of larger network delay.

4.1 Continuous State-Space Representation

The stability analysis of haptic cooperation between two users connected via a LAN or high-speed MAN is developed in this chapter as follows:

- the continuous-time state-space representation of the open loop haptic cooperation system is derived in this section, both for cooperative manipulation of a shared virtual object (Section 4.1.1) and for direct user-to-user interaction (Section 4.1.2);
- the discrete-time state-space representation of the open loop system is developed, and the communication delay is incorporated into it as proposed in [2] in Section 4.2;
- the state matrix of the open-loop multi-rate system is employed to investigate the stability of the closed-loop system for various controller gains and communication delays in Section 4.3.

Notation is used hereafter as follows: p is the number of sampling times in the open-loop haptic cooperation system; indices c and n identify signals sampled at the

[1]The local contact is the contact between the local user and the shared virtual object, while the remote contact is the contact between the remote dynamic proxy and the shared virtual object.

(fast) force control rate and at the (slow) network update rate; indices 1 and 2 indicate values related to the Peer 1 and Peer 2 site, respectively; n_x, n_y, n_u are the number of states, of outputs, and of inputs, respectively, of the continuous-time open-loop system. Furthermore: n_{cy}, n_{ny} are the number of fast and of slow system outputs; n_{1cy}, n_{1ny} are the number of fast and of slow outputs at Peer 1; n_{2cy}, n_{2ny} are the number of fast and of slow outputs at Peer 2; n_{cu}, n_{nu} are the number of fast and of slow system inputs; n_{1cu}, n_{1nu} are the number of fast and of slow inputs at Peer 1; and n_{2cu}, n_{2nu} are the number of fast and of slow inputs at Peer 2, respectively.

In the subsequent derivations, it is assumed that the force sampling times at the two peer users are equal. Hence, the haptic cooperation system is a system with two rates, the network update rate and the force control rate, i.e., $p = 2$. It is also assumed that the force and the network sampling times (T_c and T_n, respectively) are synchronized and can be written as integer multiples of a base sample time τ_0, i.e., $T_i = l_i\tau_0$ with $i \in \left\{c, n\right\}$. It then follows that a sampling time T_0 exists such that $\tau_0 = \frac{T_0}{N_0}$, $l_i = \frac{N_i}{N_0}$ for $i \in \left\{c, n\right\}$, and N_0 the least common multiple of N_i. In this dissertation in particular, the force control rate is taken to be equal to the typical haptic feedback rate of 1024Hz and the network update rate is taken to be equal to 128Hz, which is the rate of the network card in the experimental setup and is also the rate in [2]. Therefore, $\tau_0 = \frac{1}{1024}$sec, $T_0 = \frac{1}{128}$sec, $N_0 = 8$, $N_c = 8$, $N_n = 1$, $l_c = 1$, and $l_n = 8$.

The continuous state space representation of the open-loop (i.e., without the virtual coupling controller) haptic cooperation system with remote dynamic proxies is derived in this section in the general form:

$$\begin{cases} \dot{\mathbf{x}} = \mathbf{A}\,\mathbf{x} + \mathbf{B}\,\mathbf{u} \\ \mathbf{y} = \mathbf{C}\,\mathbf{x} \end{cases} \tag{4.1}$$

where $x(t) \in R^{n_x}$ is the vector of system states; $u(t) = (u_c(t) \quad u_n(t))^T \in R^{n_u}$ is the vector of (fast and slow) system inputs; $y(t) = (y_c(t) \quad y_n(t))^T \in R^{n_y}$ is the vector of (fast and slow) system outputs; and $\mathbf{A}$ is the system matrix. The specific dimensions of these vectors depend on whether Equation (4.1) models cooperative manipulation of a shared virtual object or direct user-to-user contact, and are given in the next two sections.

4.1.1 Cooperative Manipulation

Figure 4.1 schematically depicts the cooperative manipulation of a shared virtual object via the distributed architecture with remote dynamic proxies and virtual coupling coordination proposed in Section 3.2 again. The closed loop form of this architecture is shown in Figure 4.2.

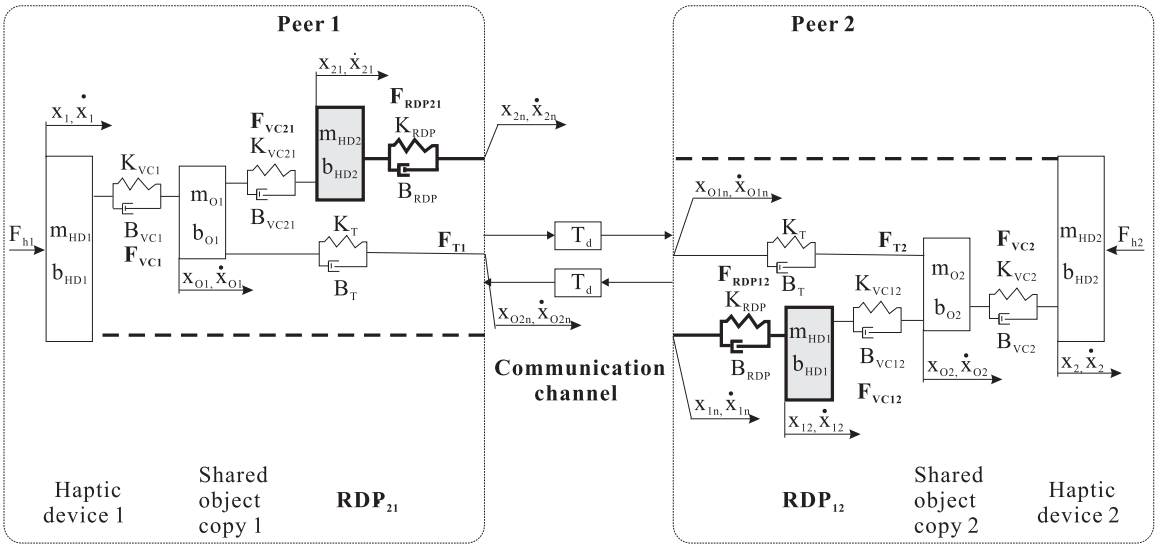

Figure 4.1: The distributed control architecture with remote dynamic proxies (RPDs) and virtual coupling coordination of two users involved in cooperative manipulation of a shared virtual object introduced in Figure 3.3. The remote dynamic proxies are shaded, and their connection to the corresponding haptic device is bolded.

The open-loop continuous-time model of the system comprises the dynamics of the haptic devices and of the peers' copies of the virtual environment which, in turn, include the local copies of the shared virtual object and the remote dynamic proxies. For cooperative manipulation, these dynamics have been derived in Equations (3.1) to (3.10). Equations (3.11) to (3.14) comprise the feedback of the system. According to these equations, the system inputs can be computed from:

- position and velocity outputs sampled at the (fast) force feedback control rate T_c: x_1, $\dot{x}_1$, x_2, $\dot{x}_2$, x_{O1}, $\dot{x}_{\mathrm{O1}}$, x_{O2}, $\dot{x}_{\mathrm{O2}}$, x_{21}, $\dot{x}_{21}$, x_{12}, $\dot{x}_{12}$;
- position and velocity outputs sampled at the (slow) network update rate T_n: x_{O1_n}, $\dot{x}_{\mathrm{O1}_n}$, x_{O2_n}, $\dot{x}_{\mathrm{O2}_n}$, x_{1_n}, $\dot{x}_{1_n}$, x_{2_n}, $\dot{x}_{2_n}$.

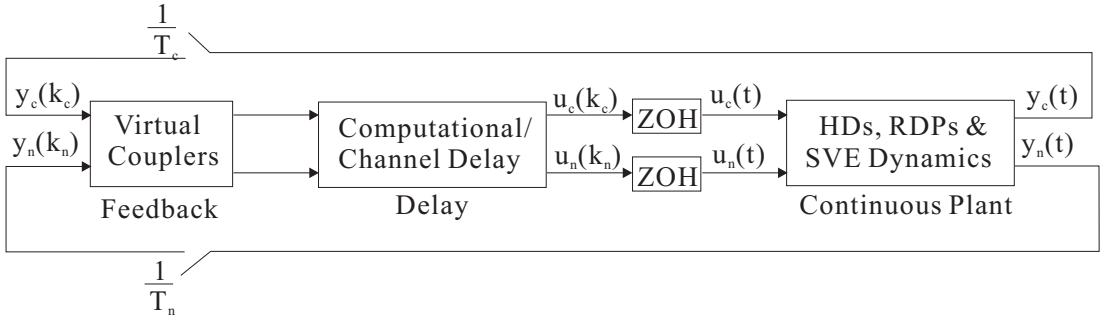

Figure 4.2: The distributed virtual coupling-based control system, including the haptic devices (HD), the remote dynamic proxies (RDP), and the shared virtual environment (SVE).

To derive the open-loop state space representation of the haptic cooperative manipulation in the form of Equation (4.1), the continuous state space dynamics of the two haptic devices (HD), of the two copies of the shared virtual object (SVO), and of the two remote dynamic proxies (RDP) can be written as:

$$\begin{pmatrix} \dot{x}_{\mathrm{HD1}} \\ \ddot{x}_{\mathrm{HD1}} \end{pmatrix} = \begin{bmatrix} 0 & 1 \\ 0 & -b_{\mathrm{HD1}}/m_{\mathrm{HD1}} \end{bmatrix} \begin{pmatrix} x_{\mathrm{HD1}} \\ \dot{x}_{\mathrm{HD1}} \end{pmatrix} + \begin{bmatrix} 0 \\ -1/m_{\mathrm{HD1}} \end{bmatrix} \begin{pmatrix} F_{\mathrm{VC1}} \end{pmatrix} \tag{4.2}$$

$$\begin{pmatrix} \dot{x}_{\mathrm{HD2}} \\ \ddot{x}_{\mathrm{HD2}} \end{pmatrix} = \begin{bmatrix} 0 & 1 \\ 0 & -b_{\mathrm{HD2}}/m_{\mathrm{HD2}} \end{bmatrix} \begin{pmatrix} x_{\mathrm{HD2}} \\ \dot{x}_{\mathrm{HD2}} \end{pmatrix} + \begin{bmatrix} 0 \\ -1/m_{\mathrm{HD2}} \end{bmatrix} \begin{pmatrix} F_{\mathrm{VC2}} \end{pmatrix} \tag{4.3}$$

$$\begin{pmatrix} \dot{x}_{\mathrm{O1}} \\ \ddot{x}_{\mathrm{O1}} \end{pmatrix} = \begin{bmatrix} 0 & 1 \\ 0 & -b_{\mathrm{O1}}/m_{\mathrm{O1}} \end{bmatrix} \begin{pmatrix} x_{\mathrm{O1}} \\ \dot{x}_{\mathrm{O1}} \end{pmatrix} + \begin{bmatrix} 0 & 0 & 0 & 0 \\ 1/m_{\mathrm{O1}} & 1/m_{\mathrm{O1}} & 1/m_{\mathrm{O1}} & 1/m_{\mathrm{O1}} \end{bmatrix} \begin{pmatrix} F_{\mathrm{VC1}} \\ F_{\mathrm{VC21}} \\ F_{\mathrm{T1}_c} \\ F_{\mathrm{T1}_n} \end{pmatrix} \tag{4.4}$$

$$\begin{pmatrix} \dot{x}_{\mathrm{O2}} \\ \ddot{x}_{\mathrm{O2}} \end{pmatrix} = \begin{bmatrix} 0 & 1 \\ 0 & -b_{\mathrm{O2}}/m_{\mathrm{O2}} \end{bmatrix} \begin{pmatrix} x_{\mathrm{O2}} \\ \dot{x}_{\mathrm{O2}} \end{pmatrix} + \begin{bmatrix} 0 & 0 & 0 & 0 \\ 1/m_{\mathrm{O2}} & 1/m_{\mathrm{O2}} & 1/m_{\mathrm{O2}} & 1/m_{\mathrm{O2}} \end{bmatrix} \begin{pmatrix} F_{\mathrm{VC2}} \\ F_{\mathrm{VC12}} \\ F_{\mathrm{T2}_c} \\ F_{\mathrm{T2}_n} \end{pmatrix} \tag{4.5}$$

$$\begin{pmatrix} \dot{x}_{21} \\ \ddot{x}_{21} \end{pmatrix} = \begin{bmatrix} 0 & 1 \\ 0 & -b_{\mathrm{HD2}}/m_{\mathrm{HD2}} \end{bmatrix} \begin{pmatrix} x_{21} \\ \dot{x}_{21} \end{pmatrix} + \begin{bmatrix} 0 & 0 & 0 \\ -1/m_{\mathrm{HD2}} & 1/m_{\mathrm{HD2}} & 1/m_{\mathrm{HD2}} \end{bmatrix} \begin{pmatrix} F_{\mathrm{VC21}} \\ F_{\mathrm{RDP21}_c} \\ F_{\mathrm{RDP21}_n} \end{pmatrix} \tag{4.6}$$

$$\begin{pmatrix} \dot{x}_{12} \\ \ddot{x}_{12} \end{pmatrix} = \begin{bmatrix} 0 & 1 \\ 0 & -b_{\mathrm{HD1}}/m_{\mathrm{HD1}} \end{bmatrix} \begin{pmatrix} x_{12} \\ \dot{x}_{12} \end{pmatrix} + \begin{bmatrix} 0 & 0 & \\ -1/m_{\mathrm{HD1}} & 1/m_{\mathrm{HD1}} & 1/m_{\mathrm{HD1}} \end{bmatrix} \begin{pmatrix} F_{\mathrm{VC12}} \\ F_{\mathrm{RDP12}_c} \\ F_{\mathrm{RDP12}_n} \end{pmatrix} \tag{4.7}$$

Equations (4.2) to (4.7) can be grouped based on the peer site. In particular, at the Peer 1 site:

$$\begin{aligned} \dot{\mathbf{x}}_{1_{6\times1}} &= \begin{pmatrix} \dot{x}_1 \\ \ddot{x}_1 \\ \dot{x}_{\mathrm{O1}} \\ \ddot{x}_{\mathrm{O1}} \\ \dot{x}_{21} \\ \ddot{x}_{21} \end{pmatrix} = \begin{bmatrix} 0 & 1 & 0 & 0 & 0 & 0 \\ 0 & -b_{\mathrm{HD1}}/m_{\mathrm{HD1}} & 0 & 0 & 0 & 0 \\ 0 & 0 & 0 & 1 & 0 & 0 \\ 0 & 0 & 0 & -b_{\mathrm{O1}}/m_{\mathrm{O1}} & 0 & 0 \\ 0 & 0 & 0 & 0 & 0 & 1 \\ 0 & 0 & 0 & 0 & 0 & -b_{\mathrm{HD2}}/m_{\mathrm{HD2}} \end{bmatrix} \begin{pmatrix} x_1 \\ \dot{x}_1 \\ x_{\mathrm{O1}} \\ \dot{x}_{\mathrm{O1}} \\ x_{21} \\ \dot{x}_{21} \end{pmatrix} \\ &+ \begin{bmatrix} 0 & 0 & 0 & 0 & 0 & 0 \\ -1/m_{\mathrm{HD1}} & 0 & 0 & 0 & 0 & 0 \\ 0 & 0 & 0 & 0 & 0 & 0 \\ 1/m_{\mathrm{O1}} & 1/m_{\mathrm{O1}} & 1/m_{\mathrm{O1}} & 0 & 1/m_{\mathrm{O1}} & 0 \\ 0 & 0 & 0 & 0 & 0 & 0 \\ 0 & -1/m_{\mathrm{HD2}} & 0 & 1/m_{\mathrm{HD2}} & 0 & 1/m_{\mathrm{HD2}} \end{bmatrix} \begin{pmatrix} F_{\mathrm{VC1}} \\ F_{\mathrm{VC21}} \\ F_{\mathrm{T1}_c} \\ F_{\mathrm{RDP21}_c} \\ F_{\mathrm{T1}_n} \\ F_{\mathrm{RDP21}_n} \end{pmatrix} \\ &= \mathbf{A}_{1_{6\times6}} \mathbf{x}_{1_{6\times1}} + \begin{bmatrix} \mathbf{B}_{1_{c_{6\times4}}} & \mathbf{B}_{1_{n_{6\times2}}} \end{bmatrix}_{6\times6} \begin{pmatrix} \mathbf{u}_{1_{c_{4\times1}}} \\ \mathbf{u}_{1_{n_{2\times1}}} \end{pmatrix}_{6\times1} \end{aligned} \tag{4.8}$$

where:

$$\mathbf{B}_{1_{c_{6\times4}}} = \begin{bmatrix} 0 & 0 & 0 & 0 \\ -1/m_{\mathrm{HD1}} & 0 & 0 & 0 \\ 0 & 0 & 0 & 0 \\ 1/m_{\mathrm{O1}} & 1/m_{\mathrm{O1}} & 1/m_{\mathrm{O1}} & 0 \\ 0 & 0 & 0 & 0 \\ 0 & -1/m_{\mathrm{HD2}} & 0 & 1/m_{\mathrm{HD2}} \end{bmatrix} \tag{4.9}$$

$$\mathbf{B}_{1_{n_{6\times 2}}} = \begin{bmatrix} 0 & 0 \\ 0 & 0 \\ 0 & 0 \\ 1/m_{\mathrm{O1}} & 0 \\ 0 & 0 \\ 0 & 1/m_{\mathrm{HD2}} \end{bmatrix} \tag{4.10}$$

and:

$$\begin{aligned} \begin{pmatrix} \mathbf{u}_{1_{c_{4\times 1}}} \\ \mathbf{u}_{1_{n_{2\times 1}}} \end{pmatrix}_{6\times 1} &= \begin{pmatrix} F_{\mathrm{VC1}} & F_{\mathrm{VC21}} & F_{\mathrm{T1}_c} & F_{\mathrm{RDP21}_c} & F_{\mathrm{T1}_n} & F_{\mathrm{RDP21}_n} \end{pmatrix}^T \\ &= \begin{bmatrix} \mathbf{F}_{1_{c_{4\times 6}}} & \mathbf{0}_{4\times 4} \\ \mathbf{0}_{2\times 6} & \mathbf{F}_{1_{n_{2\times 4}}} \end{bmatrix}_{6\times 10} \begin{pmatrix} \mathbf{y}_{1_{c_{6\times 1}}} \\ \mathbf{y}_{1_{n_{4\times 1}}} \end{pmatrix}_{10\times 1} \end{aligned} \tag{4.11}$$

with:

$$\mathbf{F}_{1_{c_{4\times 6}}} = \begin{bmatrix} K_{\mathrm{VC1}} & B_{\mathrm{VC1}} & -K_{\mathrm{VC1}} & -B_{\mathrm{VC1}} & 0 & 0 \\ 0 & 0 & -K_{\mathrm{VC21}} & -B_{\mathrm{VC21}} & K_{\mathrm{VC21}} & B_{\mathrm{VC21}} \\ 0 & 0 & -K_{\mathrm{T}} & -B_{\mathrm{T}} & 0 & 0 \\ 0 & 0 & 0 & 0 & -K_{\mathrm{RDP}} & -B_{\mathrm{RDP}} \end{bmatrix} \tag{4.12}$$

$$\mathbf{F}_{1_{n_{2\times 4}}} = \begin{bmatrix} K_{\mathrm{RDP}} & B_{\mathrm{RDP}} & 0 & 0 \\ 0 & 0 & K_{\mathrm{T}} & B_{\mathrm{T}} \end{bmatrix} \tag{4.13}$$

Similarly, at the Peer 2 site:

$$\mathbf{x}_{2_{6\times1}} = \begin{pmatrix} \dot{x}_2 \\ \ddot{x}_2 \\ \dot{x}_{O2} \\ \ddot{x}_{O2} \\ \dot{x}_{12} \\ \ddot{x}_{12} \end{pmatrix} = \begin{bmatrix} 0 & 1 & 0 & 0 & 0 & 0 \\ 0 & -b_{HD2}/m_{HD2} & 0 & 0 & 0 & 0 \\ 0 & 0 & 0 & 1 & 0 & 0 \\ 0 & 0 & 0 & -b_{O2}/m_{O2} & 0 & 0 \\ 0 & 0 & 0 & 0 & 0 & 1 \\ 0 & 0 & 0 & 0 & 0 & -b_{HD1}/m_{HD1} \end{bmatrix} \begin{pmatrix} x_2 \\ \dot{x}_2 \\ x_{O2} \\ \dot{x}_{O2} \\ x_{12} \\ \dot{x}_{12} \end{pmatrix} +$$

$$+ \begin{bmatrix} 0 & 0 & 0 & 0 & 0 & 0 \\ -1/m_{HD2} & 0 & 0 & 0 & 0 & 0 \\ 0 & 0 & 0 & 0 & 0 & 0 \\ 1/m_{O2} & 1/m_{O2} & 1/m_{O2} & 0 & 1/m_{O2} & 0 \\ 0 & 0 & 0 & 0 & 0 & 0 \\ 0 & -1/m_{HD1} & 0 & 1/m_{HD1} & 0 & 1/m_{HD1} \end{bmatrix} \begin{pmatrix} F_{VC2} \\ F_{VC12} \\ F_{T2_c} \\ F_{RDP12_c} \\ F_{T2_n} \\ F_{RDP12_n} \end{pmatrix}$$

$$= \mathbf{A}_{2_{6\times6}}\mathbf{x}_{2_{6\times1}} + \begin{bmatrix} \mathbf{B}_{2_{c_{6\times4}}} & \mathbf{B}_{2_{n_{6\times2}}} \end{bmatrix}_{6\times6} \begin{pmatrix} \mathbf{u}_{2_{c_{4\times1}}} \\ \mathbf{u}_{2_{n_{2\times1}}} \end{pmatrix}_{6\times1} \tag{4.14}$$

where:

$$\mathbf{B}_{2_{c_{6\times4}}} = \begin{bmatrix} 0 & 0 & 0 & 0 \\ -1/m_{HD2} & 0 & 0 & 0 \\ 0 & 0 & 0 & 0 \\ 1/m_{O2} & 1/m_{O2} & 1/m_{O2} & 0 \\ 0 & 0 & 0 & 0 \\ 0 & -1/m_{HD1} & 0 & 1/m_{HD1} \end{bmatrix} \tag{4.15}$$

$$\mathbf{B}_{2_{n_{6\times2}}} = \begin{bmatrix} 0 & 0 \\ 0 & 0 \\ 0 & 0 \\ 1/m_{O2} & 0 \\ 0 & 0 \\ 0 & 1/m_{HD1} \end{bmatrix} \tag{4.16}$$

and:

$$\begin{aligned}\begin{pmatrix}\mathbf{u}_{2_{c_{4\times1}}}\\ \mathbf{u}_{2_{n_{2\times1}}}\end{pmatrix}_{6\times1} &= \begin{pmatrix}F_{\mathrm{VC2}} & F_{\mathrm{VC12}} & F_{\mathrm{T2}_c} & F_{\mathrm{RDP12}_c} & F_{\mathrm{T2}_n} & F_{\mathrm{RDP12}_n}\end{pmatrix}^T \\ &= \begin{bmatrix}\mathbf{F}_{2_{c_{4\times6}}} & \mathbf{0}_{4\times4}\\ \mathbf{0}_{2\times6} & \mathbf{F}_{2_{n_{2\times4}}}\end{bmatrix}_{6\times10}\begin{pmatrix}\mathbf{y}_{2_{c_{6\times1}}}\\ \mathbf{y}_{2_{n_{4\times1}}}\end{pmatrix}_{10\times1} \end{aligned} \tag{4.17}$$

with:

$$\begin{aligned}\mathbf{F}_{2_{c_{4\times6}}} &= \begin{bmatrix}K_{\mathrm{VC1}} & B_{\mathrm{VC1}} & -K_{\mathrm{VC1}} & -B_{\mathrm{VC1}} & 0 & 0\\ 0 & 0 & -K_{\mathrm{VC21}} & -B_{\mathrm{VC21}} & K_{\mathrm{VC21}} & B_{\mathrm{VC21}}\\ 0 & 0 & -K_{\mathrm{T}} & -B_{\mathrm{T}} & 0 & 0\\ 0 & 0 & 0 & 0 & -K_{\mathrm{RDP}} & -B_{\mathrm{RDP}}\end{bmatrix} \\ &= \mathbf{F}_{1_{c_{4\times6}}} = \mathbf{F}_{\mathrm{p}_{c_{4\times6}}} \end{aligned} \tag{4.18}$$

$$\mathbf{F}_{2_{n_{2\times4}}} = \begin{bmatrix}K_{\mathrm{RDP}} & B_{\mathrm{RDP}} & 0 & 0\\ 0 & 0 & K_{\mathrm{T}} & B_{\mathrm{T}}\end{bmatrix} = \mathbf{F}_{1_{n_{2\times4}}} = \mathbf{F}_{\mathrm{p}_{n_{2\times4}}} \tag{4.19}$$

The continuous-time state-space dynamics of the entire open-loop haptic cooperation system are obtained after combining Equations (4.8) and (4.14). Specifically,

the state equation is:

$$
\begin{aligned}
\dot{\mathbf{x}}_{n_x\times 1} &= \mathbf{A}_{n_x\times n_x}\mathbf{x}_{n_x\times 1} + \mathbf{B}_{n_x\times n_u}\mathbf{u}_{n_u\times 1} \\
&= \mathbf{A}_{n_x\times n_x}\mathbf{x}_{n_x\times 1} + \begin{bmatrix}\mathbf{B}_{c_{n_x\times n_{1cu}}} & \mathbf{B}_{c_{n_x\times n_{2cu}}} & \mathbf{B}_{n_{n_x\times n_{1nu}}} & \mathbf{B}_{n_{n_x\times n_{2nu}}}\end{bmatrix}\begin{pmatrix}\mathbf{u}_{1_{c_{n_{1cu}\times 1}}} \\ \mathbf{u}_{2_{c_{n_{2cu}\times 1}}} \\ \mathbf{u}_{1_{n_{n_{1nu}\times 1}}} \\ \mathbf{u}_{2_{n_{n_{2nu}\times 1}}}\end{pmatrix} \\
\Longleftrightarrow & \\
\dot{\mathbf{x}}_{12\times 1} &= \mathbf{A}_{12\times 12}\mathbf{x}_{12\times 1} + \mathbf{B}_{12\times 12}\mathbf{u}_{12\times 1} \\
&= \mathbf{A}_{12\times 12}\mathbf{x}_{12\times 1} + \begin{bmatrix}\mathbf{B}_{c_{12\times 4}} & \mathbf{B}_{c_{12\times 4}} & \mathbf{B}_{n_{12\times 2}} & \mathbf{B}_{n_{12\times 2}}\end{bmatrix}_{12\times 12}\begin{pmatrix}\mathbf{u}_{1_{c_{4\times 1}}} \\ \mathbf{u}_{2_{c_{4\times 1}}} \\ \mathbf{u}_{1_{n_{2\times 1}}} \\ \mathbf{u}_{2_{n_{2\times 1}}}\end{pmatrix} \\
\Longleftrightarrow & \\
\begin{pmatrix}\dot{\mathbf{x}}_{1_{6\times 1}} \\ \dot{\mathbf{x}}_{2_{6\times 1}}\end{pmatrix} &= \begin{bmatrix}\mathbf{A}_{1_{6\times 6}} & \mathbf{0}_{6\times 6} \\ \mathbf{0}_{6\times 6} & \mathbf{A}_{2_{6\times 6}}\end{bmatrix}\begin{pmatrix}\mathbf{x}_{1_{6\times 1}} \\ \mathbf{x}_{2_{6\times 1}}\end{pmatrix} + \begin{bmatrix}\mathbf{B}_{1_{c_{6\times 4}}} & \mathbf{0}_{6\times 4} & \mathbf{B}_{2_{n_{6\times 2}}} & \mathbf{0}_{6\times 2} \\ \mathbf{0}_{6\times 4} & \mathbf{B}_{1_{c_{6\times 4}}} & \mathbf{0}_{6\times 2} & \mathbf{B}_{2_{n_{6\times 2}}}\end{bmatrix}\begin{pmatrix}\mathbf{u}_{1_{c_{4\times 1}}} \\ \mathbf{u}_{2_{c_{4\times 1}}} \\ \mathbf{u}_{1_{n_{2\times 1}}} \\ \mathbf{u}_{2_{n_{2\times 1}}}\end{pmatrix} \\
\Longleftrightarrow & \\
\begin{pmatrix}\dot{x}_1 \\ \ddot{x}_1 \\ \dot{x}_{\mathrm{O1}} \\ \ddot{x}_{\mathrm{O1}} \\ \dot{x}_{21} \\ \ddot{x}_{21} \\ \dot{x}_2 \\ \ddot{x}_2 \\ \dot{x}_{\mathrm{O2}} \\ \ddot{x}_{\mathrm{O2}} \\ \dot{x}_{12} \\ \ddot{x}_{12}\end{pmatrix} &= \begin{bmatrix}\mathbf{A}_{1_{6\times 6}} & \mathbf{0}_{6\times 6} \\ \mathbf{0}_{6\times 6} & \mathbf{A}_{2_{6\times 6}}\end{bmatrix}\begin{pmatrix}x_1 \\ \dot{x}_1 \\ x_{\mathrm{O1}} \\ \dot{x}_{\mathrm{O1}} \\ x_{21} \\ \dot{x}_{21} \\ x_2 \\ \dot{x}_2 \\ x_{\mathrm{O2}} \\ \dot{x}_{\mathrm{O2}} \\ x_{12} \\ \dot{x}_{12}\end{pmatrix} + \begin{bmatrix}\mathbf{B}_{1_{c_{6\times 4}}} & \mathbf{0}_{6\times 4} & \mathbf{B}_{1_{n_{6\times 2}}} & \mathbf{0}_{6\times 2} \\ \mathbf{0}_{6\times 4} & \mathbf{B}_{2_{c_{6\times 4}}} & \mathbf{0}_{6\times 2} & \mathbf{B}_{2_{n_{6\times 2}}}\end{bmatrix}\begin{pmatrix}F_{\mathrm{VC1}} \\ F_{\mathrm{VC21}} \\ F_{\mathrm{T1}_c} \\ F_{\mathrm{RDP21}_c} \\ F_{\mathrm{VC2}} \\ F_{\mathrm{VC12}} \\ F_{\mathrm{T2}_c} \\ F_{\mathrm{RDP12}_c} \\ F_{\mathrm{T1}_n} \\ F_{\mathrm{RDP21}_n} \\ F_{\mathrm{T2}_n} \\ F_{\mathrm{RDP12}_n}\end{pmatrix}
\end{aligned}
\tag{4.20}
$$

where:

$$\mathbf{u}_{1_{c_{n_{1cu}\times 1}}} = \mathbf{u}_{1_{c_{4\times 1}}} = \begin{pmatrix} F_{\mathrm{VC1}} & F_{\mathrm{VC21}} & F_{\mathrm{T1}_c} & F_{\mathrm{RDP21}_c} \end{pmatrix}^T \tag{4.21}$$

$$\mathbf{u}_{2_{c_{n_{2cu}\times 1}}} = \mathbf{u}_{2_{c_{4\times 1}}} = \begin{pmatrix} F_{\mathrm{VC2}} & F_{\mathrm{VC12}} & F_{\mathrm{T2}_c} & F_{\mathrm{RDP12}_c} \end{pmatrix}^T \tag{4.22}$$

$$\mathbf{u}_{1_{n_{n_{1nu}\times 1}}} = \mathbf{u}_{1_{n_{2\times 1}}} = \begin{pmatrix} F_{\mathrm{T1}_n} & F_{\mathrm{RDP21}_n} \end{pmatrix}^T \tag{4.23}$$

$$\mathbf{u}_{2_{n_{n_{2nu}\times 1}}} = \mathbf{u}_{2_{n_{2\times 1}}} = \begin{pmatrix} F_{\mathrm{T2}_n} & F_{\mathrm{RDP12}_n} \end{pmatrix}^T \tag{4.24}$$

The output equation is:

$$\begin{aligned} \mathbf{y}_{n_y\times 1} &= \begin{pmatrix} \mathbf{y}_{1_{c_{n_{1cy}\times 1}}} \\ \mathbf{y}_{2_{c_{n_{2cy}\times 1}}} \\ \mathbf{y}_{1_{n_{n_{1ny}\times 1}}} \\ \mathbf{y}_{2_{n_{n_{2ny}\times 1}}} \end{pmatrix} = \mathbf{C}_{n_y\times n_x}\mathbf{x}_{n_x\times 1} = \begin{bmatrix} \mathbf{C}_{1_{c_{n_{1cy}\times n_x}}} \\ \mathbf{C}_{2_{c_{n_{2cy}\times n_x}}} \\ \mathbf{C}_{1_{n_{n_{1ny}\times n_x}}} \\ \mathbf{C}_{2_{n_{n_{2ny}\times n_x}}} \end{bmatrix} \mathbf{x}_{n_x\times 1} \\ &\Longleftrightarrow \\ \mathbf{y}_{20\times 1} &= \begin{pmatrix} \mathbf{y}_{1_{c_{6\times 1}}} \\ \mathbf{y}_{2_{c_{6\times 1}}} \\ \mathbf{y}_{1_{n_{4\times 1}}} \\ \mathbf{y}_{2_{n_{4\times 1}}} \end{pmatrix} = \mathbf{C}_{20\times 12}\mathbf{x}_{12\times 1} = \begin{bmatrix} \mathbf{C}_{1_{c_{6\times 12}}} \\ \mathbf{C}_{2_{c_{6\times 12}}} \\ \mathbf{C}_{1_{n_{4\times 12}}} \\ \mathbf{C}_{2_{n_{4\times 12}}} \end{bmatrix}_{20\times 12} \mathbf{x}_{12\times 1} \\ &\Longleftrightarrow \\ \begin{pmatrix} \mathbf{x}_{12\times 1} \\ x_{2_n} \\ \dot{x}_{2_n} \\ x_{\mathrm{O2}_n} \\ \dot{x}_{\mathrm{O2}_n} \\ x_{1_n} \\ \dot{x}_{1_n} \\ x_{\mathrm{O1}_n} \\ \dot{x}_{\mathrm{O1}_n} \end{pmatrix} &= \begin{bmatrix} & \mathbf{I}_{12\times 12} & \\ \mathbf{0}_{4\times 4} & \mathbf{0}_{4\times 4} & \mathbf{I}_{4\times 4} \\ \mathbf{I}_{4\times 4} & \mathbf{0}_{4\times 4} & \mathbf{0}_{4\times 4} \end{bmatrix} \mathbf{x}_{12\times 1} \end{aligned} \tag{4.25}$$

where:

$$\begin{aligned}
\mathbf{y}_{1_{c_{n_{1cy}\times 1}}} &= \mathbf{y}_{1_{c_{6\times 1}}} = \mathbf{C}_{n_{1cy}\times n_x}\mathbf{x}_{n_x\times 1} = \mathbf{C}_{6\times 12}x_{12\times 1} && (4.26)\\
\mathbf{y}_{2_{c_{n_{2cy}\times 1}}} &= \mathbf{y}_{2_{c_{6\times 1}}} = \mathbf{C}_{n_{2cy}\times n_x}\mathbf{x}_{n_x\times 1} = \mathbf{C}_{6\times 12}x_{12\times 1} && (4.27)\\
\mathbf{y}_{1_{n_{n_{1ny}\times 1}}} &= \mathbf{y}_{1_{n_{4\times 1}}} = \begin{pmatrix} x_{2_n} & \dot{x}_{2_n} & x_{\mathrm{O}2_n} & \dot{x}_{\mathrm{O}2_n} \end{pmatrix}^T && (4.28)\\
\mathbf{y}_{2_{n_{n_{2ny}\times 1}}} &= \mathbf{y}_{2_{n_{4\times 1}}} = \begin{pmatrix} x_{1_n} & \dot{x}_{1_n} & x_{\mathrm{O}1_n} & \dot{x}_{\mathrm{O}1_n} \end{pmatrix}^T && (4.29)\\
\begin{pmatrix} \mathbf{C}_{1_{c_{n_{1cy}\times n_x}}} \\ \mathbf{C}_{2_{c_{n_{2cy}\times n_x}}} \end{pmatrix} &= \begin{pmatrix} \mathbf{C}_{1_{c_{6\times 12}}} \\ \mathbf{C}_{2_{c_{6\times 12}}} \end{pmatrix} = \mathbf{I}_{12\times 12} && (4.30)\\
\mathbf{C}_{1_{n_{n_{1ny}\times n_x}}} &= \mathbf{C}_{1_{n_{4\times 12}}} = \begin{bmatrix} \mathbf{0}_{4\times 4} & \mathbf{0}_{4\times 4} & \mathbf{I}_{4\times 4} \end{bmatrix} && (4.31)\\
\mathbf{C}_{2_{n_{n_{2ny}\times n_x}}} &= \mathbf{C}_{2_{n_{4\times 12}}} = \begin{bmatrix} \mathbf{I}_{4\times 4} & \mathbf{0}_{4\times 4} & \mathbf{0}_{4\times 4} \end{bmatrix} && (4.32)
\end{aligned}$$

The feedback equation is:

$$\begin{aligned}
\mathbf{u}_{n_u\times 1} &= \mathbf{F}_{n_u\times ny}\mathbf{y}_{n_y\times 1}\\
&\Longleftrightarrow\\
\begin{bmatrix} \mathbf{u}_{1_{c_{n_{1cu}\times 1}}} \\ \mathbf{u}_{2_{c_{n_{2cu}\times 1}}} \\ \mathbf{u}_{1_{n_{n_{1nu}\times 1}}} \\ \mathbf{u}_{2_{n_{n_{2nu}\times 1}}} \end{bmatrix} &= \begin{bmatrix} \mathbf{F}_{1_{c_{n_{1cu}\times n_{1cy}}}} & \mathbf{0}_{n_{1cu}\times n_{2cy}} & \mathbf{0}_{n_{1cu}\times n_{1ny}} & \mathbf{0}_{n_{1cu}\times n_{2ny}} \\ \mathbf{0}_{n_{2cu}\times n_{1cy}} & \mathbf{F}_{2_{c_{n_{2cu}\times n_{2cy}}}} & \mathbf{0}_{n_{2cu}\times n_{1ny}} & \mathbf{0}_{n_{2cu}\times n_{2ny}} \\ \mathbf{0}_{n_{1nu}\times n_{1cy}} & \mathbf{0}_{n_{1nu}\times n_{2cy}} & \mathbf{F}_{1_{n_{n_{1nu}\times n_{1ny}}}} & \mathbf{0}_{n_{1nu}\times n_{2ny}} \\ \mathbf{0}_{n_{2nu}\times n_{1cy}} & \mathbf{0}_{n_{2nu}\times n_{2cy}} & \mathbf{0}_{n_{2nu}\times n_{1ny}} & \mathbf{F}_{2_{n_{n_{2nu}\times n_{2ny}}}} \end{bmatrix} \begin{pmatrix} \mathbf{y}_{1_{c_{n_{1cy}\times 1}}} \\ \mathbf{y}_{2_{c_{n_{2cy}\times 1}}} \\ \mathbf{y}_{1_{n_{n_{1ny}\times 1}}} \\ \mathbf{y}_{2_{n_{n_{2ny}\times 1}}} \end{pmatrix}\\
&\Longleftrightarrow\\
\mathbf{u}_{12\times 1} &= \mathbf{F}_{12\times 20}\mathbf{y}_{20\times 1}\\
&\Longleftrightarrow\\
\mathbf{u}_{12\times 1} &= \begin{bmatrix} \mathbf{F}_{1_{c_{4\times 6}}} & \mathbf{0}_{4\times 6} & \mathbf{0}_{4\times 4} & \mathbf{0}_{4\times 4} \\ \mathbf{0}_{4\times 6} & \mathbf{F}_{2_{c_{4\times 6}}} & \mathbf{0}_{4\times 4} & \mathbf{0}_{4\times 4} \\ \mathbf{0}_{2\times 6} & \mathbf{0}_{2\times 6} & \mathbf{F}_{1_{n_{2\times 4}}} & \mathbf{0}_{2\times 4} \\ \mathbf{0}_{2\times 6} & \mathbf{0}_{2\times 6} & \mathbf{0}_{2\times 4} & \mathbf{F}_{2_{n_{2\times 4}}} \end{bmatrix} \begin{pmatrix} \mathbf{y}_{1_{c_{6\times 1}}} \\ \mathbf{y}_{2_{c_{6\times 1}}} \\ \mathbf{y}_{1_{n_{4\times 1}}} \\ \mathbf{y}_{2_{n_{4\times 1}}} \end{pmatrix}
\end{aligned} \qquad (4.33)$$

4.1.2 Direct User-to-User Interaction

Figure 4.3 schematically depicts direct user-to-user haptic interaction via the distributed architecture with remote dynamic proxies and virtual coupling coordination proposed in Section 3.2 again. The closed loop form of this architecture is shown in Figure 4.4.

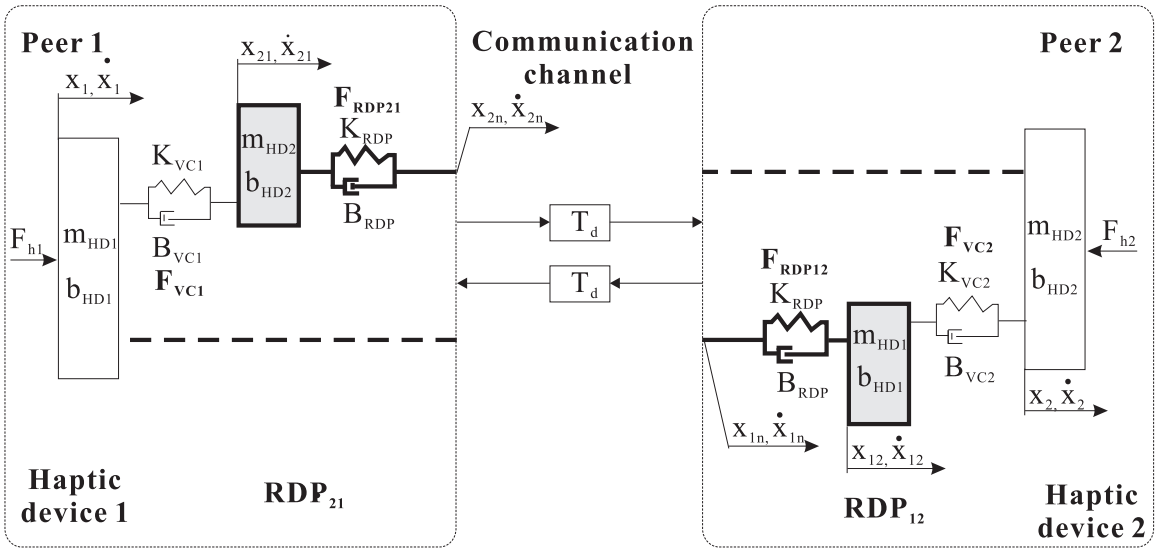

Figure 4.3: The distributed control architecture with remote dynamic proxies (RPDs) and virtual coupling coordination of two users involved in cooperative manipulation of a shared virtual object introduced in Figure 3.3. The remote dynamic proxies are shaded, and their connection to the corresponding haptic device is bolded.

The open-loop continuous-time model of the system comprises the dynamics of the haptic devices and of the peers' copies of the virtual environment which, in turn, include the remote dynamic proxies. These dynamics have been derived in Equations (3.15) to (3.18). Equations (3.11) to (3.14) comprise the feedback of the system. Equations (3.19) to (3.22) provide the feedback, according to which the system inputs can be computed from:

- position and velocity outputs sampled at the (fast) force control rate T_c: x_1, $\dot{x}_1$, x_2, $\dot{x}_2$, x_{21}, $\dot{x}_{21}$, x_{12}, $\dot{x}_{12}$;
- position and velocity outputs sampled at the (slow) network update rate T_n: x_{1_n}, $\dot{x}_{1_n}$, x_{2_n}, $\dot{x}_{2_n}$.

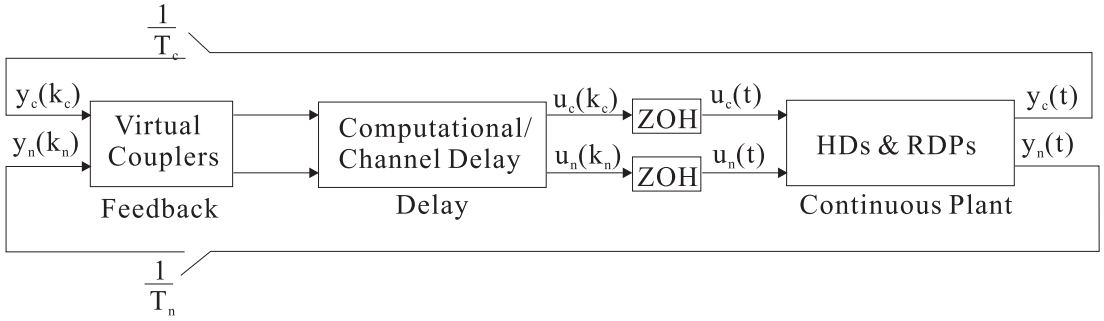

Figure 4.4: The distributed virtual coupling-based control system, including the haptic devices (HD), the remote dynamic proxies (RDP), and the shared virtual environment (SVE).

To derive the open-loop state space representation of the haptic cooperative manipulation in the form of Equation (4.1), the continuous state space dynamics of the two haptic devices (HD) and of the two remote dynamic proxies (RDP) can be written as:

$$\begin{pmatrix} \dot{x}_{\mathrm{HD1}} \\ \ddot{x}_{\mathrm{HD1}} \end{pmatrix} = \begin{bmatrix} 0 & 1 \\ 0 & -b_{\mathrm{HD1}}/m_{\mathrm{HD1}} \end{bmatrix} \begin{pmatrix} x_{\mathrm{HD1}} \\ \dot{x}_{\mathrm{HD1}} \end{pmatrix} + \begin{bmatrix} 0 \\ -1/m_{\mathrm{HD1}} \end{bmatrix} \left(F_{\mathrm{VC_1}} \right) \tag{4.34}$$

$$\begin{pmatrix} \dot{x}_{\mathrm{HD2}} \\ \ddot{x}_{\mathrm{HD2}} \end{pmatrix} = \begin{bmatrix} 0 & 1 \\ 0 & -b_{\mathrm{HD2}}/m_{\mathrm{HD2}} \end{bmatrix} \begin{pmatrix} x_{\mathrm{HD2}} \\ \dot{x}_{\mathrm{HD2}} \end{pmatrix} + \begin{bmatrix} 0 \\ -1/m_{\mathrm{HD2}} \end{bmatrix} \left(F_{\mathrm{VC2}} \right) \tag{4.35}$$

$$\begin{pmatrix} \dot{x}_{21} \\ \ddot{x}_{21} \end{pmatrix} = \begin{bmatrix} 0 & 1 \\ 0 & -b_{\mathrm{HD2}}/m_{\mathrm{HD2}} \end{bmatrix} \begin{pmatrix} x_{21} \\ \dot{x}_{21} \end{pmatrix} + \begin{bmatrix} 0 & 0 & 0 \\ 1/m_{\mathrm{HD2}} & 1/m_{\mathrm{HD2}} & 1/m_{\mathrm{HD2}} \end{bmatrix} \begin{pmatrix} F_{\mathrm{VC1}} \\ F_{\mathrm{RDP21}_c} \\ F_{\mathrm{RDP21}_n} \end{pmatrix} \tag{4.36}$$

$$\begin{pmatrix} \dot{x}_{12} \\ \ddot{x}_{12} \end{pmatrix} = \begin{bmatrix} 0 & 1 \\ 0 & -b_{\mathrm{HD1}}/m_{\mathrm{HD1}} \end{bmatrix} \begin{pmatrix} x_{12} \\ \dot{x}_{12} \end{pmatrix} + \begin{bmatrix} 0 & 0 & \\ 1/m_{\mathrm{HD1}} & 1/m_{\mathrm{HD1}} & 1/m_{\mathrm{HD1}} \end{bmatrix} \begin{pmatrix} F_{\mathrm{VC2}} \\ F_{\mathrm{RDP12}_c} \\ F_{\mathrm{RDP12}_n} \end{pmatrix} \tag{4.37}$$

Equations (4.2) to (4.7) can be grouped based on the peer site. In particular, at the

Peer 1 site:

$$\dot{\mathbf{x}}_{1_{4\times1}} = \begin{pmatrix} \dot{x}_1 \\ \ddot{x}_1 \\ \dot{x}_{21} \\ \ddot{x}_{21} \end{pmatrix} = \begin{bmatrix} 0 & 1 & 0 & 0 \\ 0 & -b_{\mathrm{HD1}}/m_{\mathrm{HD1}} & 0 & 0 \\ 0 & 0 & 0 & 1 \\ 0 & 0 & 0 & -b_{\mathrm{HD2}}/m_{\mathrm{HD2}} \end{bmatrix} \begin{pmatrix} x_1 \\ \dot{x}_1 \\ x_{21} \\ \dot{x}_{21} \end{pmatrix} + \begin{bmatrix} 0 & 0 & 0 \\ -1/m_{\mathrm{HD1}} & 0 & 0 \\ 0 & 0 & 0 \\ 1/m_{\mathrm{HD2}} & 1/m_{\mathrm{HD2}} & 1/m_{\mathrm{HD2}} \end{bmatrix} \begin{pmatrix} F_{\mathrm{VC1}} \\ F_{\mathrm{RDP21}_c} \\ F_{\mathrm{RDP21}_n} \end{pmatrix}$$

$$= \mathbf{A}_{1_{4\times4}} \mathbf{x}_{1_{4\times1}} + \begin{bmatrix} \mathbf{B}_{1_{c_{4\times2}}} & \mathbf{B}_{1_{n_{4\times1}}} \end{bmatrix}_{6\times6} \begin{pmatrix} \mathbf{u}_{1_{c_{2\times1}}} \\ \mathbf{u}_{1_{n_{1\times1}}} \end{pmatrix}_{3\times1} \tag{4.38}$$

where:

$$\mathbf{B}_{1_{c_{4\times2}}} = \begin{bmatrix} 0 & 0 \\ -1/m_{\mathrm{HD1}} & 0 \\ 0 & 0 \\ 1/m_{\mathrm{HD2}} & 1/m_{\mathrm{HD2}} \end{bmatrix} \tag{4.39}$$

$$\mathbf{B}_{1_{n_{4\times1}}} = \begin{bmatrix} 0 \\ 0 \\ 0 \\ 1/m_{\mathrm{HD2}} \end{bmatrix} \tag{4.40}$$

and:

$$\begin{aligned}
\begin{pmatrix} \mathbf{u}_{1_{c_{2\times1}}} \\ \mathbf{u}_{1_{n_{1\times1}}} \end{pmatrix}_{3\times1} &= \begin{pmatrix} F_{\mathrm{VC1}} & F_{\mathrm{RDP21}_c} & F_{\mathrm{RDP21}_n} \end{pmatrix}^T \\
&= \begin{bmatrix} K_{\mathrm{VC1}} & B_{\mathrm{VC1}} & -K_{\mathrm{VC1}} & -B_{\mathrm{VC1}} & 0 & 0 \\ 0 & 0 & -K_{\mathrm{RDP}} & -B_{\mathrm{RDP}} & 0 & 0 \\ 0 & 0 & 0 & 0 & K_{\mathrm{RDP}} & B_{\mathrm{RDP}} \end{bmatrix} \begin{pmatrix} x_1 \\ \dot{x}_1 \\ x_{21} \\ \dot{x}_{21} \\ x_{2_n} \\ \dot{x}_{2_n} \end{pmatrix} \\
&= \begin{bmatrix} \mathbf{F}_{1_{c_{2\times4}}} & \mathbf{0}_{2\times2} \\ \mathbf{0}_{1\times4} & \mathbf{F}_{1_{n_{1\times2}}} \end{bmatrix}_{3\times6} \begin{pmatrix} \mathbf{y}_{1_{c_{4\times1}}} \\ \mathbf{y}_{1_{n_{2\times1}}} \end{pmatrix}_{6\times1}
\end{aligned} \tag{4.41}$$

At the Peer 2 site:

$$\begin{aligned}
\dot{\mathbf{x}}_{2_{4\times1}} = \begin{pmatrix} \dot{x}_2 \\ \ddot{x}_2 \\ \dot{x}_{12} \\ \ddot{x}_{12} \end{pmatrix} &= \begin{bmatrix} 0 & 1 & 0 & 0 \\ 0 & -b_{\mathrm{HD2}}/m_{\mathrm{HD2}} & 0 & 0 \\ 0 & 0 & 0 & 1 \\ 0 & 0 & 0 & -b_{\mathrm{HD1}}/m_{\mathrm{HD1}} \end{bmatrix} \begin{pmatrix} x_2 \\ \dot{x}_2 \\ x_{12} \\ \dot{x}_{12} \end{pmatrix} \\
&\quad + \begin{bmatrix} 0 & 0 & 0 \\ -1/m_{\mathrm{HD2}} & 0 & 0 \\ 0 & 0 & 0 \\ 1/m_{\mathrm{HD1}} & 1/m_{\mathrm{HD1}} & 1/m_{\mathrm{HD1}} \end{bmatrix} \begin{pmatrix} F_{\mathrm{VC2}} \\ F_{\mathrm{RDP12}_c} \\ F_{\mathrm{RDP12}_n} \end{pmatrix} \\
&= \mathbf{A}_{2_{4\times4}} \mathbf{x}_{2_{4\times1}} + \begin{bmatrix} \mathbf{B}_{2_{c_{4\times2}}} & \mathbf{B}_{2_{n_{4\times1}}} \end{bmatrix}_{6\times6} \begin{pmatrix} \mathbf{u}_{2_{c_{2\times1}}} \\ \mathbf{u}_{2_{n_{1\times1}}} \end{pmatrix}_{3\times1}
\end{aligned} \tag{4.42}$$

where:

$$\mathbf{B}_{2_{c_{4\times2}}} = \begin{bmatrix} 0 & 0 \\ -1/m_{\mathrm{HD2}} & 0 \\ 0 & 0 \\ 1/m_{\mathrm{HD1}} & 1/m_{\mathrm{HD1}} \end{bmatrix} \tag{4.43}$$

$$\mathbf{B}_{2_{n_{4\times1}}} = \begin{bmatrix} 0 \\ 0 \\ 0 \\ 1/m_{\mathrm{HD1}} \end{bmatrix} \tag{4.44}$$

and:

$$\begin{aligned} \begin{pmatrix} \mathbf{u}_{2_{c_{2\times1}}} \\ \mathbf{u}_{2_{n_{1\times1}}} \end{pmatrix}_{3\times1} &= \begin{pmatrix} F_{\mathrm{VC2}} & F_{\mathrm{RDP12}_c} & F_{\mathrm{RDP12}_n} \end{pmatrix}^T \\ &= \begin{bmatrix} K_{\mathrm{VC2}} & B_{\mathrm{VC2}} & -K_{\mathrm{VC2}} & -B_{\mathrm{VC2}} & 0 & 0 \\ 0 & 0 & -K_{\mathrm{RDP}} & -B_{\mathrm{RDP}} & 0 & 0 \\ 0 & 0 & 0 & 0 & K_{\mathrm{RDP}} & B_{\mathrm{RDP}} \end{bmatrix} \begin{pmatrix} x_2 \\ \dot{x}_2 \\ x_{12} \\ \dot{x}_{12} \\ x_{1_n} \\ \dot{x}_{1_n} \end{pmatrix} \\ &= \begin{bmatrix} \mathbf{F}_{2_{c_{2\times4}}} & \mathbf{0}_{2\times2} \\ \mathbf{0}_{1\times4} & \mathbf{F}_{2_{n_{1\times2}}} \end{bmatrix}_{3\times6} \begin{pmatrix} \mathbf{y}_{2_{c_{4\times1}}} \\ \mathbf{y}_{2_{n_{2\times1}}} \end{pmatrix}_{6\times1} \end{aligned} \tag{4.45}$$

The continuous-time state-space dynamics of the open-loop direct user-to-user haptic

interaction are obtained as:

$$
\begin{aligned}
\dot{\mathbf{x}}_{8\times1} &= \mathbf{A}_{8\times8}\mathbf{x}_{8\times1} + \mathbf{B}_{8\times6}\mathbf{u}_{6\times1} \\
&= \mathbf{A}_{8\times8}\mathbf{x}_{8\times1} + \begin{bmatrix}\mathbf{B}_{c_{8\times2}} & \mathbf{B}_{c_{8\times2}} & \mathbf{B}_{n_{8\times1}} & \mathbf{B}_{n_{8\times1}}\end{bmatrix}_{8\times6} \begin{pmatrix}\mathbf{u}_{1_{c_{2\times1}}} \\ \mathbf{u}_{2_{c_{2\times1}}} \\ \mathbf{u}_{1_{n_{1\times1}}} \\ \mathbf{u}_{2_{n_{1\times1}}}\end{pmatrix} \\
\Longleftrightarrow & \\
\begin{pmatrix}\dot{\mathbf{x}}_{1_{4\times1}} \\ \dot{\mathbf{x}}_{2_{4\times1}}\end{pmatrix} &= \begin{bmatrix}\mathbf{A}_{1_{4\times4}} & \mathbf{0}_{4\times4} \\ \mathbf{0}_{4\times4} & \mathbf{A}_{2_{4\times4}}\end{bmatrix} \begin{pmatrix}\mathbf{x}_{1_{4\times1}} \\ \mathbf{x}_{2_{4\times1}}\end{pmatrix} + \begin{bmatrix}\mathbf{B}_{1_{c_{4\times2}}} & \mathbf{0}_{4\times2} & \mathbf{B}_{2_{n_{4\times1}}} & \mathbf{0}_{4\times1} \\ \mathbf{0}_{4\times2} & \mathbf{B}_{1_{c_{4\times2}}} & \mathbf{0}_{4\times1} & \mathbf{B}_{2_{n_{4\times1}}}\end{bmatrix} \begin{pmatrix}\mathbf{u}_{1_{c_{2\times1}}} \\ \mathbf{u}_{2_{c_{2\times1}}} \\ \mathbf{u}_{1_{n_{1\times1}}} \\ \mathbf{u}_{2_{n_{1\times1}}}\end{pmatrix} \\
\Longleftrightarrow & \\
\begin{pmatrix}\dot{x}_1 \\ \ddot{x}_1 \\ \dot{x}_{21} \\ \ddot{x}_{21} \\ \dot{x}_2 \\ \ddot{x}_2 \\ \dot{x}_{12} \\ \ddot{x}_{12}\end{pmatrix} &= \begin{bmatrix}\mathbf{A}_{1_{4\times4}} & \mathbf{0}_{4\times4} \\ \mathbf{0}_{4\times4} & \mathbf{A}_{2_{4\times4}}\end{bmatrix} \begin{pmatrix}x_1 \\ \dot{x}_1 \\ x_{21} \\ \dot{x}_{21} \\ x_2 \\ \dot{x}_2 \\ x_{12} \\ \dot{x}_{12}\end{pmatrix} + \begin{bmatrix}\mathbf{B}_{1_{c_{4\times2}}} & \mathbf{0}_{4\times2} & \mathbf{B}_{2_{n_{4\times1}}} & \mathbf{0}_{4\times1} \\ \mathbf{0}_{4\times2} & \mathbf{B}_{1_{c_{4\times2}}} & \mathbf{0}_{4\times1} & \mathbf{B}_{2_{n_{4\times1}}}\end{bmatrix} \begin{pmatrix}F_{\mathrm{VC1}} \\ F_{\mathrm{RDP21}_c} \\ F_{\mathrm{VC2}} \\ F_{\mathrm{RDP12}_c} \\ F_{\mathrm{RDP21}_n} \\ F_{\mathrm{RDP12}_n}\end{pmatrix}
\end{aligned}
\tag{4.46}
$$

where:

$$\mathbf{u}_{1_{c_{2\times1}}} = \begin{pmatrix}F_{\mathrm{VC1}} & F_{\mathrm{RDP21}_c}\end{pmatrix}^T \tag{4.47}$$

$$\mathbf{u}_{2_{c_{2\times1}}} = \begin{pmatrix}F_{\mathrm{VC2}} & F_{\mathrm{RDP12}_c}\end{pmatrix}^T \tag{4.48}$$

$$\mathbf{u}_{1_{n_{2\times1}}} = \begin{pmatrix}F_{\mathrm{RDP21}_n}\end{pmatrix}^T \tag{4.49}$$

$$\mathbf{u}_{2_{n_{2\times1}}} = \begin{pmatrix}F_{\mathrm{RDP12}_n}\end{pmatrix}^T \tag{4.50}$$

The output equation is:

$$\begin{aligned}
\mathbf{y}_{12\times1} &= \begin{pmatrix} \mathbf{y}_{1_{c_{4\times1}}} \\ \mathbf{y}_{2_{c_{4\times1}}} \\ \mathbf{y}_{1_{n_{2\times1}}} \\ \mathbf{y}_{2_{n_{2\times1}}} \end{pmatrix} = \mathbf{C}_{12\times8}\mathbf{x}_{8\times1} = \begin{bmatrix} \mathbf{C}_{1_{c_{4\times8}}} \\ \mathbf{C}_{2_{c_{4\times8}}} \\ \mathbf{C}_{1_{n_{2\times8}}} \\ \mathbf{C}_{2_{n_{2\times8}}} \end{bmatrix}_{12\times8} \mathbf{x}_{8\times1} \\
&\Longleftrightarrow \\
\begin{pmatrix} \mathbf{x}_{8\times1} \\ x_{2_n} \\ \dot{x}_{2_n} \\ x_{1_n} \\ \dot{x}_{1_n} \end{pmatrix} &= \begin{bmatrix} \mathbf{I}_{8\times8} \\ \mathbf{0}_{2\times2} & \mathbf{0}_{2\times2} & \mathbf{I}_{2\times2} & \mathbf{0}_{2\times2} \\ \mathbf{I}_{2\times2} & \mathbf{0}_{2\times2} & \mathbf{0}_{2\times2} & \mathbf{0}_{2\times2} \end{bmatrix} \mathbf{x}_{8\times1}
\end{aligned} \tag{4.51}$$

where:

$$\mathbf{y}_{1_{c_{4\times1}}} = \mathbf{C}_{1_{c_{4\times8}}} x_{8\times1} \tag{4.52}$$

$$\mathbf{y}_{2_{c_{4\times1}}} = \mathbf{C}_{2_{c_{4\times8}}} x_{8\times1} \tag{4.53}$$

$$\mathbf{y}_{1_{n_{2\times1}}} = \begin{pmatrix} x_{2_n} & \dot{x}_{2_n} \end{pmatrix}^T \tag{4.54}$$

$$\mathbf{y}_{2_{n_{2\times1}}} = \begin{pmatrix} x_{1_n} & \dot{x}_{1_n} \end{pmatrix}^T \tag{4.55}$$

$$\begin{pmatrix} \mathbf{C}_{1_{c_{4\times8}}} \\ \mathbf{C}_{2_{c_{4\times8}}} \end{pmatrix} = \mathbf{I}_{8\times8} \tag{4.56}$$

$$\mathbf{C}_{1_{n_{2\times8}}} = \begin{bmatrix} \mathbf{0}_{2\times2} & \mathbf{0}_{2\times2} & \mathbf{I}_{2\times2} & \mathbf{0}_{2\times2} \end{bmatrix} \tag{4.57}$$

$$\mathbf{C}_{2_{n_{2\times8}}} = \begin{bmatrix} \mathbf{I}_{2\times2} & \mathbf{0}_{2\times2} & \mathbf{0}_{2\times2} & \mathbf{0}_{2\times2} \end{bmatrix} \tag{4.58}$$

The feedback equation is:

$$\begin{aligned}
\mathbf{u}_{6\times1} &= \mathbf{F}_{6\times12}\mathbf{y}_{12\times1} \\
&\Longleftrightarrow \\
\mathbf{u}_{6\times1} &= \begin{bmatrix} \mathbf{F}_{1_{c_{2\times4}}} & \mathbf{0}_{2\times4} & \mathbf{0}_{2\times2} & \mathbf{0}_{2\times2} \\ \mathbf{0}_{2\times4} & \mathbf{F}_{2_{c_{2\times4}}} & \mathbf{0}_{2\times2} & \mathbf{0}_{2\times2} \\ \mathbf{0}_{1\times4} & \mathbf{0}_{1\times4} & \mathbf{F}_{1_{n_{1\times2}}} & \mathbf{0}_{1\times2} \\ \mathbf{0}_{1\times4} & \mathbf{0}_{1\times4} & \mathbf{0}_{1\times2} & \mathbf{F}_{2_{n_{1\times2}}} \end{bmatrix} \begin{pmatrix} \mathbf{y}_{1_{c_{4\times1}}} \\ \mathbf{y}_{2_{c_{4\times1}}} \\ \mathbf{y}_{1_{n_{1\times1}}} \\ \mathbf{y}_{2_{n_{1\times1}}} \end{pmatrix}
\end{aligned} \tag{4.59}$$

4.2 Discretization of the Control System and Delay Augmentation

The closed loop system formed by the two cooperating users, their local copies of the shared virtual environment (including the local copies of the shared virtual objects and the remote dynamic proxies) and the coordinating virtual couplers is:

- a sampled-data system because of the discrete nature of the virtual environment simulation.
- a system with multiple rates because the network transmission rate of 128 Hz is lower than the 1024 Hz rate of the local force feedback loops at the networked users.

Hence, the open-loop haptic cooperation system is discretized according to the multi-rate methodology introduced in [59][2]. The discretization is only briefly overviewed in this section, and is presented in detail in Appendix A.1 for cooperative manipulation of a shared virtual object, and in Appendix A.2 for direct user-to-user haptic interaction.

According to the methodology in [59], the expanded state vector is defined as:

$$\mathbf{x}_{\mathrm{D}}[k] = \begin{pmatrix} \mathbf{x}\left((k-1)\,T_0 + \tau_0\right) \\ \mathbf{x}\left((k-1)\,T_0 + 2\tau_0\right) \\ \vdots \\ \mathbf{x}\left((k-1)\,T_0 + (N_0-1)\,\tau_0\right) \\ \mathbf{x}\left(kT_0\right) \end{pmatrix} \tag{4.60}$$

where k is the sampling time index. The output vector is augmented via:

$$\mathbf{y}_{\mathrm{D}}[k] = \begin{pmatrix} \mathbf{y}_{\mathrm{D}_c}[k] \\ \mathbf{y}_{\mathrm{D}_n}[k] \end{pmatrix}, \text{ where } \mathbf{y}_{\mathrm{D}_i}[k] = \begin{pmatrix} \mathbf{y}_{\mathrm{D}_i}\left(kT_0\right) \\ \mathbf{y}_{\mathrm{D}_i}\left(kT_0 + T_i\right) \\ \vdots \\ \mathbf{y}_{\mathrm{D}_i}\left(kT_0 + (N_i-1)\,T_i\right) \end{pmatrix} \tag{4.61}$$

[2]The open-loop system is the system without the feedback Equations (4.33) and (4.59) for cooperative manipulation and for direct user-to-user interaction, respectively.

In the presence of computational and/or communication channel delay, the expanded input vector u_D can be defined as:

$$\mathbf{u}_{\mathrm{D}}[k] = \begin{pmatrix} \mathbf{u}_{\mathrm{D}_c}[k] \\ \mathbf{u}_{\mathrm{D}_n}[k] \end{pmatrix}, \text{ where } \mathbf{u}_{\mathrm{D}_i}[k] = \begin{pmatrix} \mathbf{u}_{\mathrm{D}_i}(kT_0) \\ \mathbf{u}_{\mathrm{D}_i}(kT_0 + T_i) \\ \vdots \\ \mathbf{u}_{\mathrm{D}_i}(kT_0 + (N_i - 1)T_i) \end{pmatrix} \tag{4.62}$$

In Equations (4.61) and (4.62), $i \in \{c, n\}$.

With the above definitions, the discrete-time state space representation of the open-loop haptic cooperation system can be written as:

$$\begin{aligned} \mathbf{x}_{\mathrm{D}}[k+1] &= \mathbf{A}_{\mathrm{D}}\mathbf{x}_{\mathrm{D}}[k] + \mathbf{B}_{\mathrm{D}}\mathbf{u}_{\mathrm{D}}[k] \\ \mathbf{y}_{\mathrm{D}}[k] &= \mathbf{C}_{\mathrm{D}}\left(\mathbf{U}_1\mathbf{x}_{\mathrm{D}}[k+1] + \mathbf{U}_2\mathbf{x}_{\mathrm{D}}[k]\right) \end{aligned} \tag{4.63}$$

where $\mathbf{U}_1 = \mathit{blockdiag}\left(\mathbf{I}_{n_x}, \ldots, \mathbf{I}_{n_x}, \mathbf{0}_{n_x}\right)$ and $\mathbf{U}_2 = \mathit{blockdiag}\left(\mathbf{0}_{n_x}, \ldots, \mathbf{0}_{n_x}, \mathbf{I}_{n_x}\right)$. Hence, the discrete-time state-space representation can be derived in the form:

$$\begin{aligned} \mathbf{x}_{\mathrm{D}}[k+1] &= \mathbf{A}_{\mathrm{D}}\mathbf{x}_{\mathrm{D}}[k] + \mathbf{B}_{\mathrm{D}}\mathbf{u}_{\mathrm{D}}[k] \\ \mathbf{y}_{\mathrm{D}}[k] &= \hat{\mathbf{C}}_{\mathrm{D}}\mathbf{x}_{\mathrm{D}}[k] + \hat{\mathbf{D}}_{\mathrm{D}}\mathbf{u}_{\mathrm{D}}[k] \end{aligned} \tag{4.64}$$

where $\hat{\mathbf{C}}_{\mathrm{D}} = \mathbf{C}_{\mathrm{D}}\mathbf{U}_1\mathbf{A}_{\mathrm{D}} + \mathbf{C}_{\mathrm{D}}\mathbf{U}_2$ and $\mathbf{C}_{\mathrm{D}}\mathbf{U}_1\mathbf{B}_{\mathrm{D}}$.

To integrate the communication channel and/or computational delay into the discrete-time state-space representation of the haptic cooperation system, the state vector can be augmented with the delayed input signals as in [2]. The delay augmentation generates the new matrices $\tilde{A}_D$, $\tilde{B}_D$, $\tilde{C}_D$, $\tilde{D}_D$, and the new augmented state vector $\tilde{x}_D[k]$ and augmented input vector $\tilde{u}_D[k]$. The detailed derivations of these matrices and vectors are presented in the Appendix A.1.2 and Appendix A.2.2. The closed-loop discrete-time system augmented with the delay can be obtained upon using the feedback law:

$$\tilde{\mathbf{u}}_{\mathrm{D}} = \mathbf{F}_{\mathrm{D}}\mathbf{y}_{\mathrm{D}} \tag{4.65}$$

The feedback gain matrix $\mathbf{F}_{\mathrm{D}}$ has constant elements that are the stiffness and damping parameters of all the virtual couplers in the control system. Given the state space representation of the open loop system augmented with computational and/or

communication delay, the state space transition matrix of the closed loop system is computed via:

$$\mathbf{A^C}_{\mathrm{D}} = \tilde{A}_D + \tilde{B}_D F_D (I - \tilde{D}_D F_D)^{-1} \tilde{C}_D \tag{4.66}$$

Lastly, the closed-loop system is stable if and only if all the eigenvalues of this matrix are inside the unit circle.

4.3 Stability Analysis

To ensure that the analysis results are comparable with previous research in [2], parameters in this analysis are chosen as [2]: $m_{\mathrm{HD}} = 0.1\mathrm{kg}$; $m_{\mathrm{O1}} = m_{\mathrm{O2}} = 0.4\mathrm{kg}$; the damping of all virtual couplers is 10Ns/m; and the update rates are $T_c = 1/1024\mathrm{s}$ for haptic rendering and $T_n = 1/128\mathrm{s}$ for network transmission. Constant combined communication/computational delays of $n_t = 0, 1, 2, 3$ network sample times are considered in the analysis.

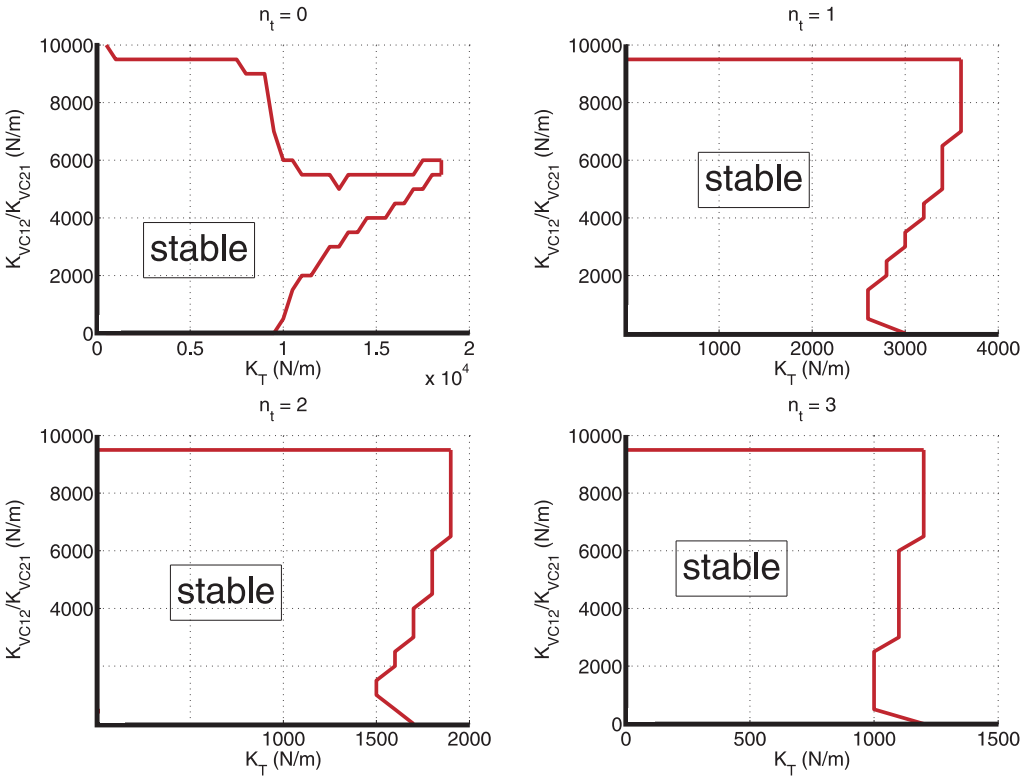

Figure 4.5: Stability region for $K_{\mathrm{VC1}} = K_{\mathrm{VC2}} = 2000\mathrm{N/m}, K_{\mathrm{RDP}} = 500\mathrm{N/m}$

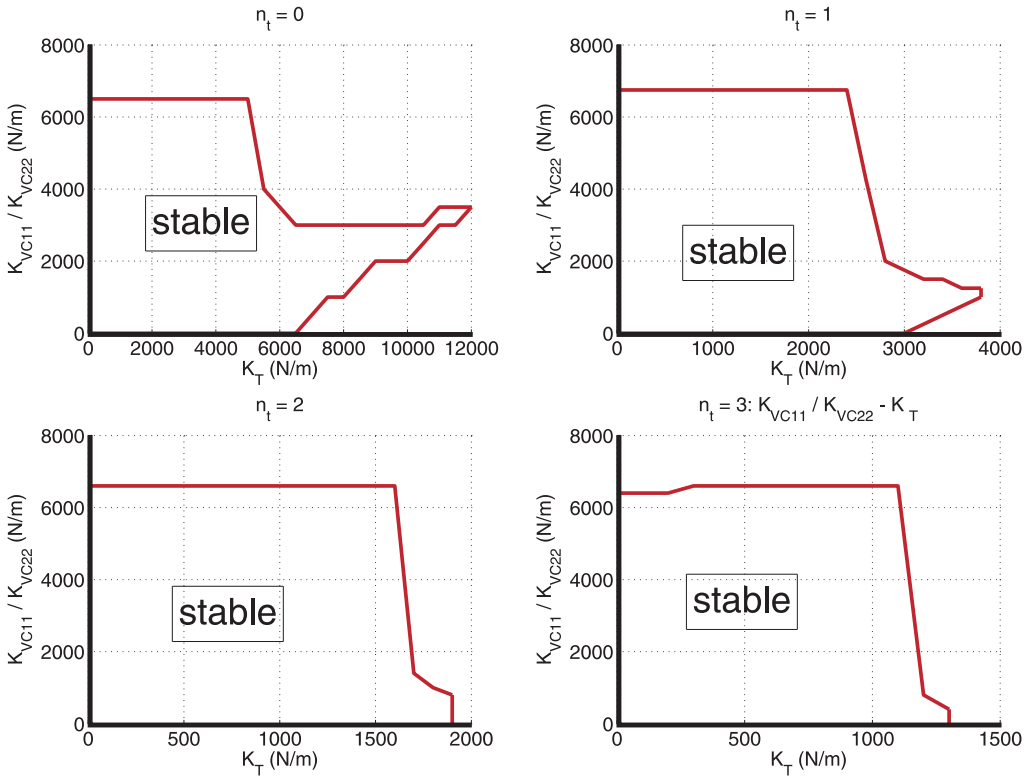

Figure 4.6: Stability region for $K_{\mathrm{VC21}} = K_{\mathrm{VC12}} = 300\mathrm{N/m}$,$K_{\mathrm{RDP}} = 500\mathrm{N/m}$.

Similar analysis is also conducted for the peer-to-peer virtual coupling scheme in [1], which consists only the local contact ($K_{\mathrm{VC1}} = K_{\mathrm{VC2}}$) and the coordinating virtual coupler between distributed copies of the shared virtual object(K_{T}). The corresponding analysis result is demonstrated in Figure 4.9 For comparison, other parameters are chosen the same as the above analysis.

Comparing to the distributed control architecture in [2] and the peer-to-peer scheme with virtual coupling in [1], the proposed control architecture is theoretically predicted to maintain similar local contact stiffness (K_{VC1} and K_{VC2}) and coordinating virtual coupler stiffness (K_{T}), yet it achieves largely improved remote contact stiffness(K_{VC21} and K_{VC12}). With this improved boundary remote contact stiffness, potentially larger position difference between the distributed copies resulting from the compliant virtual couplers controlling the remote dynamic proxies can be compensated by improving the remote contact stiffness. Note that for given local contact stiffness $K_{\mathrm{VC1}} = K_{\mathrm{VC2}}$ and remote contact stiffness $K_{\mathrm{VC21}} = K_{\mathrm{VC12}}$ in the presence of a specific delay, the K_{RDP} and the K_{T} are approximately limited within a inverse proportional boundary Figure 4.8. When applied to direct user-to-user contact, the

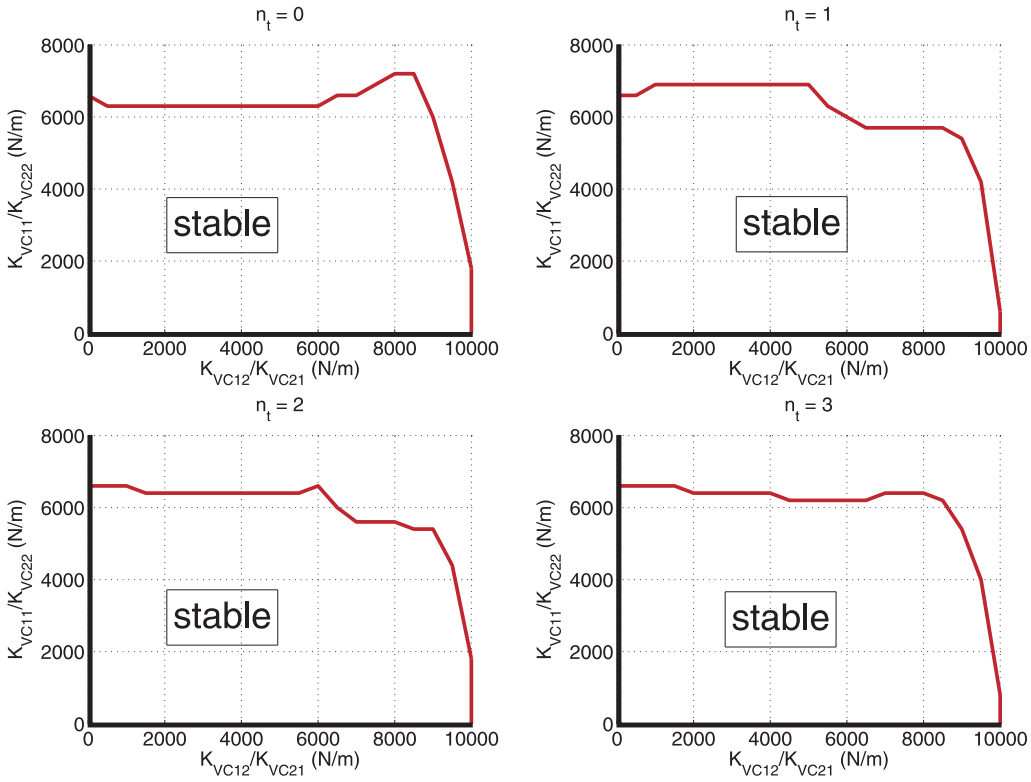

Figure 4.7: Stability region for $K_{\mathrm{T}} = 1000\mathrm{N/m}, K_{\mathrm{RDP}} = 500\mathrm{N/m}$.

proposed control architecture is predicted to achieve much stiffer contact for different delay steps (Figure 4.10).

In comparison, the distributed control architecture in [2] can maintain control stability for different delay step in the presence of much lower contact stiffness under the same other conditions.(Figure 4.11)

4.4 Summary

This Chapter theoretically analyzes the distributed control architectures with virtual coupling coordination and derives its boundary stiffness for control stability. By applying the mathematical framework for the modeling and analysis of cooperative multi-rate haptic control systems for rigid objective manipulation in [2], theoretical prediction is conducted for the proposed control architecture in the presence of 1 KHz haptic rendering rate and 128 Hz network transmission rate. Stability regions with boundary stiffness of virtual coupling controller are expressively depicted for different network delay steps when the proposed control architecture is applied to cooperative

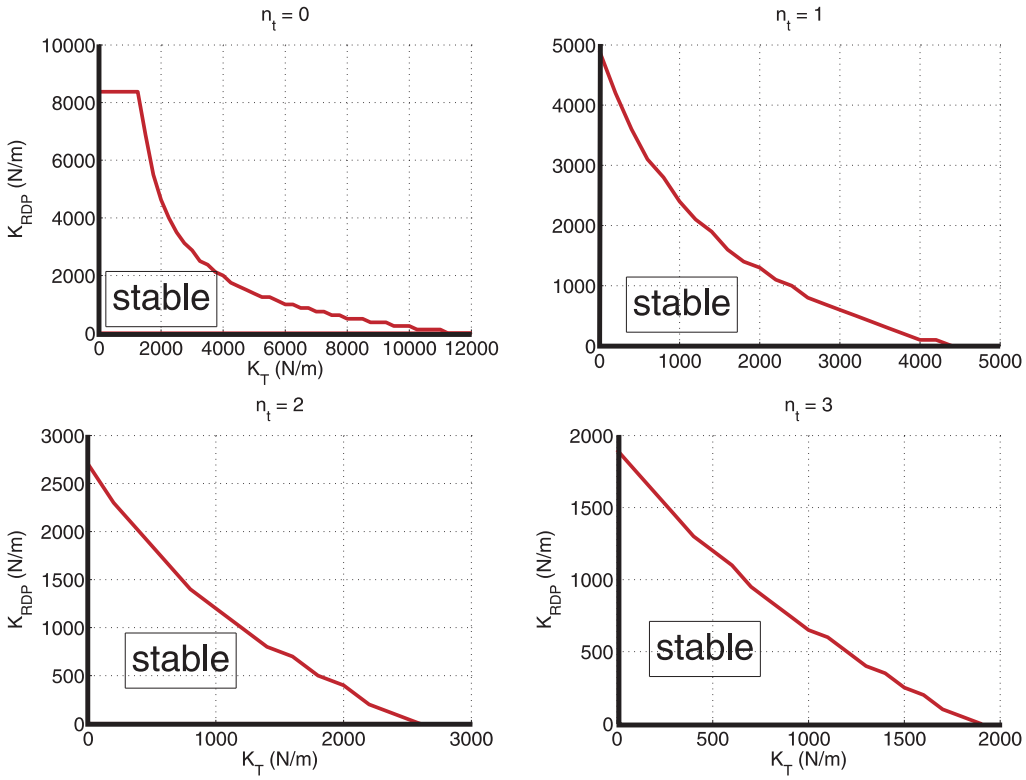

Figure 4.8: Stability region for $K_{\mathrm{VC1}} = K_{\mathrm{VC2}} = K_{\mathrm{VC21}} = K_{\mathrm{VC12}} = 4000\mathrm{N/m}$.

manipulation of the shared virtual object and direct user-to-user contact. Comparing to the peer-to-peer scheme with virtual coupling in [1] and the distributed control architecture in [2], the proposed control architecture with remote dynamic proxies and virtual coupling coordination is theoretically predicted to maintain similar local contact stiffness and coordinating virtual coupler stiffness, yet it achieves largely improved remote contact stiffness. With this improved remote contact stiffness, potentially larger position difference between the distributed copies resulting from the compliant virtual couplers controlling the remote dynamic proxies can be compensated by improving the remote contact stiffness. For the direct user-to-user contact, the proposed control architecture is predicted to render much higher contact stiffness, with smoothed users motion and force perception.

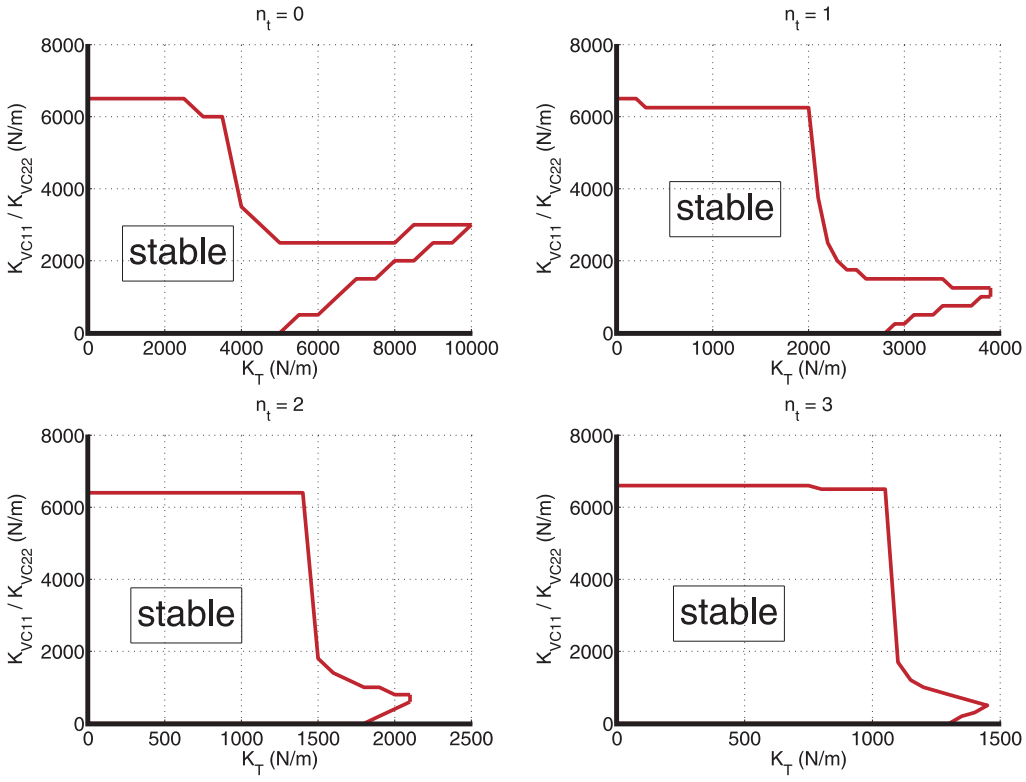

Figure 4.9: Stability region for peer-to-peer virtual coupling scheme.

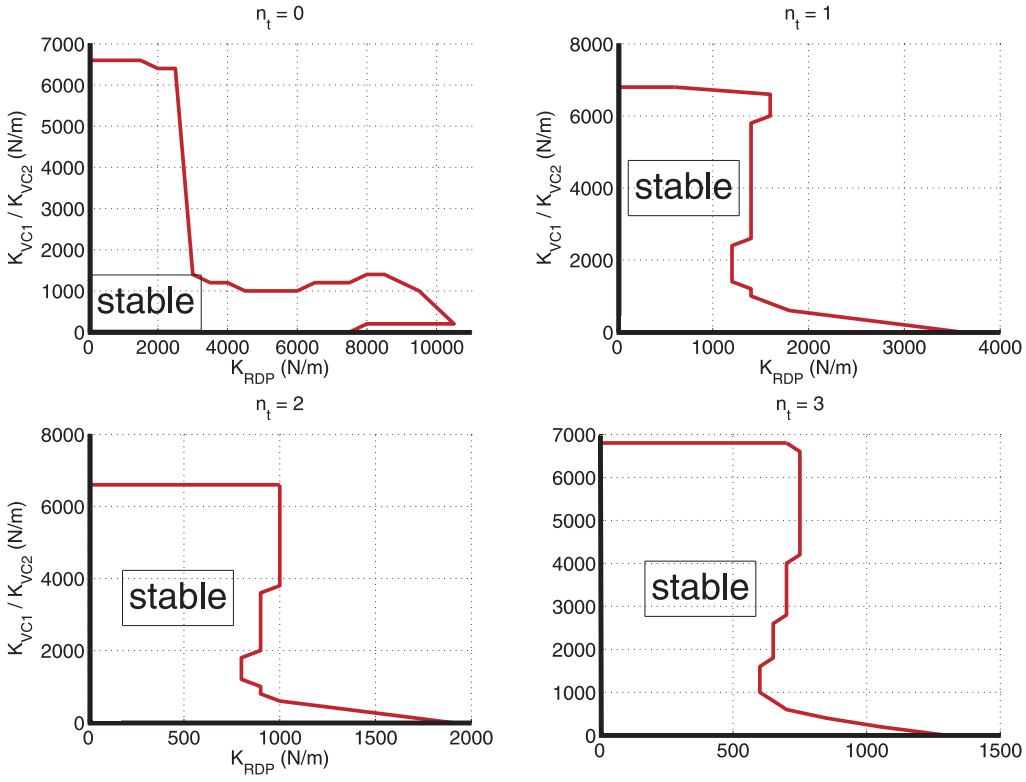

Figure 4.10: Stability region of the proposed distributed control architecture with virtual coupling and remote dynamic proxies, when applied to direct user-to-user contact.

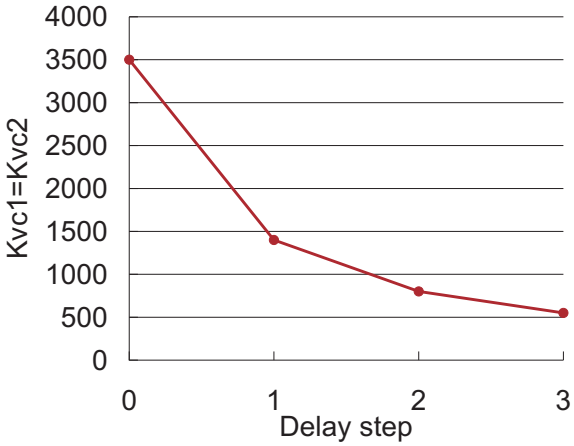

Figure 4.11: Stability region of the distributed control architecture in [2], when applied to direct user-to-user contact.

Chapter 5

Experiments

This chapter experimentally contrasts the proposed distributed control architectures to several recently designed distributed control architectures in [20], [1] and [2].

The experimental comparison among the the Proposed Control Architecture 1 (the Distributed Control Architecture with Virtual Coupling Coordination and Remote Dynamic Proxies), the Reference Control Architecture 1 (the Peer-to-peer Scheme with Virtual Coupling Controller in [20]) and the Reference Control Architecture 2 (the Distributed Control Architecture in [2]) confirms the analysis results in Chapter 4. This comparison shows that, in coordinating the distributed copies of the shared virtual object, the Proposed Control Architecture 1 achieves much higher performance than Reference Control Architecture 1, and that this performance is comparable to the performance of the Reference Control Architecture 2. In addition, the Proposed Control Architecture 1 renders smooth motion of users in the virtual environment of their distant peers, which results in continuous visual display. However, the virtual coupling control adds viscous damping to the simulated shared virtual objects in the presence of communication delay. Therefore, all the three control architectures involved in the comparison can not realistically render the motion of a shared virtual object designed as a pure mass. As the Proposed Control Architecture 1 includes the largest number of virtual coupling controllers for coordination, it introduces the largest additional damping to the shared virtual object.

The experiments involving both the cooperative manipulation and direct user-to-user contact are repeated to contrast the Proposed Control Architecture 2 (the Distributed Control Architecture with Wave-based Coordination and Remote Dynamic Proxies) to the Reference Control Architecture 3 (the Peer-to-Peer Scheme with Wave Variable Delay Compensation in [1]). Both architectures with wave-based commu-

nications outperform the control architectures with virtual coupling coordination in rendering realistic dynamic properties of the shared virtual object. Furthermore, the inertia rendered via the Proposed Control Architecture 2 has smaller variation and less derivation from the theoretical expectance than the inertia rendered via the Reference Control Architecture 3.

It is notable that the remote dynamic proxies help both proposed control architectures to maintain stable interaction and to render smooth motion of distant user in the presence of high contact stiffness regardless of whether the users cooperatively manipulate a shared virtual object or interact with each other directly. Furthermore, the performance of both architectures in coordinating the distributed copies of the shared virtual object is comparable for the same constant network delay. However, as the two proposed control architectures employ different controllers for coordination, their performance differs in several aspects. First, both during cooperative manipulation and during direct user-to-user interaction, the proposed control architecture with virtual coupling coordination adds more damping to the shared virtual environment than the control architecture with wave-based coordination. Secondly, the proposed control architecture with wave-based coordination renders stable cooperative manipulation and direct user-to-user contact in the presence of much longer constant network delay than the proposed control architecture with virtual coupling coordination.

5.1 Reference Schemes for Comparison

5.1.1 Reference Control Architecture 1: Peer-to-Peer Scheme with Virtual Coupling Controller [1]

The peer-to-peer scheme with virtual coupling controller is shown in Figure 5.1. As depicted in Figure 5.1, the virtual environment of each peer includes a copy of the shared virtual object in a rigid enclosure that allows it to move only horizontally. Note that in all the experiments in this chapter, the shared virtual object is a shared virtual cube. $m_{\mathrm{HD}i}$ and $b_{\mathrm{HD}i}$ are the mass and the damping of the haptic interfaces; $m_{\mathrm{O}i}$ and $b_{\mathrm{O}i}$ are the mass and the damping of Peer i's copy of the shared virtual object; $K_{\mathrm{VC}i}$ and $B_{\mathrm{VC}i}$ are the stiffness and the damping of the contact between Peer i and its copy of the virtual object; $F_{\mathrm{VC}i}$ is the interaction force between the haptic device of Peer i and its local copy of the virtual object; K_{T} and B_{T} are the stiffness and the damping of coordinating virtual coupling controller between the distributed copies of

the shared virtual object; $F_{\mathrm{T}i}$ is the coordinating force between the distributed copies of the shared virtual object; $x_{\mathrm{O}i}$ and $\dot{x}_{\mathrm{O}i}$ are the position and the velocity of Peer i's copy of the virtual object; $x_{\mathrm{O}i_n}$ and $\dot{x}_{\mathrm{O}i_n}$ are the position and velocity commands sent by Peer i's copy of the virtual object to the peer user; lastly, $F_{\mathrm{h}i}$ is the force applied by the i-th user to their device. The network delay is represented as T_d for both the forward and the return pathes.

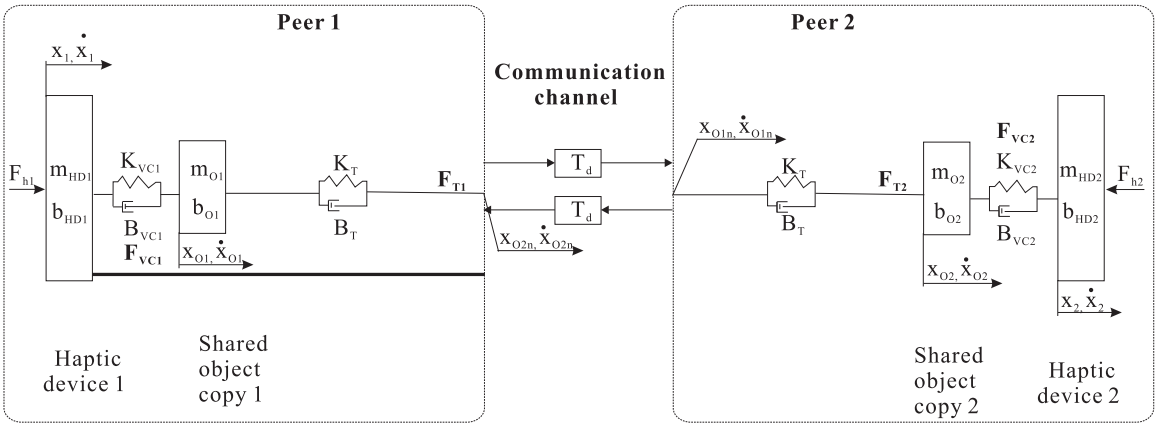

Figure 5.1: The Peer-to-Peer Scheme with Virtual Coupling Controller.

In this control architecture, the two copies of the shared virtual object are connected through a virtual coupling controller. The mass of the shared virtual object is equally divided between the two cube copies. The damping of the shared virtual object is inherited by the two cube copies. The interaction forces applied on the haptic devices and on the copies of the shared virtual object are given in Equations (5.1) to (5.8):

- for the peer haptic devices:

$$F_{\mathrm{h1}} - F_{\mathrm{VC1}} = m_{\mathrm{HD1}}\ddot{x}_1 + b_{\mathrm{HD1}}\dot{x}_1 \tag{5.1}$$

$$F_{\mathrm{h2}} - F_{\mathrm{VC2}} = m_{\mathrm{HD2}}\ddot{x}_2 + b_{\mathrm{HD2}}\dot{x}_2 \tag{5.2}$$

- for the copies of the shared virtual object:

$$F_{\mathrm{VC1}} - F_{\mathrm{T1}} = m_{\mathrm{O1}}\ddot{x}_{\mathrm{O1}} + b_{\mathrm{O}i}\dot{x}_{\mathrm{O1}} \tag{5.3}$$

$$F_{\mathrm{VC2}} - F_{\mathrm{T2}} = m_{\mathrm{O2}}\ddot{x}_{\mathrm{O2}} + b_{\mathrm{O2}}\dot{x}_{\mathrm{O2}} \tag{5.4}$$

where:

$$F_{\mathrm{VC1}} = K_{\mathrm{VC1}}(x_1 - x_{\mathrm{O1}}) + B_{\mathrm{VC1}}(\dot{x}_1 - \dot{x}_{\mathrm{O1}}) \tag{5.5}$$

$$F_{\mathrm{VC2}} = K_{\mathrm{VC1}}(x_2 - x_{\mathrm{O2}}) + B_{\mathrm{VC1}}(\dot{x}_2 - \dot{x}_{\mathrm{O2}}) \tag{5.6}$$

$$F_{\mathrm{T1}} = K_{\mathrm{T}}(x_{\mathrm{O1}} - x_{\mathrm{O2}_n}) + B_{\mathrm{T}}(\dot{x}_{\mathrm{O1}} - \dot{x}_{\mathrm{O2}_n}) \tag{5.7}$$

$$F_{\mathrm{T2}} = K_{\mathrm{T}}(x_{\mathrm{O2}} - x_{\mathrm{O1}_n}) + B_{\mathrm{T}}(\dot{x}_{\mathrm{O2}} - \dot{x}_{\mathrm{O1}_n}) \tag{5.8}$$

With the virtual coupling connection between the cube copies, this control architecture maintains control stability in the presence of constant and time-varying network delay. While achieving higher performance in position coherency between the copies of the shared virtual object, increasingly larger network delay leads to latent response of position and velocity signals from the peer sides, which makes the users feel that the shared virtual object become heavier accordingly.

5.1.2 Reference Control Architecture 2: Distributed Control Architecture [2]

As shown in Figure 5.2, the distributed control architecture in [2] transmits to the peer sides the positions and the velocities of the haptic devices in addition to the positions and the velocities of copies of the shared virtual object. Therefore, the haptic devices are kinematically represented at their remote peers' sides, which enables haptic rendering of direct user-to-user interaction among the cooperative users.

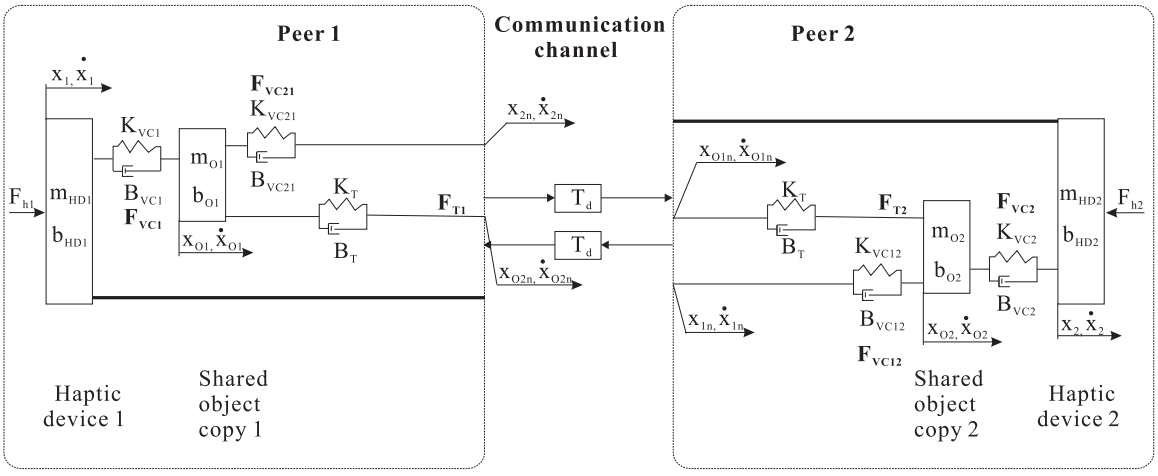

Figure 5.2: The Distributed Control Architecture in [2].

As in the Reference Control Architecture 1, the two copies of the shared virtual

object are connected through a virtual coupling controller. The mass of the shared virtual object is equally divided between the two cube copies. The damping of the shared virtual object is inherited by the two copies. The interaction forces applied on the haptic devices and on the copies of the shared virtual object are given by Equations (5.9) to (5.18):

- for the peer haptic devices:

$$F_{\mathrm{h1}} - F_{\mathrm{VC1}} = m_{\mathrm{HD1}}\ddot{x}_1 + b_{\mathrm{HD1}}\dot{x}_1 \tag{5.9}$$

$$F_{\mathrm{h2}} - F_{\mathrm{VC2}} = m_{\mathrm{HD2}}\ddot{x}_2 + b_{\mathrm{HD2}}\dot{x}_2 \tag{5.10}$$

- for the local copies of the shared virtual object:

$$F_{\mathrm{VC1}} - F_{\mathrm{T1}} + F_{\mathrm{VC21}} = m_{\mathrm{O1}}\ddot{x}_{\mathrm{O1}} + b_{\mathrm{O1}}\dot{x}_{\mathrm{O1}} \tag{5.11}$$

$$F_{\mathrm{VC2}} - F_{\mathrm{T2}} + F_{\mathrm{VC12}} = m_{\mathrm{O2}}\ddot{x}_{\mathrm{O2}} + b_{\mathrm{O2}}\dot{x}_{\mathrm{O2}} \tag{5.12}$$

where:

$$F_{\mathrm{VC1}} = K_{\mathrm{VC1}}(x_1 - x_{\mathrm{O1}}) + B_{\mathrm{VC1}}(\dot{x}_1 - \dot{x}_{\mathrm{O1}}) \tag{5.13}$$

$$F_{\mathrm{VC2}} = K_{\mathrm{VC2}}(x_2 - x_{\mathrm{O2}}) + B_{\mathrm{VC2}}(\dot{x}_2 - \dot{x}_{\mathrm{O2}}) \tag{5.14}$$

$$F_{\mathrm{T1}} = K_{\mathrm{T}}(x_{\mathrm{O1}} - x_{\mathrm{O2}_n}) + B_{\mathrm{T}}(\dot{x}_{\mathrm{O1}} - \dot{x}_{\mathrm{O2}_n}) \tag{5.15}$$

$$F_{\mathrm{T2}} = K_{\mathrm{T}}(x_{\mathrm{O2}} - x_{\mathrm{O1}_n}) + B_{\mathrm{T}}(\dot{x}_{\mathrm{O2}} - \dot{x}_{\mathrm{O1}_n}) \tag{5.16}$$

$$F_{\mathrm{VC12}} = K_{\mathrm{VC12}}(x_{1_n} - x_{\mathrm{O2}}) + B_{\mathrm{VC12}}(\dot{x}_{1_n} - \dot{x}_{\mathrm{O2}}) \tag{5.17}$$

$$F_{\mathrm{VC21}} = K_{\mathrm{VC21}}(x_{2_n} - x_{\mathrm{O1}}) + B_{\mathrm{VC21}}(\dot{x}_{2_n} - \dot{x}_{\mathrm{O1}}) \tag{5.18}$$

In Figure 5.2, $m_{\mathrm{HD}i}$ and $b_{\mathrm{HD}i}$ are the mass and the damping of the i-th haptic interface; $m_{\mathrm{O}i}$ and $b_{\mathrm{O}i}$ are the mass and the damping of Peer i's copy of the shared virtual object; $K_{\mathrm{VC}i}$ and $B_{\mathrm{VC}i}$ are the stiffness and the damping of the contact between Peer i and its copy of the virtual object; $F_{\mathrm{VC}i}$ is the interaction force between Peer i and its copy of the virtual object; K_{T} and B_{T} are the stiffness and the damping of coordinating virtual coupling controller between the distributed copies of the shared virtual object; $F_{\mathrm{VC}i}$ is the coordinating force between the distributed copies of the shared virtual object; $K_{\mathrm{VC}ij}$ and $B_{\mathrm{VC}ij}$ are the stiffness and the damping of the contact between the kinematic representation of Peer i and Peer j-th copy of the virtual object; $F_{\mathrm{VC}ij}$ is

the interaction force between the kinematic representation of Peer i and Peer j-th copy of the virtual object; x_i and $\dot{x}_i$ are the position and the velocity of the i-th haptic device; $x_{\mathrm{O}i}$ and $\dot{x}_{\mathrm{O}i}$ are the position and the velocity of Peer i's copy of the virtual object; x_{ij} and $\dot{x}_{ij}$ are the position and the velocity of the kinematic representation of Peer i in the virtual environment of Peer j; x_{i_n} and $\dot{x}_{i_n}$ are the position and the velocity commands sent by the i-th haptic device to their peers; $x_{\mathrm{O}i_n}$ and $\dot{x}_{\mathrm{O}i_n}$ are the position and velocity commands sent by Peer i's copy of the virtual object to the peer users; lastly, $F_{\mathrm{h}i}$ is the force applied by the i-th user to their device. Since $F_{\mathrm{VC}i}$ and $F_{\mathrm{VC}ij}$ represent contacts, they are unilateral forces activated by collision detection.

For direct user-to-user contact, the Reference Control Architecture 2 is shown in Figure 5.3, and the dynamics of the interaction are given by Equations (5.19) to (5.22):

- for the peer haptic devices:

$$F_{\mathrm{h1}} - F_{\mathrm{VC1}} = m_{\mathrm{HD1}}\ddot{x}_1 + b_{\mathrm{HD1}}\dot{x}_1 \tag{5.19}$$

$$F_{\mathrm{h2}} - F_{\mathrm{VC2}} = m_{\mathrm{HD2}}\ddot{x}_2 + b_{\mathrm{HD2}}\dot{x}_2 \tag{5.20}$$

where:

$$F_{\mathrm{VC1}} = K_{\mathrm{VC1}}(x_1 - x_{2_n}) + B_{\mathrm{VC1}}(\dot{x}_1 - \dot{x}_{2_n}) \tag{5.21}$$

$$F_{\mathrm{VC2}} = K_{\mathrm{VC2}}(x_2 - x_{1_n}) + B_{\mathrm{VC2}}(\dot{x}_2 - \dot{x}_{1_n}) \tag{5.22}$$

5.1.3 Reference Control Architecture 3: Peer-to-Peer Scheme with Wave Variable Delay Compensation [1]

The peer-to-peer scheme with wave variable delay compensation (Figure 5.4) employs wave-based control to coordinate the copies of the shared virtual object. In this scheme, the positions and the velocities of the copies of the shared virtual object $x_{\mathrm{O}i_d}$ and $\dot{x}_{\mathrm{O}i_d}$ are transmitted in the form of wave variables $U_{\mathrm{out}O_i}$ and $u_{\mathrm{out}O_i}$ by Peer i's copy of the virtual object to the peer user. This scheme renders realistic forces during cooperative manipulation of the shared virtual object at the expense of low position coherency between the copies of the shared virtual object. The interaction forces applied on the haptic devices and on the copies of the shared virtual object are given by Equations (5.23) to (5.30):

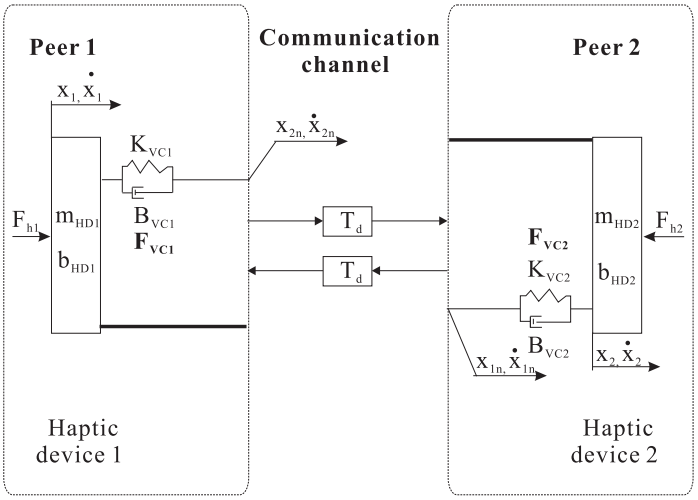

Figure 5.3: The Distributed Control Architecture in [2], applied to direct user-to-user contact.

- for the peer haptic devices:

$$F_{\mathrm{h1}} - F_{\mathrm{VC1}} = m_{\mathrm{HD1}}\ddot{x}_1 + b_{\mathrm{HD1}}\dot{x}_1 \tag{5.23}$$

$$F_{\mathrm{h2}} - F_{\mathrm{VC2}} = m_{\mathrm{HD2}}\ddot{x}_2 + b_{\mathrm{HD2}}\dot{x}_2 \tag{5.24}$$

- for the copies of the shared virtual object:

$$F_{\mathrm{VC1}} - F_{\mathrm{T1}} = m_{\mathrm{O1}}\ddot{x}_{\mathrm{O1}} + b_{\mathrm{O1}}\dot{x}_{\mathrm{O1}} \tag{5.25}$$

$$F_{\mathrm{VC2}} - F_{\mathrm{T2}} = m_{\mathrm{O2}}\ddot{x}_{\mathrm{O2}} + b_{\mathrm{O2}}\dot{x}_{\mathrm{O2}} \tag{5.26}$$

where:

$$F_{\mathrm{VC1}} = K_{\mathrm{VC1}}(x_1 - x_{\mathrm{O1}}) + B_{\mathrm{VC1}}(\dot{x}_1 - \dot{x}_{\mathrm{O1}}) \tag{5.27}$$

$$F_{\mathrm{VC2}} = K_{\mathrm{VC2}}(x_2 - x_{\mathrm{O2}}) + B_{\mathrm{VC2}}(\dot{x}_2 - \dot{x}_{\mathrm{O2}}) \tag{5.28}$$

$$F_{\mathrm{T1}} = K_{\mathrm{T}}(x_{\mathrm{O1}} - x_{\mathrm{O2}_d}) + B_{\mathrm{T}}(\dot{x}_{\mathrm{O1}} - \dot{x}_{\mathrm{O2}_d}) \tag{5.29}$$

$$F_{\mathrm{T2}} = K_{\mathrm{T}}(x_{\mathrm{O2}} - x_{\mathrm{O1}_d}) + B_{\mathrm{T}}(\dot{x}_{\mathrm{O2}} - \dot{x}_{\mathrm{O1}_d}) \tag{5.30}$$

In [1], the wave variables are only used to transmit the velocity signals. However, this dissertation will implement all wave-based controllers to transmit the wave integral for the positions in addition to wave signals. For programming simplicity,

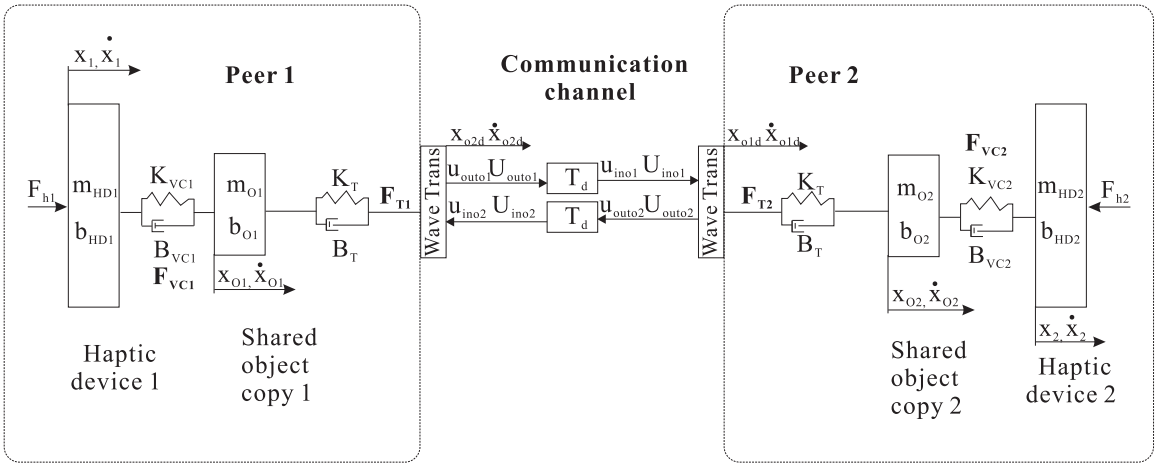

Figure 5.4: The Peer-to-Peer Scheme with Wave Variable Delay Compensation.

these wave-based controllers employ the peer-to-peer symmetric configuration of wave variable control introduced in Chapter 4.

5.2 Experiment Setup

Figure 5.5 illustrates the experimental networked haptic cooperation system. The system comprises two FALCON NOVINT haptic devices respectively connected to two personal computers. One computer runs Window XP on an Intel Core 2 Duo CPU at 2.67GHz with 2 GB RAM. The other computer runs Window Vista on an Intel Core 2 Duo CPU at 1.67GHz with 3 GB RAM. The haptic devices provide three degrees of freedom (3 DOF) displacement sensing and force rendering and, thus, enable point interaction in 3 DOF virtual environments. The computers are located in the same laboratory, and can be screened from each other to prevent users from seeing each other's display. Copies of a shared virtual environment comprising a rigid cube in a rigid enclosure are generated on each computer as C++ console applications. The computers communicate over the network via the UDP protocol. In the following experiments, the network environment is simulated via the Wide Area Network Emulator (WANem) [60]. The WANem runs on a separate personal computer. The position sensing and force rendering rate of the FALCON NOVINT haptic devices is 1KHz. The data transmission rate is 128Hz.

The experiments in Section 5.3, Section 5.4 and Section 5.5 contrast: (1) the proposed control architectures to the reference control architectures, and (2) the two

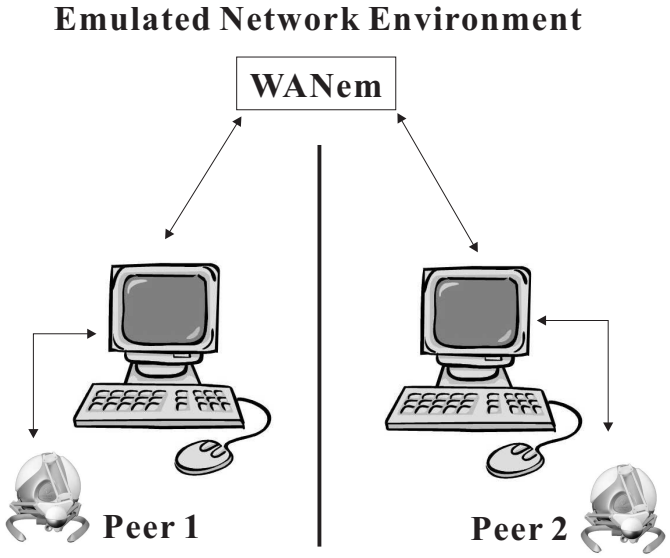

Figure 5.5: The experimental networked haptic cooperation system.

proposed control architectures against each other. In particular, the architectures involved in the experimental comparisons will be denoted as:

- **PCA 1**: the Proposed Control Architecture 1, i.e., the distributed control architecture with remote dynamic proxies and virtual coupling coordination;
- **PCA 2**: the Proposed Control Architecture 1, i.e., the distributed control architecture with remote dynamic proxies and wave-based coordination;
- **RCA 1**: the Reference Control Architecture 1, i.e., the peer-to-peer virtual coupling scheme in [1]);
- **RCA 2**: the Reference Control Architecture 2, i.e., the distributed control architecture in [2]);
- **RCA 3**: the Reference Control Architecture 3, i.e., the peer-to-peer scheme with wave variable delay compensation [1].

To ensure comparable experiments, some experiments replace the two human peers with forces applied to each FALCON NOVINT device through commands sent to motors via software. Effectively, this eliminates the inherent damping of the users' hands from the interaction. Since the two haptic interfaces are impedance type devices, the controlled forces have no stabilizing effect compared to user-applied forces. Such controlled experiments are used to investigate both the cooperative manipulation of a

shared virtual cube and the direct interaction between two remote users. Experiments with human users are also conducted for illustration purposes.

In all experiments in this chapter, general parameters are chosen consistently as: the mass of the virtual cube is $m_{\mathrm{O1}} = m_{\mathrm{O2}} = 0.5m_{\mathrm{O}} = 0.125$kg, and the mass of the remote dynamic proxies is $m_{\mathrm{HD1}} = m_{\mathrm{HD2}} = 0.01$kg; damping is incorporated neither in the remote dynamic proxies nor in the virtual cube, i.e., $b_{\mathrm{O1}} = b_{\mathrm{O2}} = b_{\mathrm{HD1}} = b_{\mathrm{HD2}} = 0$Ns/m; a constant network delay $T_d = 50$ ms is emulated via the WANem; $T_c = 1/1024$ s is the haptic rendering; $T_n = 1/128$ s is the network update rate.

In the cooperative manipulation experiments, the default parameters for the stiffness of the various controllers are: In the direct user-to-user interaction experiments,

Controller parameters	RCA 1	RCA 2	PCA 1	RCA 3	PCA 2
$K_{\mathrm{VC1}} = K_{\mathrm{VC2}}$ (N/m)	4000	4000	4000	4000	4000
$K_{\mathrm{VC21}} = K_{\mathrm{VC12}}$ (N/m)	N/A	2000	10000	N/A	10000
K_{T} (N/m)	2000	2000	2000	2000	2000
K_{RDP} (N/m)	N/A	N/A	1000	N/A	1000

Table 5.1: Default parameters of virtual coupling controllers for cooperative manipulation experiments.

the default parameters for the stiffness of the various controllers are: In all experi-

Controller parameters	RCA 2	PCA 1	PCA 2
$K_{\mathrm{VC1}} = K_{\mathrm{VC2}}$ (N/m)	2000	4000	4000
K_{RDP} (N/m)	N/A	1000	1000

Table 5.2: Default parameters of virtual coupling controllers for direct user to user interaction experiments.

ments, the damping of the various controllers are: $B_{\mathrm{VC1}} = B_{\mathrm{VC2}} = B_{\mathrm{VC21}} = B_{\mathrm{VC12}} = 3$Ns/m; $B_{\mathrm{T}} = 200$Ns/m; $B_{\mathrm{RDP}} = 200$Ns/m.

All experiments are conducted in a three dimensional shared virtual environment. The virtual environment includes a rigid enclosure that allows the users and the shared virtual object (a cube) to move only along the horizontal x-axis and thus, ensures the same initial conditions among successive experiments. In the controlled cooperative manipulation experiments, the two users are initially at rest and in contact with the shared virtual cube. Figure 5.6 is the snapshot of the initial conditions displayed to Peer 1. During the experiment, Peer 1 pushes the virtual cube and Peer 2 with a

constant controlled force $F_{h1} = 5$N, whereas Peer 2 applies no force onto the shared virtual cube.

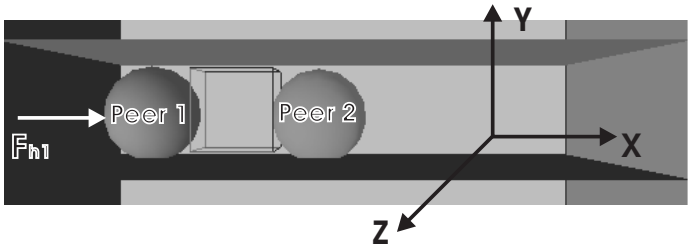

Figure 5.6: Snapshot of initial condition displayed to Peer 1 in the controlled cooperative manipulation experiments.

In the cooperative manipulation experiments with human users, the two human users are initially at rest and not in contact with the virtual cube, which is placed between them. Figure 5.7 is the snapshot of the initial conditions displayed to Peer 1. During the experiment, the two users initiate, maintain and break contact with the virtual cube. The users are instructed to perform the same manipulation during successive experiments.

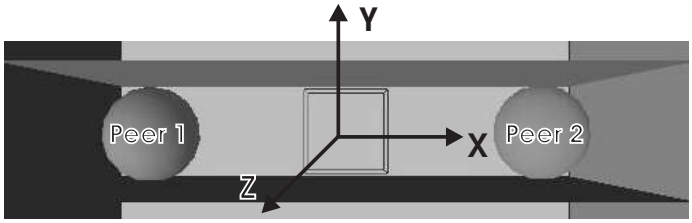

Figure 5.7: Snapshot of initial condition displayed to Peer 1 in the cooperative manipulation experiments with human users.

In the controlled experiments that investigate direct user-to-user interaction, the two users are initially at rest and in contact with each other. Figure 5.8 is the snapshot of the initial conditions displayed to Peer 1. During the experiment, Peer 1 pushes Peer 2 with a constant controlled force $F_{h1} = 5$N, whereas Peer 2 applies no force onto Peer 1.

In the experiments that investigate direct interaction between human users, the two users are initially at rest and not in contact with each other. Figure 5.9 is the snapshot of the initial conditions displayed to Peer 1. During the experiment, the

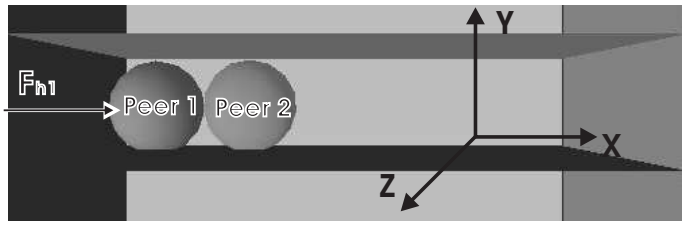

Figure 5.8: Snapshot of initial condition displayed to Peer 1 in controlled direct user-to-user interaction experiments.

two users initiate, maintain and break contact each other. The users are instructed to perform the same interaction during successive experiments.

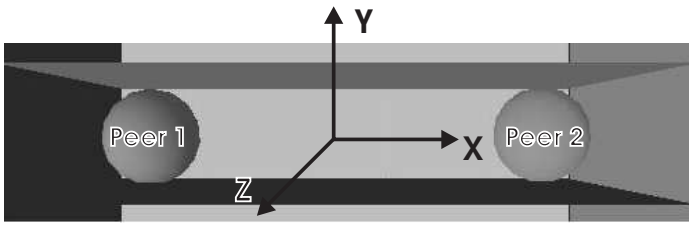

Figure 5.9: Snapshot of initial condition displayed to Peer 1 in direct user-to-user interaction with human users.

5.3 Experimental Comparison among the Reference Control Architecture 1, the Reference Control Architecture 2 and the Proposed Control Architecture 1

This section contrasts the Proposed Control Architecture 1 to the Reference Control Architecture 1 and to the Reference Control Architecture 2. Experiment I (Section 5.3.1) illustrates controlled cooperative manipulation. Experiment II (Section 5.3.2) demonstrates cooperative manipulation between two human users. Experiment III (Section 5.3.3) depicts controlled direct user-to-user interaction. Lastly, experiment IV (Section 5.3.4) presents direct user-to-user interaction between two human users. As the Reference Control Architecture 1 can not render direct user-to-user interaction,

only the Reference Control Architecture 2 and the Proposed Control Architecture 1 are employed in the Experiment III and Experiment IV.

5.3.1 Experiment I - Controlled Cooperative Manipulation of the Shared Virtual Cube

Section 5.3.1 contrasts the Proposed Control Architecture 1 to the Reference Control Architecture 1 and to the Reference Control Architecture 2 in controlled cooperative manipulation experiments. Figure 5.10, Figure 5.11 and Figure 5.12 demonstrate the position and the force feedback during controlled cooperative manipulation of the shared virtual cube via the Reference Control Architecture 1, via the Reference Control Architecture 2 and via the Proposed Control Architecture 1, respectively. The dynamics of all elements in the shared virtual environment and the task completion times demonstrate the features and the performance of the different control architectures. These figures show that the Proposed Control Architecture 1 renders the smoothest motion of the remote user, which results in smooth force feedback to the users. However, due to the virtual coupling coordination of the shared virtual object and of the remote dynamic proxies, the Proposed Control Architecture 1 renders a predominantly viscous virtual environment.

Figure 5.13 shows the position coherency performance of the three control architectures with virtual coupling coordination. As Figure 5.13 illustrates, the much higher stiffness of the remote contact helps the Proposed Control Architecture 1 to achieve better performance than that of the Reference Control Architecture 1 in coordinating the distributed cube copies. This performance is comparable to the performance of the Reference Control Architecture 2. Among the three control architectures in comparison, the Proposed Control Architecture 1 leads to the longest task completion time. This result confirms that virtual couplers implemented over communication channels with network delay add viscous damping to the simulated virtual elements that they connect [2].

5.3.2 Experiment II - Cooperative Manipulation of the Shared Virtual Cube by Human Users

Section 5.3.2 contrasts the Proposed Control Architecture 1 to the Reference Control Architecture 1 and to the Reference Control Architecture 2 through cooperative

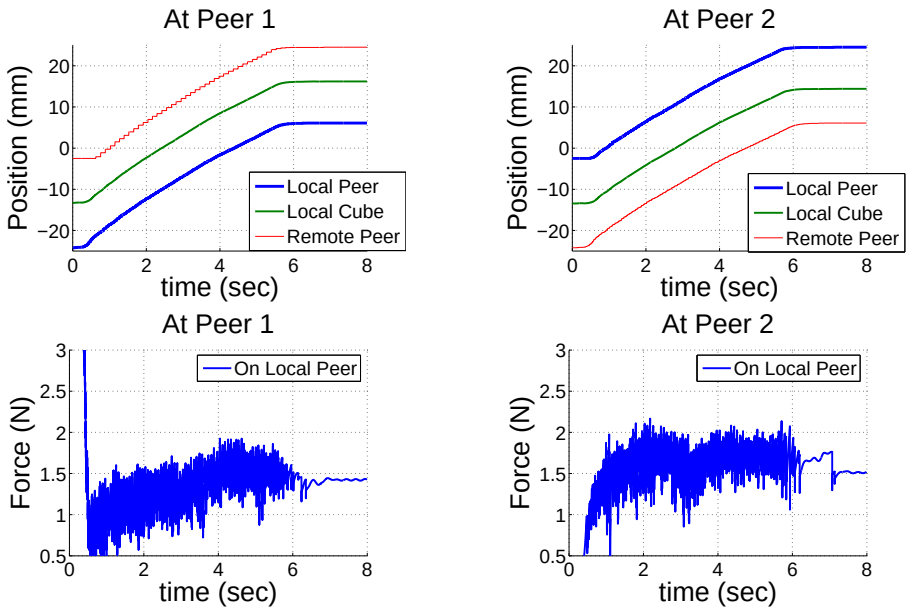

Figure 5.10: Controlled cooperative manipulation of the shared virtual cube, rendered via the Reference Control Architecture 1. $K_{\mathrm{VC1}} = K_{\mathrm{VC2}} = 4000\mathrm{N/m}$, $K_{\mathrm{T}} = 2000$ N/m.

manipulations of the virtual cube performed by with human users. Figure 5.14, Figure 5.15 and Figure 5.16 demonstrate the position and the force feedback rendered by the Reference Control Architecture 1, by the Reference Control Architecture 2 and by the Proposed Control Architecture 1, respectively. These figures confirm that Proposed Control Architecture 1: (1) renders smooth motion of the remote users; and (2) renders a predominantly viscous virtual environment.

Figure 5.17 shows the position coherency performance of the three control architectures that use virtual coupling coordination during cooperative manipulation of a shared virtual cube by two human users. The experimental results in this figure confirm the conclusion in Section 5.3.2: the remote dynamic proxies help the Proposed Control Architecture 1 to achieve higher position coherency than the Reference Control Architecture 1 and this performance is comparable to that of Reference Control Architecture 2.

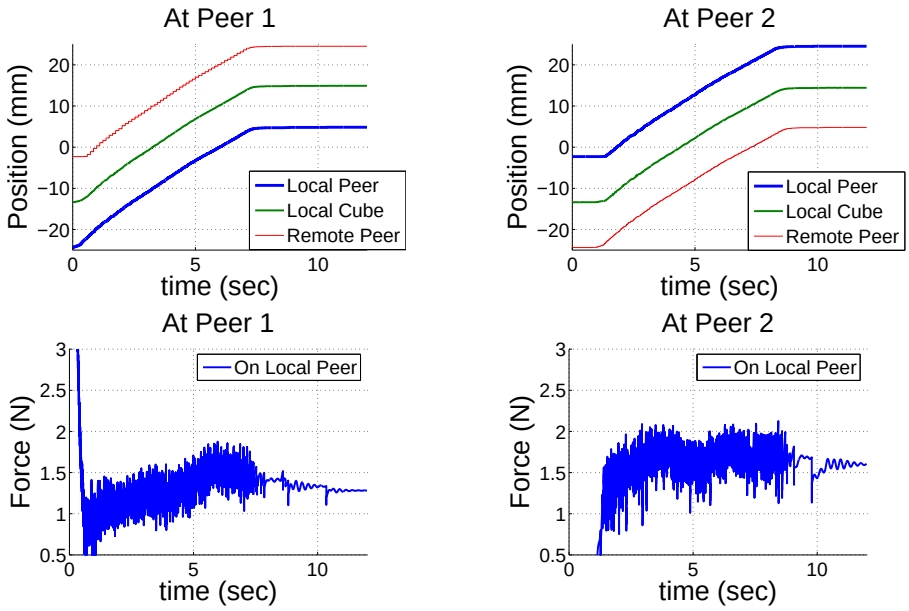

Figure 5.11: Controlled cooperative manipulation of the shared virtual cube, rendered via the Reference Control Architecture 2. $K_{\mathrm{VC1}} = K_{\mathrm{VC2}} = 4000\mathrm{N/m}$,$K_{\mathrm{VC21}} = K_{\mathrm{VC12}} = 2000\mathrm{N/m}$, $K_{\mathrm{T}} = 2000$ N/m.

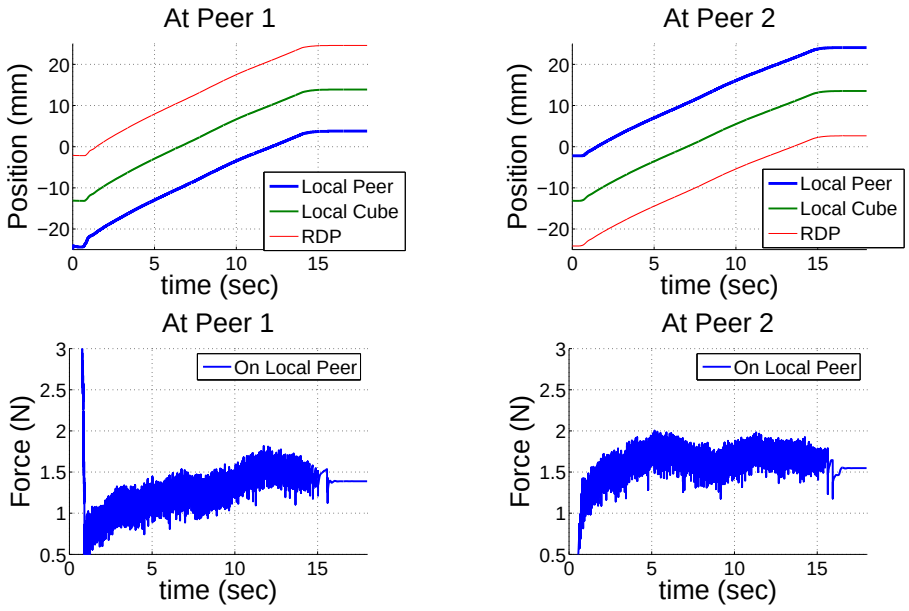

Figure 5.12: Controlled cooperative manipulation of the shared virtual cube, rendered via the Proposed Control Architecture 1. $K_{\mathrm{VC1}} = K_{\mathrm{VC2}} = 4000\mathrm{N/m}$, $K_{\mathrm{VC21}} = K_{\mathrm{VC12}} = 10000\mathrm{N/m}$, $K_{\mathrm{T}} = 2000\mathrm{N/m}$, $K_{\mathrm{RDP}} = 1000\mathrm{Ns/m}$.

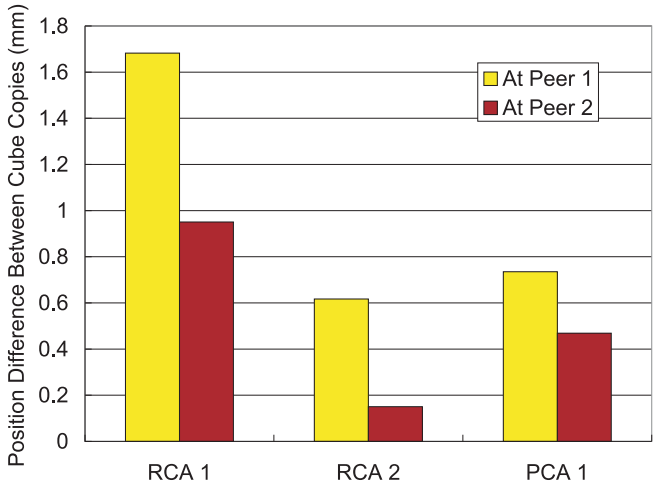

Figure 5.13: Position coherency for Cooperative Manipulation with controlled forces rendered (1) via the Reference Control Architecture 1 (RCA 1), (2) via the Reference Control Architecture 2 (RCA 2), and (3) via the Proposed Control Architecture 1 (PCA 1).

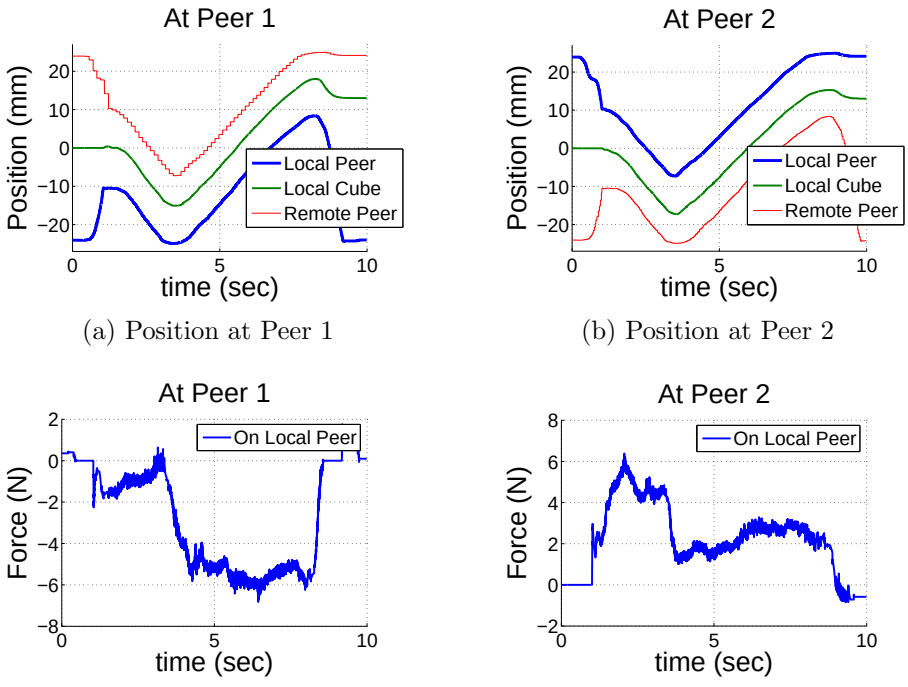

(a) Position at Peer 1

(b) Position at Peer 2

(c) Direct Force applied to Peer 1

(d) Direct Force applied to Peer 2

Figure 5.14: Cooperative manipulation of the shared virtual cube by human users, rendered via the Reference Control Architecture 1. $K_{\mathrm{VC1}} = K_{\mathrm{VC2}} = 4000\mathrm{N/m}$, $K_{\mathrm{T}} = 2000$ N/m.

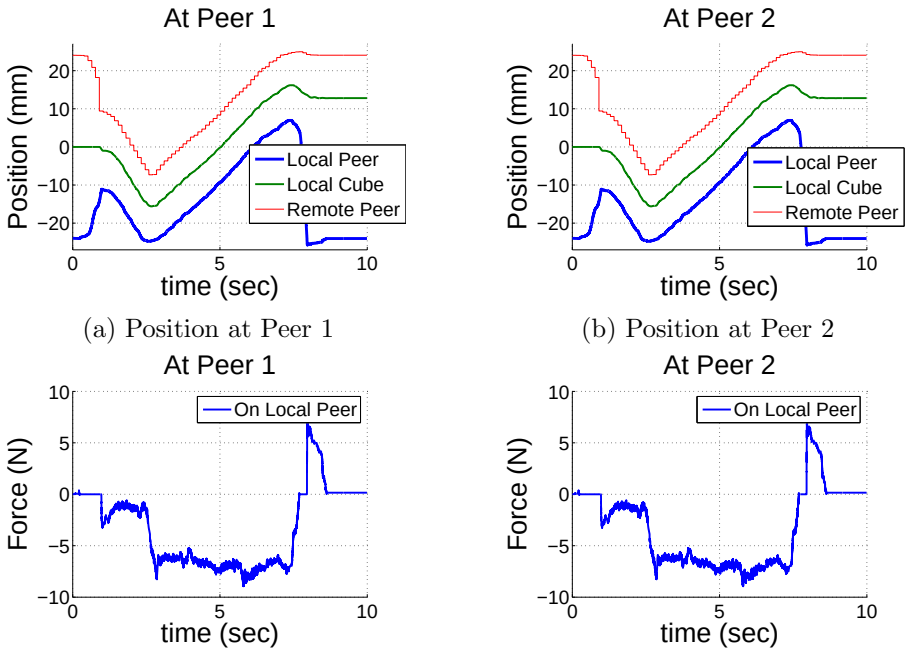

(a) Position at Peer 1

(b) Position at Peer 2

(c) Direct Force applied to Peer 1

(d) Direct Force applied to Peer 2

Figure 5.15: Cooperative manipulation of the shared virtual cube by human users, rendered via the Reference Control Architecture 2. $K_{\mathrm{VC1}} = K_{\mathrm{VC2}} = 4000\mathrm{N/m}$,$K_{\mathrm{VC21}} = K_{\mathrm{VC12}} = 2000\mathrm{N/m}$, $K_{\mathrm{T}} = 2000$ N/m.

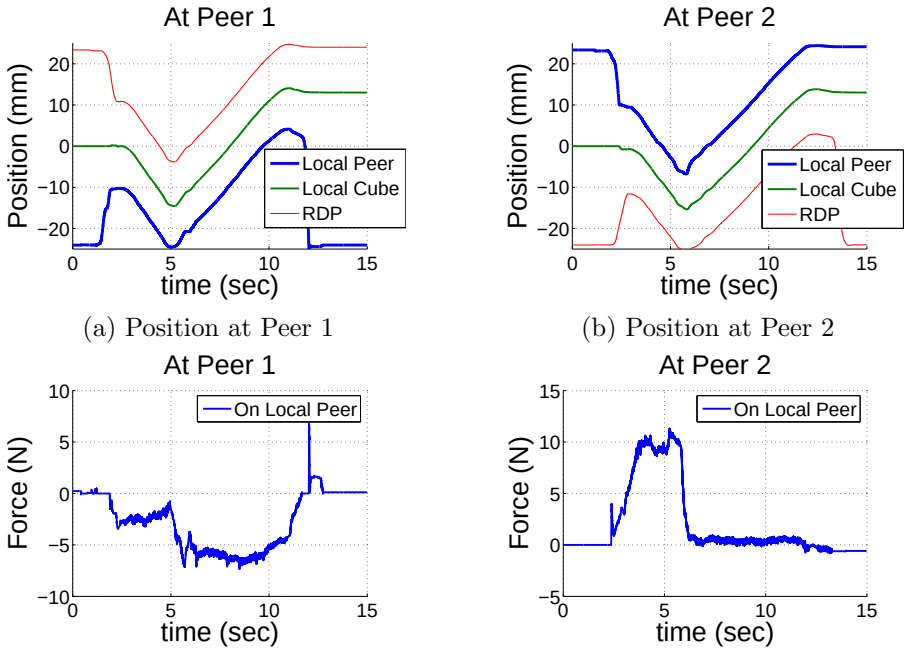

(a) Position at Peer 1

(b) Position at Peer 2

(c) Direct Force applied to Peer 1

(d) Direct Force applied to Peer 2

Figure 5.16: Cooperative manipulation of the shared virtual cube by human users, rendered via the Proposed Control Architecture 1. $K_{\mathrm{VC1}} = K_{\mathrm{VC2}} = 4000\mathrm{N/m}$, $K_{\mathrm{VC21}} = K_{\mathrm{VC12}} = 10000\mathrm{N/m}$, $K_{\mathrm{T}} = 2000\mathrm{N/m}$, $K_{\mathrm{RDP}} = 1000\mathrm{Ns/m}$.

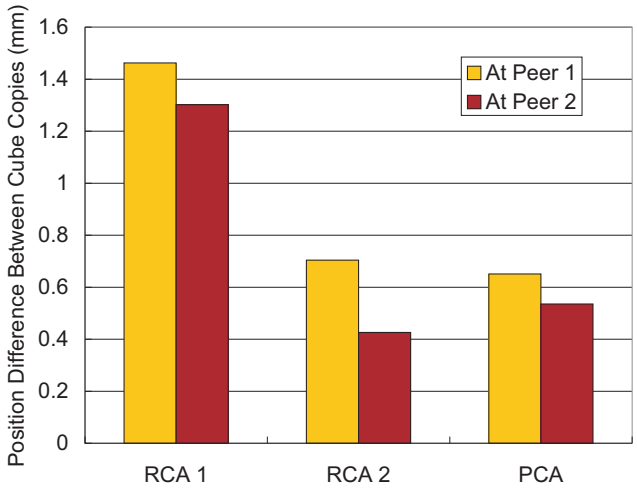

Figure 5.17: Position coherency in Cooperative Manipulation with human users rendered (1) via the Reference Control Architecture 1 (RCA 1), (2) via the Reference Control Architecture 2 (RCA 2), and (3) via the Proposed Control Architecture 1 (PCA 1).

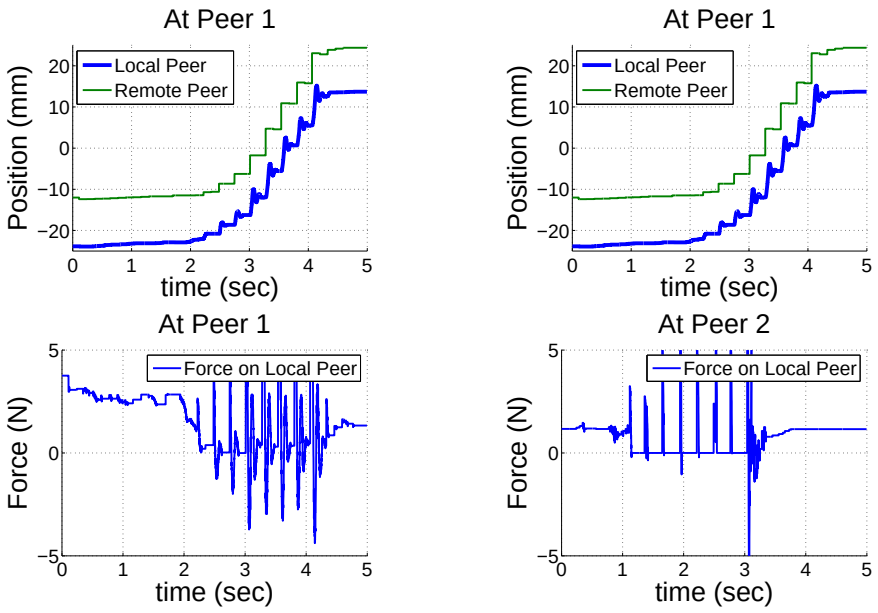

Figure 5.18: Controlled direct user-to-user interaction, rendered via the Reference Control Architecture 2. $K_{\mathrm{VC1}} = K_{\mathrm{VC2}} = 2000\mathrm{N/m}$, $T_d = 50$ ms

5.3.3 Experiment III - Controlled Direct User-to-User Interaction

This section illustrates the position and the force feedback during controlled direct user-to-user interaction rendered via the Reference Control Architecture 2 (Figure 5.18) and via the Proposed Control Architecture 1 (Figure 5.19), respectively[1]. These figures show that the Proposed Control Architecture 1 renders smooth motion of the remote user, which results in the smooth force feedback applied to the users. The discontinuous motion of the remote users rendered by the Reference Control Architecture 2 prevents it from rendering high contact stiffness during direct user-to-user interaction. As Figure 5.18 shows, the interaction rendered via the Reference Control Architecture 2 is stable for a contact stiffness of up to 2000 N/m, although the motion of the remote users is perceived as discontinuous. However, the Proposed Control Architecture 1 maintains the interaction stable for a contact stiffness of up to 4000 N/m in the presence of 50 ms constant network delay. For the same contact stiffness and network delay, the interaction becomes unstable when rendered via the Reference Control Architecture 2.

[1]Note that the Reference Control Architecture 1 cannot render direct user-to-user interaction.

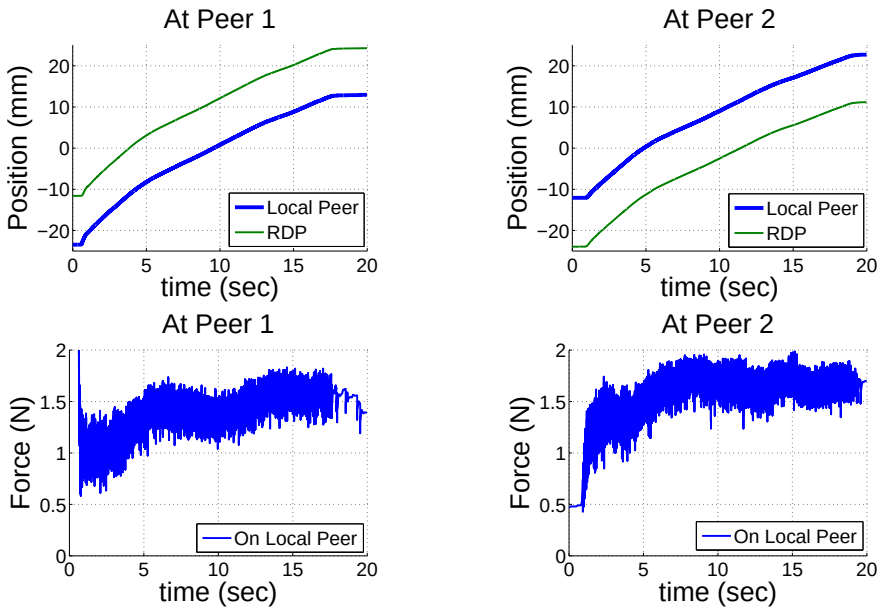

Figure 5.19: Controlled direct user-to-user interaction, rendered via the Proposed Control Architecture 1. $K_{\mathrm{VC1}} = K_{\mathrm{VC2}} = 4000\mathrm{N/m}$, $K_{\mathrm{RDP}} = 1000\mathrm{Ns/m}$, $T_d = 50$ ms

5.3.4 Experiment IV - Direct Interaction between Human Users

This section illustrates the position and the force feedback during direct interaction between two human users rendered via the Reference Control Architecture 2 (Figure 5.20) and via the Proposed Control Architecture 1 (Figure 5.21), respectively. As shown in Figure 5.21, direct user-to-user contact via the Proposed Control Architecture 1 can achieve higher contact stiffness (4000 N/m) with smooth rendering of user motion and of forces. The Reference Control Architecture 2 renders discontinuous forces and users motion even with much lower contact stiffness (2000 N/m), as shown in Figure 5.20.

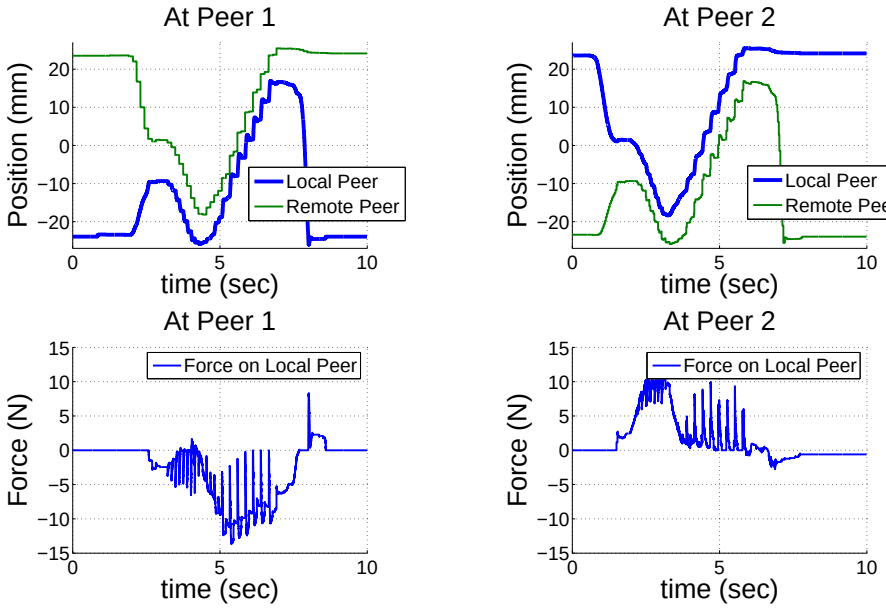

Figure 5.20: Direct interaction between human users, rendered via the Reference Control Architecture 2. $K_{\mathrm{VC1}} = K_{\mathrm{VC2}} = 2000\mathrm{N/m}$.

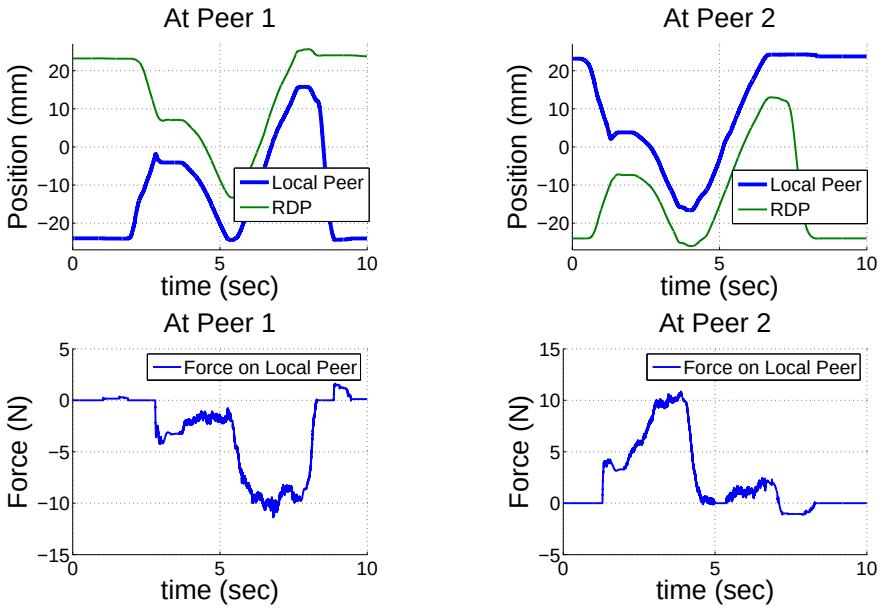

Figure 5.21: Direct interaction between human users, rendered via the Proposed Control Architecture 1. $K_{\mathrm{VC1}} = K_{\mathrm{VC2}} = 4000\mathrm{N/m}$, $K_{\mathrm{RDP}} = 1000\mathrm{Ns/m}$.

5.4 Experimental Comparison between the Reference Control Architecture 3 and the Proposed Control Architecture 2

In this section, the Proposed Control Architecture 2 is contrasted to the Reference Control Architecture 3. In cooperative manipulation experiments, Experiment I (Section 5.4.1) involves the controlled force and Experiment II (Section 5.4.2) involves human users. As the Reference Control Architecture 3 cannot render direct user-to-user contact, experiments involving direct interaction between human users are only presented for the Proposed Control Architecture 2. All wave-based controllers in the Reference Control Architecture 3 and the Proposed Control Architecture 2 employ a wave impedance of $b = 50$ N/m.

5.4.1 Experiment I - Controlled Cooperative Manipulation of the Shared Virtual Cube

In this section, Figure 5.22 and Figure 5.23 demonstrate controlled cooperative manipulation of the shared virtual cube via the Reference Control Architecture 3 and via the Proposed Control Architecture 2 in the presence of 50 ms constant network delay, respectively. The experiment is later repeated for various constant network delays. Figure 5.24 demonstrates the position coherency performance (1) via the Reference Control Architecture 3 and (2) via the Proposed Control Architecture 2. While the Reference Control Architecture 3 (RCA 3) generally renders an average position difference of 3.62 mm between cube copies, the Proposed Control Architecture 2 (PCA 2) maintains an average position difference of 1.30 mm between the cube copies for the various constant network delays.

Note that with the wave-based coordination, both the Reference Control Architecture 3 and the Proposed Control Architecture 2 can render stable cooperative manipulation in the presence of long network delay (for example $T_d = 400$ ms as in Figure 5.25 and in Figure 5.26). For a network delay of $T_d = 400$ ms, all control architectures with virtual coupling coordination are unstable.

When Peer 1 pushes the shared virtual cube and Peer 2 with a constant hand force, the control architectures with wave-based coordination lead to parabolic user trajectories instead of the linear user trajectories rendered by the control architectures

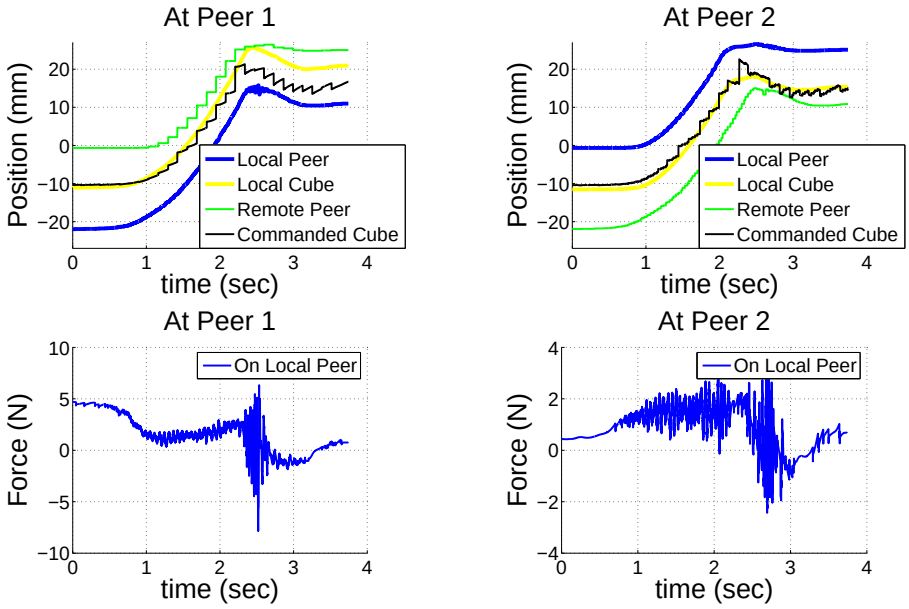

Figure 5.22: Controlled cooperative manipulation of the shared virtual cube, rendered via the Reference Control Architecture 3. $T_d = 50$ ms.

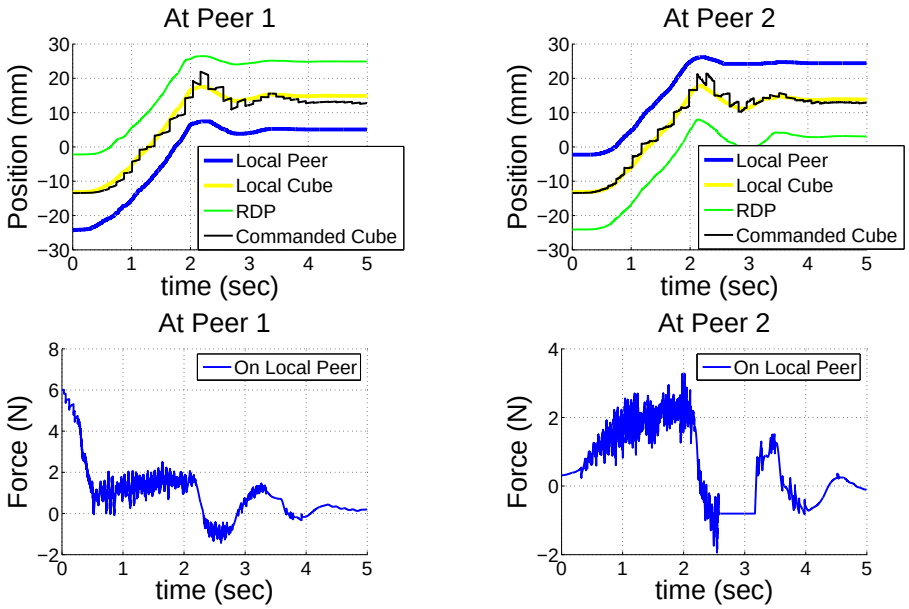

Figure 5.23: Controlled cooperative manipulation of the shared virtual cube, rendered via the Proposed Control Architecture 2. $T_d = 50$ ms.

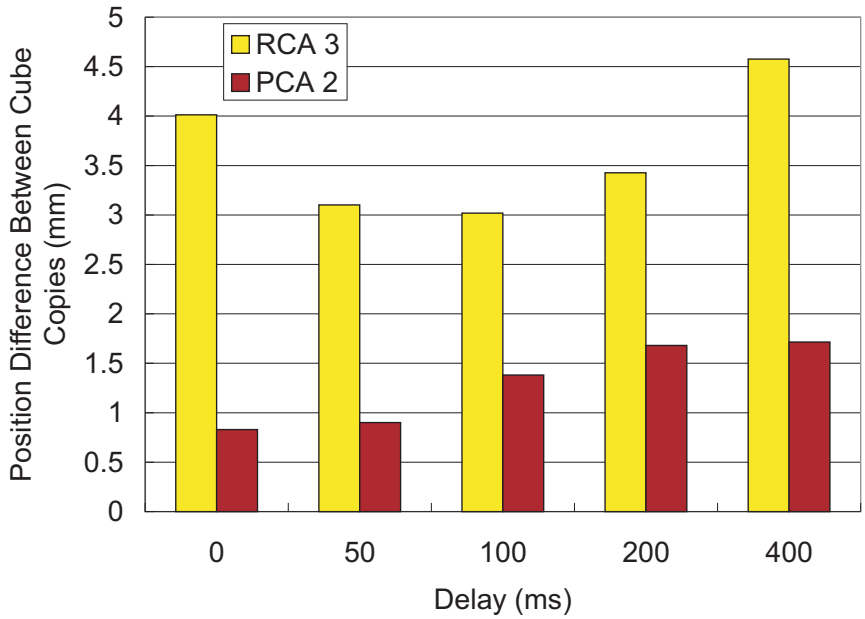

Figure 5.24: Position coherency in cooperative manipulation controlled force rendered (1) via the Reference Control Architecture 3 and (2) via the Proposed Control Architecture 2

with virtual coupling control. The parabolic user trajectories demonstrate that users perceive a predominantly inertial virtual environment when their networked haptic cooperation is rendered using wave-based coordination. As the shared virtual object and the two peer users in the experiments in this chapter are designed to be pure masses in free space. It follows that wave-based coordination of networked haptic cooperation renders the dynamics of the virtual environment more realistically than virtual coupling coordination.

Figure 5.27 shows the mass rendered during cooperative manipulation (1) via the Reference Control Architecture 3 and (2) via the Proposed Control Architecture 2. In this experiment, Peer 1 pushes a mass of 0.45 kg (labeled as "Expectance" in Figure 5.27) in free space, i.e. the sum of the mass of the shared virtual cube and the mass of Peer 2. Both control architectures with wave-based coordination render mass that varies with the network delay. However, the mass perceived via the Proposed Control Architecture 2 varies less with the network delay and deviates less from the theoretical expectance.

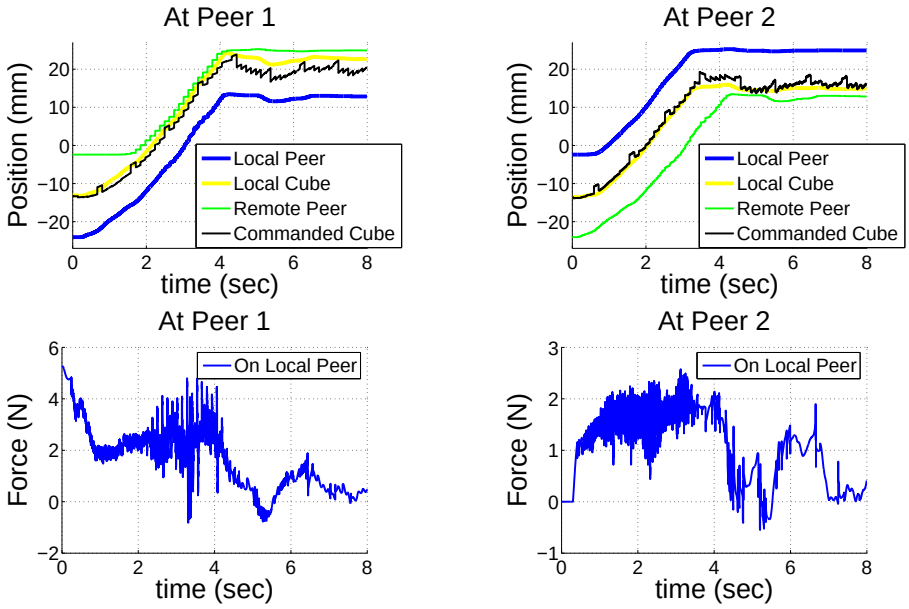

Figure 5.25: Controlled cooperative manipulation of the shared virtual cube, rendered via the Reference Control Architecture 3. $T_d = 400$ ms.

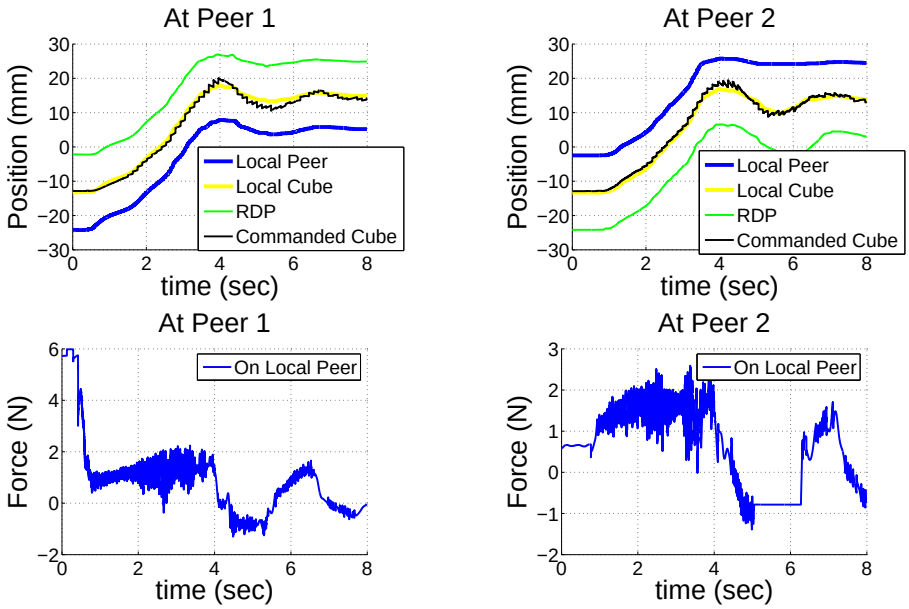

Figure 5.26: Controlled cooperative manipulation of the shared virtual cube, rendered via the Proposed Control Architecture 2. $T_d = 400$ ms.

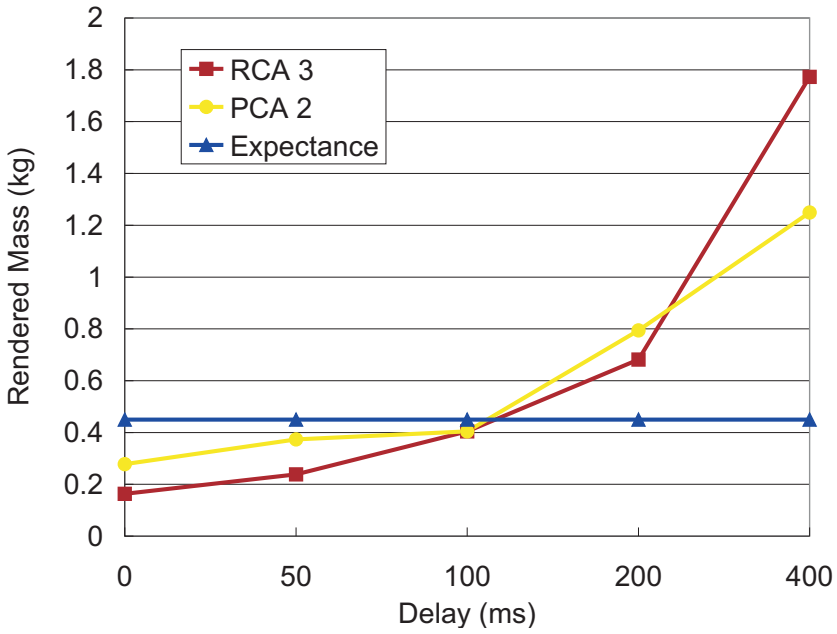

Figure 5.27: Perceived mass in controlled cooperative manipulation rendered (1) via the Reference Control Architecture 3 and (2) via the Proposed Control Architecture 2.

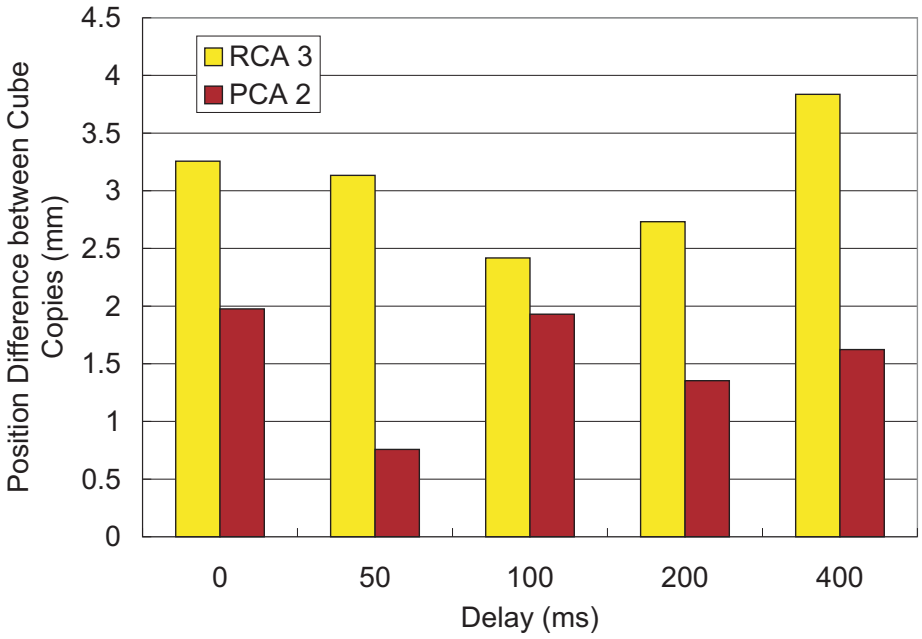

Figure 5.28: Position coherency in cooperative manipulation of the shared virtual cube by human users rendered (1) via the Reference Control Architecture 3 and (2) via the Proposed Control Architecture 2.

5.4.2 Experiment II - Cooperative Manipulation of the Shared Virtual Cube by Human Users

Section 5.4.2 contrasts the Proposed Control Architecture 2 to the Reference Control Architecture 3 in cooperative manipulation experiments with human users. Figure 5.28 illustrates the performance of the Proposed Control Architecture 2 and of the Reference Control Architecture 3 during cooperative manipulation of the shared virtual cube by two human users. This figure confirms that the the remote dynamic proxies help the Proposed Control Architecture 2 to improve the position coherency of the distributed cube copies. Note that both control architectures with wave-based controllers can render stable cooperative manipulation in the presence of long network delay ($T_d = 400$ ms).

5.4.3 Experiment III - Controlled Direct User-to-User Interaction

Figure 5.29 illustrates that controlled direct user-to-user interaction can be rendered via the Proposed Control Architecture 2 in the presence of constant network delays up to $T_d = 400$ ms. The Reference Control Architecture 3 cannot be used to render direct user-to-user interaction.

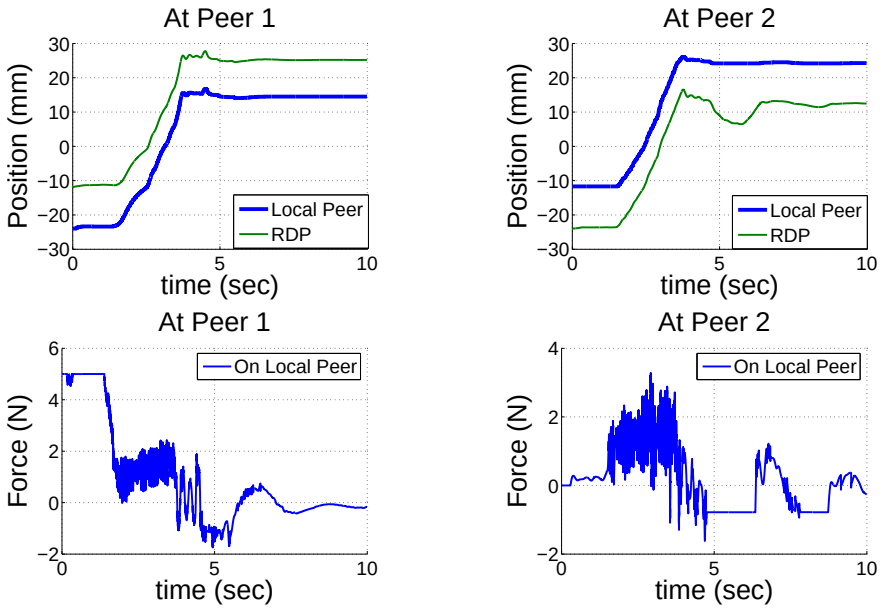

Figure 5.29: Controlled direct user-to-user interaction rendered via the Proposed Control Architecture 2. $T_d = 400$ ms.

5.4.4 Experiment IV - Direct Interaction between Human Users

Figure 5.30 validates that the Proposed Control Architecture 2 can render direct interaction between human users for constant network delays up to $T_d = 400$ ms.

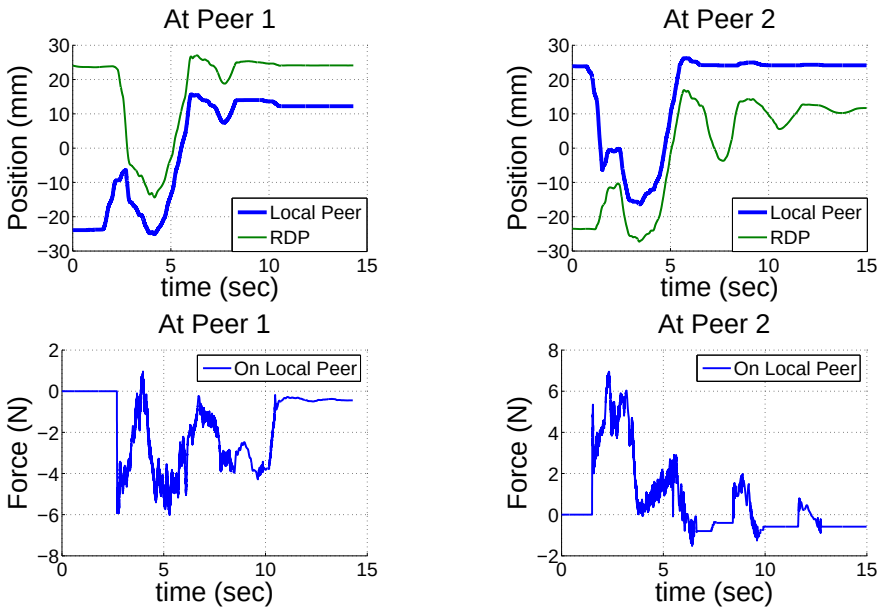

Figure 5.30: Direct interaction between human users, rendered via the Proposed Control Architecture 2, $T_d = 400$ ms.

5.5 Experimental Comparison between the Two Proposed Control Architectures with Remote Dynamic Proxies

This section compares the two distributed control architectures that integrate the remote dynamic proxies with the two different coordination controllers. The two architectures demonstrate their performance in cooperative manipulation as well as in the direct user-to-user interaction via the experimental networked haptic cooperation system shown in Figure 5.5.

In Experiment I (Section 5.5.1) and Experiment II (5.5.2), cooperative manipulation and direct user-to-user contact is implemented via the two distributed control architectures for different constant network delays. The performance of the two architectures is evaluated and compared from the perspective of: (1) maintaining position coherency among the distributed copies of the shared virtual object, and (2) realistic rendering of the dynamic properties of the shared virtual object in the presence of different constant network delays. In the cooperative manipulation experiments, Experiment I (Section 5.5.1) employs controlled forces and Experiment II (Section 5.5.2) involves human users. In addition, Experiment III (Section 5.5.3) shows that the Pro-

posed Control Architecture 2 maintains the interaction stable in the presence of longer constant network delay.

5.5.1 Experiment I - Experiments with Controlled Forces

This section demonstrates the haptic rendering of cooperative manipulation and of direct user-to-user interaction via the proposed control architectures in the presence of two constant network delays, $T_d = 50$ ms and $T_d = 100$ ms, respectively.

Figure 5.31 illustrates the position coherency performance for controlled cooperative manipulation of the shared virtual cube shown in Figure 5.6. As Figure 5.31 illustrates, both architectures achieve comparable position coherency performance.

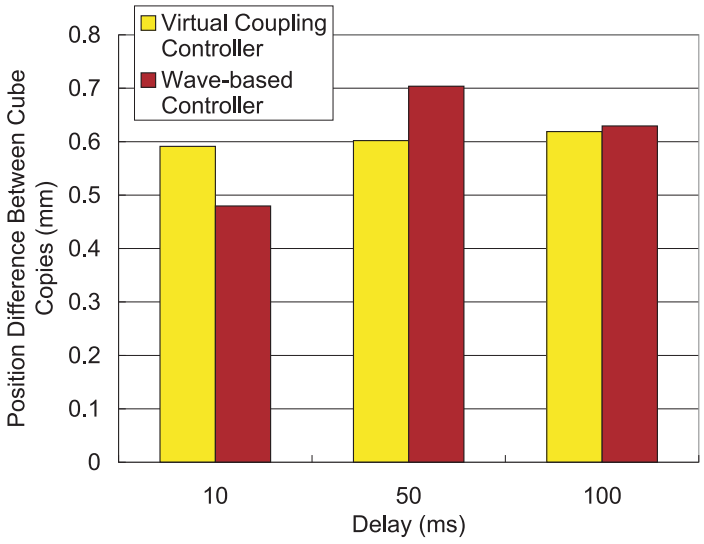

Figure 5.31: Position coherency in cooperative manipulation with controlled force rendered via the proposed control architectures with remote dynamic proxies governed (1) by the virtual coupling controller and (2) by wave-based controller.

Figure 5.32 and Figure 5.33 show the position and the force feedback during controlled cooperative manipulation of the shared virtual cube rendered via the Proposed Control Architecture 1 and the Proposed Control Architecture 2, respectively, in the presence of a constant network delay of 50 ms. Note that the architecture with virtual coupling leads to longer task completion time. This is because virtual couplers implemented over communication channels with delay add viscous damping to the simulated elements that they connect [2]. Meanwhile, the Proposed Control Architecture 2 renders the dynamic properties more realistically.

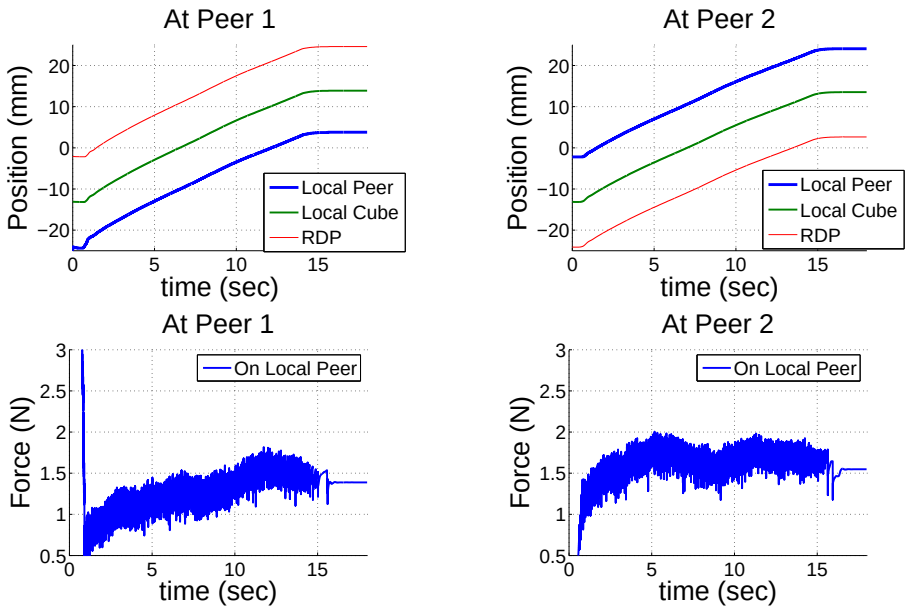

Figure 5.32: Controlled cooperative manipulation of the shared virtual cube, rendered via the Proposed Control Architecture 1. $T_d = 50$ms.

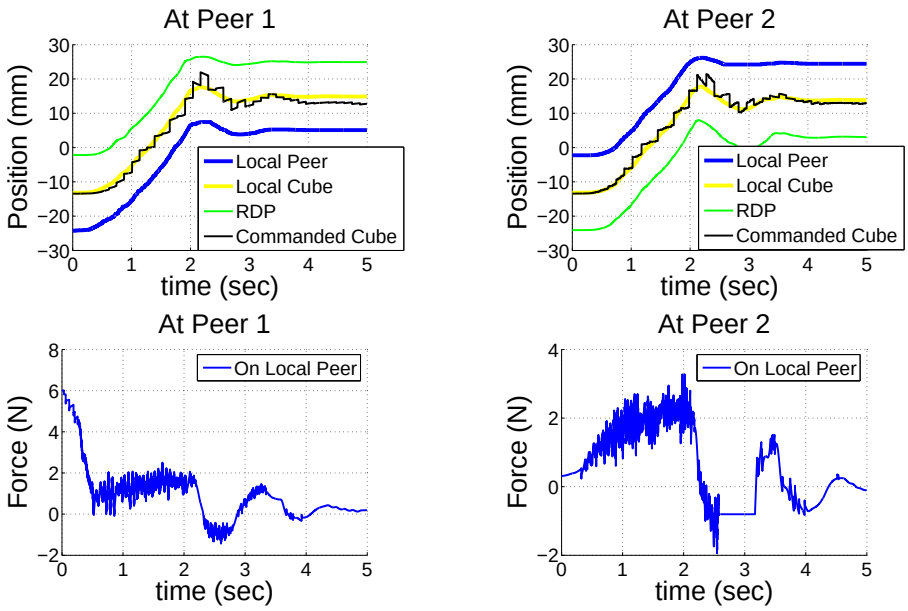

Figure 5.33: Controlled cooperative manipulation of the shared virtual cube, rendered via the Proposed Control Architecture 2. $T_d = 50$ms.

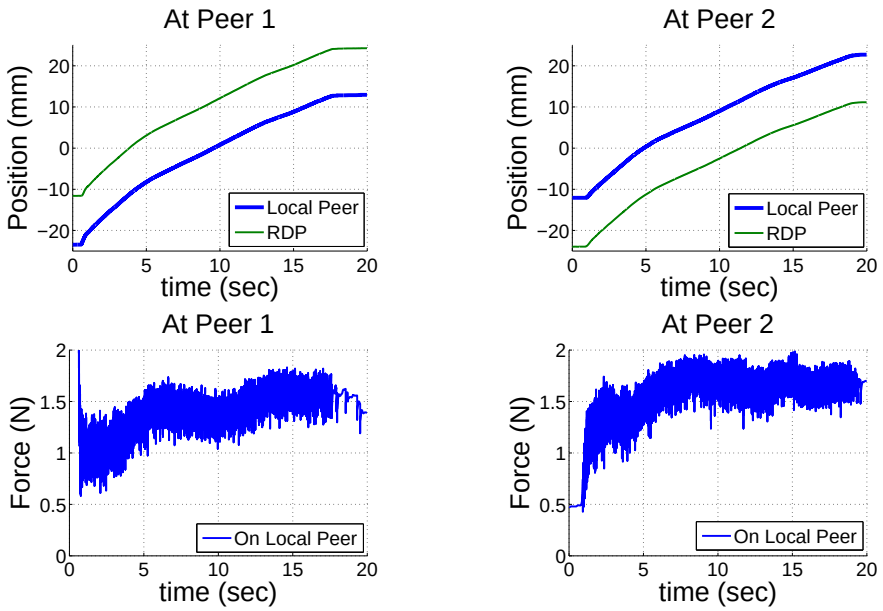

Figure 5.34: Controlled user-to-user interaction, rendered via the Proposed Control Architecture 1. $T_d = 50$ms.

Controlled direct user-to-user interactions via the two proposed architectures are depicted in Figure 5.34 and Figure 5.35. As the remote dynamic proxies representing the distant users have only pure mass, these experiments confirm that the Proposed Control Architecture 2 (that integrates the remote dynamic proxies with wave-based coordination) renders direct user-to-user interaction more realistically than the Proposed Control Architecture 1 (that integrates the remote dynamic proxies with the virtual coupling controllers).

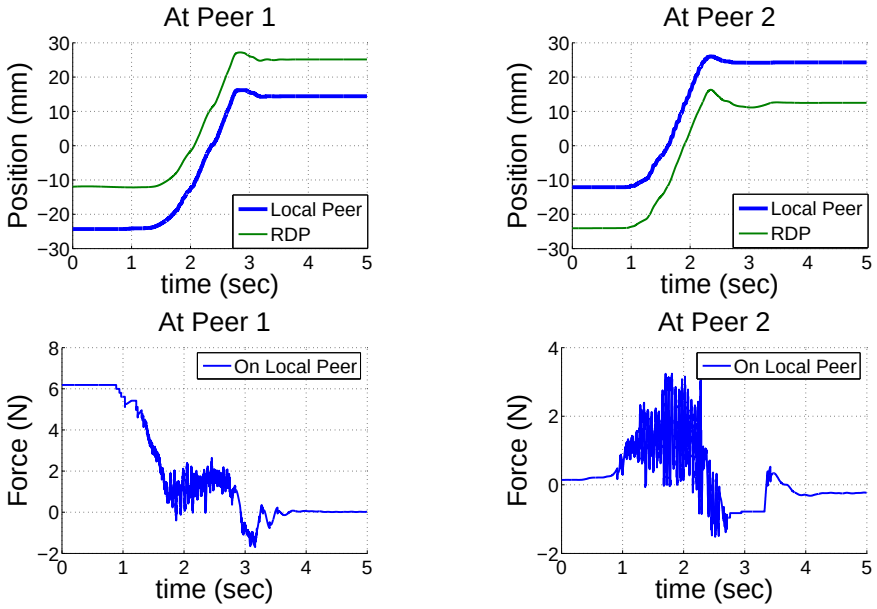

Figure 5.35: Controlled user-to-user interaction, rendered via the Proposed Control Architecture 2. $T_d = 50$ms.

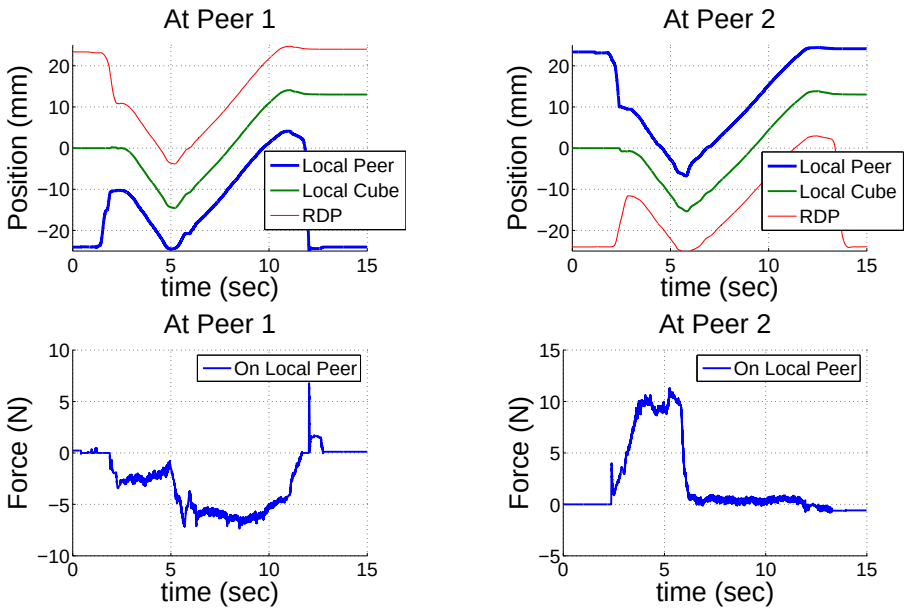

Figure 5.36: Cooperative manipulation of the shared virtual cube by two human users, rendered via the Proposed Control Architecture 1. $T_d = 50$ms.

5.5.2 Experiment II - Experiments with Human Users

This section illustrates the cooperative manipulation of the shared virtual cube by two human users via the two proposed architectures. Figure 5.36 and Figure 5.37 illustrate the position and the force feedback during cooperative manipulation, while Figure 5.38 and Figure 5.39 illustrate the position and the force feedback during direct interaction. These experiments with human users confirm the conclusion of Experiment I (Section 5.5.1): both for cooperative manipulation and for direct user-to-user interaction, the Proposed Control Architecture 1 with virtual coupling coordination renders a predominantly viscous virtual environment, while the Proposed Control Architecture 2 with wave-based coordination renders the dynamics of the shared virtual object realistically.

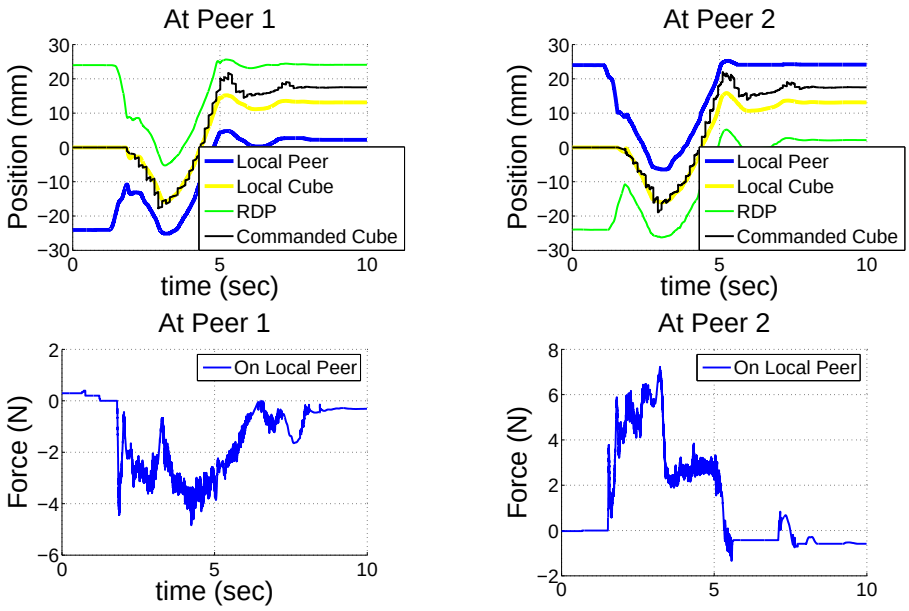

Figure 5.37: Cooperative manipulation of the shared virtual cube by two human users, rendered via the Proposed Control Architecture 2. $T_d = 50$ms.

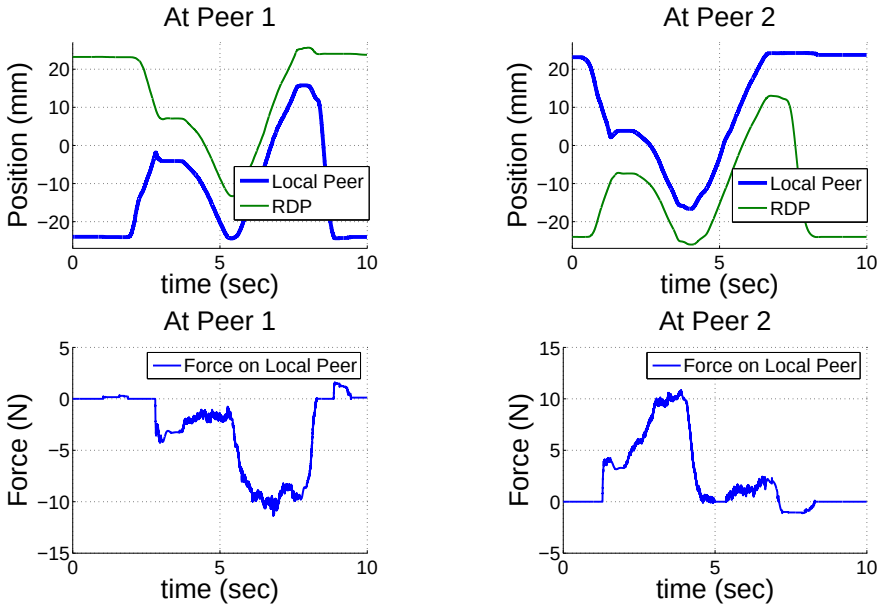

Figure 5.38: Direct interaction between two human users, rendered via the Proposed Control Architecture 1. $T_d = 50$ms.

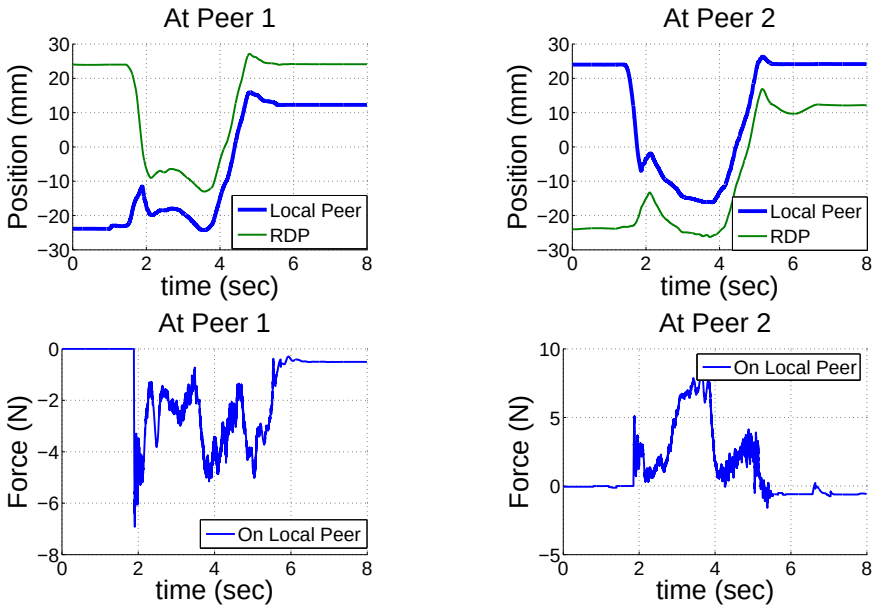

Figure 5.39: Direct interaction between two human users, rendered via the Proposed Control Architecture 2. $T_d = 50$ms.

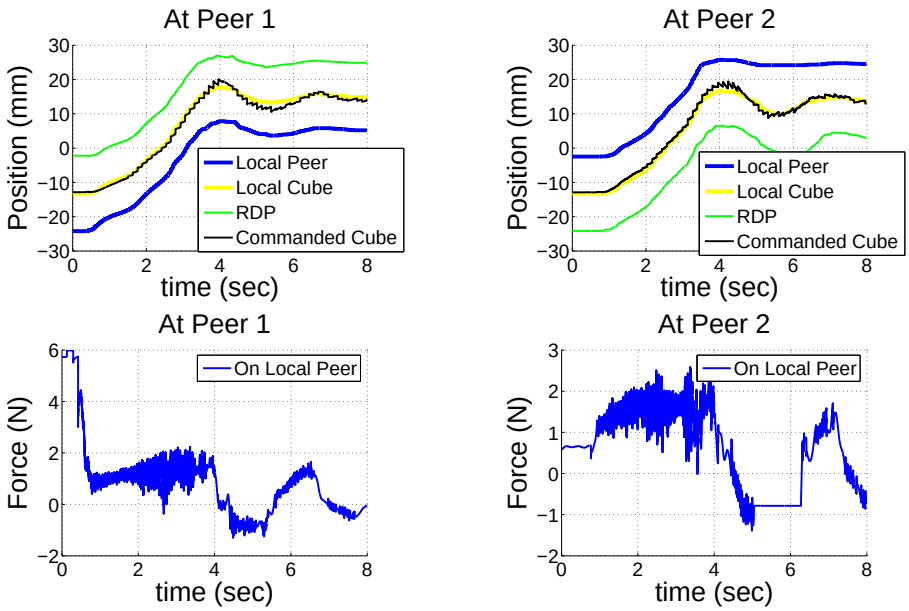

Figure 5.40: Cooperative manipulation of the shared virtual cube by controlled forces, rendered via the Proposed Control Architecture 2. $T_d = 400$ms.

5.5.3 Experiment III - Experiments for Long Network Delay

This section experimentally demonstrates that the Proposed Control Architecture 2 with wave-based coordination can maintain the networked haptic cooperation stable in the presence of longer network delay than the Proposed Control Architecture 1 with virtual coupling coordination, which becomes unstable for $T_d = 200$ms. Specifically, the Proposed Control Architecture 2 with wave-based coordination renders stable cooperative manipulation (Figure 5.40 and Figure 5.41) and stable direct user-to-user interaction (Figure 5.42 and Figure 5.43) for $T_d = 400$ms.

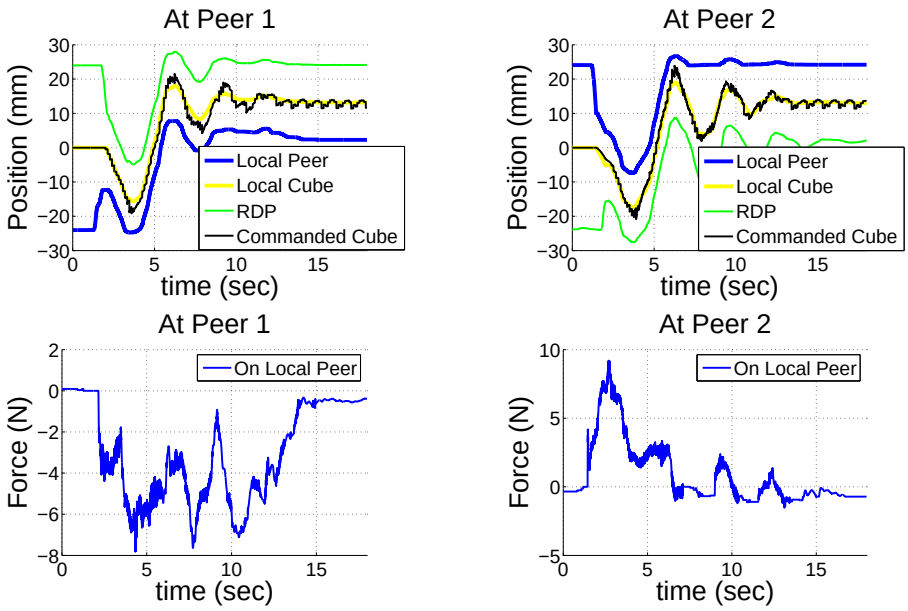

Figure 5.41: Cooperative manipulation of the shared virtual cube by two human users, rendered via the Proposed Control Architecture 2. $T_d = 400$ms.

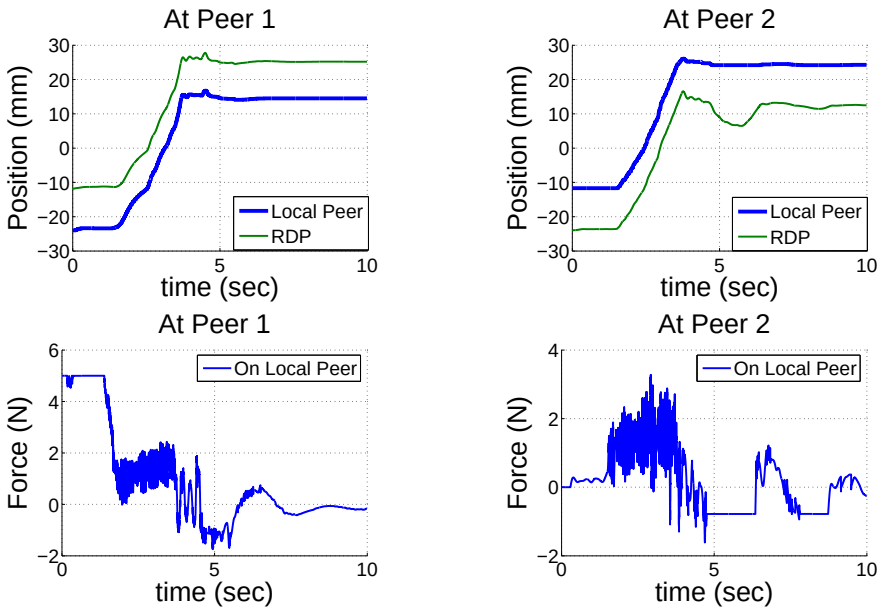

Figure 5.42: Controlled direct user-to-user interaction, rendered via the Proposed Control Architecture 2. $T_d = 400$ms.

5.6 Summary

This chapter has compared through experiments the two proposed control architectures with remote dynamic proxies to the recently designed distributed control architectures [20], [1] and [2].

The Proposed Control Architecture 1 (the Proposed Distributed Control Architecture with Remote Dynamic Proxies and Virtual Coupling Coordination) has been contrasted to the Reference Control Architecture 1 (the Peer-to-peer Scheme with Virtual Coupling Controller in [20]) and to the Reference Control Architecture 2 (the Distributed Control Architecture in [2]) via cooperative manipulation of a shared virtual object and direct user-to-user interaction experiments. The experimental comparison has validated that the Proposed Control Architecture 1: (1) can render stable direct user-to-user interaction in the presence of much higher contact stiffness; (2) coordinates the distributed copies of the shared virtual object better than the Reference Control Architecture 1 and comparably to the Reference Control Architecture 2; and (3)renders smooth user motion to their distant peers, leading to continuous visual display and to smooth interaction forces. However, the virtual couplers crossing the communication channel with delay add significant viscous damping to the simulated shared virtual objects. Therefore, similarly to the two prior control architectures with

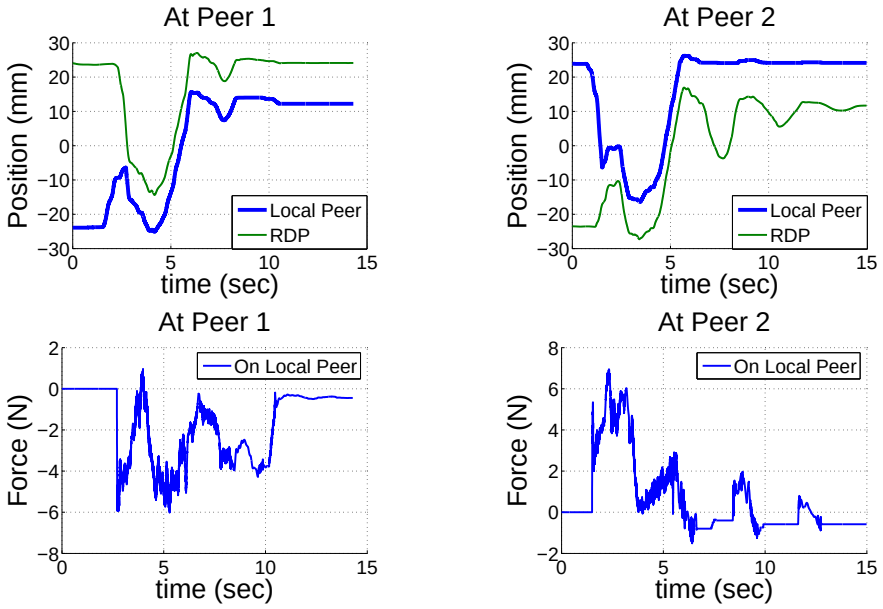

Figure 5.43: Direct interaction between two human users, rendered via the Proposed Control Architecture 2. $T_d = 400$ms.

virtual coupling coordination, the Proposed Control Architecture 1 does not render the motion of an inertial shared virtual object realistically. Furthermore, the Proposed Control Architecture 1 adds more damping to the shared virtual object than the two prior architectures because it includes the largest number of coordinating virtual couplers.

The Proposed Control Architecture 2 (the Distributed Control Architecture with Remote Dynamic Proxies and Wave-based Coordination) has been compared to the Reference Control Architecture 3 (the Peer-to-Peer Scheme with Wave Variable Delay Compensation in [1]) and to the Reference Control Architecture 3 (the Peer-to-Peer Scheme with Wave Variable Delay Compensation in [1]) via cooperative manipulation of a shared virtual object and direct user-to-user interaction experiments similar to those employed in the analysis of the architectures with virtual coupling coordination. These experiments have demonstrated: (1) all architectures with wave-based coordination render the inertia of the shared virtual object and of the haptic device of the remote peer more realistic than the architectures with virtual coupling coordination; (2) the Proposed Architecture 2 renders this inertia most faithfully and leads to its smallest variation as the delay in the communication channel increases; and (3) the Proposed Architecture 2 achieves similar coordination performance to the control architectures with virtual coupling coordination.

In conclusion, the remote dynamic proxies enable two networked users to perceive high contact stiffness and smooth motion of the distant peer both during cooperative manipulation a shared virtual object and during direct interaction with each other regardless whether a virtual coupling controller or a wave-based controller connects the networked users. Furthermore, the remote dynamic proxies lead to a wave-based controller with performance in coordinating the distributed copies of the shared virtual object similar to the performance of the virtual coupling controller. However, the remote dynamic proxies mitigate: neither (1) the significant damping added to the shared virtual object by the virtual coupling controller; nor (2) the inability of virtual coupling control to maintain the networked cooperation stable for large delays. Therefore, the Proposed Control Architecture 2 (with remote dynamic proxies and wave-based control) renders the inertia of the virtual objects more realistically and maintains the networked cooperation stable for larger constant network delays than the Proposed Control Architecture 1 (with remote dynamic proxies and virtual coupling control).

Chapter 6

Conclusions and Future Work

6.1 Conclusion

This dissertation has set out to enable direct haptic interaction between distant peer users in addition to allowing the peers to cooperatively manipulate a shared virtual object. Direct user-to-user haptic interaction over a network is expected to benefit applications like tele-rehabilitation and on-line multi-user computer games. To allow direct networked haptic interaction, this work has:

- proposed to distribute the peer users across the network via avatars with second order dynamics called remote dynamic proxies.
- integrated the remote dynamic proxies into two distributed haptic control architectures, one using virtual coupling and one using wave-based communications between the networked sites.
- analyzed the stability of networked haptic cooperation rendered via remote dynamic proxies with virtual coupling coordination using the state space representation of the two-users multi-rate haptic system. For direct user-to-user interaction, the analysis has predicted that the remote dynamic proxies can render much stiffer contact and can maintain the interaction stable for longer constant network delays than prior architectures. Furthermore, these improvements are achieved without sacrificing performance as measured via position coherency.
- experimentally validated the advantages and the limitations of networked haptic cooperation rendered via the two proposed distributed architectures with remote

dynamic proxies. The validation has contrasted the architectures with remote dynamic proxies to three existing architectures that employ similar time delay compensation techniques. The comparison has shown that both architectures enable users to feel and see their peers moving smoothly in the presence of limited network update rates and constant network delays. Compared to prior architectures:

- the architecture with remote dynamic proxies and virtual coupling coordination allows the peers to perceive much stiffer direct contact and to touch each other under longer constant network delays. However, the remote dynamic proxies do not lessen users' perception of a predominantly viscous virtual environment in the presence of network delay.
- the architecture with remote dynamic proxies and wave-based coordination mitigates the poor position coherency typical to wave-based control. Furthermore, it renders the inertia of the virtual objects more realistically regardless of the network delay.

In conclusion, this dissertation has proposed remote dynamic proxies to allow peer networked users both to interact with each other directly and to cooperatively manipulated a shared virtual object. It has also shown that the remote dynamic proxies improve networked haptic cooperation in both distributed architectures in which they have been integrated although they cannot overcome all limitations specific to those architectures. In particular, networked haptic cooperation feels as if happening in a predominantly viscous virtual environment and is stable for much shorter network delay when rendered via remote dynamic proxies with virtual coupling coordination. Therefore, future work should investigate alternative coordination strategies in order to further increase the stability and improve the performance of networked haptic cooperation rendered via remote dynamic proxies.

6.2 Future Work

The current framework for enabling remote users to touch and feel each other both directly and through a shared virtual object that they cooperatively manipulate can be broadened in several ways:

- The stability analysis for networked haptic cooperation with remote dynamic

proxies and wave-based control should be developed in order to provide useful design guidelines to application developers using wave domain communications between remote users.

- The stability analysis presented in Chapter 4 addresses only the case of two users connected via an Ethernet-based Local Area Network (LAN) or a Metropolitan Area Network (MAN), i.e., a network with fixed and relatively small delay. To enable Internet-based haptic cooperation, future work should investigate the stability of networked haptics with remote dynamic proxies over networks with variable communication delay and packet loss.

- The integration of the remote dynamic proxies into other distributed architectures presents another avenue for extending this work. Architectures that employ passivity-based methods to compensate the network effects are of special interest.

- remote dynamic proxies with geometric attributes in addition to dynamic properties could be developed in order to allow 6DOF body interaction between peer users. Such remote dynamic proxies are expected to increase the complexity both of collision detection and of collision response algorithms in the virtual environment.

- Haptic cooperation among multiple users could be pursued from the control, the network, and the synchronization perspectives. For example, methods for guaranteeing the equivalent control gain can be developed to ensure stability independent of the (possibly varying) number of cooperating users. Buffering can be implemented to smooth network delay jitter. Advanced protocols can be employed to synchronize a large number of users and to expand their connectivity gracefully.

Our hope is that the broader framework will transform haptic devices into computer interfaces that people use every time they connect to other people over the Internet.

Bibliography

[1] G. Sankaranarayanan and B. Hannaford, "Experimental comparison of internet haptic collaboration with time-delay compensation techniques," in *IEEE Int Conf Robot Autom*, vol. 1, pp. 206–211, 2008.

[2] M. Fotoohi, S. Sirouspour, and D. Capson, "Stability and Performance Analysis of Centralized and Distributed Multi-rate Control Architectures for Multi-user Haptic Interaction," *Int J Robot Res*, vol. 26, no. 9, p. 977C994, 2007.

[3] K. Salisbury, F. Conti, and F. Barbagli, "Haptic rendering: introductory concepts," *Computer Graphics and Applications, IEEE*, vol. 24, pp. 24–32, 2004.

[4] M. Capps, P. McDowell, and M. Zyda, "A future for entertainment-defense research collaboration," in *Computer Graphics and Applications, IEEE*, vol. 21, (Naval Postgraduate Sch., Monterey, CA), pp. 37–43, 2001.

[5] J. Marsh, M. Glencross, and S. Pettifer, "A Network Architecture Supporting Consistent Rich Behavior in Collaborative Interactive Applications," in *IEEE Transactions on Visualization and Computer Graphics*, vol. 12, pp. 405–416, 2006.

[6] C. Gunn, M. Hutchins, D. Stevenson, M. Adcock, and P. Youngblood, "Using collaborative haptics in remote surgical training," in *Eurohaptics Conference, 2005 and Symposium on Haptic Interfaces for Virtual Environment and Teleoperator Systems, 2005. World Haptics 2005. First Joint*, (ICT Centre, CSIRO, Australia), pp. 481–482, 2005.

[7] G. Guthart and J. Salisbury, J.K., "The Intuitive telesurgery system: overview andapplication," in *Robotics and Automation, 2000. Proceedings. ICRA '00. IEEE International Conference*, vol. 1, (Intuitive Surg. Inc., Mountain View, CA), pp. 618–621, 2000.

[8] B. Baxter, V. Scheib, M. Lin, and D. Manocha, "nteractive Haptic Painting with 3D Virtual Brushes," in *ACM SIGGRAPH Computer Graphics and Interactive Techniques*, (Department of Computer Science, University of North Carolina, Chapel Hill), pp. 461–486, 2001.

[9] M. Foskey, M. Otaduy, and M. Lin, "ArtNova: touch-enabled 3D model design," in *Virtual Reality, 2002. Proceedings. IEEE*, (North Carolina Univ., Chapel Hill, NC), pp. 119–126, 2002.

[10] R. Williams II, J. Howell, and R. Conatser Jr., *Digital Human Modeling for Palpatory Medical Training with Haptic Feedback*. Society of Automotive Engineers, 2007.

[11] J. Cha, S. Kim, Y. Ho, and J. Ryu, "3D video player system with haptic interaction based on depth image-based representation," in *Consumer Electronics, IEEE Transactions*, vol. 52, (Dept. of Mechatronics, Gwangju Inst. of Sci. & Technol., South Korea), pp. 477–484, 2006.

[12] P. Buttolo, R. Oboe, and B. Hannaford, "Architectures for Shared Haptic Virtual Environments," *Comput Graphics*, vol. 21, no. 4, pp. 421–429, 1997.

[13] E. Salln and S. Zhai, "Collaboration meets Fittslaw: Passing Virtual Objects with and without Haptic Force Feedback," in *INTERACT 2003, IFIP Conference on Human-Computer Interaction*, (Lab. for Intelligent Mech. Syst., Northwestern Univ., Evanston, IL;), pp. 97–104, 2003.

[14] G. Sankaranarayanan and B. Hannaford, "Virtual Coupling Schemes for Position Coherency in Networked Haptic Environments," in *Biomedical Robot. & Biomechatronics, 2006. BioRob 2006. The First IEEE/RAS-EMBS Int. Conf*, vol. 1, pp. 853–858, 2006.

[15] J. Kim, H. Kim, B. Tay, M. Muniyandi, M. Srinivasan, J. Jordan, J. Mortensen, M. Oliveira, and M. Slater, "Transatlantic Touch: A Study of Haptic Collaboration over Long Distance," *Presence*, vol. 13, no. 3, pp. 328–337, 2004.

[16] M. Glencross, C. Jay, J. Feasel, L. Kohli, M. Whitton, and R. Hubbold, "Effective Cooperative Haptic Interaction over the Internet," in *Virt Real Conf, 2007. VR '07. IEEE*, vol. 1, (Manchester Univ.), pp. 115–122, 2007.

[17] H. Sugarman, E. Dayan, A. Weisel-Eichler, and J. Tiran, "The Jerusalem Telerehabilitation System, a New, Low-Cost, Haptic Rehabilitation Approach," *CyberPsychology & Behavior*, vol. 9, no. 2, pp. 178–182, 2006.

[18] S. Aggarwal, H. Banavar, A. Khandelwal, S. Mukherjee, and S. Rangarajan, "Accuracy in DeadReckoning Based Distributed MultiPlayer Games," in *3rd ACM SIGCOMM workshop on Network and system support for games*, (Department of Computer Science, Florida State University, Tallahassee, FL & Center for Networking Research Lucent Technologies Bell Laboratories, Holmdel, NJ), pp. 161–165, 2004.

[19] M. Fujimoto and Y. Ishibashi, "Packetization interval of haptic media in networked virtual environments," in *Network and System Support for Games*, vol. 1, (Nagoya Institute of Technology, Nagoya, Japan), pp. 1–6, 2005.

[20] G. Sankaranarayanan and B. Hannaford, "Experimental Internet Haptic Collaboration using Virtual Coupling Scheme," in *IEEE Symp Haptic Interf Virt Envir Teleop Syst*, pp. 259–266, 2008.

[21] J. Colgate, P. Grafing, M. Stanley, and G. Schenkel, "Implementation of Stiff Virtual Walls in Force-Reflecting Interfaces," in *Proceedings of the IEEE Virtual Reality Annual International Symposium*, (Seattle, WA), pp. 202–208, 1993.

[22] A. M.O.1, H. S., and K. S., "An experimental study on the effects of Network delay in Cooperative Shared Haptic Virtual Environment," *Comput Graphics*, vol. 27, no. 2, pp. 205–213, 2003.

[23] C. Jay, M. Glencross, and R. Hubbold, "Modeling the effects of delayed haptic and visual feedback in a collaborative virtual environment," *ACM Trans. Comput.-Hum. Interact*, vol. 14, no. 2, pp. 8–39, 2007.

[24] K. Park and R. Kenyon, "Effects of network characteristics on human performance in a collaborative virtual environment," in *Virtual Reality, 1999. Proceedings., IEEE*, vol. 1, (Electron. Visualization Lab., Illinois Univ., Chicago, IL, US), pp. 104–111, 1999.

[25] K. Hikichi, H. Morino, I. Arimoto, K. Sezaki, and Y. Yasuda, "The evaluation of delay jitter for haptics collaboration over the Internet," in *Global Telecommu-*

nications Conference, 2002. GLOBECOM '02. IEEE, vol. 2, (Graduate Sch. of Sci. and Eng., Waseda Univ., Tokyo, Japan), pp. 1492–1496, 2002.

[26] K. Hikichi, H. Morino, Y. Yasuda, I. Arimoto, and K. Sezaki, "The Evaluation of Adaptation Control for Haptics Collaboration over the Internet," in *the International CQR Workshop*, (Waseda University, Japan, University of Tokyo, Japan), 2002.

[27] L. Chen, " Effects of network characteristics on task performance in a desktop CVE system," in *Advanced Information Networking and Applications, 2005. AINA 2005. 19th International Conference*, vol. 1, (Coll. of Comput. Sci., Zhejiang Univ., Hangzhou, China), pp. 821 – 826, 2005.

[28] A. Boukerche, S. Shirmohammadi, and A. Hossain, "Moderating simulation lag in haptic virtual environments," in *Proceedings of the 39th annual Symposium on Simulation*, vol. 1, (PARADISE Research Laborator,Canada), pp. 269–277, 2006.

[29] I. Goncharenko, M. Svinin, S. Matsumoto, Y. Masui, Y. Kanou, and S. Hosoe, "Cooperative Control with Haptic Visualization in Shared Virtual Environments," in *Information Visualisation, 2004. IV 2004. Proceedings. Eighth International Conference*, vol. 1, (3D Inc., Yokohama, Japan), pp. 533–538, 2004.

[30] S. Shirmohammadi, N. Woo, and S. Alavi, "Network lag mitigation methods in collaborative distributed simulations," in *Collaborative Technologies and Systems, 2005. Proceedings of the 2005 International Symposium*, (Distributed Collaborative Virtual Environments Res. Lab., Ottawa Univ., Ont., Canada), pp. 244 – 250, 2005.

[31] Y. You, M. Sung, N. Kim, and K. Jun, "An experimental study on the performance of haptic data transmission in networked haptic collaboration," in *Advanced Communication Technology, The 9th International Conference*, vol. 1, (Dept. of Electr. Eng. and Comput. Sci., Michigan Univ.), pp. 657–662, 2007.

[32] S. Shirmohammadi and N. Georganas, "Collaborating in 3D virtual environments: a synchronous architecture," in *Enabling Technologies: Infrastructure for Collaborative Enterprises, 2000. (WET ICE 2000). Proeedings. IEEE 9th International Workshops*, (Sch. of Inf. Technol. and Eng., Ottawa Univ., Ont.), pp. 35–42, 2000.

[33] M. Y. Sung, Y. Yoo, K. Jun, N.-J. Kim, and J. Chae, "Experiments for a Collaborative Haptic Virtual Reality," in *Artificial Reality and Telexistence–Workshops, 2006. ICAT '06. 16th International Conference*, vol. 1, (University of Incheon, South Korea), pp. 174–179, 2006.

[34] A. Boukerche and H. Maamar, "An efficient hybrid multicast transport protocol for collaborative virtual environment with networked haptic," in *Haptic Audio Visual Environments and their Applications, 2006. HAVE 2006. IEEE International Workshop*, (PARADISE Res. Lab., Ottawa Univ., Ont.), pp. 78–83, 2006.

[35] G. Sankaranarayanan and B. Hannaford, "Experimental comparison of internet haptic collaboration with time-delay compensation techniques," in *IEEE Int Conf Robot Autom*, vol. 1, pp. 206–211, 2008.

[36] O. Wongwirat and S. Ohara, "Moving average based adaptive buffer for haptic media synchronization in telehaptics," in *Advanced Intelligent Mechatronics. Proceedings, 2005 IEEE/ASME International Conference*, vol. 1, (Graduate Sch. of Eng., Tokai Univ., Kanagawa), pp. 1305–1311, 2005.

[37] S. Lee, S. Moon, and J. Kim, "A network-adaptive transport scheme for haptic-based collaborative virtual environments," in *Proceedings of 5th ACM SIGCOMM workshop on Network and system support for games*, vol. 1, (Gwangju Institute of Science and Technology (GIST)), p. 13, 2006.

[38] S. Shirmohammadi and N. Ho Woo, "Evaluating decorators for haptic collaboration over Internet," in *Haptic, Audio and Visual Environments and Their Applications, 2004. HAVE 2004. Proceedings. The 3rd IEEE International Workshop*, vol. 1, (Sch. of Inf. Technol. and Eng., Ottawa Univ., Ont., Canada;), pp. 105–109, 2004.

[39] S. Shirmohammadi and N. H. Woo, "Shared Object Manipulation with Decorators in Virtual Environments," in *Distributed Simulation and Real-Time Applications, 2004. DS-RT 2004. Eighth IEEE International Symposium*, vol. 1, (School of Information Technology and Engineering University of Ottawa, Ottawa, Canada boukerch@site.uottawa.ca), pp. 230–233, 2004.

[40] A. Boukerche, S. Shirmohammadi, and A. Hossain, "A prediction algorithm for haptic collaboration," in *Haptic Audio Visual Environments and their Applica-*

tions, 2005. IEEE International Workshop, vol. 1, (Sch. of Inf. Technol. and Eng., Ottawa Univ., Ont., Canada), pp. 154–158, 2005.

[41] A. Boukerche, S. Shirmohammadi, and A. Hossain, "The Effect of Prediction on Collaborative Haptic Applications," in *Haptic Interfaces for Virtual Environment and Teleoperator Systems, 2006 14th Symposium*, vol. 1, (School of Information Technology and Engineering University of Ottawa, Ottawa, Canada boukerch@site.uottawa.ca), pp. 515–516, 2006.

[42] S. Singhal and M. Zyda, *Networked virtual environments: design and implementation*. ACM Press/Addison-Wesley Publishing Co. New York, NY, USA, 1999.

[43] C. Gutwin, J. Dyck, and J. Burkitt, "Using cursor prediction to smooth telepointer jitter," in *Proceedings of the 2003 international ACM SIGGROUP conference on Supporting group work*, vol. 1, (University of Saskatchewan, Saskatoon, Canada), pp. 294–301, 2003.

[44] J. Dyck, C. Gutwin, S. Subramanian, and C. Fedak, "High-Performance Telepointers," in *CSCW04, Chicago, Illinois, USA*, vol. 1, (Department of Computer Science, University of Saskatchewan), pp. 172–181, 2004.

[45] P. Buttolo, R. Oboe, and B. Hannaford, "Architectures for Shared Haptic Virtual Environments," *Computer & Graphics*, pp. 1–10, 1997.

[46] J. Cheong, S.-I. Niculescu, A. Annaswamy, and M. Srinivasan, "Motion synchronization in virtual environments with shared haptics and large time delays," in *Eurohaptics Conf, 2005 & Symp on Haptic Interfaces for Virtual Environment & Teleoperator Syst, 2005. World Haptics 2005. First Joint*, vol. 1, pp. 277– 282, 2005.

[47] J. Colgate, M. Stanley, and J. Brown, "Issues in the Haptic Display of Tool Use," in *Proceedings of the IEEE/RSJ International Conference on Intelligent Robots and Systems*, (Pittsburgh, PA), pp. 140–145, 1995.

[48] B. Hannaford and J. H. Ryu, "Time-Domain Passivity of Haptic Interfaces," *IEEE Transactions on Robotics and Automation*, vol. 18, pp. 1–10, February 2002.

[49] J. H. Ryu, C. Preusche, B. Hannaford, and G. Hirzinger, "Time domain passivity control with reference energy following," in *Control Systems Technology, IEEE Transactions*, vol. 13, (Sch. of Mech. Eng., Korea Univ. of Technol. and Educ., Cheoan-City, South Korea), pp. 737–742, 2005.

[50] G. Niemeyer, *Using wave varialbes in time delayed force reflecting teleoperation.* PhD thesis, Massachusetts institute of technology, 1997.

[51] C. Secchi, S. Stramigioli, and C. Fantuzzi, "Digital passive geometric telemanipulation," in *Robotics and Automation, 2003. Proceedings. ICRA '03. IEEE International Conference*, vol. 3, (DISMI, Modena Univ., Reggio Emilia, Italy;), pp. 3290–3295, 2003.

[52] C. Zilles and J. Salisbury, "A Constraint-based God Object Method for Haptic Display," in *ASME Haptic Interf Virt Envir Teleop Syst*, (Chicago, IL), pp. 146–150, 1994.

[53] D. Ruspini, K. Koralov, and O. Khatib, "Haptic Interaction in Virtual Environments," in *IEEE/RSJ Int Conf Intell Robot Syst*, (Genoble, France), 1997.

[54] P. Mitra and G. Niemeyer, "Dynamic Proxy Objects in Haptic Simulations," in *IEEE Conf Robot Autom Mechatronics*, pp. 1054–1059, 2004.

[55] D. Constantinescu, S. Salcudean, and E. Croft, "Local Models of Interaction for Realistic manipulation of Rigid Virtual Worlds," *Int J Robot Res*, vol. 24, no. 10, pp. 789–804, 2005.

[56] R. Anderson and M. Spong, "Bilateral Control of Teleoperation with Time Delay," *IEEE Trans. Autom. Control*, vol. 34, no. 5, pp. 494–501, 1989.

[57] G. Niemeyer and J. E. Slotine, "Stable Adaptive Teleoperation," *IEEE J. Oceanic Eng.*, vol. 16, no. 1, pp. 152–162, 1991.

[58] G. Niemeyer and J. E. Slotine, "Telemanipulation with Time Delays," *Int. J. Robot. Res.*, vol. 23, no. 9, pp. 873–890, 2004.

[59] M. Araki and K. Yamamoto, "Multivariable multirate sampled-data systems: State-space description, transfer characteristics, and Nyquist criterion," in *Automatic Control, IEEE Transactions*, vol. 31, (Kyoto University, Yoshida, Kyoto, Japan;), pp. 145–154, 1986.

[60] *WANem 1.1 Wide Area Network Emulator User Guide*. Performance Engineering Research Centre, 2007.

Appendix A

Appendix

This appendix presents the detailed procedure of deriving the stability region for the proposed distributed control architecture with remote dynamic proxies and virtual coupling coordination. When applied to cooperative manipulation, the control system of the proposed control architecture is a sampled-data system because of the discrete nature of the virtual environment simulation, as well as a system with multiple rates because of the inherent limitations of the communication port (particularly, data from remote peers is sampled at frequencies of 128Hz, and the local control loop runs at 1 KHz). Therefore, the continuous state space representation of the control system presented in Chapter 4 is to be discretized with state vector that expanded according to the multiple sampling rates. Furthermore, the computational delay and network delay will be augmented to the discrete state space representation of the control system, which renders the stability region of the control system in the presence of different delay step.

Furthermore, this appendix will provide detailed procedure of setting up WANem for network condition emulation. This detailed procedure consists: (1) configuring WANem on a PC for network emulation, (2) setting up routing between connected users, and (3) adjusting emulated network condition via web-based interface.

In the following sections, the following values apply both to cooperative manipulation and to direct user-to-user interaction:

$p = 2$	number of sample times in the system (T_c and T_n in this case)
$T_c = \frac{1}{1024}$	control sampling rate
$T_n = \frac{1}{128}$	network sampling rate
$T_0 = \frac{1}{128}$	smallest sampling rate integer multiple of all sampling rates in the system
$N_c = \frac{T_0}{T_c} = \frac{\frac{1}{128}}{\frac{1}{1024}} = 8$	number of control sampling periods in T_0
$N_n = \frac{T_0}{T_n} = \frac{\frac{1}{128}}{\frac{1}{128}} = 1$	number of network sampling periods in T_0
$\bar{N} = N_c + N_n = 8 + 1 = 9$	sum of all N-s
$\tau_0 = \frac{1}{1024}$	base sampling rate, i.e., largest sampling rate that fits an integer number of times in all system sampling rates
$l_c = \frac{T_c}{\tau_0} = \frac{\frac{1}{1024}}{\frac{1}{1024}} = 1$	number of fundamental sampling periods in T_c
$l_n = \frac{T_n}{\tau_0} = \frac{\frac{1}{128}}{\frac{1}{1024}} = 8$	number of fundamental sampling periods in T_n
$N_0 = 8$	the least common multiple of N_c and N_n

A.1 Cooperative Manipulation

For cooperative manipulation, the dimensions of the state, the input, and the output vectors are as follows:

$n_x = 12$	number of states of continuous-time system
$n_{cu} = 8$	number of fast inputs (updated at the control rate) of continuous-time system
$n_{1cu} = 4$	number of fast inputs (updated at the control rate) of continuous-time system at the Peer 1 side
$n_{2cu} = 4$	number of fast inputs (updated at the control rate) of continuous-time system at the Peer 2 side
$n_{nu} = 4$	number of slow inputs (updated at the network rate) of continuous-time system
$n_{1nu} = 2$	number of slow inputs (updated at the network rate) of continuous-time system at the Peer 1 side
$n_{2nu} = 2$	number of slow inputs (updated at the network rate) of continuous-time system at the Peer 2 side
$n_u = n_{cu} + n_{nu} = 12$	number of inputs of continuous-time system
$n_{cy} = 12$	number of fast outputs (updated at the control rate) of continuous-time system
$n_{1cy} = 6$	number of fast outputs (updated at the control rate) of continuous-time system at the Peer 1 side
$n_{2cy} = 6$	number of fast outputs (updated at the control rate) of continuous-time system at the Peer 2 side
$n_{ny} = 8$	number of slow outputs (updated at the network rate) of continuous-time system
$n_{1ny} = 4$	number of slow outputs (updated at the network rate) of continuous-time system at the Peer 1 side
$n_{2ny} = 4$	number of slow outputs (updated at the network rate) of continuous-time system at the Peer 2 side
$n_y = n_{cy} + n_{ny} = 20$	number of outputs of continuous-time system

A.1.1 Discretization of the Continuous State Space Representation

With the multiple sampling rates existing in the control system, the state vector for the discrete-time system is expanded as:

$$\begin{aligned}
\mathbf{x}_{\mathrm{D}_{N_0 \cdot n_x \times 1}}[k] &= \mathbf{x}_{\mathrm{D}_{8 \cdot 12 \times 1}}[k] = \mathbf{x}_{\mathrm{D}_{96 \times 1}}[k] \\
&= \begin{pmatrix} \mathbf{x}_{n_x \times 1}\left((k-1)\,T_0 + \tau_0\right) \\ \mathbf{x}_{n_x \times 1}\left((k-1)\,T_0 + 2\tau_0\right) \\ \vdots \\ \mathbf{x}_{n_x \times 1}\left((k-1)\,T_0 + (N_0-1)\,\tau_0\right) \\ \mathbf{x}_{n_x \times 1}\left(kT_0\right) \end{pmatrix} = \begin{pmatrix} \mathbf{x}_{12 \times 1}\left((k-1)\,T_0 + \tau_0\right) \\ \mathbf{x}_{12 \times 1}\left((k-1)\,T_0 + 2\tau_0\right) \\ \vdots \\ \mathbf{x}_{12 \times 1}\left((k-1)\,T_0 + 7\tau_0\right) \\ \mathbf{x}_{12 \times 1}\left(kT_0\right) \end{pmatrix} \\
&= \begin{pmatrix} \mathbf{x}_{n_x \times 1}\left(kT_0 - (N_0-1)\,\tau_0\right) \\ \mathbf{x}_{n_x \times 1}\left(kT_0 - (N_0-2)\,\tau_0\right) \\ \vdots \\ \mathbf{x}_{n_x \times 1}\left(kT_0 - \tau_0\right) \\ \mathbf{x}_{n_x \times 1}\left(kT_0\right) \end{pmatrix} = \begin{pmatrix} \mathbf{x}_{12 \times 1}\left(kT_0 - 7\tau_0\right) \\ \mathbf{x}_{12 \times 1}\left(kT_0 - 6\tau_0\right) \\ \vdots \\ \mathbf{x}_{12 \times 1}\left(kT_0 - \tau_0\right) \\ \mathbf{x}_{12 \times 1}\left(kT_0\right) \end{pmatrix}
\end{aligned} \tag{A.1}$$

The output vector is expanded as:

$$\begin{aligned}
\mathbf{y}_{\mathrm{D}_{(N_c \cdot n_{cy} + N_n \cdot n_{ny}) \times 1}}[k] &= \mathbf{y}_{\mathrm{D}_{(8 \cdot 12 + 1 \cdot 8) \times 1}}[k] = \mathbf{y}_{\mathrm{D}_{104 \times 1}}[k] = \begin{pmatrix} \mathbf{y}_{\mathrm{D}_{c_{N_c \cdot n_{cy} \times 1}}}[k] \\ \mathbf{y}_{\mathrm{D}_{n_{N_n \cdot n_{ny} \times 1}}}[k] \end{pmatrix} \\
&= \begin{pmatrix} \mathbf{y}_{\mathrm{D}_{c_{8 \cdot 12 \times 1}}}[k] \\ \mathbf{y}_{\mathrm{D}_{n_{1 \cdot 8 \times 1}}}[k] \end{pmatrix} = \begin{pmatrix} \mathbf{y}_{\mathrm{D}_{c_{96 \times 1}}}[k] \\ \mathbf{y}_{\mathrm{D}_{n_{8 \times 1}}}[k] \end{pmatrix}
\end{aligned} \tag{A.2}$$

where:

$$
\begin{aligned}
\mathbf{y}_{\mathrm{D}_{c_{N_c\times n_{cy}}}}[k] &= \mathbf{y}_{\mathrm{D}_{c_{8\cdot 12\times 1}}}[k] = \mathbf{y}_{\mathrm{D}_{c_{96\times 1}}}[k] \\
&= \begin{pmatrix} \mathbf{y}_{\mathrm{D}_{c_{n_{cy}\times 1}}}(kT_0) \\ \mathbf{y}_{\mathrm{D}_{c_{n_{cy}\times 1}}}(kT_0+T_c) \\ \vdots \\ \mathbf{y}_{\mathrm{D}_{c_{n_{cy}\times 1}}}(kT_0+(N_c-1)T_c) \end{pmatrix} = \begin{pmatrix} \mathbf{y}_{\mathrm{D}_{c_{12\times 1}}}(kT_0) \\ \mathbf{y}_{\mathrm{D}_{c_{12\times 1}}}(kT_0+T_c) \\ \vdots \\ \mathbf{y}_{c_{12\times 1}}(kT_0+7T_c) \end{pmatrix} \\
&= \begin{pmatrix} \mathbf{y}_{\mathrm{D}_{1c_{n_{1cy}\times 1}}}(kT_0) \\ \mathbf{y}_{\mathrm{D}_{2c_{n_{2cy}\times 1}}}(kT_0) \\ \mathbf{y}_{\mathrm{D}_{1c_{n_{1cy}\times 1}}}(kT_0+T_c) \\ \mathbf{y}_{\mathrm{D}_{2c_{n_{2cy}\times 1}}}(kT_0+T_c) \\ \vdots \\ \mathbf{y}_{\mathrm{D}_{1c_{n_{1cy}\times 1}}}(kT_0+7T_c) \\ \mathbf{y}_{\mathrm{D}_{2c_{n_{2cy}\times 1}}}(kT_0+7T_c) \end{pmatrix} = \begin{pmatrix} \mathbf{y}_{\mathrm{D}_{1c_{6\times 1}}}(kT_0) \\ \mathbf{y}_{\mathrm{D}_{2c_{6\times 1}}}(kT_0) \\ \mathbf{y}_{\mathrm{D}_{1c_{6\times 1}}}(kT_0+T_c) \\ \mathbf{y}_{\mathrm{D}_{2c_{6\times 1}}}(kT_0+T_c) \\ \vdots \\ \mathbf{y}_{\mathrm{D}_{1c_{6\times 1}}}(kT_0+7T_c) \\ \mathbf{y}_{\mathrm{D}_{2c_{6\times 1}}}(kT_0+7T_c) \end{pmatrix}
\end{aligned}
\tag{A.3}
$$

$$
\begin{aligned}
\mathbf{y}_{\mathrm{D}_{n_{N_n\times n_{ny}}}}[k] &= \mathbf{y}_{\mathrm{D}_{n_{1\cdot 8\times 1}}}[k] = \mathbf{y}_{\mathrm{D}_{n_{8\times 1}}}[k] \\
&= \begin{pmatrix} \mathbf{y}_{\mathrm{D}_{n_{n_{ny}\times 1}}}(kT_0) \\ \mathbf{y}_{\mathrm{D}_{n_{n_{ny}\times 1}}}(kT_0+T_n) \\ \vdots \\ \mathbf{y}_{\mathrm{D}_{n_{n_{ny}\times 1}}}(kT_0+(N_n-1)T_n) \end{pmatrix} = \left[\mathbf{y}_{\mathrm{D}_{n_{8\times 1}}}(kT_0)\right] \\
&= \begin{pmatrix} \mathbf{y}_{\mathrm{D}_{1n_{n_{1ny}\times 1}}}(kT_0) \\ \mathbf{y}_{\mathrm{D}_{2n_{n_{2ny}\times 1}}}(kT_0) \\ \mathbf{y}_{\mathrm{D}_{1n_{n_{1ny}\times 1}}}(kT_0+T_n) \\ \mathbf{y}_{\mathrm{D}_{2n_{n_{2ny}\times 1}}}(kT_0+T_n) \\ \vdots \\ \mathbf{y}_{\mathrm{D}_{1n_{n_{1ny}\times 1}}}(kT_0+(N_n-1)T_n) \\ \mathbf{y}_{\mathrm{D}_{2n_{n_{2ny}\times 1}}}(kT_0+(N_n-1)T_n) \end{pmatrix} = \begin{bmatrix} \mathbf{y}_{1n_{4\times 1}}(kT_0) \\ \mathbf{y}_{2n_{4\times 1}}(kT_0) \end{bmatrix}
\end{aligned}
\tag{A.4}
$$

The input vector is expanded as:

$$\begin{aligned}\mathbf{u}_{\mathrm{D}_{(N_c\cdot n_{cu}+N_n\cdot n_{nu})\times 1}}[k] &= \mathbf{u}_{\mathrm{D}_{(8\cdot 8+1\cdot 4)\times 1}}[k] = \mathbf{u}_{\mathrm{D}_{68\times 1}}[k] \\ &= \begin{pmatrix}\mathbf{u}_{\mathrm{D}_{c_{N_c\cdot n_{cu}\times 1}}}[k] \\ \mathbf{u}_{\mathrm{D}_{n_{N_n\cdot n_{nu}\times 1}}}[k]\end{pmatrix} = \begin{pmatrix}\mathbf{u}_{\mathrm{D}_{c_{8\cdot 8\times 1}}}[k] \\ \mathbf{u}_{\mathrm{D}_{n_{1\cdot 4\times 1}}}[k]\end{pmatrix} = \begin{pmatrix}\mathbf{u}_{\mathrm{D}_{c_{64\times 1}}}[k] \\ \mathbf{u}_{\mathrm{D}_{n_{4\times 1}}}[k]\end{pmatrix}\end{aligned} \tag{A.5}$$

where $\mathbf{u}_{\mathrm{D}_{c_{N_c\cdot n_{cu}\times 1}}}[k]$ depends on positions & velocities measured locally at the control sampling rate T_c:

$$\begin{aligned}\mathbf{u}_{\mathrm{D}_{c_{N_c\cdot n_{cu}\times 1}}}[k] &= \mathbf{u}_{\mathrm{D}_{c_{8\cdot 8\times 1}}}[k] = \mathbf{u}_{\mathrm{D}_{c_{64\times 1}}}[k] = \\ &= \begin{pmatrix}\mathbf{u}_{c_{n_{cu}\times 1}}(kT_0) \\ \vdots \\ \mathbf{u}_{c_{n_{cu}\times 1}}(kT_0+(N_c-1)T_c)\end{pmatrix} = \begin{pmatrix}\mathbf{u}_{c_{8\times 1}}(kT_0) \\ \vdots \\ \mathbf{u}_{c_{8\times 1}}(kT_0+7T_c)\end{pmatrix} \\ &= \begin{pmatrix}\mathbf{u}_{1c_{n_{1cu}\times 1}}(kT_0) \\ \mathbf{u}_{2c_{n_{2cu}\times 1}}(kT_0) \\ \vdots \\ \mathbf{u}_{1c_{n_{1cu}\times 1}}(kT_0+(N_c-1)T_c) \\ \mathbf{u}_{2c_{n_{2cu}\times 1}}(kT_0+(N_c-1)T_c)\end{pmatrix} = \begin{pmatrix}\mathbf{u}_{1c_{4\times 1}}(kT_0) \\ \mathbf{u}_{2c_{4\times 1}}(kT_0) \\ \vdots \\ \mathbf{u}_{1c_{4\times 1}}(kT_0+7T_c) \\ \mathbf{u}_{2c_{4\times 1}}(kT_0+7T_c)\end{pmatrix}\end{aligned} \tag{A.6}$$

and $\mathbf{u}_{\mathrm{D}_{n_{N_n\cdot n_{nu}\times 1}}}[k]$ depends on positions & velocities received from the remote peer

at the network sampling rate T_n:

$$\begin{aligned}
\mathbf{u}_{\mathrm{D}_{n_{N_n \cdot n_{nu} \times 1}}}[k] &= \mathbf{u}_{\mathrm{D}_{n_{1 \cdot 4 \times 1}}}[k] = \mathbf{u}_{\mathrm{D}_{n_{4 \times 1}}}[k] = \\
&= \begin{pmatrix} \mathbf{u}_{n_{n_{nu} \times 1}}(kT_0) \\ \vdots \\ \mathbf{u}_{n_{n_{nu} \times 1}}(T_0 + (N_n - 1)\,T_n) \end{pmatrix} = \left(\mathbf{u}_{n_{4 \times 1}}(kT_0)\right) \\
&= \begin{pmatrix} \mathbf{u}_{1n_{n_{1nu} \times 1}}(kT_0) \\ \mathbf{u}_{2n_{n_{2nu} \times 1}}(kT_0) \\ \vdots \\ \mathbf{u}_{1n_{n_{1nu} \times 1}}(T_0 + (N_n - 1)\,T_n) \\ \mathbf{u}_{2n_{n_{2nu} \times 1}}(T_0 + (N_n - 1)\,T_n) \end{pmatrix} = \begin{pmatrix} \mathbf{u}_{n_{2 \times 1}}(kT_0) \\ \mathbf{u}_{n_{2 \times 1}}(kT_0) \end{pmatrix}
\end{aligned} \tag{A.7}$$

Hence, the discrete-time state-space representation of the open-loop system is:

$$\begin{aligned}
\mathbf{x}_{\mathrm{D}}[k+1] &= \mathbf{A}_{\mathrm{D}}\,\mathbf{x}_{\mathrm{D}}[k] + \mathbf{B}_{\mathrm{D}}\,\mathbf{u}_{\mathrm{D}}[k] \\
\mathbf{y}_{\mathrm{D}}[k] &= \mathbf{C}_{\mathrm{D}}\left(\mathbf{U}_1\,\mathbf{x}_{\mathrm{D}}[k+1] + \mathbf{U}_2\,\mathbf{x}_{\mathrm{D}}[k]\right)
\end{aligned} \tag{A.8}$$

The computation of all matrices in Equation (A.8) is detailed in the following.

$$\begin{aligned}
\mathbf{A}_{\mathrm{D}_{N_0 \cdot n_x \times N_0 \cdot n_x}} &= \mathbf{A}_{\mathrm{D}_{8 \cdot 12 \times 8 \cdot 12}} = \mathbf{A}_{\mathrm{D}_{96 \times 96}} = \\
&= \begin{bmatrix}
\mathbf{0}_{12\times12} & \cdots & \mathbf{0}_{12\times12} & \mathbf{A}_{\mathrm{D}_1 12\times12} \\
\mathbf{0}_{12\times12} & \cdots & \mathbf{0}_{12\times12} & \mathbf{A}_{\mathrm{D}_2 12\times12} \\
\mathbf{0}_{12\times12} & \cdots & \mathbf{0}_{12\times12} & \mathbf{A}_{\mathrm{D}_3 12\times12} \\
\mathbf{0}_{12\times12} & \cdots & \mathbf{0}_{12\times12} & \mathbf{A}_{\mathrm{D}_4 12\times12} \\
\mathbf{0}_{12\times12} & \cdots & \mathbf{0}_{12\times12} & \mathbf{A}_{\mathrm{D}_5 12\times12} \\
\mathbf{0}_{12\times12} & \cdots & \mathbf{0}_{12\times12} & \mathbf{A}_{\mathrm{D}_6 12\times12} \\
\mathbf{0}_{12\times12} & \cdots & \mathbf{0}_{12\times12} & \mathbf{A}_{\mathrm{D}_7 12\times12} \\
\mathbf{0}_{12\times12} & \cdots & \mathbf{0}_{12\times12} & \mathbf{A}_{\mathrm{D}_8 12\times12}
\end{bmatrix}_{96\times96}
\end{aligned} \tag{A.9}$$

in which:

$$\mathbf{A}_{\mathrm{D}_{l_{12\times12}}} = e^{\mathbf{A}_{12\times12}\cdot l\cdot\tau_0} = e^{\mathbf{A}_{12\times12}\cdot l\cdot\frac{1}{1024}} \qquad l = 1,\cdots,N_0 = 1,\cdots,8 \tag{A.10}$$

$$\begin{aligned}
\mathbf{B}_{\mathrm{D}_{N_0\cdot n_x\times(N_c\cdot n_{cu}+N_n\cdot n_{nu})}} &= \left[\mathbf{B}_{\mathrm{D}_{c_{N_0\cdot n_x\times N_c\cdot n_{cu}}}} \quad \mathbf{B}_{\mathrm{D}_{n_{N_0\cdot n_x\times N_n\cdot n_{nu}}}}\right] \Longleftrightarrow \\
\mathbf{B}_{\mathrm{D}_{8\cdot12\times(8\cdot8+1\cdot4)}} &= \left[\mathbf{B}_{\mathrm{D}_{c_{8\cdot12\times8\cdot8}}} \quad \mathbf{B}_{\mathrm{D}_{n_{8\cdot12\times1\cdot4}}}\right] \Longleftrightarrow \\
\mathbf{B}_{\mathrm{D}_{96\times68}} &= \left[\mathbf{B}_{\mathrm{D}_{c_{96\times64}}} \quad \mathbf{B}_{\mathrm{D}_{n_{96\times4}}}\right]
\end{aligned} \tag{A.11}$$

with the $\mathbf{B}_{\mathrm{D}_{c_{96\times64}}}$ and $\mathbf{B}_{\mathrm{D}_{n_{96\times4}}}$ matrices detailed in the following. Specifically, the $\mathbf{B}_{\mathrm{D}_{c_{96\times64}}}$ matrix is an $N_0 \times N_c = 8\times8$ block matrix:

$$\begin{aligned}
\mathbf{B}_{\mathrm{D}_{c_{N_0\cdot n_x\times N_c\cdot n_{cu}}}} &= \left[\mathbf{b}_{\mathrm{D}_{c,l\mu_{n_x\times n_{cu}}}}\right] = \left[\left(\mathbf{b}_{\mathrm{D}_{1c,l\mu_{n_x\times n_{1cu}}}} \quad \mathbf{b}_{\mathrm{D}_{2c,l\mu_{n_x\times n_{2cu}}}}\right)\right] \\
l &= 1,\ldots,N_0;\ \mu = 0,\ldots,N_c-1 \\
&\Longleftrightarrow \\
\mathbf{B}_{\mathrm{D}_{c_{96\times64}}} &= \left[\mathbf{b}_{\mathrm{D}_{c,l\mu_{12\times8}}}\right] = \left[\left(\mathbf{b}_{\mathrm{D}_{1c,l\mu_{12\times4}}}, \mathbf{b}_{\mathrm{D}_{2c,l\mu_{12\times4}}}\right)\right] \\
l &= 1,\ldots,8;\ \mu = 0,\ldots,7
\end{aligned} \tag{A.12}$$

with the $l\mu$ block computed via:

$$\mathbf{b}_{\mathrm{D}_{ic,l\mu_{n_x\times n_{ic}}}} = \begin{cases} \mathbf{0}_{n_x\times n_{ic}} & l \le l_c\cdot\mu \\ \int_{\mu\cdot l_c\cdot\tau_0}^{l\cdot\tau_0} e^{\mathbf{A}_{n_x\times n_x}(l\cdot\tau_0-\tau)}\mathbf{B}_{ic_{n_x\times n_{ic}}}d\tau & l_c\cdot\mu < l \le l_c\cdot(\mu+1) \\ \int_{\mu\cdot l_c\cdot\tau_0}^{(\mu+1)\cdot l_c\cdot\tau_0} e^{\mathbf{A}_{n_x\times n_x}(l\cdot\tau_0-\tau)}\mathbf{B}_{ic_{n_x\times n_{ic}}}d\tau & l_c\cdot(\mu+1) < l \end{cases}$$

$(i=1,2)$

$$\Longleftrightarrow$$

$$\mathbf{b}_{\mathrm{D}_{1c,l\mu_{12\times4}}} = \begin{cases} \mathbf{0}_{12\times4} & l \le 1\cdot\mu \\ \int_{\mu\cdot1\cdot\tau_0}^{l\cdot\tau_0} e^{\mathbf{A}_{12\times12}(l\cdot\tau_0-\tau)}\mathbf{B}_{1c_{12\times4}}d\tau & 1\cdot\mu < l \le 1\cdot(\mu+1) \\ \int_{\mu\cdot1\cdot\tau_0}^{(\mu+1)\cdot1\cdot\tau_0} e^{\mathbf{A}_{12\times12}(l\cdot\tau_0-\tau)}\mathbf{B}_{1c_{12\times4}}d\tau & 1\cdot(\mu+1) < l \end{cases}$$

$$\mathbf{b}_{\mathrm{D}_{2c,l\mu_{12\times8}}} = \begin{cases} \mathbf{0}_{12\times4} & l \le 1\cdot\mu \\ \int_{\mu\cdot1\cdot\tau_0}^{l\cdot\tau_0} e^{\mathbf{A}_{12\times12}(l\cdot\tau_0-\tau)}\mathbf{B}_{2c_{12\times4}}d\tau & 1\cdot\mu < l \le 1\cdot(\mu+1) \\ \int_{\mu\cdot1\cdot\tau_0}^{(\mu+1)\cdot1\cdot\tau_0} e^{\mathbf{A}_{12\times12}(l\cdot\tau_0-\tau)}\mathbf{B}_{2c_{12\times4}}d\tau & 1\cdot(\mu+1) < l \end{cases} \tag{A.13}$$

Hence:

$$\begin{aligned} \mathbf{B}_{\mathrm{D}_{c_{N_0\cdot n_x\times N_c\cdot n_{cu}=8\cdot12\times8\cdot8=96\times64}}} &= \begin{bmatrix} \mathbf{b}_{\mathrm{D}_{c,10_{12\times8}}} & \mathbf{0}_{12\times8} & \cdots & \mathbf{0}_{12\times8} & \mathbf{0}_{12\times8} \\ \mathbf{b}_{\mathrm{D}_{c,20_{12\times8}}} & \mathbf{b}_{\mathrm{D}_{c,21_{12\times8}}} & \cdots & \mathbf{0}_{12\times8} & \mathbf{0}_{12\times8} \\ \mathbf{b}_{\mathrm{D}_{c,30_{12\times8}}} & \mathbf{b}_{\mathrm{D}_{c,31_{12\times8}}} & \cdots & \mathbf{0}_{12\times8} & \mathbf{0}_{12\times8} \\ \mathbf{b}_{\mathrm{D}_{c,40_{12\times8}}} & \mathbf{b}_{\mathrm{D}_{c,41_{12\times8}}} & \cdots & \mathbf{0}_{12\times8} & \mathbf{0}_{12\times8} \\ \mathbf{b}_{\mathrm{D}_{c,50_{12\times8}}} & \mathbf{b}_{\mathrm{D}_{c,51_{12\times8}}} & \cdots & \mathbf{0}_{12\times8} & \mathbf{0}_{12\times8} \\ \mathbf{b}_{\mathrm{D}_{c,60_{12\times8}}} & \mathbf{b}_{\mathrm{D}_{c,61_{12\times8}}} & \cdots & \mathbf{0}_{12\times8} & \mathbf{0}_{12\times8} \\ \mathbf{b}_{\mathrm{D}_{c,70_{12\times8}}} & \mathbf{b}_{\mathrm{D}_{c,71_{12\times8}}} & \cdots & \mathbf{b}_{\mathrm{D}_{c,76_{12\times8}}} & \mathbf{0}_{12\times8} \\ \mathbf{b}_{\mathrm{D}_{c,80_{12\times8}}} & \mathbf{b}_{\mathrm{D}_{c,81_{12\times8}}} & \cdots & \mathbf{b}_{\mathrm{D}_{c,86_{12\times8}}} & \mathbf{b}_{\mathrm{D}_{c,87_{12\times8}}} \end{bmatrix} \\ &= \begin{bmatrix} \mathbf{b}_{\mathrm{D}_{c,0_{96\times8}}} & \mathbf{b}_{\mathrm{D}_{c,1_{96\times8}}} & \cdots & \mathbf{b}_{\mathrm{D}_{c,6_{96\times8}}} & \mathbf{b}_{\mathrm{D}_{c,2_{96\times8}}} \end{bmatrix} \end{aligned} \tag{A.14}$$

Where:

$$\begin{aligned}
\mathbf{b}_{\mathrm{D}_{c,l\mu_{nx\times ncu}}} &= \left(\mathbf{b}_{\mathrm{D}_{1c,l\mu_{nx\times n1cu}}} \quad \mathbf{b}_{\mathrm{D}_{2c,l\mu_{nx\times n2cu}}}\right) \\
l &= 1,\ldots,N_0;\ \mu = 0,\ldots,N_c-1 \\
\mathbf{b}_{\mathrm{D}_{c,\mu_{96\times 8}}} &= \left(\mathbf{b}_{\mathrm{D}_{1c,l\mu_{96\times 4}}}, \mathbf{b}_{\mathrm{D}_{2c,\mu_{96\times 4}}}\right) \\
l &= 1,\ldots,8;\ \mu = 0,\ldots,7
\end{aligned} \tag{A.15}$$

The $\mathbf{B}_{\mathrm{D}_{n_{96\times 4}}}$ matrix is an $N_0 \times N_n = 8 \times 1$ block matrix:

$$\begin{aligned}
\mathbf{B}_{\mathrm{D}_{n_{N_0\cdot nx\times N_n\cdot nnu}}} &= \left[\mathbf{b}_{\mathrm{D}_{n,l\mu_{nx\times nnu}}}\right] = \left[\left(\mathbf{b}_{\mathrm{D}_{1n,l\mu_{nx\times n1nu}}} \quad \mathbf{b}_{\mathrm{D}_{2c,l\mu_{nx\times n2nu}}}\right)\right] \\
l &= 1,\ldots,N_0;\ \mu = 0,\ldots,N_n-1 \\
&\Longleftrightarrow \\
\mathbf{B}_{\mathrm{D}_{n_{96\times 4}}} &= \left[\mathbf{b}_{\mathrm{D}_{n,l\mu_{12\times 4}}}\right] = \left[\left(\mathbf{b}_{\mathrm{D}_{1n,l\mu_{12\times 2}}}, \mathbf{b}_{\mathrm{D}_{2n,l\mu_{12\times 2}}}\right)\right] \\
l &= 1,\ldots,8;\ \mu = 0
\end{aligned} \tag{A.16}$$

with the $l\mu$ block computed via:

$$\begin{aligned}
\mathbf{b}_{\mathrm{D}_{in,l\mu_{n_x\times n_{in}}}} &= \begin{cases} \mathbf{0}_{n_x\times n_{in}} & l \le l_n\cdot\mu \\ \int_{\mu\cdot l_n\cdot\tau_0}^{l\cdot\tau_0} e^{\mathbf{A}_{n_x\times n_x}(l\cdot\tau_0-\tau)}\mathbf{B}_{in_{n_x\times n_{in}}}d\tau & l_n\cdot\mu < l \le l_n\cdot(\mu+1) \\ \int_{\mu\cdot l_n\cdot\tau_0}^{(\mu+1)\cdot l_n\cdot\tau_0} e^{\mathbf{A}_{n_x\times n_x}(l\cdot\tau_0-\tau)}\mathbf{B}_{in_{n_x\times n_{in}}}d\tau & l_n\cdot(\mu+1) < l \end{cases} \\
(i=1,2) \\
&\Longleftrightarrow \\
\mathbf{b}_{\mathrm{D}_{1n,l\mu_{12\times 2}}} &= \begin{cases} \mathbf{0}_{12\times 2} & l \le 8\cdot\mu = 0 \\ \int_{\mu\cdot 8\cdot\tau_0}^{l\cdot\tau_0} e^{\mathbf{A}_{12\times 12}(l\cdot\tau_0-\tau)}\mathbf{B}_{1n_{12\times 2}}d\tau & 8\cdot\mu = 0 < l \le 8\cdot(\mu+1) = 8 \\ \int_{\mu\cdot 8\cdot\tau_0}^{(\mu+1)\cdot 8\cdot\tau_0} e^{\mathbf{A}_{12\times 12}(l\cdot\tau_0-\tau)}\mathbf{B}_{1n_{12\times 2}}d\tau & 8\cdot(\mu+1) = 8 < l \end{cases} \\
&\Longleftrightarrow \\
\mathbf{b}_{\mathrm{D}_{1n,l\mu_{12\times 2}}} &= \int_{\mu\cdot 8\cdot\tau_0}^{l\cdot\tau_0} e^{\mathbf{A}_{12\times 12}(l\cdot\tau_0-\tau)}\mathbf{B}_{1n_{12\times 2}}d\tau \qquad 0 < l \le 8 \\
\mathbf{b}_{\mathrm{D}_{2n,l\mu_{12\times 2}}} &= \begin{cases} \mathbf{0}_{12\times 2} & l \le 8\cdot\mu = 0 \\ \int_{\mu\cdot 8\cdot\tau_0}^{l\cdot\tau_0} e^{\mathbf{A}_{12\times 12}(l\cdot\tau_0-\tau)}\mathbf{B}_{2n_{12\times 2}}d\tau & 8\cdot\mu = 0 < l \le 8\cdot(\mu+1) = 8 \\ \int_{\mu\cdot 8\cdot\tau_0}^{(\mu+1)\cdot 8\cdot\tau_0} e^{\mathbf{A}_{12\times 12}(l\cdot\tau_0-\tau)}\mathbf{B}_{2n_{12\times 2}}d\tau & 8\cdot(\mu+1) = 8 < l \end{cases} \\
&\Longleftrightarrow \\
\mathbf{b}_{\mathrm{D}_{2n,l\mu_{12\times 2}}} &= \int_{\mu\cdot 8\cdot\tau_0}^{l\cdot\tau_0} e^{\mathbf{A}_{12\times 12}(l\cdot\tau_0-\tau)}\mathbf{B}_{2n_{12\times 2}}d\tau \qquad 0 < l \le 8
\end{aligned} \tag{A.17}$$

Hence:

$$\begin{aligned}
\mathbf{B}_{\mathrm{D}_{n_{N_0\cdot n_x\times N_n\cdot n_{nu}=8\cdot 12\times 1\cdot 4=96\times 4}}} &= \begin{bmatrix} \mathbf{b}_{\mathrm{D}_{n,1_{0_{12\times 4}}}} \\ \mathbf{b}_{\mathrm{D}_{n,2_{0_{12\times 4}}}} \\ \vdots \\ \mathbf{b}_{\mathrm{D}_{n,7_{0_{12\times 4}}}} \\ \mathbf{b}_{\mathrm{D}_{n,8_{0_{12\times 4}}}} \end{bmatrix} = \begin{bmatrix} \mathbf{b}_{\mathrm{D}_{1n,1_{0_{12\times 2}}}} & \mathbf{b}_{\mathrm{D}_{2n,1_{0_{12\times 2}}}} \\ \mathbf{b}_{\mathrm{D}_{1n,2_{0_{12\times 2}}}} & \mathbf{b}_{\mathrm{D}_{2n,2_{0_{12\times 2}}}} \\ \vdots & \\ \mathbf{b}_{\mathrm{D}_{1n,7_{0_{12\times 2}}}} & \mathbf{b}_{\mathrm{D}_{2n,7_{0_{12\times 2}}}} \\ \mathbf{b}_{\mathrm{D}_{1n,8_{0_{12\times 2}}}} & \mathbf{b}_{\mathrm{D}_{2n,8_{0_{12\times 2}}}} \end{bmatrix} \\
&= \begin{bmatrix} \mathbf{b}_{\mathrm{D}_{n,0_{96\times 4}}} \end{bmatrix} = \begin{bmatrix} \mathbf{b}_{\mathrm{D}_{1n,0_{96\times 2}}} & \mathbf{b}_{\mathrm{D}_{2n,0_{96\times 2}}} \end{bmatrix}
\end{aligned} \tag{A.18}$$

$$\begin{aligned}
\mathbf{C}_{\mathrm{D}_{(N_c\cdot n_{cy}+N_n\cdot n_{ny})\times N_0\cdot n_x}} &= \begin{bmatrix} \mathbf{C}_{\mathrm{D}_{c_{N_c\cdot n_{cy}\times N_0\cdot n_x}}} \\ \mathbf{C}_{\mathrm{D}_{n_{N_n\cdot n_{ny}\times N_0\cdot n_x}}} \end{bmatrix} \\
\Longleftrightarrow \mathbf{C}_{\mathrm{D}_{(8\cdot 12+1\cdot 8)\times 8\cdot 12}} &= \begin{bmatrix} \mathbf{C}_{\mathrm{D}_{c_{8\cdot 12\times 8\cdot 12}}} \\ \mathbf{C}_{\mathrm{D}_{n_{1\cdot 8\times 8\cdot 12}}} \end{bmatrix} \\
\Longleftrightarrow \mathbf{C}_{\mathrm{D}_{104\times 96}} &= \begin{bmatrix} \mathbf{C}_{\mathrm{D}_{c_{96\times 96}}} \\ \mathbf{C}_{\mathrm{D}_{n_{8\times 96}}} \end{bmatrix}
\end{aligned} \tag{A.19}$$

with the $\mathbf{C}_{\mathrm{D}_{c_{96\times 96}}}$ and $\mathbf{C}_{\mathrm{D}_{n_{8\times 96}}}$ matrices detailed in the following. Specifically, the $\mathbf{C}_{\mathrm{D}_{c_{96\times 96}}}$ matrix is an $N_c \times N_0 = 8 \times 8$ block matrix:

$$\begin{aligned}
\mathbf{C}_{\mathrm{D}_{c_{N_c\cdot n_{cy}\times N_0\cdot n_x}}} &= \left[\mathbf{c}_{\mathrm{D}_{c,\nu l_{n_{cy}\times n_x}}}\right] = \left[\begin{pmatrix} \mathbf{c}_{\mathrm{D}_{1c,\nu l_{n_{1cy}\times n_x}}} \\ \mathbf{c}_{\mathrm{D}_{2c,\nu l_{n_{2cy}\times n_x}}} \end{pmatrix}\right] \\
\nu &= 0,\ldots,N_c-1;\, l=1,\ldots,N_0 \\
&\Longleftrightarrow \\
\mathbf{C}_{\mathrm{D}_{c_{96\times 96}}} &= \left[\mathbf{c}_{\mathrm{D}_{c,\nu l_{12\times 12}}}\right] = \left[\begin{pmatrix} \mathbf{c}_{\mathrm{D}_{1c,\nu l_{6\times 12}}} \\ \mathbf{c}_{\mathrm{D}_{2c,\nu l_{6\times 12}}} \end{pmatrix}\right] \\
\nu &= 0,\ldots,7;\, l=1,\ldots,8
\end{aligned} \tag{A.20}$$

with the νl block computed via:

$$\begin{aligned}
\mathbf{c}_{\mathrm{D}_{ic,\nu l_{n_{icy}\times n_x}}} &= \begin{cases} \mathbf{C}_{ic_{n_{icy}\times n_x}} & \nu = 0, l = N_0 \quad or \quad l_c \cdot \nu = l \\ \mathbf{0}_{n_{icy}\times n_x} & otherwise \end{cases} \\
&\Longleftrightarrow \\
&(i = 1, 2) \\
\mathbf{c}_{\mathrm{D}_{1c,\nu l_{6\times 12}}} &= \begin{cases} \mathbf{C}_{1c_{6\times 12}} & \nu = 0, l = 8 \quad or \quad 1 \cdot \nu = l \\ \mathbf{0}_{6\times 12} & otherwise \end{cases}, \\
\mathbf{c}_{\mathrm{D}_{2c,\nu l_{6\times 12}}} &= \begin{cases} \mathbf{C}_{2c_{6\times 12}} & \nu = 0, l = 8 \quad or \quad 1 \cdot \nu = l \\ \mathbf{0}_{6\times 12} & otherwise \end{cases}
\end{aligned} \tag{A.21}$$

Hence:

$$\begin{aligned}
&\mathbf{C}_{\mathrm{D}c_{N_c \cdot n_{cy}\times N_0 \cdot n_x = 8\cdot 12\times 8\cdot 12 = 96\times 96}} \\
&= \begin{bmatrix}
\mathbf{0}_{12\times 12} & \mathbf{0}_{12\times 12} & \mathbf{0}_{12\times 12} & \mathbf{0}_{12\times 12} & \mathbf{0}_{12\times 12} & \mathbf{0}_{12\times 12} & \mathbf{0}_{12\times 12} & \mathbf{C}_{c_{12\times 12}} \\
\mathbf{C}_{c_{12\times 12}} & \mathbf{0}_{12\times 12} & \mathbf{0}_{12\times 12} & \mathbf{0}_{12\times 12} & \mathbf{0}_{12\times 12} & \mathbf{0}_{12\times 12} & \mathbf{0}_{12\times 12} & \mathbf{0}_{12\times 12} \\
\mathbf{0}_{12\times 12} & \mathbf{C}_{c_{12\times 12}} & \mathbf{0}_{12\times 12} & \mathbf{0}_{12\times 12} & \mathbf{0}_{12\times 12} & \mathbf{0}_{12\times 12} & \mathbf{0}_{12\times 12} & \mathbf{0}_{12\times 12} \\
\mathbf{0}_{12\times 12} & \mathbf{0}_{12\times 12} & \mathbf{C}_{c_{12\times 12}} & \mathbf{0}_{12\times 12} & \mathbf{0}_{12\times 12} & \mathbf{0}_{12\times 12} & \mathbf{0}_{12\times 12} & \mathbf{0}_{12\times 12} \\
\mathbf{0}_{12\times 12} & \mathbf{0}_{12\times 12} & \mathbf{0}_{12\times 12} & \mathbf{C}_{c_{12\times 12}} & \mathbf{0}_{12\times 12} & \mathbf{0}_{12\times 12} & \mathbf{0}_{12\times 12} & \mathbf{0}_{12\times 12} \\
\mathbf{0}_{12\times 12} & \mathbf{0}_{12\times 12} & \mathbf{0}_{12\times 12} & \mathbf{0}_{12\times 12} & \mathbf{C}_{c_{12\times 12}} & \mathbf{0}_{12\times 12} & \mathbf{0}_{12\times 12} & \mathbf{0}_{12\times 12} \\
\mathbf{0}_{12\times 12} & \mathbf{0}_{12\times 12} & \mathbf{0}_{12\times 12} & \mathbf{0}_{12\times 12} & \mathbf{0}_{12\times 12} & \mathbf{C}_{c_{12\times 12}} & \mathbf{0}_{12\times 12} & \mathbf{0}_{12\times 12} \\
\mathbf{0}_{12\times 12} & \mathbf{0}_{12\times 12} & \mathbf{0}_{12\times 12} & \mathbf{0}_{12\times 12} & \mathbf{0}_{12\times 12} & \mathbf{0}_{12\times 12} & \mathbf{C}_{c_{12\times 12}} & \mathbf{0}_{12\times 12}
\end{bmatrix}
\end{aligned} \tag{A.22}$$

Where

$$\mathbf{C}_{c_{12\times 12}} = \left(\mathbf{C}_{1c_{6\times 12}} \mathbf{C}_{2c_{6\times 12}}\right) \tag{A.23}$$

The $\mathbf{C}_{\mathrm{D}_{n_{8\times 96}}}$ matrix is a $N_n \times N_0 = 1 \times 8$ block matrix:

$$\begin{aligned}
\mathbf{C}_{\mathrm{D}_{n_{N_n \cdot n_{ny} \times N_0 \cdot n_x}}} &= \left[\mathbf{c}_{\mathrm{D}_{n,\nu l_{n_{ny} \times n_x}}}\right] = \left[\begin{pmatrix} \mathbf{c}_{\mathrm{D}_{1n,\nu l_{n_{1ny} \times n_x}}} \\ \mathbf{c}_{\mathrm{D}_{2n,\nu l_{n_{2ny} \times n_x}}} \end{pmatrix}\right] \\
\nu &= 0, \ldots, N_n - 1;\, l = 1, \ldots, N_0 \\
&\Longleftrightarrow \\
\mathbf{C}_{\mathrm{D}_{n_{8\times 96}}} &= \left[\mathbf{c}_{\mathrm{D}_{n,\nu l_{8\times 12}}}\right] = \left[\begin{pmatrix} \mathbf{c}_{\mathrm{D}_{1n,\nu l_{4\times 12}}} \\ \mathbf{c}_{\mathrm{D}_{2n,\nu l_{4\times 12}}} \end{pmatrix}\right] \\
\nu &= 0;\, l = 1, \ldots, 8
\end{aligned} \tag{A.24}$$

with the νl block computed via:

$$\begin{aligned}
\mathbf{c}_{\mathrm{D}_{in,l\nu_{8\times 12}}} &= \begin{cases} \mathbf{C}_{in_{n_{iny} \times n_x}} & \nu = 0, l = N_0 \quad or \quad l_n \cdot \nu = l \\ \\ \mathbf{0}_{8\times 12} & otherwise \end{cases} \qquad (i = 1, 2) \\
&\Longleftrightarrow \\
\mathbf{c}_{\mathrm{D}_{1n,l\nu_{4\times 12}}} &= \begin{cases} \mathbf{C}_{1n_{4\times 12}} & \nu = 0, l = 8 \quad or \quad 8 \cdot \nu = l \\ \\ \mathbf{0}_{4\times 12} & otherwise \end{cases} \\
\mathbf{c}_{\mathrm{D}_{2n,l\nu_{4\times 12}}} &= \begin{cases} \mathbf{C}_{2n_{4\times 12}} & \nu = 0, l = 8 \quad or \quad 8 \cdot \nu = l \\ \\ \mathbf{0}_{4\times 12} & otherwise \end{cases}
\end{aligned} \tag{A.25}$$

Hence:

$$\mathbf{C}_{\mathrm{D}_{n_{N_n \cdot n_{ny} \times N_0 \cdot n_x = 1\cdot 8\times 8\cdot 12 = 8\times 96}}} = \begin{bmatrix} \mathbf{0}_{8\times 12} & \mathbf{0}_{8\times 12} & \mathbf{0}_{8\times 12} & \mathbf{0}_{8\times 12} & \mathbf{0}_{8\times 12} & \mathbf{0}_{8\times 12} & \mathbf{0}_{8\times 12} & \mathbf{C}_{n_{8\times 12}} \end{bmatrix} \tag{A.26}$$

Where

$$\mathbf{C}_{n_{8\times 12}} = \begin{pmatrix} \mathbf{C}_{1n_{4\times 12}} \\ \mathbf{C}_{2n_{4\times 12}} \end{pmatrix} \tag{A.27}$$

Lastly, $\mathbf{U}1_{N_0 \cdot n_x \times N_0 \cdot n_x = 8 \cdot 12 \times 8 \cdot 12 = 96 \times 96}$ and $\mathbf{U}2_{N_0 \cdot n_x \times N_0 \cdot n_x = 8 \cdot 12 \times 8 \cdot 12 = 96 \times 96}$ are $N_0 \times N_0 = 8$ blocks diagonal matrices having the following $n_x \times n_x = 12 \times 12$ blocks on their diagonals:

$$\begin{array}{l} \left\{ \begin{array}{rcl} \mathbf{U}1_{N_0 \cdot n_x \times N_0 \cdot n_x} & = & blockdiag\left(\mathbf{I}_{n_x \times n_x}, \ldots, \mathbf{I}_{n_x \times n_x}, \mathbf{0}_{n_x \times n_x}\right) \\ \mathbf{U}2_{N_0 \cdot n_x \times N_0 \cdot n_x} & = & blockdiag\left(\mathbf{0}_{n_x \times n_x}, \ldots, \mathbf{0}_{n_x \times n_x}, \mathbf{I}_{n_x \times n_x}\right) \end{array} \right. \\ \Longleftrightarrow \\ \left\{ \begin{array}{rcl} \mathbf{U}1_{8 \cdot 12 \times 8 \cdot 12} & = & \mathbf{U}1_{96 \times 96} = blockdiag\left(\mathbf{I}_{12 \times 12}, \ldots, \mathbf{I}_{12 \times 12}, \mathbf{0}_{12 \times 12}\right) \\ \mathbf{U}2_{8 \cdot 12 \times 8 \cdot 12} & = & \mathbf{U}2_{96 \times 96} = blockdiag\left(\mathbf{0}_{12 \times 12}, \ldots, \mathbf{0}_{12 \times 12}, \mathbf{I}_{12 \times 12}\right) \end{array} \right. \end{array} \tag{A.28}$$

Therefore,

$$\begin{array}{rcl} \hat{\mathbf{C}}_{\mathrm{D}_{104 \times 96}} & = & \mathbf{C}_{\mathrm{D}_{104 \times 96}} \cdot \mathbf{U}1_{96 \times 96} \cdot \mathbf{A}_{\mathrm{D}_{96 \times 96}} + \mathbf{C}_{\mathrm{D}_{104 \times 96}} \cdot \mathbf{U}2_{96 \times 96} \\ \hat{\mathbf{D}}_{\mathrm{D}_{104 \times 68}} & = & \mathbf{C}_{\mathrm{D}_{104 \times 96}} \cdot \mathbf{U}1_{96 \times 96} \cdot \mathbf{B}_{\mathrm{D}_{96 \times 68}} \end{array} \tag{A.29}$$

The closed-loop dynamics can be obtained from the open-loop discrete-time difference equations using the feedback law:

$$\begin{array}{rcl} \mathbf{u}_{\mathrm{D}_{(N_c \cdot n_{cu} + N_n \cdot n_{nu}) \times 1}} & = & \mathbf{F}_{\mathrm{D}_{(N_c \cdot n_{cu} + N_n \cdot n_{nu}) \times (N_c \cdot n_{cy} + N_n \cdot n_{ny})}} \mathbf{y}_{\mathrm{D}_{(N_c \cdot n_{cy} + N_n \cdot n_{ny}) \times 1}} \Longleftrightarrow \\ \mathbf{u}_{\mathrm{D}_{68 \times 1}} & = & \mathbf{F}_{\mathrm{D}_{(8 \cdot 8 + 1 \cdot 4) \times (8 \cdot 12 + 1 \cdot 8)}} \mathbf{y}_{\mathrm{D}_{(8 \cdot 12 + 1 \cdot 8) \times 1}} = \mathbf{F}_{\mathrm{D}_{68 \times 104}} \mathbf{y}_{\mathrm{D}_{104 \times 1}} \end{array} \tag{A.30}$$

According to Equation 4.33, given

$$\begin{aligned}
\mathbf{F}_{cc_{N_c\cdot n_{cu}\times N_c\cdot n_{cy}}} = \mathbf{F}_{cc_{8\cdot 8\times 8\cdot 12}} &= \begin{bmatrix} \mathbf{F}_{1c_{n_{1cu}\times n_{1cy}}} & \mathbf{0}_{n_{1cu}\times n_{2cy}} \\ \mathbf{0}_{n_{2cu}\times n_{1cy}} & \mathbf{F}_{2c_{n_{2cu}\times n_{2cy}}} \end{bmatrix} = \begin{bmatrix} \mathbf{F}_{1c_{4\times 6}} & \mathbf{0}_{4\times 6} \\ \mathbf{0}_{4\times 6} & \mathbf{F}_{2c_{4\times 6}} \end{bmatrix} \\
\mathbf{F}_{cn_{N_c\cdot n_{cu}\times N_n\cdot n_{ny}}} = \mathbf{F}_{cn_{8\cdot 8\times 1\cdot 8}} &= \begin{bmatrix} \mathbf{0}_{n_{1cu}\times n_{1ny}} & \mathbf{0}_{n_{1cu}\times n_{2ny}} \\ \mathbf{0}_{n_{2cu}\times n_{1ny}} & \mathbf{0}_{n_{2cu}\times n_{2ny}} \end{bmatrix} = \begin{bmatrix} \mathbf{0}_{4\times 4} & \mathbf{0}_{4\times 4} \\ \mathbf{0}_{4\times 4} & \mathbf{0}_{4\times 4} \end{bmatrix} \\
\mathbf{F}_{nc_{N_n\cdot n_{nu}\times N_c\cdot n_{cy}}} = \mathbf{F}_{nc_{1\cdot 4\times 8\cdot 12}} &= \begin{bmatrix} \mathbf{0}_{n_{1nu}\times n_{1cy}} & \mathbf{0}_{n_{1nu}\times n_{2cy}} \\ \mathbf{0}_{n_{2nu}\times n_{1cy}} & \mathbf{0}_{n_{2nu}\times n_{2cy}} \end{bmatrix} = \begin{bmatrix} \mathbf{0}_{2\times 6} & \mathbf{0}_{2\times 6} \\ \mathbf{0}_{2\times 6} & \mathbf{0}_{2\times 6} \end{bmatrix} \\
\mathbf{F}_{nn_{N_n\cdot n_{nu}\times N_n\cdot n_{ny}}} = \mathbf{F}_{nn_{1\cdot 4\times 1\cdot 8}} &= \begin{bmatrix} \mathbf{F}_{1n_{n_{1nu}\times n_{1ny}}} & \mathbf{0}_{n_{1nu}\times n_{2ny}} \\ \mathbf{0}_{n_{2nu}\times n_{1ny}} & \mathbf{F}_{2n_{n_{2nu}\times n_{2ny}}} \end{bmatrix} = \begin{bmatrix} \mathbf{F}_{1n_{n_{2\times 4}}} & \mathbf{0}_{2\times 4} \\ \mathbf{0}_{2\times 4} & \mathbf{F}_{2n_{n_{2\times 4}}} \end{bmatrix}
\end{aligned} \tag{A.31}$$

The discrete-time feedback matrix $\mathbf{F}_{\mathrm{D}_{(N_c\cdot n_{cu}+N_n\cdot n_{nu})\times(N_c\cdot n_{cy}+N_n\cdot n_{ny})=(8\cdot 8+1\cdot 4)\times(8\cdot 12+1\cdot 8)=68\times 104}}$ is:

$$\begin{aligned}
&\mathbf{F}_{\mathrm{D}_{(N_c\cdot n_{cu}+N_n\cdot n_{nu})\cdot\times(N_c\cdot n_{cy}+N_n\cdot n_{ny})}} = \begin{bmatrix} \mathbf{F}_{\mathrm{D}cc_{N_c\cdot n_{cu}\times N_c\cdot n_{cy}}} & \mathbf{F}_{\mathrm{D}cn_{N_c\cdot n_{cu}\times N_n\cdot n_{ny}}} \\ \mathbf{F}_{\mathrm{D}nc_{N_n\cdot n_{nu}\times N_c\cdot n_{cy}}} & \mathbf{F}_{\mathrm{D}nn_{N_n\cdot n_{nu}\times N_n\cdot n_{ny}}} \end{bmatrix} \\
\Longleftrightarrow& \\
&\mathbf{F}_{\mathrm{D}_{(64+4)\times(96+8)}} = \begin{bmatrix} \mathbf{F}_{\mathrm{D}cc_{64\times 96}} & \mathbf{F}_{\mathrm{D}cn_{64\times 8}} \\ \mathbf{F}_{\mathrm{D}nc_{4\times 96}} & \mathbf{F}_{\mathrm{D}nn_{4\times 8}} \end{bmatrix} = \begin{bmatrix} \mathbf{F}_{\mathrm{D}cc_{64\times 96}} & \mathbf{0}_{64\times 8} \\ \mathbf{0}_{4\times 96} & \mathbf{F}_{\mathrm{D}nn_{4\times 8}} \end{bmatrix}
\end{aligned} \tag{A.32}$$

and the $\mathbf{F}_{\mathrm{D}cc_{N_c\cdot n_{cu}\times N_c\cdot n_{cy}=64\times 96}}$ and $\mathbf{F}_{\mathrm{D}nn_{N_n\cdot n_{nu}\times N_n\cdot n_{ny}=4\times 8}}$ matrices are block matrices computed as detailed next. In particular, $\mathbf{F}_{\mathrm{D}cc_{N_c\cdot n_{cu}\times N_c\cdot n_{cy}}}$ has $N_c\times N_c = 8\times 8$ blocks of dimension $n_{cu}\times n_{cy} = 8\times 12$:

$$\begin{aligned}
\mathbf{F}_{\mathrm{D}cc_{N_c\cdot n_{cu}\times N_c\cdot n_{cy}}} &= \left[\mathbf{f}_{\mathrm{D}cc,\mu\nu_{n_{cu}\times n_{cy}}}\right] \quad \mu = 0,\ldots,N_c-1;\ \nu = 0,\ldots,N_c-1 \\
&\Longleftrightarrow \\
\mathbf{F}_{\mathrm{D}cc_{8\cdot 8\times 8\cdot 12=64\times 96}} &= \left[\mathbf{f}_{\mathrm{D}cc,\mu\nu_{8\times 12}}\right] \quad \mu = 0,\ldots,7;\ \nu = 0,\ldots,7
\end{aligned} \tag{A.33}$$

with the $\mu\nu$ block computed via:

$$\begin{aligned}
\mathbf{f}_{\mathrm{D}_{cc,\mu\nu_{n_{cu}\times n_{cy}}}} &= \begin{cases} \mathbf{F}_{cc_{n_{cu}\times n_{cy}}} & \nu l_c \leq \mu l_c < (\nu+1)\, l_c \\ \mathbf{0}_{n_{cu}\times n_{cy}} & otherwise. \end{cases} \\
&\Longleftrightarrow \\
\mathbf{f}_{\mathrm{D}_{cc,\mu\nu_{n_{cu}\times n_{cy}}}} &= \begin{cases} \mathbf{F}_{cc_{8\times 12}} & \nu \leq \mu < (\nu+1) \\ \mathbf{0}_{8\times 12} & otherwise. \end{cases}
\end{aligned} \tag{A.34}$$

Hence:

$$\mathbf{F}_{\mathrm{D}_{cc_{64\times 96}}} = \begin{bmatrix}
\mathbf{F}_{cc_{8\times 12}} & \mathbf{0}_{8\times 12} & \mathbf{0}_{8\times 12} & \mathbf{0}_{8\times 12} & \mathbf{0}_{8\times 12} & \mathbf{0}_{8\times 12} & \mathbf{0}_{8\times 12} & \mathbf{0}_{8\times 12} \\
\mathbf{0}_{8\times 12} & \mathbf{F}_{cc_{8\times 12}} & \mathbf{0}_{8\times 12} & \mathbf{0}_{8\times 12} & \mathbf{0}_{8\times 12} & \mathbf{0}_{8\times 12} & \mathbf{0}_{8\times 12} & \mathbf{0}_{8\times 12} \\
\mathbf{0}_{8\times 12} & \mathbf{0}_{8\times 12} & \mathbf{F}_{cc_{8\times 12}} & \mathbf{0}_{8\times 12} & \mathbf{0}_{8\times 12} & \mathbf{0}_{8\times 12} & \mathbf{0}_{8\times 12} & \mathbf{0}_{8\times 12} \\
\mathbf{0}_{8\times 12} & \mathbf{0}_{8\times 12} & \mathbf{0}_{8\times 12} & \mathbf{F}_{cc_{8\times 12}} & \mathbf{0}_{8\times 12} & \mathbf{0}_{8\times 12} & \mathbf{0}_{8\times 12} & \mathbf{0}_{8\times 12} \\
\mathbf{0}_{8\times 12} & \mathbf{0}_{8\times 12} & \mathbf{0}_{8\times 12} & \mathbf{0}_{8\times 12} & \mathbf{F}_{cc_{8\times 12}} & \mathbf{0}_{8\times 12} & \mathbf{0}_{8\times 12} & \mathbf{0}_{8\times 12} \\
\mathbf{0}_{8\times 12} & \mathbf{0}_{8\times 12} & \mathbf{0}_{8\times 12} & \mathbf{0}_{8\times 12} & \mathbf{0}_{8\times 12} & \mathbf{F}_{cc_{8\times 12}} & \mathbf{0}_{8\times 12} & \mathbf{0}_{8\times 12} \\
\mathbf{0}_{8\times 12} & \mathbf{0}_{8\times 12} & \mathbf{0}_{8\times 12} & \mathbf{0}_{8\times 12} & \mathbf{0}_{8\times 12} & \mathbf{0}_{8\times 12} & \mathbf{F}_{cc_{8\times 12}} & \mathbf{0}_{8\times 12} \\
\mathbf{0}_{8\times 12} & \mathbf{0}_{8\times 12} & \mathbf{0}_{8\times 12} & \mathbf{0}_{8\times 12} & \mathbf{0}_{8\times 12} & \mathbf{0}_{8\times 12} & \mathbf{0}_{8\times 12} & \mathbf{F}_{cc_{8\times 12}}
\end{bmatrix} \tag{A.35}$$

The $\mathbf{F}_{\mathrm{D}_{nn_{N_n\cdot n_{nu}\times N_n\cdot n_{ny}}}}$ has $N_n \times N_n = 1\times 1$ blocks of dimension $n_{nu}\times n_{ny} = 4\times 8$:

$$\begin{aligned}
\mathbf{F}_{\mathrm{D}_{nn_{N_n\cdot n_{nu}\times N_n\cdot n_{ny}}}} &= \left[\mathbf{f}_{\mathrm{D}_{nn,\mu\nu_{n_{nu}\times n_{ny}}}}\right] \quad \mu = 0,\ldots,N_n-1;\ \nu = 0,\ldots,N_n-1 \\
&\Longleftrightarrow \\
\mathbf{F}_{\mathrm{D}_{nn_{1\cdot 4\times 1\cdot 8=4\times 8}}} &= \left[\mathbf{f}_{\mathrm{D}_{nn,\mu\nu_{4\times 8}}}\right] \quad \mu = 0;\ \nu = 0
\end{aligned} \tag{A.36}$$

with the $\mu\nu$-th block computed via:

$$\begin{aligned}
\mathbf{f}_{\mathrm{D}_{nn,\mu\nu_{n_{cu}\times n_{cy}}}} &= \begin{cases} \mathbf{F}_{nn_{n_{nu}\times n_{ny}}} & \nu l_n \leq \mu l_n < (\nu+1)\, l_n \\ \mathbf{0}_{nnu\times n_{cny}} & otherwise. \end{cases} \\
&\Longleftrightarrow \\
\mathbf{f}_{\mathrm{D}_{nn,\mu\nu_{4\times 8}}} &= \begin{cases} \mathbf{F}_{nn_{4\times 8}} & 8\nu \leq 8\mu < 8\,(\nu+1) \\ \mathbf{0}_{4\times 8} & otherwise. \end{cases}
\end{aligned} \tag{A.37}$$

Hence:

$$\mathbf{F}_{\mathrm{D}_{nn_{4\times 8}}} = \mathbf{F}_{nn_{4\times 8}} \tag{A.38}$$

A.1.2 Delay Augmentation

The network and computational delay can be integrated into the discrete-time dynamics of the system using the method in Appendix B of [2]. For the general case of a computational delay $T_{VE} = n_{_{VE}} T_c$ (i.e., an integer multiple of the control sampling rate) and a network delay $T_D = n_{_D} T_n$ (i.e., an integer multiple of the network

sampling rate), the discrete-time system:

$$
\begin{aligned}
\mathbf{x}_{\mathrm{D}_{N_0\cdot n_x\times 1}}[k+1] &= \mathbf{A}_{\mathrm{D}_{N_0\cdot n_x\times N_0\cdot n_x}}\mathbf{x}_{\mathrm{D}_{N_0\cdot n_x\times 1}}[k] \\
&+ \begin{bmatrix}\mathbf{B}_{\mathrm{D}_{c_{N_0\cdot n_x\times N_c\cdot n_{cu}}}} & \mathbf{B}_{\mathrm{D}_{n_{N_0\cdot n_x\times N_n\cdot n_{nu}}}}\end{bmatrix}\begin{pmatrix}\mathbf{u}_{\mathrm{D}_{c_{N_0\cdot n_x\times N_c\cdot n_{cu}}}}[k] \\ \mathbf{u}_{\mathrm{D}_{n_{N_0\cdot n_x\times N_n\cdot n_{nu}}}}[k]\end{pmatrix} \\
\begin{pmatrix}\mathbf{y}_{\mathrm{D}_{c_{N_c\cdot n_{cy}\times 1}}}[k] \\ \mathbf{y}_{\mathrm{D}_{c_{N_n\cdot n_{ny}\times 1}}}[k]\end{pmatrix} &= \hat{\mathbf{C}}_{\mathrm{D}_{(N_c\cdot n_{cy}+N_n\cdot n_{ny})\times N_0\cdot n_x}}\mathbf{x}_{\mathrm{D}_{N_0\cdot n_x\times 1}}[k] \\
&+ \begin{bmatrix}\hat{\mathbf{D}}_{\mathrm{D}_{c_{(N_c\cdot n_{cy}+N_n\cdot n_{ny})\times N_c\cdot n_{cu}}}} & \hat{\mathbf{D}}_{\mathrm{D}_{n_{(N_c\cdot n_{cy}+N_n\cdot n_{ny})\times N_n\cdot n_{nu}}}}\end{bmatrix}\begin{pmatrix}\mathbf{u}_{\mathrm{D}_{c_{N_c\cdot n_{cu}\times 1}}}[k] \\ \mathbf{u}_{\mathrm{D}_{n_{N_n\cdot n_{nu}\times 1}}}[k]\end{pmatrix} \\
&\Longleftrightarrow \\
\mathbf{x}_{\mathrm{D}_{96\times 1}}[k+1] &= \mathbf{A}_{\mathrm{D}_{96\times 96}}\mathbf{x}_{\mathrm{D}_{96\times 1}}[k] + \begin{bmatrix}\mathbf{B}_{\mathrm{D}_{c_{96\times 64}}} & \mathbf{B}_{\mathrm{D}_{n_{96\times 4}}}\end{bmatrix}\begin{pmatrix}\mathbf{u}_{\mathrm{D}_{c_{96\times 64}}}[k] \\ \mathbf{u}_{\mathrm{D}_{n_{96\times 4}}}[k]\end{pmatrix} \\
\begin{pmatrix}\mathbf{y}_{\mathrm{D}_{c_{96\times 1}}}[k] \\ \mathbf{y}_{\mathrm{D}_{c_{8\times 1}}}[k]\end{pmatrix} &= \hat{\mathbf{C}}_{\mathrm{D}_{104\times 96}}\mathbf{x}_{\mathrm{D}_{96\times 1}}[k] + \begin{bmatrix}\hat{\mathbf{D}}_{\mathrm{D}_{c_{104\times 64}}} & \hat{\mathbf{D}}_{\mathrm{D}_{n_{104\times 4}}}\end{bmatrix}\begin{pmatrix}\mathbf{u}_{\mathrm{D}_{c_{64\times 1}}}[k] \\ \mathbf{u}_{\mathrm{D}_{n_{4\times 1}}}[k]\end{pmatrix}
\end{aligned}
\tag{A.39}
$$

has the delayed feedback:

$$
\begin{aligned}
\begin{pmatrix}\mathbf{u}_{\mathrm{D}_{c_{N_c\cdot n_{cu}\times 1}}}[k] \\ \mathbf{u}_{\mathrm{D}_{n_{N_n\cdot n_{nu}\times 1}}}[k]\end{pmatrix} &= \mathbf{F}_{\mathrm{D}_{(N_c\cdot n_{cu}+N_n\cdot n_{nu})\times(N_c\cdot n_{cy}+N_n\cdot n_{ny})}}\begin{pmatrix}\mathbf{y}_{\mathrm{D}_{c_{N_c\cdot n_{cy}\times 1}}}[k-n_{_{VE}}T_c] \\ \mathbf{y}_{\mathrm{D}_{c_{N_n\cdot n_{ny}\times 1}}}[k-n_{_D}T_n]\end{pmatrix} \\
&\Longleftrightarrow \\
\begin{pmatrix}\mathbf{u}_{\mathrm{D}_{c_{64\times 1}}}[k] \\ \mathbf{u}_{\mathrm{D}_{n_{4\times 1}}}[k]\end{pmatrix} &= \mathbf{F}_{\mathrm{D}_{68\times 104}}\begin{pmatrix}\mathbf{y}_{\mathrm{D}_{c_{96\times 1}}}[k-n_{_{VE}}T_c] \\ \mathbf{y}_{\mathrm{D}_{c_{8\times 1}}}[k-n_{_D}T_n]\end{pmatrix}
\end{aligned}
\tag{A.40}
$$

In this case, the state vector is augmented with the delayed inputs:

$$\tilde{\mathbf{x}}_{\mathrm{D}_{\left(N_0\cdot n_x+n_{VE}\cdot n_{cu}+n_D\cdot n_{nu}\right)\times 1}}[k] = \begin{bmatrix} \mathbf{x}_{\mathrm{D}_{N_0\cdot n_x\times 1}}[k] \\ \mathbf{u}_{c_{n_{cu}\times 1}}(kT_0-n_{VE}T_c) \\ \vdots \\ \mathbf{u}_{c_{n_{cu}\times 1}}(kT_0-T_c) \\ \mathbf{u}_{n_{nnu}\times 1}(kT_0-n_DT_n) \\ \vdots \\ \mathbf{u}_{n_{nnu}\times 1}(kT_0-T_n) \end{bmatrix} = \begin{bmatrix} \mathbf{x}_{\mathrm{D}_{N_0\cdot n_x\times 1}}[k] \\ \mathbf{u}_{1c_{n_{1cu}\times 1}}(kT_0-n_{VE}T_c) \\ \mathbf{u}_{2c_{n_{2cu}\times 1}}(kT_0-n_{VE}T_c) \\ \vdots \\ \mathbf{u}_{1c_{n_{1cu}\times 1}}(kT_0-T_c) \\ \mathbf{u}_{2c_{n_{2cu}\times 1}}(kT_0-T_c) \\ \mathbf{u}_{1n_{n_{1nu}\times 1}}(kT_0-n_DT_n) \\ \mathbf{u}_{2n_{n_{2nu}\times 1}}(kT_0-n_DT_n) \\ \vdots \\ \mathbf{u}_{1n_{n_{1nu}\times 1}}(kT_0-T_n) \\ \mathbf{u}_{2n_{n_{2nu}\times 1}}(kT_0-T_n) \end{bmatrix}$$

$$\Longleftrightarrow$$

$$\tilde{\mathbf{x}}_{\mathrm{D}_{\left(96+8\cdot n_{VE}+4\cdot n_D\right)\times 1}}[k] = \begin{bmatrix} \mathbf{x}_{\mathrm{D}_{96\times 1}}[k] \\ \mathbf{u}_{c_{8\times 1}}(kT_0-n_{VE}T_c) \\ \vdots \\ \mathbf{u}_{c_{8\times 1}}(kT_0-T_c) \\ \mathbf{u}_{n_{4\times 1}}(kT_0-n_DT_n) \\ \vdots \\ \mathbf{u}_{n_{4\times 1}}(kT_0-T_n) \\ \mathbf{u}_{n_{4\times 1}}(kT_0-T_n) \end{bmatrix} = \begin{bmatrix} \mathbf{x}_{\mathrm{D}_{96\times 1}}[k] \\ \mathbf{u}_{1c_{4\times 1}}(kT_0-n_{VE}T_c) \\ \mathbf{u}_{2c_{4\times 1}}(kT_0-n_{VE}T_c) \\ \vdots \\ \mathbf{u}_{1c_{4\times 1}}(kT_0-T_c) \\ \mathbf{u}_{2c_{4\times 1}}(kT_0-T_c) \\ \mathbf{u}_{1n_{2\times 1}}(kT_0-n_DT_n) \\ \mathbf{u}_{2n_{2\times 1}}(kT_0-n_DT_n) \\ \vdots \\ \mathbf{u}_{1n_{2\times 1}}(kT_0-T_n) \\ \mathbf{u}_{2n_{2\times 1}}(kT_0-T_n) \end{bmatrix} \tag{A.41}$$

and the transition matrices are modified as follows:

$$\tilde{\mathbf{A}}_{\mathrm{D}_{\left(N_0\cdot n_x+n_{VE}\cdot n_{cu}+n_D\cdot n_{nu}\right)\times\left(N_0\cdot n_x+n_{VE}\cdot n_{cu}+n_D\cdot n_{nu}\right)}} = \begin{bmatrix} \bar{\mathbf{A}}_{\mathrm{D}_{\left(N_0\cdot n_x+n_{VE}\cdot n_{cu}+n_D\cdot n_{nu}\right)\times N_0\cdot n_x}} \\ \bar{\mathbf{b}}_{\mathrm{Dc}_{aug}\left(N_0\cdot n_x+n_{VE}\cdot n_{cu}+n_D\cdot n_{nu}\right)\times n_{VE}\cdot n_{cu}} \\ \bar{\mathbf{b}}_{\mathrm{Dn}_{aug}\left(N_0\cdot n_x+n_{VE}\cdot n_{cu}+n_D\cdot n_{nu}\right)\times n_D\cdot n_{nu}} \end{bmatrix}^T \tag{A.42}$$

$$\begin{aligned} \bar{\mathbf{A}}_{\mathrm{D}_{\left(N_0\cdot n_x+n_{VE}\cdot n_{cu}+n_D\cdot n_{nu}\right)\times N_0\cdot n_x}} &= \bar{\mathbf{A}}_{\mathrm{D}_{\left(8\cdot 12+n_{VE}\cdot 8+n_D\cdot 4\right)\times 8\cdot 12}} \\ &= \begin{bmatrix} \mathbf{A}_{\mathrm{D}_{N_0\cdot n_x\times N_0\cdot n_x}} \\ \mathbf{0}_{n_{1cu}\times N_0\cdot n_x} \\ \mathbf{0}_{n_{2cu}\times N_0\cdot n_x} \\ \vdots \\ \mathbf{0}_{n_{1cu}\times N_0\cdot n_x} \\ \mathbf{0}_{n_{2cu}\times N_0\cdot n_x} \\ \mathbf{0}_{n_{1nu}\times N_0\cdot n_x} \\ \mathbf{0}_{n_{2nu}\times N_0\cdot n_x} \\ \vdots \\ \mathbf{0}_{n_{1nu}\times N_0\cdot n_x} \\ \mathbf{0}_{n_{2nu}\times N_0\cdot n_x} \end{bmatrix} = \begin{bmatrix} \mathbf{A}_{\mathrm{D}_{8\cdot 12\times 8\cdot 12}} \\ \mathbf{0}_{4\times 8\cdot 12} \\ \mathbf{0}_{4\times 8\cdot 12} \\ \vdots \\ \mathbf{0}_{4\times 8\cdot 12} \\ \mathbf{0}_{4\times 8\cdot 12} \\ \mathbf{0}_{2\times 8\cdot 12} \\ \mathbf{0}_{2\times 8\cdot 12} \\ \vdots \\ \mathbf{0}_{2\times 8\cdot 12} \\ \mathbf{0}_{2\times 8\cdot 12} \end{bmatrix} \end{aligned} \tag{A.43}$$

$$\bar{\mathbf{b}}_{\mathrm{Dc}_{aug}\left(N_0\cdot n_x+n_{VE}\cdot n_{cu}+n_D\cdot n_{nu}\right)\times n_{VE}\cdot n_{cu}} = \bar{\mathbf{b}}_{\mathrm{Dc}_{aug}\left(8\cdot 12+n_{VE}\cdot 8+n_D\cdot 4\right)\times n_{VE}\cdot 8}$$

$$= \begin{bmatrix}
\mathbf{b}_{\mathrm{D}_{1c,1}{}_{N_0\cdot n_x\times n_{1cu}}} & \mathbf{b}_{\mathrm{D}_{2c,1}{}_{N_0\cdot n_x\times n_{2cu}}} & \mathbf{0}_{N_0\cdot n_x\times n_{1cu}} & \mathbf{0}_{N_0\cdot n_x\times n_{1cu}} & \dots & \mathbf{0}_{N_0\cdot n_x\times n_{1cu}} & \mathbf{0}_{N_0\cdot n_x\times n_{2cu}} \\
\mathbf{0}_{n_{1cu}\times n_{1cu}} & \mathbf{0}_{n_{1cu}\times n_{2cu}} & \mathbf{I}_{n_{1cu}\times n_{1cu}} & \mathbf{0}_{n_{1cu}\times n_{2cu}} & \dots & \mathbf{0}_{n_{1cu}\times n_{1cu}} & \mathbf{0}_{n_{1cu}\times n_{2cu}} \\
\mathbf{0}_{n_{2cu}\times n_{1cu}} & \mathbf{0}_{n_{2cu}\times n_{2cu}} & \mathbf{0}_{n_{2cu}\times n_{1cu}} & \mathbf{I}_{n_{2cu}\times n_{2cu}} & \dots & \mathbf{0}_{n_{2cu}\times n_{1cu}} & \mathbf{0}_{n_{2cu}\times n_{2cu}} \\
\vdots & & & & & & \\
\mathbf{0}_{n_{1cu}\times n_{1cu}} & \mathbf{0}_{n_{1cu}\times n_{2cu}} & \mathbf{0}_{n_{1cu}\times n_{1cu}} & \mathbf{0}_{n_{1cu}\times n_{2cu}} & \dots & \mathbf{I}_{n_{1cu}\times n_{1cu}} & \mathbf{0}_{n_{1cu}\times n_{2cu}} \\
\mathbf{0}_{n_{1cu}\times n_{1cu}} & \mathbf{0}_{n_{1cu}\times n_{2cu}} & \mathbf{0}_{n_{1cu}\times n_{1cu}} & \mathbf{0}_{n_{1cu}\times n_{2cu}} & \dots & \mathbf{0}_{n_{1cu}\times n_{1cu}} & \mathbf{I}_{n_{1cu}\times n_{2cu}} \\
\mathbf{0}_{n_{1nu}\times n_{1cu}} & \mathbf{0}_{n_{1nu}\times n_{2cu}} & \mathbf{0}_{n_{1nu}\times n_{1cu}} & \mathbf{0}_{n_{1nu}\times n_{2cu}} & \dots & \mathbf{0}_{n_{1nu}\times n_{1cu}} & \mathbf{0}_{n_{1nu}\times n_{2cu}} \\
\mathbf{0}_{n_{2nu}\times n_{1cu}} & \mathbf{0}_{n_{2nu}\times n_{2cu}} & \mathbf{0}_{n_{2nu}\times n_{1cu}} & \mathbf{0}_{n_{2nu}\times n_{2cu}} & \dots & \mathbf{0}_{n_{2nu}\times n_{1cu}} & \mathbf{0}_{n_{2nu}\times n_{2cu}} \\
\vdots & & & & & & \\
\mathbf{0}_{n_{1nu}\times n_{1cu}} & \mathbf{0}_{n_{1nu}\times n_{2cu}} & \mathbf{0}_{n_{1nu}\times n_{1cu}} & \mathbf{0}_{n_{1nu}\times n_{2cu}} & \dots & \mathbf{0}_{n_{1nu}\times n_{1cu}} & \mathbf{0}_{n_{1nu}\times n_{2cu}} \\
\mathbf{0}_{n_{2nu}\times n_{1cu}} & \mathbf{0}_{n_{2nu}\times n_{2cu}} & \mathbf{0}_{n_{2nu}\times n_{1cu}} & \mathbf{0}_{n_{2nu}\times n_{2cu}} & \dots & \mathbf{0}_{n_{2nu}\times n_{1cu}} & \mathbf{0}_{n_{2nu}\times n_{2cu}}
\end{bmatrix}$$

$$= \begin{bmatrix}
\mathbf{b}_{\mathrm{D}_{1c,1}{}_{8\cdot 12\times 4}} & \mathbf{b}_{\mathrm{D}_{2c,1}{}_{8\cdot 12\times 4}} & \mathbf{0}_{8\cdot 12\times 4} & \mathbf{0}_{8\cdot 12\times 4} & \dots & \mathbf{0}_{8\cdot 12\times 4} & \mathbf{0}_{8\cdot 12\times 4} \\
\mathbf{0}_{4\times 4} & \mathbf{0}_{4\times 4} & \mathbf{I}_{4\times 4} & \mathbf{0}_{4\times 4} & \dots & \mathbf{0}_{4\times 4} & \mathbf{0}_{4\times 4} \\
\mathbf{0}_{4\times 4} & \mathbf{0}_{4\times 4} & \mathbf{0}_{4\times 4} & \mathbf{I}_{4\times 4} & \dots & \mathbf{0}_{4\times 4} & \mathbf{0}_{4\times 4} \\
\vdots & & & & & & \\
\mathbf{0}_{4\times 4} & \mathbf{0}_{4\times 4} & \mathbf{0}_{4\times 4} & \mathbf{0}_{4\times 4} & \dots & \mathbf{I}_{4\times 4} & \mathbf{0}_{4\times 4} \\
\mathbf{0}_{4\times 4} & \mathbf{0}_{4\times 4} & \mathbf{0}_{4\times 4} & \mathbf{0}_{4\times 4} & \dots & \mathbf{0}_{4\times 4} & \mathbf{I}_{4\times 4} \\
\mathbf{0}_{2\times 4} & \mathbf{0}_{2\times 4} & \mathbf{0}_{2\times 4} & \mathbf{0}_{2\times 4} & \dots & \mathbf{0}_{2\times 4} & \mathbf{0}_{2\times 4} \\
\mathbf{0}_{2\times 4} & \mathbf{0}_{2\times 4} & \mathbf{0}_{2\times 4} & \mathbf{0}_{2\times 4} & \dots & \mathbf{0}_{2\times 4} & \mathbf{0}_{2\times 4} \\
\vdots & & & & & & \\
\mathbf{0}_{2\times 4} & \mathbf{0}_{2\times 4} & \mathbf{0}_{2\times 4} & \mathbf{0}_{2\times 4} & \dots & \mathbf{0}_{2\times 4} & \mathbf{0}_{2\times 4} \\
\mathbf{0}_{2\times 4} & \mathbf{0}_{2\times 4} & \mathbf{0}_{2\times 4} & \mathbf{0}_{2\times 4} & \dots & \mathbf{0}_{2\times 4} & \mathbf{0}_{2\times 4}
\end{bmatrix} \tag{A.44}$$

$$
\begin{aligned}
\bar{\mathbf{b}}_{\mathrm{Dn}_{aug}{}_{\left(N_0\cdot n_x+n_{VE}\cdot n_{cu}+n_D\cdot n_{nu}\right)\times n_D\cdot n_{nu}}} &= \bar{\mathbf{b}}_{\mathrm{Dn}_{aug}{}_{\left(8\cdot 12+n_{VE}\cdot 8+n_D\cdot 4\right)\times n_D\cdot 4}} \\
&= \begin{bmatrix}
\mathbf{b}_{\mathrm{D}_{2n,1}{}_{N_0\cdot n_x\times n_{1nu}}} & \mathbf{b}_{\mathrm{D}_{2n,1}{}_{N_0\cdot n_x\times n_{2nu}}} & \mathbf{0}_{N_0\cdot n_x\times n_{1nu}} & \mathbf{0}_{N_0\cdot n_x\times n_{1nu}} & \dots & \mathbf{0}_{N_0\cdot n_x\times n_{1nu}} & \mathbf{0}_{N_0\cdot n_x\times n_{2nu}} \\
\mathbf{0}_{n_{1cu}\times n_{1nu}} & \mathbf{0}_{n_{1cu}\times n_{2nu}} & \mathbf{0}_{n_{1cu}\times n_{1nu}} & \mathbf{0}_{n_{1cu}\times n_{2nu}} & \dots & \mathbf{0}_{n_{1cu}\times n_{1nu}} & \mathbf{0}_{n_{1cu}\times n_{2nu}} \\
\mathbf{0}_{n_{2cu}\times n_{1nu}} & \mathbf{0}_{n_{2cu}\times n_{2nu}} & \mathbf{0}_{n_{2cu}\times n_{1nu}} & \mathbf{0}_{n_{2cu}\times n_{2nu}} & \dots & \mathbf{0}_{n_{2cu}\times n_{1nu}} & \mathbf{0}_{n_{2cu}\times n_{2nu}} \\
\vdots & & & & & & \\
\mathbf{0}_{n_{1cu}\times n_{1nu}} & \mathbf{0}_{n_{1cu}\times n_{2nu}} & \mathbf{0}_{n_{1cu}\times n_{1nu}} & \mathbf{0}_{n_{1cu}\times n_{2nu}} & \dots & \mathbf{0}_{n_{1cu}\times n_{1nu}} & \mathbf{0}_{n_{1cu}\times n_{2nu}} \\
\mathbf{0}_{n_{1cu}\times n_{1nu}} & \mathbf{0}_{n_{1cu}\times n_{2nu}} & \mathbf{0}_{n_{1cu}\times n_{1nu}} & \mathbf{0}_{n_{1cu}\times n_{2nu}} & \dots & \mathbf{0}_{n_{1cu}\times n_{1nu}} & \mathbf{0}_{n_{1cu}\times n_{2nu}} \\
\mathbf{0}_{n_{1nu}\times n_{1nu}} & \mathbf{0}_{n_{1nu}\times n_{2nu}} & \mathbf{I}_{n_{1nu}\times n_{1nu}} & \mathbf{0}_{n_{1nu}\times n_{2nu}} & \dots & \mathbf{0}_{n_{1nu}\times n_{1nu}} & \mathbf{0}_{n_{1nu}\times n_{2nu}} \\
\mathbf{0}_{n_{2nu}\times n_{1nu}} & \mathbf{0}_{n_{2nu}\times n_{2nu}} & \mathbf{0}_{n_{2nu}\times n_{1nu}} & \mathbf{I}_{n_{2nu}\times n_{2nu}} & \dots & \mathbf{0}_{n_{2nu}\times n_{1nu}} & \mathbf{0}_{n_{2nu}\times n_{2nu}} \\
\vdots & & & & & & \\
\mathbf{0}_{n_{1nu}\times n_{1nu}} & \mathbf{0}_{n_{1nu}\times n_{2nu}} & \mathbf{0}_{n_{1nu}\times n_{1nu}} & \mathbf{0}_{n_{1nu}\times n_{2nu}} & \dots & \mathbf{I}_{n_{1nu}\times n_{1nu}} & \mathbf{0}_{n_{1nu}\times n_{2nu}} \\
\mathbf{0}_{n_{2nu}\times n_{1nu}} & \mathbf{0}_{n_{2nu}\times n_{2nu}} & \mathbf{0}_{n_{2nu}\times n_{1nu}} & \mathbf{0}_{n_{2nu}\times n_{2nu}} & \dots & \mathbf{0}_{n_{2nu}\times n_{1nu}} & \mathbf{I}_{n_{2nu}\times n_{2nu}}
\end{bmatrix} \\
&= \begin{bmatrix}
\mathbf{b}_{\mathrm{D}_{2n,1}{}_{8\cdot 12\times 2}} & \mathbf{b}_{\mathrm{D}_{2n,1}{}_{8\cdot 12\times 2}} & \mathbf{0}_{8\cdot 12\times 2} & \mathbf{0}_{8\cdot 12\times 2} & \dots & \mathbf{0}_{8\cdot 12\times 2} & \mathbf{0}_{8\cdot 12\times 2} \\
\mathbf{0}_{4\times 2} & \mathbf{0}_{4\times 2} & \mathbf{0}_{4\times 2} & \mathbf{0}_{4\times 2} & \dots & \mathbf{0}_{4\times 2} & \mathbf{0}_{4\times 2} \\
\mathbf{0}_{4\times 2} & \mathbf{0}_{4\times 2} & \mathbf{0}_{4\times 2} & \mathbf{0}_{4\times 2} & \dots & \mathbf{0}_{4\times 2} & \mathbf{0}_{4\times 2} \\
\vdots & & & & & & \\
\mathbf{0}_{4\times 2} & \mathbf{0}_{4\times 2} & \mathbf{0}_{4\times 2} & \mathbf{0}_{4\times 2} & \dots & \mathbf{0}_{4\times 2} & \mathbf{0}_{4\times 2} \\
\mathbf{0}_{4\times 2} & \mathbf{0}_{4\times 2} & \mathbf{0}_{4\times 2} & \mathbf{0}_{4\times 2} & \dots & \mathbf{0}_{4\times 2} & \mathbf{0}_{4\times 2} \\
\mathbf{0}_{2\times 2} & \mathbf{0}_{2\times 2} & \mathbf{I}_{2\times 2} & \mathbf{0}_{2\times 2} & \dots & \mathbf{0}_{2\times 2} & \mathbf{0}_{2\times 2} \\
\mathbf{0}_{2\times 2} & \mathbf{0}_{2\times 2} & \mathbf{0}_{2\times 2} & \mathbf{I}_{2\times 2} & \dots & \mathbf{0}_{2\times 2} & \mathbf{0}_{2\times 2} \\
\vdots & & & & & & \\
\mathbf{0}_{2\times 2} & \mathbf{0}_{2\times 2} & \mathbf{0}_{2\times 2} & \mathbf{0}_{2\times 2} & \dots & \mathbf{I}_{2\times 2} & \mathbf{0}_{2\times 2} \\
\mathbf{0}_{2\times 2} & \mathbf{0}_{2\times 2} & \mathbf{0}_{2\times 2} & \mathbf{0}_{2\times 2} & \dots & \mathbf{0}_{2\times 2} & \mathbf{I}_{2\times 2}
\end{bmatrix}
\end{aligned}
\tag{A.45}
$$

$$
\begin{aligned}
&\tilde{\mathbf{B}}_{\mathrm{D}_{\left(N_0\cdot n_x+n_{VE}\cdot n_{cu}+n_D\cdot n_{nu}\right)\times\left(N_c\cdot n_{cu}+N_n\cdot n_{nu}\right)}} \\
&= \begin{bmatrix}
\bar{\mathbf{b}}_{\mathrm{D}_{c}{}_{\left(N_0\cdot n_x+n_{VE}\cdot n_{cu}+n_D\cdot n_{nu}\right)\times N_c\cdot n_{cu}}} & \bar{\mathbf{b}}_{\mathrm{D}_{n}{}_{\left(N_0\cdot n_x+n_{VE}\cdot n_{cu}+n_D\cdot n_{nu}\right)\times N_n\cdot n_{nu}}}
\end{bmatrix}
\end{aligned}
\tag{A.46}
$$

$$\bar{\mathbf{b}}_{\mathrm{D}_{c_{\left(N_0\cdot n_x+n_{VE}\cdot n_{cu}+n_D\cdot n_{nu}\right)\times N_c\cdot n_{cu}}}} = \bar{\mathbf{b}}_{\mathrm{D}_{c_{\left(8\cdot 12+n_{VE}\cdot 8+n_D\cdot 4\right)\times 8\cdot 8}}} = \begin{bmatrix}\bar{\mathbf{b}}_{\mathrm{D}_{c_1}} & \bar{\mathbf{b}}_{\mathrm{D}_{c_2}}\end{bmatrix}$$

$$\bar{\mathbf{b}}_{\mathrm{D}_{c_1}} = \begin{bmatrix}
\mathbf{b}_{\mathrm{D}_{1c,2_{N_0\cdot n_x\times n_{1cu}}}} & \mathbf{b}_{\mathrm{D}_{1c,2_{N_0\cdot n_x\times n_{2cu}}}} & \dots & \mathbf{b}_{\mathrm{D}_{1c,N_c N_0\cdot n_x\times n_{1cu}}} & \mathbf{b}_{\mathrm{D}_{2c,N_c N_0\cdot n_x\times n_{2cu}}} \\
\mathbf{0}_{n_{1cu}\times n_{1cu}} & \mathbf{0}_{n_{1cu}\times n_{2cu}} & \dots & \mathbf{0}_{n_{1cu}\times n_{1cu}} & \mathbf{0}_{n_{1cu}\times n_{2cu}} \\
\mathbf{0}_{n_{2cu}\times n_{1cu}} & \mathbf{0}_{n_{2cu}\times n_{2cu}} & \dots & \mathbf{0}_{n_{2cu}\times n_{1cu}} & \mathbf{0}_{n_{2cu}\times n_{2cu}} \\
\vdots & & & & \\
\mathbf{0}_{n_{1cu}\times n_{1cu}} & \mathbf{0}_{n_{1cu}\times n_{2cu}} & \dots & \mathbf{0}_{n_{1cu}\times n_{1cu}} & \mathbf{0}_{n_{1cu}\times n_{2cu}} \\
\mathbf{0}_{n_{2cu}\times n_{1cu}} & \mathbf{0}_{n_{2cu}\times n_{2cu}} & \dots & \mathbf{0}_{n_{2cu}\times n_{1cu}} & \mathbf{0}_{n_{2cu}\times n_{2cu}} \\
\mathbf{0}_{n_{1nu}\times n_{1cu}} & \mathbf{0}_{n_{1nu}\times n_{2cu}} & \dots & \mathbf{0}_{n_{1nu}\times n_{1cu}} & \mathbf{0}_{n_{1nu}\times n_{2cu}} \\
\mathbf{0}_{n_{2nu}\times n_{1cu}} & \mathbf{0}_{n_{2nu}\times n_{2cu}} & \dots & \mathbf{0}_{n_{2nu}\times n_{1cu}} & \mathbf{0}_{n_{2nu}\times n_{2cu}} \\
\vdots & & & & \\
\mathbf{0}_{n_{1nu}\times n_{1cu}} & \mathbf{0}_{n_{1nu}\times n_{2cu}} & \dots & \mathbf{0}_{n_{1nu}\times n_{1cu}} & \mathbf{0}_{n_{1nu}\times n_{2cu}} \\
\mathbf{0}_{n_{2nu}\times n_{1cu}} & \mathbf{0}_{n_{2nu}\times n_{2cu}} & \dots & \mathbf{0}_{n_{2nu}\times n_{1cu}} & \mathbf{0}_{n_{2nu}\times n_{2cu}}
\end{bmatrix}$$

$$= \begin{bmatrix}
\mathbf{b}_{\mathrm{D}_{1c,2_{8\cdot 12\times 4}}} & \mathbf{b}_{\mathrm{D}_{1c,2_{8\cdot 12\times 4}}} & \dots & \mathbf{b}_{\mathrm{D}_{1c,8_{8\cdot 12\times 4}}} & \mathbf{b}_{\mathrm{D}_{2c,8_{8\cdot 12\times 4}}} \\
\mathbf{0}_{4\times 4} & \mathbf{0}_{4\times 4} & \dots & \mathbf{0}_{4\times 4} & \mathbf{0}_{4\times 4} \\
\mathbf{0}_{4\times 4} & \mathbf{0}_{4\times 4} & \dots & \mathbf{0}_{4\times 4} & \mathbf{0}_{4\times 4} \\
\vdots & & & & \\
\mathbf{0}_{4\times 4} & \mathbf{0}_{4\times 4} & \dots & \mathbf{0}_{4\times 4} & \mathbf{0}_{4\times 4} \\
\mathbf{0}_{4\times 4} & \mathbf{0}_{4\times 4} & \dots & \mathbf{0}_{4\times 4} & \mathbf{0}_{4\times 4} \\
\mathbf{0}_{2\times 4} & \mathbf{0}_{2\times 4} & \dots & \mathbf{0}_{2\times 4} & \mathbf{0}_{2\times 4} \\
\mathbf{0}_{2\times 4} & \mathbf{0}_{2\times 4} & \dots & \mathbf{0}_{2\times 4} & \mathbf{0}_{2\times 4} \\
\vdots & & & & \\
\mathbf{0}_{2\times 4} & \mathbf{0}_{2\times 4} & \dots & \mathbf{0}_{2\times 4} & \mathbf{0}_{2\times 4} \\
\mathbf{0}_{2\times 4} & \mathbf{0}_{2\times 4} & \dots & \mathbf{0}_{2\times 4} & \mathbf{0}_{2\times 4}
\end{bmatrix}$$

$$\bar{\mathbf{b}}_{\mathrm{D}_{c_2}} = \begin{bmatrix}
\mathbf{0}_{N_0\cdot n_x\times n_{1cu}} & \mathbf{0}_{N_0\cdot n_x\times n_{2cu}} \\
\mathbf{0}_{n_{1cu}\times n_{1cu}} & \mathbf{0}_{n_{1cu}\times n_{2cu}} \\
\mathbf{0}_{n_{2cu}\times n_{1cu}} & \mathbf{0}_{n_{2cu}\times n_{2cu}} \\
\vdots & \\
\mathbf{I}_{n_{1cu}\times n_{1cu}} & \mathbf{0}_{n_{1cu}\times n_{2cu}} \\
\mathbf{0}_{n_{2cu}\times n_{1cu}} & \mathbf{I}_{n_{2cu}\times n_{2cu}} \\
\mathbf{0}_{n_{1nu}\times n_{1cu}} & \mathbf{0}_{n_{1nu}\times n_{2cu}} \\
\mathbf{0}_{n_{2nu}\times n_{1cu}} & \mathbf{0}_{n_{2nu}\times n_{2cu}} \\
\vdots & \\
\mathbf{0}_{n_{1nu}\times n_{1cu}} & \mathbf{0}_{n_{1nu}\times n_{2cu}} \\
\mathbf{0}_{n_{2nu}\times n_{1cu}} & \mathbf{0}_{n_{2nu}\times n_{2cu}}
\end{bmatrix} = \begin{bmatrix}
\mathbf{0}_{8\cdot 12\times 4} & \mathbf{0}_{8\cdot 12\times 4} \\
\mathbf{0}_{4\times 4} & \mathbf{0}_{4\times 4} \\
\mathbf{0}_{4\times 4} & \mathbf{0}_{4\times 4} \\
\vdots & \\
\mathbf{I}_{4\times 4} & \mathbf{0}_{4\times 4} \\
\mathbf{0}_{4\times 4} & \mathbf{I}_{4\times 4} \\
\mathbf{0}_{2\times 4} & \mathbf{0}_{2\times 4} \\
\mathbf{0}_{2\times 4} & \mathbf{0}_{2\times 4} \\
\vdots & \\
\mathbf{0}_{2\times 4} & \mathbf{0}_{2\times 4} \\
\mathbf{0}_{2\times 4} & \mathbf{0}_{2\times 4}
\end{bmatrix} \tag{A.47}$$

$$\bar{\mathbf{b}}_{\mathrm{D}_{n_{\left(N_0\cdot n_x+n_{VE}\cdot n_{cu}+n_D\cdot n_{nu}\right)\times N_n\cdot n_{nu}}}} = \bar{\mathbf{b}}_{\mathrm{D}_{n_{\left(8\cdot 12+n_{VE}\cdot 8+n_D\cdot 4\right)\times 1\cdot 4}}} = \begin{bmatrix}\bar{\mathbf{b}}_{\mathrm{D}_{n_1}} & \bar{\mathbf{b}}_{\mathrm{D}_{n_2}}\end{bmatrix}$$

$$\bar{\mathbf{b}}_{\mathrm{D}_{n_1}} = \begin{bmatrix} \mathbf{b}_{\mathrm{D}_{1n,2_{N_0\cdot n_x\times n_{1nu}}}} & \mathbf{b}_{\mathrm{D}_{1n,2_{N_0\cdot n_x\times n_{2nu}}}} & \dots & \mathbf{b}_{\mathrm{D}_{1n,N_n N_0\cdot n_x\times n_{1nu}}} & \mathbf{b}_{\mathrm{D}_{2n,N_n N_0\cdot n_x\times n_{2nu}}} \\ \mathbf{0}_{n_{1cu}\times n_{1nu}} & \mathbf{0}_{n_{1cu}\times n_{2nu}} & \dots & \mathbf{0}_{n_{1cu}\times n_{1nu}} & \mathbf{0}_{n_{1cu}\times n_{2nu}} \\ \mathbf{0}_{n_{2cu}\times n_{1nu}} & \mathbf{0}_{n_{2cu}\times n_{2nu}} & \dots & \mathbf{0}_{n_{2cu}\times n_{1nu}} & \mathbf{0}_{n_{2cu}\times n_{2nu}} \\ \vdots & & & & \\ \mathbf{0}_{n_{1cu}\times n_{1nu}} & \mathbf{0}_{n_{1cu}\times n_{2nu}} & \dots & \mathbf{0}_{n_{1cu}\times n_{1nu}} & \mathbf{0}_{n_{1cu}\times n_{2nu}} \\ \mathbf{0}_{n_{2cu}\times n_{1nu}} & \mathbf{0}_{n_{2cu}\times n_{2nu}} & \dots & \mathbf{0}_{n_{2cu}\times n_{1nu}} & \mathbf{0}_{n_{2cu}\times n_{2nu}} \\ \mathbf{0}_{n_{1nu}\times n_{1nu}} & \mathbf{0}_{n_{1nu}\times n_{2nu}} & \dots & \mathbf{0}_{n_{1nu}\times n_{1nu}} & \mathbf{0}_{n_{1nu}\times n_{2nu}} \\ \mathbf{0}_{n_{2nu}\times n_{1nu}} & \mathbf{0}_{n_{2nu}\times n_{2nu}} & \dots & \mathbf{0}_{n_{2nu}\times n_{1nu}} & \mathbf{0}_{n_{2nu}\times n_{2nu}} \\ \vdots & & & & \\ \mathbf{0}_{n_{1nu}\times n_{1nu}} & \mathbf{0}_{n_{1nu}\times n_{2nu}} & \dots & \mathbf{0}_{n_{1nu}\times n_{1nu}} & \mathbf{0}_{n_{1nu}\times n_{2nu}} \\ \mathbf{0}_{n_{2nu}\times n_{1nu}} & \mathbf{0}_{n_{2nu}\times n_{2nu}} & \dots & \mathbf{0}_{n_{2nu}\times n_{1nu}} & \mathbf{0}_{n_{2nu}\times n_{2nu}} \end{bmatrix}$$

$$\bar{\mathbf{b}}_{\mathrm{D}_{n_2}} = \begin{bmatrix} \mathbf{0}_{N_0\cdot n_x\times n_{1nu}} & \mathbf{0}_{N_0\cdot n_x\times n_{2nu}} \\ \mathbf{0}_{n_{1cu}\times n_{1nu}} & \mathbf{0}_{n_{1cu}\times n_{2nu}} \\ \mathbf{0}_{n_{2cu}\times n_{1nu}} & \mathbf{0}_{n_{2cu}\times n_{2nu}} \\ \vdots & \\ \mathbf{I}_{n_{1cu}\times n_{1nu}} & \mathbf{0}_{n_{1cu}\times n_{2nu}} \\ \mathbf{0}_{n_{2cu}\times n_{1nu}} & \mathbf{I}_{n_{2cu}\times n_{2nu}} \\ \mathbf{0}_{n_{1nu}\times n_{1nu}} & \mathbf{0}_{n_{1nu}\times n_{2nu}} \\ \mathbf{0}_{n_{2nu}\times n_{1nu}} & \mathbf{0}_{n_{2nu}\times n_{2nu}} \\ \vdots & \\ \mathbf{0}_{n_{1nu}\times n_{1nu}} & \mathbf{0}_{n_{1nu}\times n_{2nu}} \\ \mathbf{0}_{n_{2nu}\times n_{1nu}} & \mathbf{0}_{n_{2nu}\times n_{2nu}} \end{bmatrix} = \begin{bmatrix} \mathbf{0}_{8\cdot 12\times 2} & \mathbf{0}_{8\cdot 12\times 2} \\ \mathbf{0}_{4\times 2} & \mathbf{0}_{4\times 2} \\ \mathbf{0}_{4\times 2} & \mathbf{0}_{4\times 2} \\ \vdots & \\ \mathbf{I}_{4\times 2} & \mathbf{0}_{4\times 2} \\ \mathbf{0}_{4\times 2} & \mathbf{I}_{4\times 2} \\ \mathbf{0}_{2\times 2} & \mathbf{0}_{2\times 2} \\ \mathbf{0}_{2\times 2} & \mathbf{0}_{2\times 2} \\ \vdots & \\ \mathbf{0}_{2\times 2} & \mathbf{0}_{2\times 2} \\ \mathbf{0}_{2\times 2} & \mathbf{0}_{2\times 2} \end{bmatrix} \tag{A.48}$$

$$\tilde{\mathbf{C}}_{\mathrm{D}_{\left(N_c\cdot n_{cy}+N_n\cdot n_{ny}\right)\times\left(N_0\cdot n_x+n_{VE}\cdot n_{cu}+n_D\cdot n_{nu}\right)}} = \begin{bmatrix}\bar{\mathbf{C}}_{\mathrm{D}_{\left(N_c\cdot n_{cy}+N_n\cdot n_{ny}\right)\times N_0\cdot n_x}} & \bar{\mathbf{d}}_{\mathrm{Dc}_{aug}\left(N_c\cdot n_{cy}+N_n\cdot n_{ny}\right)\times n_{VE}\cdot n_{cu}} & \bar{\mathbf{d}}_{\mathrm{Dn}_{aug}\left(N_c\cdot n_{cy}+N_n\cdot n_{ny}\right)\times n_D\cdot n_{nu}}\end{bmatrix} \tag{A.49}$$

$$\begin{aligned}\bar{\mathbf{C}}_{\mathrm{D}_{(N_c\cdot n_{cy}+N_n\cdot n_{ny})\times N_0\cdot n_x}} &= \bar{\mathbf{C}}_{\mathrm{D}_{(8\cdot 12+1\cdot 8)\times 8\cdot 12}} = \left[\hat{\mathbf{C}}_{\mathrm{D}_{(N_c\cdot n_{cy}+N_n\cdot n_{ny})\times N_0\cdot n_x}}\right] \\ &= \left[\hat{\mathbf{C}}_{\mathrm{D}_{(8\cdot 12+1\cdot 8)\times 8\cdot 12}}\right] = \left[\hat{\mathbf{C}}_{\mathrm{D}_{104\times 96}}\right] \end{aligned} \tag{A.50}$$

$$\begin{aligned}\bar{\mathbf{d}}_{\mathrm{Dc}_{aug}{}_{(N_c\cdot n_{cy}+N_n\cdot n_{ny})\times n_{VE}\cdot n_{cu}}} &= \bar{\mathbf{d}}_{\mathrm{Dc}_{aug}{}_{(8\cdot 12+1\cdot 8)\times n_{VE}\cdot 8}} \\ &= \begin{bmatrix} \hat{\mathbf{d}}_{\mathrm{D}_{1c,1}{}_{(N_c\cdot n_{cy}+N_n\cdot n_{ny})\times n_{1cu}}} \\ \hat{\mathbf{d}}_{\mathrm{D}_{2c,1}{}_{(N_c\cdot n_{cy}+N_n\cdot n_{ny})\times n_{2cu}}} \\ \mathbf{0}_{(N_c\cdot n_{cy}+N_n\cdot n_{ny})\times n_{1cu}} \\ \mathbf{0}_{(N_c\cdot n_{cy}+N_n\cdot n_{ny})\times n_{2cu}} \\ \vdots \\ \mathbf{0}_{(N_c\cdot n_{cy}+N_n\cdot n_{ny})\times n_{1cu}} \\ \mathbf{0}_{(N_c\cdot n_{cy}+N_n\cdot n_{ny})\times n_{2cu}} \end{bmatrix}^T = \begin{bmatrix} \hat{\mathbf{d}}_{\mathrm{D}_{1c,1}{}_{(8\cdot 12+1\cdot 8)\times 4}} \\ \hat{\mathbf{d}}_{\mathrm{D}_{2c,1}{}_{(8\cdot 12+1\cdot 8)\times 4}} \\ \mathbf{0}_{(8\cdot 12+1\cdot 8)\times 4} \\ \mathbf{0}_{(8\cdot 12+1\cdot 8)\times 4} \\ \vdots \\ \mathbf{0}_{(8\cdot 12+1\cdot 8)\times 4} \\ \mathbf{0}_{(8\cdot 12+1\cdot 8)\times 4} \end{bmatrix}^T \end{aligned} \tag{A.51}$$

$$\begin{aligned}\bar{\mathbf{d}}_{\mathrm{Dn}_{aug}{}_{(N_c\cdot n_{cy}+N_n\cdot n_{ny})\times n_D\cdot n_{nu}}} &= \bar{\mathbf{d}}_{\mathrm{Dn}_{aug}{}_{(8\cdot 12+1\cdot 8)\times n_D\cdot 4}} \\ &= \begin{bmatrix} \hat{\mathbf{d}}_{\mathrm{D}_{1n,1}{}_{(N_c\cdot n_{cy}+N_n\cdot n_{ny})\times n_{1nu}}} \\ \hat{\mathbf{d}}_{\mathrm{D}_{2n,1}{}_{(N_c\cdot n_{cy}+N_n\cdot n_{ny})\times n_{2nu}}} \\ \mathbf{0}_{(N_c\cdot n_{cy}+N_n\cdot n_{ny})\times n_{1nu}} \\ \mathbf{0}_{(N_c\cdot n_{cy}+N_n\cdot n_{ny})\times n_{2nu}} \\ \vdots \\ \mathbf{0}_{(N_c\cdot n_{cy}+N_n\cdot n_{ny})\times n_{1nu}} \\ \mathbf{0}_{(N_c\cdot n_{cy}+N_n\cdot n_{ny})\times n_{2nu}} \end{bmatrix}^T = \begin{bmatrix} \hat{\mathbf{d}}_{\mathrm{D}_{1n,1}{}_{(8\cdot 12+1\cdot 8)\times 2}} \\ \hat{\mathbf{d}}_{\mathrm{D}_{2n,1}{}_{(8\cdot 12+1\cdot 8)\times 2}} \\ \mathbf{0}_{(8\cdot 12+1\cdot 8)\times 2} \\ \mathbf{0}_{(8\cdot 12+1\cdot 8)\times 2} \\ \vdots \\ \mathbf{0}_{(8\cdot 12+1\cdot 8)\times 2} \\ \mathbf{0}_{(8\cdot 12+1\cdot 8)\times 2} \end{bmatrix}^T \end{aligned} \tag{A.52}$$

$$\tilde{\mathbf{D}}_{D_{(N_c\cdot n_{cy}+N_n\cdot n_{ny})\times(N_c\cdot n_{cu}+N_n\cdot n_{nu})}} = \begin{bmatrix} \hat{\mathbf{d}}_{\mathrm{D}_{1c,2}{}_{(N_c\cdot n_{cy}+N_n\cdot n_{ny})\times n_{1cu}}} \\ \hat{\mathbf{d}}_{\mathrm{D}_{2c,2}{}_{(N_c\cdot n_{cy}+N_n\cdot n_{ny})\times n_{2cu}}} \\ \vdots \\ \hat{\mathbf{d}}_{\mathrm{D}_{1c,N_c}{}_{(N_c\cdot n_{cy}+N_n\cdot n_{ny})\times n_{1cu}}} \\ \hat{\mathbf{d}}_{\mathrm{D}_{2c,N_c}{}_{(N_c\cdot n_{cy}+N_n\cdot n_{ny})\times n_{2cu}}} \\ \mathbf{0}_{(N_c\cdot n_{cy}+N_n\cdot n_{ny})\times n_{1cu}} \\ \mathbf{0}_{(N_c\cdot n_{cy}+N_n\cdot n_{ny})\times n_{2cu}} \\ \hat{\mathbf{d}}_{\mathrm{D}_{1n,2}{}_{(N_c\cdot n_{cy}+N_n\cdot n_{ny})\times n_{1nu}}} \\ \hat{\mathbf{d}}_{\mathrm{D}_{2n,2}{}_{(N_c\cdot n_{cy}+N_n\cdot n_{ny})\times n_{2nu}}} \\ \vdots \\ \hat{\mathbf{d}}_{\mathrm{D}_{1n,N_n}{}_{(N_c\cdot n_{cy}+N_n\cdot n_{ny})\times n_{1nu}}} \\ \hat{\mathbf{d}}_{\mathrm{D}_{2n,N_n}{}_{(N_c\cdot n_{cy}+N_n\cdot n_{ny})\times n_{2nu}}} \\ \mathbf{0}_{(N_c\cdot n_{cy}+N_n\cdot n_{ny})\times n_{1nu}} \\ \mathbf{0}_{(N_c\cdot n_{cy}+N_n\cdot n_{ny})\times n_{2nu}} \end{bmatrix}^T$$

$$\Longleftrightarrow$$

$$\tilde{\mathbf{D}}_{D_{104\times 68}} = \begin{bmatrix} \hat{\mathbf{d}}_{\mathrm{D}_{1c,2}{}_{104\times 4}} \\ \hat{\mathbf{d}}_{\mathrm{D}_{2c,2}{}_{104\times 4}} \\ \cdots \\ \hat{\mathbf{d}}_{\mathrm{D}_{1c,8}{}_{104\times 4}} \\ \hat{\mathbf{d}}_{\mathrm{D}_{2c,8}{}_{104\times 4}} \\ \mathbf{0}_{104\times 4} \\ \mathbf{0}_{104\times 4} \\ \mathbf{0}_{104\times 2} \\ \mathbf{0}_{104\times 2} \end{bmatrix}^T \tag{A.53}$$

A.2 Direct User-to-User Contact

For direct user-to-user contact, the dimensions of the state, the input, and the output vectors are as follows:

$n_x = 8$	number of states of continuous-time system
$n_{cu} = 4$	number of fast inputs (updated at the control rate) of continuous-time system
$n_{1cu} = 2$	number of fast inputs (updated at the control rate) of continuous-time system at the Peer 1 side
$n_{2cu} = 2$	number of fast inputs (updated at the control rate) of continuous-time system at the Peer 2 side
$n_{nu} = 2$	number of slow inputs (updated at the network rate) of continuous-time system
$n_{1nu} = 1$	number of slow inputs (updated at the network rate) of continuous-time system at the Peer 1 side
$n_{2nu} = 1$	number of slow inputs (updated at the network rate) of continuous-time system at the Peer 2 side
$n_u = n_{cu} + n_{nu} = 6$	number of inputs of continuous-time system
$n_{cy} = 8$	number of fast outputs (updated at the control rate) of continuous-time system
$n_{1cy} = 4$	number of fast outputs (updated at the control rate) of continuous-time system at the Peer 1 side
$n_{2cy} = 4$	number of fast outputs (updated at the control rate) of continuous-time system at the Peer 2 side
$n_{ny} = 4$	number of slow outputs (updated at the network rate) of continuous-time system
$n_{1ny} = 2$	number of slow outputs (updated at the network rate) of continuous-time system at the Peer 1 side
$n_{2ny} = 2$	number of slow outputs (updated at the network rate) of continuous-time system at the Peer 2 side
$n_y = n_{cy} + n_{ny} = 12$	number of outputs of continuous-time system

A.2.1 Discretization of the Continuous State Space Representation

With the multiple sampling rates existing in the control system, the state vector for the discrete-time system is expanded as:

$$\begin{aligned}
\mathbf{x}_{\mathrm{D}_{N_0 \cdot n_x \times 1}}[k] &= \mathbf{x}_{\mathrm{D}_{8\cdot 8\times 1}}[k] = \mathbf{x}_{\mathrm{D}_{64\times 1}}[k] \\
&= \begin{pmatrix} \mathbf{x}_{n_x\times 1}\left((k-1)\,T_0+\tau_0\right) \\ \mathbf{x}_{n_x\times 1}\left((k-1)\,T_0+2\tau_0\right) \\ \vdots \\ \mathbf{x}_{n_x\times 1}\left((k-1)\,T_0+(N_0-1)\,\tau_0\right) \\ \mathbf{x}_{n_x\times 1}\left(kT_0\right) \end{pmatrix} = \begin{pmatrix} \mathbf{x}_{8\times 1}\left((k-1)\,T_0+\tau_0\right) \\ \mathbf{x}_{8\times 1}\left((k-1)\,T_0+2\tau_0\right) \\ \vdots \\ \mathbf{x}_{8\times 1}\left((k-1)\,T_0+7\tau_0\right) \\ \mathbf{x}_{8\times 1}\left(kT_0\right) \end{pmatrix} \\
&= \begin{pmatrix} \mathbf{x}_{n_x\times 1}\left(kT_0-(N_0-1)\,\tau_0\right) \\ \mathbf{x}_{n_x\times 1}\left(kT_0-(N_0-2)\,\tau_0\right) \\ \vdots \\ \mathbf{x}_{n_x\times 1}\left(kT_0-\tau_0\right) \\ \mathbf{x}_{n_x\times 1}\left(kT_0\right) \end{pmatrix} = \begin{pmatrix} \mathbf{x}_{8\times 1}\left(kT_0-7\tau_0\right) \\ \mathbf{x}_{8\times 1}\left(kT_0-6\tau_0\right) \\ \vdots \\ \mathbf{x}_{8\times 1}\left(kT_0-\tau_0\right) \\ \mathbf{x}_{8\times 1}\left(kT_0\right) \end{pmatrix}
\end{aligned} \tag{A.54}$$

The output vector is expanded as:

$$\begin{aligned}
\mathbf{y}_{\mathrm{D}_{(N_c\cdot n_{cy}+N_n\cdot n_{ny})\times 1}}[k] &= \mathbf{y}_{\mathrm{D}_{(8\cdot 8+1\cdot 4)\times 1}}[k] = \mathbf{y}_{\mathrm{D}_{68\times 1}}[k] = \begin{pmatrix} \mathbf{y}_{\mathrm{D}_{c_{N_c\cdot n_{cy}\times 1}}}[k] \\ \mathbf{y}_{\mathrm{D}_{n_{N_n\cdot n_{ny}\times 1}}}[k] \end{pmatrix} \\
&= \begin{pmatrix} \mathbf{y}_{\mathrm{D}_{c_{8\cdot 8\times 1}}}[k] \\ \mathbf{y}_{\mathrm{D}_{n_{1\cdot 4\times 1}}}[k] \end{pmatrix} = \begin{pmatrix} \mathbf{y}_{\mathrm{D}_{c_{64\times 1}}}[k] \\ \mathbf{y}_{\mathrm{D}_{n_{4\times 1}}}[k] \end{pmatrix}
\end{aligned} \tag{A.55}$$

where:

$$
\begin{aligned}
\mathbf{y}_{\mathrm{D}_{c_{N_c\times n_{cy}}}}[k] &= \mathbf{y}_{\mathrm{D}_{c_{8\cdot 8\times 1}}}[k] = \mathbf{y}_{\mathrm{D}_{c_{64\times 1}}}[k] \\
&= \begin{pmatrix} \mathbf{y}_{\mathrm{D}_{c_{n_{cy}\times 1}}}(kT_0) \\ \mathbf{y}_{\mathrm{D}_{c_{n_{cy}\times 1}}}(kT_0+T_c) \\ \vdots \\ \mathbf{y}_{\mathrm{D}_{c_{n_{cy}\times 1}}}(kT_0+(N_c-1)T_c) \end{pmatrix} = \begin{pmatrix} \mathbf{y}_{\mathrm{D}_{c_{8\times 1}}}(kT_0) \\ \mathbf{y}_{\mathrm{D}_{c_{8\times 1}}}(kT_0+T_c) \\ \vdots \\ \mathbf{y}_{c_{8\times 1}}(kT_0+7T_c) \end{pmatrix} \\
&= \begin{pmatrix} \mathbf{y}_{\mathrm{D}_{1c_{n_{1cy}\times 1}}}(kT_0) \\ \mathbf{y}_{\mathrm{D}_{2c_{n_{2cy}\times 1}}}(kT_0) \\ \mathbf{y}_{\mathrm{D}_{1c_{n_{1cy}\times 1}}}(kT_0+T_c) \\ \mathbf{y}_{\mathrm{D}_{2c_{n_{2cy}\times 1}}}(kT_0+T_c) \\ \vdots \\ \mathbf{y}_{\mathrm{D}_{1c_{n_{1cy}\times 1}}}(kT_0+7T_c) \\ \mathbf{y}_{\mathrm{D}_{2c_{n_{2cy}\times 1}}}(kT_0+7T_c) \end{pmatrix} = \begin{pmatrix} \mathbf{y}_{\mathrm{D}_{1c_{4\times 1}}}(kT_0) \\ \mathbf{y}_{\mathrm{D}_{2c_{4\times 1}}}(kT_0) \\ \mathbf{y}_{\mathrm{D}_{1c_{4\times 1}}}(kT_0+T_c) \\ \mathbf{y}_{\mathrm{D}_{2c_{4\times 1}}}(kT_0+T_c) \\ \vdots \\ \mathbf{y}_{\mathrm{D}_{1c_{4\times 1}}}(kT_0+7T_c) \\ \mathbf{y}_{\mathrm{D}_{2c_{4\times 1}}}(kT_0+7T_c) \end{pmatrix}
\end{aligned}
\tag{A.56}
$$

$$
\begin{aligned}
\mathbf{y}_{\mathrm{D}_{n_{N_n\times n_{ny}}}}[k] &= \mathbf{y}_{\mathrm{D}_{n_{1\cdot 4\times 1}}}[k] = \mathbf{y}_{\mathrm{D}_{n_{4\times 1}}}[k] \\
&= \begin{pmatrix} \mathbf{y}_{\mathrm{D}_{n_{n_{ny}\times 1}}}(kT_0) \\ \mathbf{y}_{\mathrm{D}_{n_{n_{ny}\times 1}}}(kT_0+T_n) \\ \vdots \\ \mathbf{y}_{\mathrm{D}_{n_{n_{ny}\times 1}}}(kT_0+(N_n-1)T_n) \end{pmatrix} = \left[\mathbf{y}_{\mathrm{D}_{n_{4\times 1}}}(kT_0)\right] \\
&= \begin{pmatrix} \mathbf{y}_{\mathrm{D}_{1n_{n_{1ny}\times 1}}}(kT_0) \\ \mathbf{y}_{\mathrm{D}_{2n_{n_{2ny}\times 1}}}(kT_0) \\ \mathbf{y}_{\mathrm{D}_{1n_{n_{1ny}\times 1}}}(kT_0+T_n) \\ \mathbf{y}_{\mathrm{D}_{2n_{n_{2ny}\times 1}}}(kT_0+T_n) \\ \vdots \\ \mathbf{y}_{\mathrm{D}_{1n_{n_{1ny}\times 1}}}(kT_0+(N_n-1)T_n) \\ \mathbf{y}_{\mathrm{D}_{2n_{n_{2ny}\times 1}}}(kT_0+(N_n-1)T_n) \end{pmatrix} = \begin{bmatrix} \mathbf{y}_{1n_{2\times 1}}(kT_0) \\ \mathbf{y}_{2n_{2\times 1}}(kT_0) \end{bmatrix}
\end{aligned}
\tag{A.57}
$$

The input vector is expanded as:

$$\begin{aligned}\mathbf{u}_{\mathrm{D}_{(N_c\cdot n_{cu}+N_n\cdot n_{nu})\times 1}}[k] &= \mathbf{u}_{\mathrm{D}_{(8\cdot 4+1\cdot 2)\times 1}}[k] = \mathbf{u}_{\mathrm{D}_{34\times 1}}[k] \\ &= \begin{pmatrix}\mathbf{u}_{\mathrm{D}_{c_{N_c\cdot n_{cu}\times 1}}}[k] \\ \mathbf{u}_{\mathrm{D}_{n_{N_n\cdot n_{nu}\times 1}}}[k]\end{pmatrix} = \begin{pmatrix}\mathbf{u}_{\mathrm{D}_{c_{8\cdot 4\times 1}}}[k] \\ \mathbf{u}_{\mathrm{D}_{n_{1\cdot 2\times 1}}}[k]\end{pmatrix} = \begin{pmatrix}\mathbf{u}_{\mathrm{D}_{c_{32\times 1}}}[k] \\ \mathbf{u}_{\mathrm{D}_{n_{2\times 1}}}[k]\end{pmatrix}\end{aligned} \tag{A.58}$$

where $\mathbf{u}_{\mathrm{D}_{c_{N_c\cdot n_{cu}\times 1}}}[k]$ depends on positions and velocities measured locally at the control sampling rate T_c:

$$\begin{aligned}\mathbf{u}_{\mathrm{D}_{c_{N_c\cdot n_{cu}\times 1}}}[k] &= \mathbf{u}_{\mathrm{D}_{c_{8\cdot 4\times 1}}}[k] = \mathbf{u}_{\mathrm{D}_{c_{32\times 1}}}[k] \\ &= \begin{pmatrix}\mathbf{u}_{c_{n_{cu}\times 1}}(kT_0) \\ \vdots \\ \mathbf{u}_{c_{n_{cu}\times 1}}(kT_0+(N_c-1)T_c)\end{pmatrix} = \begin{pmatrix}\mathbf{u}_{c_{4\times 1}}(kT_0) \\ \vdots \\ \mathbf{u}_{c_{4\times 1}}(kT_0+7T_c)\end{pmatrix} \\ &= \begin{pmatrix}\mathbf{u}_{1c_{n_{1cu}\times 1}}(kT_0) \\ \mathbf{u}_{2c_{n_{2cu}\times 1}}(kT_0) \\ \vdots \\ \mathbf{u}_{1c_{n_{1cu}\times 1}}(kT_0+(N_c-1)T_c) \\ \mathbf{u}_{2c_{n_{2cu}\times 1}}(kT_0+(N_c-1)T_c)\end{pmatrix} = \begin{pmatrix}\mathbf{u}_{1c_{2\times 1}}(kT_0) \\ \mathbf{u}_{2c_{2\times 1}}(kT_0) \\ \vdots \\ \mathbf{u}_{1c_{2\times 1}}(kT_0+7T_c) \\ \mathbf{u}_{2c_{2\times 1}}(kT_0+7T_c)\end{pmatrix}\end{aligned} \tag{A.59}$$

and $\mathbf{u}_{\mathrm{D}_{n_{N_n\cdot n_{nu}\times 1}}}[k]$ depends on positions and velocities received from the remote peer

at the network sampling rate T_n:

$$\begin{aligned}
\mathbf{u}_{\mathrm{D}_{n_{N_n \cdot n_{nu} \times 1}}}[k] &= \mathbf{u}_{\mathrm{D}_{n_{1 \cdot 2 \times 1}}}[k] = \mathbf{u}_{\mathrm{D}_{n_{2 \times 1}}}[k] \\
&= \begin{pmatrix} \mathbf{u}_{n_{n_{nu} \times 1}}(kT_0) \\ \vdots \\ \mathbf{u}_{n_{n_{nu} \times 1}}(T_0 + (N_n - 1)\,T_n) \end{pmatrix} = \left(\mathbf{u}_{n_{2 \times 1}}(kT_0)\right) \\
&= \begin{pmatrix} \mathbf{u}_{1n_{n_{1nu} \times 1}}(kT_0) \\ \mathbf{u}_{2n_{n_{2nu} \times 1}}(kT_0) \\ \vdots \\ \mathbf{u}_{1n_{n_{1nu} \times 1}}(T_0 + (N_n - 1)\,T_n) \\ \mathbf{u}_{2n_{n_{2nu} \times 1}}(T_0 + (N_n - 1)\,T_n) \end{pmatrix} = \begin{pmatrix} \mathbf{u}_{n_{1 \times 1}}(kT_0) \\ \mathbf{u}_{n_{1 \times 1}}(kT_0) \end{pmatrix}
\end{aligned} \tag{A.60}$$

Hence, the discrete-time state-space representation of the open-loop system is:

$$\begin{aligned}
\mathbf{x}_{\mathrm{D}}[k+1] &= \mathbf{A}_{\mathrm{D}}\,\mathbf{x}_{\mathrm{D}}[k] + \mathbf{B}_{\mathrm{D}}\,\mathbf{u}_{\mathrm{D}}[k] \\
\mathbf{y}_{\mathrm{D}}[k] &= \mathbf{C}_{\mathrm{D}}\left(\mathbf{U}_1\,\mathbf{x}_{\mathrm{D}}[k+1] + \mathbf{U}_2\,\mathbf{x}_{\mathrm{D}}[k]\right)
\end{aligned} \tag{A.61}$$

The computation of all matrices in Equation (A.61) is detailed in the following.

$$\begin{aligned}
\mathbf{A}_{\mathrm{D}_{N_0 \cdot n_x \times N_0 \cdot n_x}} &= \mathbf{A}_{\mathrm{D}_{8 \cdot 12 \times 8 \cdot 12}} = \mathbf{A}_{\mathrm{D}_{96 \times 96}} \\
&= \begin{bmatrix}
\mathbf{0}_{8\times8} & \cdots & \mathbf{0}_{8\times8} & \mathbf{A}_{\mathrm{D}_{1_{8\times8}}} \\
\mathbf{0}_{8\times8} & \cdots & \mathbf{0}_{8\times8} & \mathbf{A}_{\mathrm{D}_{2_{8\times8}}} \\
\mathbf{0}_{8\times8} & \cdots & \mathbf{0}_{8\times8} & \mathbf{A}_{\mathrm{D}_{3_{8\times8}}} \\
\mathbf{0}_{8\times8} & \cdots & \mathbf{0}_{8\times8} & \mathbf{A}_{\mathrm{D}_{4_{8\times8}}} \\
\mathbf{0}_{8\times8} & \cdots & \mathbf{0}_{8\times8} & \mathbf{A}_{\mathrm{D}_{5_{8\times8}}} \\
\mathbf{0}_{8\times8} & \cdots & \mathbf{0}_{8\times8} & \mathbf{A}_{\mathrm{D}_{6_{8\times8}}} \\
\mathbf{0}_{8\times8} & \cdots & \mathbf{0}_{8\times8} & \mathbf{A}_{\mathrm{D}_{7_{8\times8}}} \\
\mathbf{0}_{8\times8} & \cdots & \mathbf{0}_{8\times8} & \mathbf{A}_{\mathrm{D}_{8_{8\times8}}}
\end{bmatrix}_{64\times64}
\end{aligned} \tag{A.62}$$

in which:

$$\mathbf{A}_{\mathrm{D}_{l_{8\times 8}}} = e^{\mathbf{A}_{8\times 8}\cdot l\cdot \tau_0} = e^{\mathbf{A}_{8\times 8}\cdot l\cdot \frac{1}{1024}} \qquad l = 1, \cdots, N_0 = 1, \cdots, 8 \tag{A.63}$$

$$\begin{aligned} \mathbf{B}_{\mathrm{D}_{N_0\cdot n_x\times(N_c\cdot n_{cu}+N_n\cdot n_{nu})}} &= \left[\mathbf{B}_{\mathrm{D}_{c_{N_0\cdot n_x\times N_c\cdot n_{cu}}}} \quad \mathbf{B}_{\mathrm{D}_{n_{N_0\cdot n_x\times N_n\cdot n_{nu}}}}\right] \\ &\Longleftrightarrow \\ \mathbf{B}_{\mathrm{D}_{8\cdot 8\times(8\cdot 4+1\cdot 2)}} &= \left[\mathbf{B}_{\mathrm{D}_{c_{8\cdot 8\times 8\cdot 4}}} \quad \mathbf{B}_{\mathrm{D}_{n_{8\cdot 8\times 1\cdot 2}}}\right] \\ &\Longleftrightarrow \\ \mathbf{B}_{\mathrm{D}_{64\times 34}} &= \left[\mathbf{B}_{\mathrm{D}_{c_{64\times 32}}} \quad \mathbf{B}_{\mathrm{D}_{n_{64\times 2}}}\right] \end{aligned} \tag{A.64}$$

with the $\mathbf{B}_{\mathrm{D}_{c_{64\times 32}}}$ and $\mathbf{B}_{\mathrm{D}_{n_{64\times 2}}}$ matrices detailed in the following. Specifically, the $\mathbf{B}_{\mathrm{D}_{c_{64\times 32}}}$ matrix is an $N_0 \times N_c = 8 \times 8$ block matrix:

$$\begin{aligned} \mathbf{B}_{\mathrm{D}_{c_{N_0\cdot n_x\times N_c\cdot n_{cu}}}} &= \left[\mathbf{b}_{\mathrm{D}_{c,l\mu_{n_x\times n_{cu}}}}\right] = \left[\left(\mathbf{b}_{\mathrm{D}_{1c,l\mu_{n_x\times n_{1cu}}}} \quad \mathbf{b}_{\mathrm{D}_{2c,l\mu_{n_x\times n_{2cu}}}}\right)\right] \\ l &= 1, \ldots, N_0;\ \mu = 0, \ldots, N_c - 1 \\ &\Longleftrightarrow \\ \mathbf{B}_{\mathrm{D}_{c_{64\times 32}}} &= \left[\mathbf{b}_{\mathrm{D}_{c,l\mu_{8\times 4}}}\right] = \left[\left(\mathbf{b}_{\mathrm{D}_{1c,l\mu_{8\times 2}}}, \mathbf{b}_{\mathrm{D}_{2c,l\mu_{8\times 2}}}\right)\right] \\ l &= 1, \ldots, 8;\ \mu = 0, \ldots, 7 \end{aligned} \tag{A.65}$$

with the $l\mu$ block computed via:

$$\mathbf{b}_{\mathrm{D}_{ic,l\mu_{n_x\times n_{ic}}}} = \begin{cases} \mathbf{0}_{n_x\times n_{ic}} & l \le l_c\cdot\mu \\ \int_{\mu\cdot l_c\cdot\tau_0}^{l\cdot\tau_0} e^{\mathbf{A}_{n_x\times n_x}(l\cdot\tau_0-\tau)}\mathbf{B}_{ic_{n_x\times n_{ic}}}d\tau & l_c\cdot\mu < l \le l_c\cdot(\mu+1) \\ \int_{\mu\cdot l_c\cdot\tau_0}^{(\mu+1)\cdot l_c\cdot\tau_0} e^{\mathbf{A}_{n_x\times n_x}(l\cdot\tau_0-\tau)}\mathbf{B}_{ic_{n_x\times n_{ic}}}d\tau & l_c\cdot(\mu+1) < l \end{cases}$$

$(i=1,2)$

$$\Longleftrightarrow$$

$$\mathbf{b}_{\mathrm{D}_{1c,l\mu_{8\times 2}}} = \begin{cases} \mathbf{0}_{8\times 2} & l \le 1\cdot\mu \\ \int_{\mu\cdot 1\cdot\tau_0}^{l\cdot\tau_0} e^{\mathbf{A}_{8\times 8}(l\cdot\tau_0-\tau)}\mathbf{B}_{1c_{8\times 2}}d\tau & 1\cdot\mu < l \le 1\cdot(\mu+1) \\ \int_{\mu\cdot 1\cdot\tau_0}^{(\mu+1)\cdot 1\cdot\tau_0} e^{\mathbf{A}_{8\times 8}(l\cdot\tau_0-\tau)}\mathbf{B}_{1c_{8\times 2}}d\tau & 1\cdot(\mu+1) < l \end{cases}$$

$$\mathbf{b}_{\mathrm{D}_{2c,l\mu_{8\times 2}}} = \begin{cases} \mathbf{0}_{12\times 2} & l \le 1\cdot\mu \\ \int_{\mu\cdot 1\cdot\tau_0}^{l\cdot\tau_0} e^{\mathbf{A}_{8\times 8}(l\cdot\tau_0-\tau)}\mathbf{B}_{2c_{8\times 2}}d\tau & 1\cdot\mu < l \le 1\cdot(\mu+1) \\ \int_{\mu\cdot 1\cdot\tau_0}^{(\mu+1)\cdot 1\cdot\tau_0} e^{\mathbf{A}_{8\times 8}(l\cdot\tau_0-\tau)}\mathbf{B}_{2c_{8\times 2}}d\tau & 1\cdot(\mu+1) < l \end{cases} \tag{A.66}$$

Hence:

$$\begin{aligned} \mathbf{B}_{\mathrm{D}_{c_{N_0\cdot n_x\times N_c\cdot n_{cu}=8\cdot 8\times 8\cdot 4=64\times 32}}} &= \begin{bmatrix} \mathbf{b}_{\mathrm{D}_{c,10_{8\times 4}}} & \mathbf{0}_{8\times 4} & \cdots & \mathbf{0}_{8\times 4} & \mathbf{0}_{8\times 4} \\ \mathbf{b}_{\mathrm{D}_{c,20_{8\times 4}}} & \mathbf{b}_{\mathrm{D}_{c,21_{8\times 4}}} & \cdots & \mathbf{0}_{8\times 4} & \mathbf{0}_{8\times 4} \\ \mathbf{b}_{\mathrm{D}_{c,30_{8\times 4}}} & \mathbf{b}_{\mathrm{D}_{c,31_{8\times 4}}} & \cdots & \mathbf{0}_{8\times 4} & \mathbf{0}_{8\times 4} \\ \mathbf{b}_{\mathrm{D}_{c,40_{8\times 4}}} & \mathbf{b}_{\mathrm{D}_{c,41_{8\times 4}}} & \cdots & \mathbf{0}_{8\times 4} & \mathbf{0}_{8\times 4} \\ \mathbf{b}_{\mathrm{D}_{c,50_{8\times 4}}} & \mathbf{b}_{\mathrm{D}_{c,51_{8\times 4}}} & \cdots & \mathbf{0}_{8\times 4} & \mathbf{0}_{8\times 4} \\ \mathbf{b}_{\mathrm{D}_{c,60_{8\times 4}}} & \mathbf{b}_{\mathrm{D}_{c,61_{8\times 4}}} & \cdots & \mathbf{0}_{8\times 4} & \mathbf{0}_{8\times 4} \\ \mathbf{b}_{\mathrm{D}_{c,70_{8\times 4}}} & \mathbf{b}_{\mathrm{D}_{c,71_{8\times 4}}} & \cdots & \mathbf{b}_{\mathrm{D}_{c,76_{8\times 4}}} & \mathbf{0}_{8\times 4} \\ \mathbf{b}_{\mathrm{D}_{c,80_{8\times 4}}} & \mathbf{b}_{\mathrm{D}_{c,81_{8\times 4}}} & \cdots & \mathbf{b}_{\mathrm{D}_{c,86_{8\times 4}}} & \mathbf{b}_{\mathrm{D}_{c,87_{8\times 4}}} \end{bmatrix} \\ &= \begin{bmatrix} \mathbf{b}_{\mathrm{D}_{c,0_{64\times 4}}} & \mathbf{b}_{\mathrm{D}_{c,1_{64\times 4}}} & \cdots & \mathbf{b}_{\mathrm{D}_{c,6_{64\times 4}}} & \mathbf{b}_{\mathrm{D}_{c,2_{64\times 4}}} \end{bmatrix} \end{aligned} \tag{A.67}$$

Where:

$$\begin{aligned}
\mathbf{b}_{\mathrm{D}_{c,l\mu_{nx\times ncu}}} &= \begin{pmatrix}\mathbf{b}_{\mathrm{D}_{1c,l\mu_{nx\times n1cu}}} & \mathbf{b}_{\mathrm{D}_{2c,l\mu_{nx\times n2cu}}}\end{pmatrix} \\
l &= 1,\ldots,N_0;\ \mu=0,\ldots,N_c-1 \\
\mathbf{b}_{\mathrm{D}_{c,\mu_{64\times 4}}} &= \left(\mathbf{b}_{\mathrm{D}_{1c,l\mu_{64\times 2}}},\mathbf{b}_{\mathrm{D}_{2c,\mu_{64\times 2}}}\right) \\
l &= 1,\ldots,8;\ \mu=0,\ldots,7
\end{aligned} \tag{A.68}$$

The $\mathbf{B}_{\mathrm{D}_{n_{64\times 2}}}$ matrix is an $N_0\times N_n = 8\times 1$ block matrix:

$$\begin{aligned}
\mathbf{B}_{\mathrm{D}_{n_{N_0\cdot nx\times N_n\cdot nnu}}} &= \left[\mathbf{b}_{\mathrm{D}_{n,l\mu_{nx\times nnu}}}\right] = \left[\begin{pmatrix}\mathbf{b}_{\mathrm{D}_{1n,l\mu_{nx\times n1nu}}} & \mathbf{b}_{\mathrm{D}_{2c,l\mu_{nx\times n2nu}}}\end{pmatrix}\right] \\
l &= 1,\ldots,N_0;\ \mu=0,\ldots,N_n-1 \\
&\Longleftrightarrow \\
\mathbf{B}_{\mathrm{D}_{n_{64\times 2}}} &= \left[\mathbf{b}_{\mathrm{D}_{n,l\mu_{8\times 2}}}\right] = \left[\left(\mathbf{b}_{\mathrm{D}_{1n,l\mu_{8\times 1}}},\mathbf{b}_{\mathrm{D}_{2n,l\mu_{8\times 1}}}\right)\right] \\
l &= 1,\ldots,8;\ \mu=0
\end{aligned} \tag{A.69}$$

with the $l\mu$ block computed via:

$$\begin{aligned}
\mathbf{b}_{\mathrm{D}_{in,l\mu_{n_x\times n_{in}}}} &= \begin{cases} \mathbf{0}_{n_x\times n_{in}} & l \le l_n\cdot\mu \\ \int_{\mu\cdot l_n\cdot\tau_0}^{l\cdot\tau_0} e^{\mathbf{A}_{n_x\times n_x}(l\cdot\tau_0-\tau)}\mathbf{B}_{in_{n_x\times n_{in}}}d\tau & l_n\cdot\mu < l \le l_n\cdot(\mu+1) \\ \int_{\mu\cdot l_n\cdot\tau_0}^{(\mu+1)\cdot l_n\cdot\tau_0} e^{\mathbf{A}_{n_x\times n_x}(l\cdot\tau_0-\tau)}\mathbf{B}_{in_{n_x\times n_{in}}}d\tau & l_n\cdot(\mu+1) < l \end{cases} \\
(i=1,2) & \\
\Longleftrightarrow & \\
\mathbf{b}_{\mathrm{D}_{1n,l\mu_{8\times 1}}} &= \begin{cases} \mathbf{0}_{8\times 1} & l \le 8\cdot\mu = 0 \\ \int_{\mu\cdot 8\cdot\tau_0}^{l\cdot\tau_0} e^{\mathbf{A}_{8\times 8}(l\cdot\tau_0-\tau)}\mathbf{B}_{1n_{8\times 1}}d\tau & 8\cdot\mu = 0 < l \le 8\cdot(\mu+1) = 8 \\ \int_{\mu\cdot 8\cdot\tau_0}^{(\mu+1)\cdot 8\cdot\tau_0} e^{\mathbf{A}_{12\times 12}(l\cdot\tau_0-\tau)}\mathbf{B}_{1n_{12\times 2}}d\tau & 8\cdot(\mu+1) = 8 < l \end{cases} \\
\Longleftrightarrow & \\
\mathbf{b}_{\mathrm{D}_{1n,l\mu_{8\times 1}}} &= \int_{\mu\cdot 8\cdot\tau_0}^{l\cdot\tau_0} e^{\mathbf{A}_{8\times 8}(l\cdot\tau_0-\tau)}\mathbf{B}_{1n_{12\times 2}}d\tau \qquad 0 < l \le 8 \\
\mathbf{b}_{\mathrm{D}_{2n,l\mu_{8\times 1}}} &= \begin{cases} \mathbf{0}_{8\times 1} & l \le 8\cdot\mu = 0 \\ \int_{\mu\cdot 8\cdot\tau_0}^{l\cdot\tau_0} e^{\mathbf{A}_{8\times 8}(l\cdot\tau_0-\tau)}\mathbf{B}_{2n_{8\times 1}}d\tau & 8\cdot\mu = 0 < l \le 8\cdot(\mu+1) = 8 \\ \int_{\mu\cdot 8\cdot\tau_0}^{(\mu+1)\cdot 8\cdot\tau_0} e^{\mathbf{A}_{8\times 8}(l\cdot\tau_0-\tau)}\mathbf{B}_{2n_{12\times 2}}d\tau & 8\cdot(\mu+1) = 8 < l \end{cases} \\
\Longleftrightarrow & \\
\mathbf{b}_{\mathrm{D}_{2n,l\mu_{8\times 1}}} &= \int_{\mu\cdot 8\cdot\tau_0}^{l\cdot\tau_0} e^{\mathbf{A}_{8\times 8}(l\cdot\tau_0-\tau)}\mathbf{B}_{2n_{8\times 1}}d\tau \qquad 0 < l \le 8
\end{aligned} \tag{A.70}$$

Hence:

$$\begin{aligned}
\mathbf{B}_{\mathrm{D}_{n_{N_0\cdot n_x\times N_n\cdot n_{nu}=8\cdot 8\times 1\cdot 2=64\times 2}}} &= \begin{bmatrix} \mathbf{b}_{\mathrm{D}_{n,1_{8\times 2}}} \\ \mathbf{b}_{\mathrm{D}_{n,2_{8\times 2}}} \\ \vdots \\ \mathbf{b}_{\mathrm{D}_{n,7_{8\times 2}}} \\ \mathbf{b}_{\mathrm{D}_{n,8_{8\times 2}}} \end{bmatrix} = \begin{bmatrix} \mathbf{b}_{\mathrm{D}_{1n,1_{8\times 1}}} & \mathbf{b}_{\mathrm{D}_{2n,1_{8\times 1}}} \\ \mathbf{b}_{\mathrm{D}_{1n,2_{8\times 1}}} & \mathbf{b}_{\mathrm{D}_{2n,2_{8\times 1}}} \\ \vdots & \\ \mathbf{b}_{\mathrm{D}_{1n,7_{8\times 1}}} & \mathbf{b}_{\mathrm{D}_{2n,7_{8\times 1}}} \\ \mathbf{b}_{\mathrm{D}_{1n,8_{8\times 1}}} & \mathbf{b}_{\mathrm{D}_{2n,8_{8\times 1}}} \end{bmatrix} \\
&= \begin{bmatrix} \mathbf{b}_{\mathrm{D}_{n,0_{64\times 2}}} \end{bmatrix} = \begin{bmatrix} \mathbf{b}_{\mathrm{D}_{1n,0_{64\times 1}}} & \mathbf{b}_{\mathrm{D}_{2n,0_{64\times 1}}} \end{bmatrix}
\end{aligned} \tag{A.71}$$

$$\begin{aligned}
\mathbf{C}_{\mathrm{D}_{(N_c\cdot n_{cy}+N_n\cdot n_{ny})\times N_0\cdot n_x}} &= \begin{bmatrix} \mathbf{C}_{\mathrm{D}_{c_{N_c\cdot n_{cy}\times N_0\cdot n_x}}} \\ \mathbf{C}_{\mathrm{D}_{n_{N_n\cdot n_{ny}\times N_0\cdot n_x}}} \end{bmatrix} \\
&\Longleftrightarrow \\
\mathbf{C}_{\mathrm{D}_{(8\cdot 8+1\cdot 4)\times 8\cdot 8}} &= \begin{bmatrix} \mathbf{C}_{\mathrm{D}_{c_{8\cdot 8\times 8\cdot 8}}} \\ \mathbf{C}_{\mathrm{D}_{n_{1\cdot 4\times 8\cdot 8}}} \end{bmatrix} \\
&\Longleftrightarrow \\
\mathbf{C}_{\mathrm{D}_{68\times 64}} &= \begin{bmatrix} \mathbf{C}_{\mathrm{D}_{c_{64\times 64}}} \\ \mathbf{C}_{\mathrm{D}_{n_{4\times 64}}} \end{bmatrix}
\end{aligned} \tag{A.72}$$

with the $\mathbf{C}_{\mathrm{D}_{c_{64\times 64}}}$ and $\mathbf{C}_{\mathrm{D}_{n_{4\times 64}}}$ matrices detailed in the following. Specifically, the $\mathbf{C}_{\mathrm{D}_{c_{64\times 64}}}$ matrix is an $N_c \times N_0 = 8 \times 8$ block matrix:

$$\begin{aligned}
\mathbf{C}_{\mathrm{D}_{c_{N_c\cdot n_{cy}\times N_0\cdot n_x}}} &= \left[\mathbf{c}_{\mathrm{D}_{c,\nu l_{n_{cy}\times n_x}}}\right] = \left[\begin{pmatrix} \mathbf{c}_{\mathrm{D}_{1c,\nu l_{n_{1cy}\times n_x}}} \\ \mathbf{c}_{\mathrm{D}_{2c,\nu l_{n_{2cy}\times n_x}}} \end{pmatrix}\right] \\
\nu &= 0,\ldots,N_c-1;\, l=1,\ldots,N_0 \\
&\Longleftrightarrow \\
\mathbf{C}_{\mathrm{D}_{c_{64\times 64}}} &= \left[\mathbf{c}_{\mathrm{D}_{c,\nu l_{8\times 8}}}\right] = \left[\begin{pmatrix} \mathbf{c}_{\mathrm{D}_{1c,\nu l_{4\times 18}}} \\ \mathbf{c}_{\mathrm{D}_{2c,\nu l_{4\times 8}}} \end{pmatrix}\right] \\
\nu &= 0,\ldots,7;\, l=1,\ldots,8
\end{aligned} \tag{A.73}$$

with the νl block computed via:

$$\begin{aligned}
\mathbf{c}_{\mathrm{D}_{ic,\nu l_{n_{icy}\times n_x}}} &= \begin{cases} \mathbf{C}_{ic_{n_{icy}\times n_x}} & \nu = 0, l = N_0 \quad or \quad l_c \cdot \nu = l \\ \mathbf{0}_{n_{icy}\times n_x} & otherwise \end{cases} \\
(i = 1, 2) & \\
\Longleftrightarrow & \\
\mathbf{c}_{\mathrm{D}_{1c,\nu l_{4\times 8}}} &= \begin{cases} \mathbf{C}_{1c_{4\times 8}} & \nu = 0, l = 8 \quad or \quad 1 \cdot \nu = l \\ \mathbf{0}_{4\times 8} & otherwise \end{cases} \\
\mathbf{c}_{\mathrm{D}_{2c,\nu l_{4\times 8}}} &= \begin{cases} \mathbf{C}_{2c_{4\times 8}} & \nu = 0, l = 8 \quad or \quad 1 \cdot \nu = l \\ \mathbf{0}_{4\times 8} & otherwise \end{cases}
\end{aligned} \tag{A.74}$$

Hence:

$$\begin{aligned}
&\mathbf{C}_{\mathrm{D}_{c_{N_c\cdot n_{cy}\times N_0\cdot n_x=8\cdot 8\times 8\cdot 8=64\times 64}}} \\
&= \begin{bmatrix}
\mathbf{0}_{8\times 8} & \mathbf{0}_{8\times 8} & \mathbf{0}_{8\times 8} & \mathbf{0}_{8\times 8} & \mathbf{0}_{8\times 8} & \mathbf{0}_{8\times 8} & \mathbf{0}_{8\times 8} & \mathbf{C}_{c_{8\times 8}} \\
\mathbf{C}_{c_{8\times 8}} & \mathbf{0}_{8\times 8} & \mathbf{0}_{8\times 8} & \mathbf{0}_{8\times 8} & \mathbf{0}_{8\times 8} & \mathbf{0}_{8\times 8} & \mathbf{0}_{8\times 8} & \mathbf{0}_{8\times 8} \\
\mathbf{0}_{8\times 8} & \mathbf{C}_{c_{8\times 8}} & \mathbf{0}_{8\times 8} & \mathbf{0}_{8\times 8} & \mathbf{0}_{8\times 8} & \mathbf{0}_{8\times 8} & \mathbf{0}_{8\times 8} & \mathbf{0}_{8\times 8} \\
\mathbf{0}_{8\times 8} & \mathbf{0}_{8\times 8} & \mathbf{C}_{c_{8\times 8}} & \mathbf{0}_{8\times 8} & \mathbf{0}_{8\times 8} & \mathbf{0}_{8\times 8} & \mathbf{0}_{8\times 8} & \mathbf{0}_{8\times 8} \\
\mathbf{0}_{8\times 8} & \mathbf{0}_{8\times 8} & \mathbf{0}_{8\times 8} & \mathbf{C}_{c_{8\times 8}} & \mathbf{0}_{8\times 8} & \mathbf{0}_{8\times 8} & \mathbf{0}_{8\times 8} & \mathbf{0}_{8\times 8} \\
\mathbf{0}_{8\times 8} & \mathbf{0}_{8\times 8} & \mathbf{0}_{8\times 8} & \mathbf{0}_{8\times 8} & \mathbf{C}_{c_{8\times 8}} & \mathbf{0}_{8\times 8} & \mathbf{0}_{8\times 8} & \mathbf{0}_{8\times 8} \\
\mathbf{0}_{8\times 8} & \mathbf{0}_{8\times 8} & \mathbf{0}_{8\times 8} & \mathbf{0}_{8\times 8} & \mathbf{0}_{8\times 8} & \mathbf{C}_{c_{8\times 8}} & \mathbf{0}_{8\times 8} & \mathbf{0}_{8\times 8} \\
\mathbf{0}_{8\times 8} & \mathbf{0}_{8\times 8} & \mathbf{0}_{8\times 8} & \mathbf{0}_{8\times 8} & \mathbf{0}_{8\times 8} & \mathbf{0}_{8\times 8} & \mathbf{C}_{c_{8\times 8}} & \mathbf{0}_{8\times 8}
\end{bmatrix}
\end{aligned} \tag{A.75}$$

Where

$$\mathbf{C}_{c_{8\times 8}} = \left(\mathbf{C}_{1c_{4\times 8}}\mathbf{C}_{2c_{4\times 8}}\right) \tag{A.76}$$

The $\mathbf{C}_{\mathrm{D}_{n_{4\times 64}}}$ matrix is a $N_n \times N_0 = 1 \times 8$ block matrix:

$$\begin{aligned}
\mathbf{C}_{\mathrm{D}_{n_{N_n \cdot n_{ny} \times N_0 \cdot n_x}}} &= \left[\mathbf{c}_{\mathrm{D}_{n,\nu l_{n_{ny} \times n_x}}}\right] = \left[\begin{pmatrix} \mathbf{c}_{\mathrm{D}_{1n,\nu l_{n_{1ny} \times n_x}}} \\ \mathbf{c}_{\mathrm{D}_{2n,\nu l_{n_{2ny} \times n_x}}} \end{pmatrix}\right] \\
\nu &= 0, \ldots, N_n - 1;\, l = 1, \ldots, N_0 \\
&\Longleftrightarrow \\
\mathbf{C}_{\mathrm{D}_{n_{4\times 64}}} &= \left[\mathbf{c}_{\mathrm{D}_{n,\nu l_{4\times 8}}}\right] = \left[\begin{pmatrix} \mathbf{c}_{\mathrm{D}_{1n,\nu l_{2\times 8}}} \\ \mathbf{c}_{\mathrm{D}_{2n,\nu l_{2\times 8}}} \end{pmatrix}\right] \\
\nu &= 0;\, l = 1, \ldots, 8
\end{aligned} \tag{A.77}$$

with the νl block computed via:

$$\begin{aligned}
\mathbf{c}_{\mathrm{D}_{in,l\nu_{2\times 8}}} &= \begin{cases} \mathbf{C}_{in_{n_{iny} \times n_x}} & \nu = 0, l = N_0 \quad or \quad l_n \cdot \nu = l \\ \\ \mathbf{0}_{2\times 8} & otherwise \end{cases} \\
(i &= 1, 2) \\
&\Longleftrightarrow \\
\mathbf{c}_{\mathrm{D}_{1n,l\nu_{2\times 8}}} &= \begin{cases} \mathbf{C}_{1n_{2\times 4}} & \nu = 0, l = 8 \quad or \quad 8 \cdot \nu = l \\ \\ \mathbf{0}_{2\times 4} & otherwise \end{cases} \\
\mathbf{c}_{\mathrm{D}_{2n,l\nu_{2\times 8}}} &= \begin{cases} \mathbf{C}_{2n_{2\times 8}} & \nu = 0, l = 8 \quad or \quad 8 \cdot \nu = l \\ \\ \mathbf{0}_{2\times 8} & otherwise \end{cases}
\end{aligned} \tag{A.78}$$

Hence:

$$\mathbf{C}_{\mathrm{D}_{n_{N_n \cdot n_{ny} \times N_0 \cdot n_x = 1 \cdot 4 \times 8 \cdot 8 = 4 \times 64}}} = \begin{bmatrix} \mathbf{0}_{4\times 8} & \mathbf{0}_{4\times 8} & \mathbf{0}_{4\times 8} & \mathbf{0}_{4\times 8} & \mathbf{0}_{4\times 8} & \mathbf{0}_{4\times 8} & \mathbf{0}_{4\times 8} & \mathbf{C}_{n_{4\times 8}} \end{bmatrix} \tag{A.79}$$

Where

$$\mathbf{C}_{n_{4\times 8}} = \begin{pmatrix} \mathbf{C}_{1n_{2\times 8}} \\ \mathbf{C}_{2n_{2\times 8}} \end{pmatrix} \tag{A.80}$$

Lastly, $\mathbf{U}1_{N_0\cdot n_x \times N_0\cdot n_x = 8\cdot 8\times 8\cdot 8 = 64\times 64}$ and $\mathbf{U}2_{N_0\cdot n_x \times N_0\cdot n_x = 8\cdot 8\times 8\cdot 8 = 64\times 64}$ are $N_0 \times N_0 = 8$ blocks diagonal matrices having the following $n_x \times n_x = 8 \times 8$ blocks on their diagonals:

$$\begin{aligned} & \begin{cases} \mathbf{U}1_{N_0\cdot n_x \times N_0\cdot n_x} &= blockdiag\left(\mathbf{I}_{n_x\times n_x}, \ldots, \mathbf{I}_{n_x\times n_x}, \mathbf{0}_{n_x\times n_x}\right) \\ \mathbf{U}2_{N_0\cdot n_x \times N_0\cdot n_x} &= blockdiag\left(\mathbf{0}_{n_x\times n_x}, \ldots, \mathbf{0}_{n_x\times n_x}, \mathbf{I}_{n_x\times n_x}\right) \end{cases} \\ \Longleftrightarrow \quad & \begin{cases} \mathbf{U}1_{8\cdot 8\times 8\cdot 8} &= \mathbf{U}1_{64\times 64} = blockdiag\left(\mathbf{I}_{8\times 8}, \ldots, \mathbf{I}_{8\times 8}, \mathbf{0}_{8\times 8}\right) \\ \mathbf{U}2_{8\cdot 8\times 8\cdot 8} &= \mathbf{U}2_{64\times 64} = blockdiag\left(\mathbf{0}_{8\times 8}, \ldots, \mathbf{0}_{8\times 8}, \mathbf{I}_{8\times 8}\right) \end{cases} \end{aligned} \tag{A.81}$$

Therefore,

$$\begin{aligned} \hat{\mathbf{C}}_{\mathrm{D}_{68\times 64}} &= \mathbf{C}_{\mathrm{D}_{68\times 64}} \cdot \mathbf{U}1_{64\times 64} \cdot \mathbf{A}_{\mathrm{D}_{64\times 64}} + \mathbf{C}_{\mathrm{D}_{68\times 64}} \cdot \mathbf{U}2_{64\times 64} \\ \hat{\mathbf{D}}_{\mathrm{D}_{68\times 34}} &= \mathbf{C}_{\mathrm{D}_{68\times 64}} \cdot \mathbf{U}1_{64\times 64} \cdot \mathbf{B}_{\mathrm{D}_{64\times 34}} \end{aligned} \tag{A.82}$$

The closed-loop dynamics can be obtained from the open-loop discrete-time difference equations using the feedback law:

$$\begin{aligned} \mathbf{u}_{\mathrm{D}_{(N_c\cdot n_{cu}+N_n\cdot n_{nu})\times 1}} &= \mathbf{F}_{\mathrm{D}_{(N_c\cdot n_{cu}+N_n\cdot n_{nu})\times (N_c\cdot n_{cy}+N_n\cdot n_{ny})}} \mathbf{y}_{\mathrm{D}_{(N_c\cdot n_{cy}+N_n\cdot n_{ny})\times 1}} \Longleftrightarrow \\ \mathbf{u}_{\mathrm{D}_{68\times 1}} &= \mathbf{F}_{\mathrm{D}_{(8\cdot 4+1\cdot 2)\times (8\cdot 8+1\cdot 4)}} \mathbf{y}_{\mathrm{D}_{(8\cdot 8+1\cdot 4)\times 1}} = \mathbf{F}_{\mathrm{D}_{34\times 68}} \mathbf{y}_{\mathrm{D}_{68\times 1}} \end{aligned} \tag{A.83}$$

According to Equation 4.33, given

$$\begin{aligned}
\mathbf{F}_{cc_{N_c\cdot n_{cu}\times N_c\cdot n_{cy}}} = \mathbf{F}_{cc_{8\cdot 8\times 8\cdot 12}} &= \begin{bmatrix} \mathbf{F}_{1c_{n_{1cu}\times n_{1cy}}} & \mathbf{0}_{n_{1cu}\times n_{2cy}} \\ \mathbf{0}_{n_{2cu}\times n_{1cy}} & \mathbf{F}_{2c_{n_{2cu}\times n_{2cy}}} \end{bmatrix} = \begin{bmatrix} \mathbf{F}_{1c_{2\times 4}} & \mathbf{0}_{2\times 4} \\ \mathbf{0}_{2\times 4} & \mathbf{F}_{2c_{2\times 4}} \end{bmatrix} \\
\mathbf{F}_{cn_{N_c\cdot n_{cu}\times N_n\cdot n_{ny}}} = \mathbf{F}_{cn_{8\cdot 8\times 1\cdot 8}} &= \begin{bmatrix} \mathbf{0}_{n_{1cu}\times n_{1ny}} & \mathbf{0}_{n_{1cu}\times n_{2ny}} \\ \mathbf{0}_{n_{2cu}\times n_{1ny}} & \mathbf{0}_{n_{2cu}\times n_{2ny}} \end{bmatrix} = \begin{bmatrix} \mathbf{0}_{2\times 2} & \mathbf{0}_{2\times 2} \\ \mathbf{0}_{2\times 2} & \mathbf{0}_{2\times 2} \end{bmatrix} \\
\mathbf{F}_{nc_{N_n\cdot n_{nu}\times N_c\cdot n_{cy}}} = \mathbf{F}_{nc_{1\cdot 4\times 8\cdot 12}} &= \begin{bmatrix} \mathbf{0}_{n_{1nu}\times n_{1cy}} & \mathbf{0}_{n_{1nu}\times n_{2cy}} \\ \mathbf{0}_{n_{2nu}\times n_{1cy}} & \mathbf{0}_{n_{2nu}\times n_{2cy}} \end{bmatrix} = \begin{bmatrix} \mathbf{0}_{1\times 4} & \mathbf{0}_{1\times 4} \\ \mathbf{0}_{1\times 4} & \mathbf{0}_{1\times 4} \end{bmatrix} \\
\mathbf{F}_{nn_{N_n\cdot n_{nu}\times N_n\cdot n_{ny}}} = \mathbf{F}_{nn_{1\cdot 4\times 1\cdot 8}} &= \begin{bmatrix} \mathbf{F}_{1n_{n_{1nu}\times n_{1ny}}} & \mathbf{0}_{n_{1nu}\times n_{2ny}} \\ \mathbf{0}_{n_{2nu}\times n_{1ny}} & \mathbf{F}_{2n_{n_{2nu}\times n_{2ny}}} \end{bmatrix} = \begin{bmatrix} \mathbf{F}_{1n_{1\times 2}} & \mathbf{0}_{1\times 2} \\ \mathbf{0}_{1\times 2} & \mathbf{F}_{2n_{1\times 2}} \end{bmatrix}
\end{aligned} \tag{A.84}$$

The discrete-time feedback matrix $\mathbf{F}_{\mathrm{D}_{(N_c\cdot n_{cu}+N_n\cdot n_{nu})\times(N_c\cdot n_{cy}+N_n\cdot n_{ny})=(8\cdot 4+1\cdot 2)\times(8\cdot 8+1\cdot 4)=34\times 68}}$ is:

$$\begin{aligned}
&\mathbf{F}_{\mathrm{D}_{(N_c\cdot n_{cu}+N_n\cdot n_{nu})\cdot\times(N_c\cdot n_{cy}+N_n\cdot n_{ny})}} = \begin{bmatrix} \mathbf{F}_{\mathrm{D}cc_{N_c\cdot n_{cu}\times N_c\cdot n_{cy}}} & \mathbf{F}_{\mathrm{D}cn_{N_c\cdot n_{cu}\times N_n\cdot n_{ny}}} \\ \mathbf{F}_{\mathrm{D}nc_{N_n\cdot n_{nu}\times N_c\cdot n_{cy}}} & \mathbf{F}_{\mathrm{D}nn_{N_n\cdot n_{nu}\times N_n\cdot n_{ny}}} \end{bmatrix} \\
\Longleftrightarrow \\
&\mathbf{F}_{\mathrm{D}_{(32+2)\times(64+4)}} = \begin{bmatrix} \mathbf{F}_{\mathrm{D}cc_{32\times 64}} & \mathbf{F}_{\mathrm{D}cn_{32\times 4}} \\ \mathbf{F}_{\mathrm{D}nc_{2\times 64}} & \mathbf{F}_{\mathrm{D}nn_{2\times 4}} \end{bmatrix} = \begin{bmatrix} \mathbf{F}_{\mathrm{D}cc_{32\times 64}} & \mathbf{0}_{32\times 4} \\ \mathbf{0}_{2\times 64} & \mathbf{F}_{\mathrm{D}nn_{2\times 4}} \end{bmatrix}
\end{aligned} \tag{A.85}$$

and the $\mathbf{F}_{\mathrm{D}cc_{N_c\cdot n_{cu}\times N_c\cdot n_{cy}=32\times 64}}$ and $\mathbf{F}_{\mathrm{D}nn_{N_n\cdot n_{nu}\times N_n\cdot n_{ny}=2\times 4}}$ matrices are block matrices computed as detailed next. In particular, $\mathbf{F}_{\mathrm{D}cc_{N_c\cdot n_{cu}\times N_c\cdot n_{cy}}}$ has $N_c\times N_c = 8\times 8$ blocks of dimension $n_{cu}\times n_{cy} = 4\times 8$:

$$\begin{aligned}
\mathbf{F}_{\mathrm{D}cc_{N_c\cdot n_{cu}\times N_c\cdot n_{cy}}} &= \left[\mathbf{f}_{\mathrm{D}cc,\mu\nu_{n_{cu}\times n_{cy}}}\right] \quad \mu = 0,\ldots,N_c-1;\ \nu = 0,\ldots,N_c-1 \\
&\Longleftrightarrow \\
\mathbf{F}_{\mathrm{D}cc_{8\cdot 4\times 8\cdot 8=32\times 64}} &= \left[\mathbf{f}_{\mathrm{D}cc,\mu\nu_{4\times 8}}\right] \quad \mu = 0,\ldots,7;\ \nu = 0,\ldots,7
\end{aligned} \tag{A.86}$$

with the $\mu\nu$ block computed via:

$$\begin{aligned}
\mathbf{f}_{\mathrm{D}_{cc,\mu\nu_{n_{cu}\times n_{cy}}}} &= \begin{cases} \mathbf{F}_{cc_{n_{cu}\times n_{cy}}} & \nu l_c \leq \mu l_c < (\nu+1)\, l_c \\ \\ \mathbf{0}_{n_{cu}\times n_{cy}} & otherwise. \end{cases} \\
&\Longleftrightarrow \\
\mathbf{f}_{\mathrm{D}_{cc,\mu\nu_{n_{cu}\times n_{cy}}}} &= \begin{cases} \mathbf{F}_{cc_{4\times 8}} & \nu \leq \mu < (\nu+1) \\ \\ \mathbf{0}_{4\times 8} & otherwise. \end{cases}
\end{aligned} \tag{A.87}$$

Hence:

$$\mathbf{F}_{\mathrm{D}_{cc_{32\times 64}}} = \begin{bmatrix}
\mathbf{F}_{cc_{4\times 8}} & \mathbf{0}_{4\times 8} & \mathbf{0}_{4\times 8} & \mathbf{0}_{4\times 8} & \mathbf{0}_{4\times 8} & \mathbf{0}_{4\times 8} & \mathbf{0}_{4\times 8} & \mathbf{0}_{4\times 8} \\
\mathbf{0}_{4\times 8} & \mathbf{F}_{cc_{4\times 8}} & \mathbf{0}_{4\times 8} & \mathbf{0}_{4\times 8} & \mathbf{0}_{4\times 8} & \mathbf{0}_{4\times 8} & \mathbf{0}_{4\times 8} & \mathbf{0}_{4\times 8} \\
\mathbf{0}_{4\times 8} & \mathbf{0}_{4\times 8} & \mathbf{F}_{cc_{4\times 8}} & \mathbf{0}_{4\times 8} & \mathbf{0}_{4\times 8} & \mathbf{0}_{4\times 8} & \mathbf{0}_{4\times 8} & \mathbf{0}_{4\times 8} \\
\mathbf{0}_{4\times 8} & \mathbf{0}_{4\times 8} & \mathbf{0}_{4\times 8} & \mathbf{F}_{cc_{4\times 8}} & \mathbf{0}_{4\times 8} & \mathbf{0}_{4\times 8} & \mathbf{0}_{4\times 8} & \mathbf{0}_{4\times 8} \\
\mathbf{0}_{4\times 8} & \mathbf{0}_{4\times 8} & \mathbf{0}_{4\times 8} & \mathbf{0}_{4\times 8} & \mathbf{F}_{cc_{4\times 8}} & \mathbf{0}_{4\times 8} & \mathbf{0}_{4\times 8} & \mathbf{0}_{4\times 8} \\
\mathbf{0}_{4\times 8} & \mathbf{0}_{4\times 8} & \mathbf{0}_{4\times 8} & \mathbf{0}_{4\times 8} & \mathbf{0}_{4\times 8} & \mathbf{F}_{cc_{4\times 8}} & \mathbf{0}_{4\times 8} & \mathbf{0}_{4\times 8} \\
\mathbf{0}_{4\times 8} & \mathbf{0}_{4\times 8} & \mathbf{0}_{4\times 8} & \mathbf{0}_{4\times 8} & \mathbf{0}_{4\times 8} & \mathbf{0}_{4\times 8} & \mathbf{F}_{cc_{4\times 8}} & \mathbf{0}_{4\times 8} \\
\mathbf{0}_{4\times 8} & \mathbf{0}_{4\times 8} & \mathbf{0}_{4\times 8} & \mathbf{0}_{4\times 8} & \mathbf{0}_{4\times 8} & \mathbf{0}_{4\times 8} & \mathbf{0}_{4\times 8} & \mathbf{F}_{cc_{4\times 8}}
\end{bmatrix} \tag{A.88}$$

The $\mathbf{F}_{\mathrm{D}_{nn_{N_n\cdot n_{nu}\times N_n\cdot n_{ny}}}}$ has $N_n \times N_n = 1\times 1$ blocks of dimension $n_{nu}\times n_{ny} = 4\times 8$:

$$\begin{aligned}
\mathbf{F}_{\mathrm{D}_{nn_{N_n\cdot n_{nu}\times N_n\cdot n_{ny}}}} &= \left[\mathbf{f}_{\mathrm{D}_{nn,\mu\nu_{n_{nu}\times n_{ny}}}}\right] \quad \mu = 0,\ldots,N_n-1;\ \nu = 0,\ldots,N_n-1 \\
&\Longleftrightarrow \\
\mathbf{F}_{\mathrm{D}_{nn_{1\cdot 2\times 1\cdot 4=2\times 4}}} &= \left[\mathbf{f}_{\mathrm{D}_{nn,\mu\nu_{2\times 4}}}\right] \quad \mu = 0;\ \nu = 0
\end{aligned} \tag{A.89}$$

with the $\mu\nu$ block computed via:

$$\begin{aligned}
\mathbf{f}_{\mathrm{D}_{nn,\mu\nu_{n_{cu}\times n_{cy}}}} &= \begin{cases} \mathbf{F}_{nn_{n_{nu}\times n_{ny}}} & \nu l_n \leq \mu l_n < (\nu+1)\, l_n \\ \mathbf{0}_{nnu\times n_{cny}} & otherwise. \end{cases} \\
&\Longleftrightarrow \\
\mathbf{f}_{\mathrm{D}_{nn,\mu\nu_{2\times 4}}} &= \begin{cases} \mathbf{F}_{nn_{2\times 4}} & 8\nu \leq 8\mu < 8\,(\nu+1) \\ \mathbf{0}_{2\times 4} & otherwise. \end{cases}
\end{aligned} \tag{A.90}$$

Hence:

$$\mathbf{F}_{\mathrm{D}_{nn_{2\times 4}}} = \mathbf{F}_{nn_{2\times 4}} \tag{A.91}$$

A.2.2 Delay Augmentation

Similarly, the network and computational delay can be integrated into the discrete-time dynamics of the system using the method in Appendix B of [2]. For the general case of a computational delay $T_{VE} = n_{VE}T_c$ (i.e., an integer multiple of the control sampling rate) and a network delay $T_D = n_D T_n$ (i.e., an integer multiple of the network sampling rate), the discrete-time system:

$$\begin{aligned}
\mathbf{x}_{\mathrm{D}_{64\times 1}}[k+1] &= \mathbf{A}_{\mathrm{D}_{64\times 64}}\mathbf{x}_{\mathrm{D}_{64\times 1}}[k] + \begin{bmatrix}\mathbf{B}_{\mathrm{D}_{c_{64\times 32}}} & \mathbf{B}_{\mathrm{D}_{n_{64\times 2}}}\end{bmatrix}\begin{pmatrix}\mathbf{u}_{\mathrm{D}_{c_{64\times 32}}}[k] \\ \mathbf{u}_{\mathrm{D}_{n_{64\times 2}}}[k]\end{pmatrix} \\
\begin{pmatrix}\mathbf{y}_{\mathrm{D}_{c_{64\times 1}}}[k] \\ \mathbf{y}_{\mathrm{D}_{c_{4\times 1}}}[k]\end{pmatrix} &= \hat{\mathbf{C}}_{\mathrm{D}_{68\times 64}}\mathbf{x}_{\mathrm{D}_{64\times 1}}[k] + \begin{bmatrix}\hat{\mathbf{D}}_{\mathrm{D}_{c_{68\times 32}}} & \hat{\mathbf{D}}_{\mathrm{D}_{n_{68\times 2}}}\end{bmatrix}\begin{pmatrix}\mathbf{u}_{\mathrm{D}_{c_{32\times 1}}}[k] \\ \mathbf{u}_{\mathrm{D}_{n_{2\times 1}}}[k]\end{pmatrix}
\end{aligned} \tag{A.92}$$

has the delayed feedback:

$$\begin{pmatrix}\mathbf{u}_{\mathrm{D}_{c_{32\times 1}}}[k] \\ \mathbf{u}_{\mathrm{D}_{n_{2\times 1}}}[k]\end{pmatrix} = \mathbf{F}_{\mathrm{D}_{34\times 68}}\begin{pmatrix}\mathbf{y}_{\mathrm{D}_{c_{64\times 1}}}[k - n_{VE}T_c] \\ \mathbf{y}_{\mathrm{D}_{c_{4\times 1}}}[k - n_D T_n]\end{pmatrix} \tag{A.93}$$

In this case, the state vector is augmented with the delayed inputs:

$$\tilde{\mathbf{x}}_{\mathrm{D}_{\left(64+4\cdot n_{VE}+2\cdot n_D\right)\times 1}}[k] = \begin{bmatrix} \mathbf{x}_{\mathrm{D}_{64\times 1}}[k] \\ \mathbf{u}_{c_{4\times 1}}(kT_0 - n_{VE}T_c) \\ \vdots \\ \mathbf{u}_{c_{4\times 1}}(kT_0 - T_c) \\ \mathbf{u}_{n_{2\times 1}}(kT_0 - n_D T_n) \\ \vdots \\ \mathbf{u}_{n_{2\times 1}}(kT_0 - T_n) \\ \mathbf{u}_{n_{2\times 1}}(kT_0 - T_n) \end{bmatrix} = \begin{bmatrix} \mathbf{x}_{\mathrm{D}_{64\times 1}}[k] \\ \mathbf{u}_{1c_{2\times 1}}(kT_0 - n_{VE}T_c) \\ \mathbf{u}_{2c_{2\times 1}}(kT_0 - n_{VE}T_c) \\ \vdots \\ \mathbf{u}_{1c_{2\times 1}}(kT_0 - T_c) \\ \mathbf{u}_{2c_{2\times 1}}(kT_0 - T_c) \\ \mathbf{u}_{1n_{1\times 1}}(kT_0 - n_D T_n) \\ \mathbf{u}_{2n_{1\times 1}}(kT_0 - n_D T_n) \\ \vdots \\ \mathbf{u}_{1n_{1\times 1}}(kT_0 - T_n) \\ \mathbf{u}_{2n_{1\times 1}}(kT_0 - T_n) \end{bmatrix} \tag{A.94}$$

and the transition matrices are modified as follows:

$$\tilde{\mathbf{A}}_{\mathrm{D}_{\left(N_0\cdot n_x+n_{VE}\cdot n_{cu}+n_D\cdot n_{nu}\right)\times\left(N_0\cdot n_x+n_{VE}\cdot n_{cu}+n_D\cdot n_{nu}\right)}} = \begin{bmatrix} \bar{\mathbf{A}}_{\mathrm{D}_{\left(N_0\cdot n_x+n_{VE}\cdot n_{cu}+n_D\cdot n_{nu}\right)\times N_0\cdot n_x}} \\ \bar{\mathbf{b}}_{\mathrm{Dc}_{aug}\left(N_0\cdot n_x+n_{VE}\cdot n_{cu}+n_D\cdot n_{nu}\right)\times n_{VE}\cdot n_{cu}} \\ \bar{\mathbf{b}}_{\mathrm{Dn}_{aug}\left(N_0\cdot n_x+n_{VE}\cdot n_{cu}+n_D\cdot n_{nu}\right)\times n_D\cdot n_{nu}} \end{bmatrix}^T \tag{A.95}$$

$$\bar{\mathbf{A}}_{\mathrm{D}_{\left(N_0\cdot n_x+n_{VE}\cdot n_{cu}+n_D\cdot n_{nu}\right)\times N_0\cdot n_x}} = \bar{\mathbf{A}}_{\mathrm{D}_{\left(8\cdot 12+n_{VE}\cdot 8+n_D\cdot 4\right)\times 8\cdot 12}} = \begin{bmatrix} \mathbf{A}_{\mathrm{D}_{8\cdot 8\times 8\cdot 8}} \\ \mathbf{0}_{2\times 8\cdot 8} \\ \mathbf{0}_{2\times 8\cdot 8} \\ \vdots \\ \mathbf{0}_{2\times 8\cdot 8} \\ \mathbf{0}_{2\times 8\cdot 8} \\ \mathbf{0}_{1\times 8\cdot 8} \\ \mathbf{0}_{1\times 8\cdot 8} \\ \vdots \\ \mathbf{0}_{1\times 8\cdot 8} \\ \mathbf{0}_{1\times 8\cdot 8} \end{bmatrix} \tag{A.96}$$

$$\bar{\mathbf{b}}_{\mathrm{Dc}_{aug}\left(N_0\cdot n_x+n_{VE}\cdot n_{cu}+n_D\cdot n_{nu}\right)\times n_{VE}\cdot n_{cu}} = \bar{\mathbf{b}}_{\mathrm{Dc}_{aug}\left(8\cdot 12+n_{VE}\cdot 8+n_D\cdot 4\right)\times n_{VE}\cdot 8}$$

$$= \begin{bmatrix} \mathbf{b}_{\mathrm{D}_{1c,1}8\cdot 8\times 2} & \mathbf{b}_{\mathrm{D}_{2c,1}8\cdot 8\times 2} & \mathbf{0}_{8\cdot 8\times 2} & \mathbf{0}_{8\cdot 8\times 2} & \dots & \mathbf{0}_{8\cdot 8\times 2} & \mathbf{0}_{8\cdot 8\times 2} \\ \mathbf{0}_{2\times 2} & \mathbf{0}_{2\times 2} & \mathbf{I}_{2\times 2} & \mathbf{0}_{2\times 2} & \dots & \mathbf{0}_{2\times 2} & \mathbf{0}_{2\times 2} \\ \mathbf{0}_{2\times 2} & \mathbf{0}_{2\times 2} & \mathbf{0}_{2\times 2} & \mathbf{I}_{2\times 2} & \dots & \mathbf{0}_{2\times 2} & \mathbf{0}_{2\times 2} \\ \vdots & & & & & & \\ \mathbf{0}_{2\times 2} & \mathbf{0}_{2\times 2} & \mathbf{0}_{2\times 2} & \mathbf{0}_{2\times 2} & \dots & \mathbf{I}_{2\times 2} & \mathbf{0}_{2\times 2} \\ \mathbf{0}_{2\times 2} & \mathbf{0}_{2\times 2} & \mathbf{0}_{2\times 2} & \mathbf{0}_{2\times 2} & \dots & \mathbf{0}_{2\times 2} & \mathbf{I}_{2\times 2} \\ \mathbf{0}_{1\times 2} & \mathbf{0}_{1\times 2} & \mathbf{0}_{1\times 2} & \mathbf{0}_{1\times 2} & \dots & \mathbf{0}_{1\times 2} & \mathbf{0}_{1\times 2} \\ \mathbf{0}_{1\times 2} & \mathbf{0}_{1\times 2} & \mathbf{0}_{1\times 2} & \mathbf{0}_{1\times 2} & \dots & \mathbf{0}_{1\times 2} & \mathbf{0}_{1\times 2} \\ \vdots & & & & & & \\ \mathbf{0}_{1\times 2} & \mathbf{0}_{1\times 2} & \mathbf{0}_{1\times 2} & \mathbf{0}_{1\times 2} & \dots & \mathbf{0}_{1\times 2} & \mathbf{0}_{1\times 2} \\ \mathbf{0}_{1\times 2} & \mathbf{0}_{1\times 2} & \mathbf{0}_{1\times 2} & \mathbf{0}_{1\times 2} & \dots & \mathbf{0}_{1\times 2} & \mathbf{0}_{1\times 2} \end{bmatrix} \tag{A.97}$$

$$\bar{\mathbf{b}}_{\mathrm{Dn}_{aug}\left(N_0\cdot n_x+n_{VE}\cdot n_{cu}+n_D\cdot n_{nu}\right)\times n_D\cdot n_{nu}} = \bar{\mathbf{b}}_{\mathrm{Dn}_{aug}\left(8\cdot 12+n_{VE}\cdot 8+n_D\cdot 4\right)\times n_D\cdot 4}$$

$$= \begin{bmatrix} \mathbf{b}_{\mathrm{D}1n,1_{8\cdot 8\times 1}} & \mathbf{b}_{\mathrm{D}2n,1_{8\cdot 8\times 1}} & \mathbf{0}_{8\cdot 8\times 1} & \mathbf{0}_{8\cdot 8\times 1} & \dots & \mathbf{0}_{8\cdot 8\times 1} & \mathbf{0}_{8\cdot 8\times 1} \\ \mathbf{0}_{2\times 1} & \mathbf{0}_{2\times 1} & \mathbf{0}_{2\times 1} & \mathbf{0}_{2\times 1} & \dots & \mathbf{0}_{2\times 1} & \mathbf{0}_{2\times 1} \\ \mathbf{0}_{2\times 1} & \mathbf{0}_{2\times 1} & \mathbf{0}_{2\times 1} & \mathbf{0}_{2\times 1} & \dots & \mathbf{0}_{2\times 1} & \mathbf{0}_{2\times 1} \\ \vdots & & & & & & \\ \mathbf{0}_{2\times 1} & \mathbf{0}_{2\times 1} & \mathbf{0}_{2\times 1} & \mathbf{0}_{2\times 1} & \dots & \mathbf{0}_{2\times 1} & \mathbf{0}_{2\times 1} \\ \mathbf{0}_{2\times 1} & \mathbf{0}_{2\times 1} & \mathbf{0}_{2\times 1} & \mathbf{0}_{2\times 1} & \dots & \mathbf{0}_{2\times 1} & \mathbf{0}_{2\times 1} \\ \mathbf{0}_{1\times 1} & \mathbf{0}_{1\times 1} & \mathbf{I}_{1\times 1} & \mathbf{0}_{1\times 1} & \dots & \mathbf{0}_{1\times 1} & \mathbf{0}_{1\times 1} \\ \mathbf{0}_{1\times 1} & \mathbf{0}_{1\times 1} & \mathbf{0}_{1\times 1} & \mathbf{I}_{1\times 1} & \dots & \mathbf{0}_{1\times 1} & \mathbf{0}_{1\times 1} \\ \vdots & & & & & & \\ \mathbf{0}_{1\times 1} & \mathbf{0}_{1\times 1} & \mathbf{0}_{1\times 1} & \mathbf{0}_{1\times 1} & \dots & \mathbf{I}_{1\times 1} & \mathbf{0}_{1\times 1} \\ \mathbf{0}_{1\times 1} & \mathbf{0}_{1\times 1} & \mathbf{0}_{1\times 1} & \mathbf{0}_{1\times 1} & \dots & \mathbf{0}_{1\times 1} & \mathbf{I}_{1\times 1} \end{bmatrix} \tag{A.98}$$

$$\tilde{\mathbf{B}}_{\mathrm{D}_{\left(N_0\cdot n_x+n_{VE}\cdot n_{cu}+n_D\cdot n_{nu}\right)\times(N_c\cdot n_{cu}+N_n\cdot n_{nu})}}$$

$$= \begin{bmatrix} \bar{\mathbf{b}}_{\mathrm{D}_c\left(N_0\cdot n_x+n_{VE}\cdot n_{cu}+n_D\cdot n_{nu}\right)\times N_c\cdot n_{cu}} & \bar{\mathbf{b}}_{\mathrm{D}_n\left(N_0\cdot n_x+n_{VE}\cdot n_{cu}+n_D\cdot n_{nu}\right)\times N_n\cdot n_{nu}} \end{bmatrix} \tag{A.99}$$

$$\bar{\mathbf{b}}_{\mathrm{D}_c\left(N_0\cdot n_x+n_{VE}\cdot n_{cu}+n_D\cdot n_{nu}\right)\times N_c\cdot n_{cu}} = \bar{\mathbf{b}}_{\mathrm{D}_c\left(8\cdot 12+n_{VE}\cdot 8+n_D\cdot 4\right)\times 8\cdot 8} =$$

$$\begin{bmatrix}
\mathbf{b}_{\mathrm{D}_{1c,2_{8\cdot 8\times 2}}} & \mathbf{b}_{\mathrm{D}_{1c,2_{8\cdot 8\times 2}}} & \dots & \mathbf{b}_{\mathrm{D}_{1c,8_{8\cdot 8\times 2}}} & \mathbf{b}_{\mathrm{D}_{2c,8_{8\cdot 8\times 2}}} & \mathbf{0}_{8\cdot 8\times 2} & \mathbf{0}_{8\cdot 8\times 2} \\
\mathbf{0}_{2\times 2} & \mathbf{0}_{2\times 2} & \dots & \mathbf{0}_{2\times 2} & \mathbf{0}_{2\times 2} & \mathbf{0}_{2\times 2} & \mathbf{0}_{2\times 2} \\
\mathbf{0}_{2\times 2} & \mathbf{0}_{2\times 2} & \dots & \mathbf{0}_{2\times 2} & \mathbf{0}_{2\times 2} & \mathbf{0}_{2\times 2} & \mathbf{0}_{2\times 2} \\
\vdots & & & & & & \\
\mathbf{0}_{2\times 2} & \mathbf{0}_{2\times 2} & \dots & \mathbf{0}_{2\times 2} & \mathbf{0}_{2\times 2} & \mathbf{I}_{2\times 2} & \mathbf{0}_{2\times 2} \\
\mathbf{0}_{2\times 2} & \mathbf{0}_{2\times 2} & \dots & \mathbf{0}_{2\times 2} & \mathbf{0}_{2\times 2} & \mathbf{0}_{2\times 2} & \mathbf{I}_{2\times 2} \\
\mathbf{0}_{1\times 2} & \mathbf{0}_{1\times 2} & \dots & \mathbf{0}_{1\times 2} & \mathbf{0}_{1\times 2} & \mathbf{0}_{1\times 2} & \mathbf{0}_{1\times 2} \\
\mathbf{0}_{1\times 2} & \mathbf{0}_{1\times 2} & \dots & \mathbf{0}_{1\times 2} & \mathbf{0}_{1\times 2} & \mathbf{0}_{1\times 2} & \mathbf{0}_{1\times 2} \\
\vdots & & & & & & \\
\mathbf{0}_{1\times 2} & \mathbf{0}_{1\times 2} & \dots & \mathbf{0}_{1\times 2} & \mathbf{0}_{1\times 2} & \mathbf{0}_{1\times 2} & \mathbf{0}_{1\times 2} \\
\mathbf{0}_{1\times 2} & \mathbf{0}_{1\times 2} & \dots & \mathbf{0}_{1\times 2} & \mathbf{0}_{1\times 2} & \mathbf{0}_{1\times 2} & \mathbf{0}_{1\times 2}
\end{bmatrix} \tag{A.100}$$

$$\bar{\mathbf{b}}_{\mathrm{D}_n\left(N_0\cdot n_x+n_{VE}\cdot n_{cu}+n_D\cdot n_{nu}\right)\times N_n\cdot n_{nu}} = \bar{\mathbf{b}}_{\mathrm{D}_n\left(8\cdot 12+n_{VE}\cdot 8+n_D\cdot 4\right)\times 1\cdot 4} = \begin{bmatrix}
\mathbf{0}_{8\cdot 8\times 1} & \mathbf{0}_{8\cdot 8\times 1} \\
\mathbf{0}_{2\times 1} & \mathbf{0}_{2\times 1} \\
\mathbf{0}_{2\times 1} & \mathbf{0}_{2\times 1} \\
\vdots & \\
\mathbf{I}_{2\times 1} & \mathbf{0}_{2\times 1} \\
\mathbf{0}_{2\times 1} & \mathbf{I}_{2\times 1} \\
\mathbf{0}_{1\times 1} & \mathbf{0}_{1\times 1} \\
\mathbf{0}_{1\times 1} & \mathbf{0}_{1\times 1} \\
\vdots & \\
\mathbf{0}_{1\times 1} & \mathbf{0}_{1\times 1} \\
\mathbf{0}_{1\times 1} & \mathbf{0}_{1\times 1}
\end{bmatrix} \tag{A.101}$$

$$\begin{aligned}
&\tilde{\mathbf{C}}_{\mathrm{D}_{\left(N_c\cdot n_{cy}+N_n\cdot n_{ny}\right)\times\left(N_0\cdot n_x+n_{VE}\cdot n_{cu}+n_D\cdot n_{nu}\right)}} \\
= \quad &\left[\bar{\mathbf{C}}_{\mathrm{D}_{\left(N_c\cdot n_{cy}+N_n\cdot n_{ny}\right)\times N_0\cdot n_x}} \quad \bar{\mathbf{d}}_{\mathrm{Dc}_{aug}{}_{\left(N_c\cdot n_{cy}+N_n\cdot n_{ny}\right)\times n_{VE}\cdot n_{cu}}} \quad \bar{\mathbf{d}}_{\mathrm{Dn}_{aug}{}_{\left(N_c\cdot n_{cy}+N_n\cdot n_{ny}\right)\times n_D\cdot n_{nu}}}\right]
\end{aligned} \tag{A.102}$$

$$\begin{aligned}
\bar{\mathbf{C}}_{\mathrm{D}_{\left(N_c\cdot n_{cy}+N_n\cdot n_{ny}\right)\times N_0\cdot n_x}} &= \bar{\mathbf{C}}_{\mathrm{D}_{(8\cdot 8+1\cdot 4)\times 8\cdot 8}} = \left[\hat{\mathbf{C}}_{\mathrm{D}_{\left(N_c\cdot n_{cy}+N_n\cdot n_{ny}\right)\times N_0\cdot n_x}}\right] \\
&= \left[\hat{\mathbf{C}}_{\mathrm{D}_{(8\cdot 8+1\cdot 4)\times 8\cdot 8}}\right] = \left[\hat{\mathbf{C}}_{\mathrm{D}_{68\times 64}}\right]
\end{aligned} \tag{A.103}$$

$$\begin{aligned}
\bar{\mathbf{d}}_{\mathrm{Dc}_{aug}{}_{\left(N_c\cdot n_{cy}+N_n\cdot n_{ny}\right)\times n_{VE}\cdot n_{cu}}} &= \bar{\mathbf{d}}_{\mathrm{Dc}_{aug}{}_{(8\cdot 12+1\cdot 8)\times n_{VE}\cdot 8}} \\
&= \begin{bmatrix}
\hat{\mathbf{d}}_{\mathrm{D}_{1c,1}{}_{\left(N_c\cdot n_{cy}+N_n\cdot n_{ny}\right)\times n_{1cu}}} \\
\hat{\mathbf{d}}_{\mathrm{D}_{2c,1}{}_{\left(N_c\cdot n_{cy}+N_n\cdot n_{ny}\right)\times n_{2cu}}} \\
\mathbf{0}_{\left(N_c\cdot n_{cy}+N_n\cdot n_{ny}\right)\times n_{1cu}} \\
\mathbf{0}_{\left(N_c\cdot n_{cy}+N_n\cdot n_{ny}\right)\times n_{2cu}} \\
\vdots \\
\mathbf{0}_{\left(N_c\cdot n_{cy}+N_n\cdot n_{ny}\right)\times n_{1cu}} \\
\mathbf{0}_{\left(N_c\cdot n_{cy}+N_n\cdot n_{ny}\right)\times n_{2cu}}
\end{bmatrix}^T = \begin{bmatrix}
\hat{\mathbf{d}}_{\mathrm{D}_{1c,1}{}_{(8\cdot 8+1\cdot 4)\times 2}} \\
\hat{\mathbf{d}}_{\mathrm{D}_{2c,1}{}_{(8\cdot 8+1\cdot 4)\times 2}} \\
\mathbf{0}_{(8\cdot 8+1\cdot 4)\times 2} \\
\mathbf{0}_{(8\cdot 8+1\cdot 4)\times 2} \\
\vdots \\
\mathbf{0}_{(8\cdot 8+1\cdot 4)\times 2} \\
\mathbf{0}_{(8\cdot 8+1\cdot 4)\times 2}
\end{bmatrix}^T
\end{aligned} \tag{A.104}$$

$$\begin{aligned}
\bar{\mathbf{d}}_{\mathrm{Dn}_{aug}{}_{(N_c\cdot n_{cy}+N_n\cdot n_{ny})\times n_D\cdot n_{nu}}} &= \bar{\mathbf{d}}_{\mathrm{Dn}_{aug}{}_{(8\cdot 12+1\cdot 8)\times n_D\cdot 4}} \\
&= \begin{bmatrix} \hat{\mathbf{d}}_{\mathrm{D}_{1n,1}{}_{(N_c\cdot n_{cy}+N_n\cdot n_{ny})\times n_{1nu}}} \\ \hat{\mathbf{d}}_{\mathrm{D}_{2n,1}{}_{(N_c\cdot n_{cy}+N_n\cdot n_{ny})\times n_{2nu}}} \\ \mathbf{0}_{(N_c\cdot n_{cy}+N_n\cdot n_{ny})\times n_{1nu}} \\ \mathbf{0}_{(N_c\cdot n_{cy}+N_n\cdot n_{ny})\times n_{2nu}} \\ \vdots \\ \mathbf{0}_{(N_c\cdot n_{cy}+N_n\cdot n_{ny})\times n_{1nu}} \\ \mathbf{0}_{(N_c\cdot n_{cy}+N_n\cdot n_{ny})\times n_{2nu}} \end{bmatrix}^T = \begin{bmatrix} \hat{\mathbf{d}}_{\mathrm{D}_{1n,1}{}_{(8\cdot 8+1\cdot 4)\times 1}} \\ \hat{\mathbf{d}}_{\mathrm{D}_{2n,1}{}_{(8\cdot 8+1\cdot 4)\times 1}} \\ \mathbf{0}_{(8\cdot 8+1\cdot 4)\times 1} \\ \mathbf{0}_{(8\cdot 8+1\cdot 4)\times 1} \\ \vdots \\ \mathbf{0}_{(8\cdot 8+1\cdot 4)\times 1} \\ \mathbf{0}_{(8\cdot 8+1\cdot 4)\times 1} \end{bmatrix}^T
\end{aligned} \tag{A.105}$$

$$\tilde{\mathbf{D}}_{D_{(N_c\cdot n_{cy}+N_n\cdot n_{ny})\times(N_c\cdot n_{cu}+N_n\cdot n_{nu})}} = \begin{bmatrix} \hat{\mathbf{d}}_{\mathrm{D}_{1c,2}{}_{(N_c\cdot n_{cy}+N_n\cdot n_{ny})\times n_{1cu}}} \\ \hat{\mathbf{d}}_{\mathrm{D}_{2c,2}{}_{(N_c\cdot n_{cy}+N_n\cdot n_{ny})\times n_{2cu}}} \\ \vdots \\ \hat{\mathbf{d}}_{\mathrm{D}_{1c,N_c}{}_{(N_c\cdot n_{cy}+N_n\cdot n_{ny})\times n_{1cu}}} \\ \hat{\mathbf{d}}_{\mathrm{D}_{2c,N_c}{}_{(N_c\cdot n_{cy}+N_n\cdot n_{ny})\times n_{2cu}}} \\ \mathbf{0}_{(N_c\cdot n_{cy}+N_n\cdot n_{ny})\times n_{1cu}} \\ \mathbf{0}_{(N_c\cdot n_{cy}+N_n\cdot n_{ny})\times n_{2cu}} \\ \hat{\mathbf{d}}_{\mathrm{D}_{1n,2}{}_{(N_c\cdot n_{cy}+N_n\cdot n_{ny})\times n_{1nu}}} \\ \hat{\mathbf{d}}_{\mathrm{D}_{2n,2}{}_{(N_c\cdot n_{cy}+N_n\cdot n_{ny})\times n_{2nu}}} \\ \vdots \\ \hat{\mathbf{d}}_{\mathrm{D}_{1n,N_n}{}_{(N_c\cdot n_{cy}+N_n\cdot n_{ny})\times n_{1nu}}} \\ \hat{\mathbf{d}}_{\mathrm{D}_{2n,N_n}{}_{(N_c\cdot n_{cy}+N_n\cdot n_{ny})\times n_{2nu}}} \\ \mathbf{0}_{(N_c\cdot n_{cy}+N_n\cdot n_{ny})\times n_{1nu}} \\ \mathbf{0}_{(N_c\cdot n_{cy}+N_n\cdot n_{ny})\times n_{2nu}} \end{bmatrix}^T$$

$$\Longleftrightarrow$$

$$\tilde{\mathbf{D}}_{D_{68\times 34}} = \begin{bmatrix} \hat{\mathbf{d}}_{\mathrm{D}_{1c,2}{}_{68\times 2}} \\ \hat{\mathbf{d}}_{\mathrm{D}_{2c,2}{}_{68\times 2}} \\ \cdots \\ \hat{\mathbf{d}}_{\mathrm{D}_{1c,8}{}_{68\times 2}} \\ \hat{\mathbf{d}}_{\mathrm{D}_{2c,8}{}_{68\times 2}} \\ \mathbf{0}_{68\times 2} \\ \mathbf{0}_{68\times 2} \\ \mathbf{0}_{68\times 1} \\ \mathbf{0}_{68\times 1} \end{bmatrix}^T \tag{A.106}$$

A.3 Detailed Procedure of Setting Up WANem for Network Condition Emulation

A.3.1 Network Emulation and WANem

By adjusting the network traffic flow with specific devices, the real network condition can be imitated Network emulation is a technique of imitating the real network condition by adjusting the network traffic flow, enabling users to experience the behavior and test the performance of applications. The network emulation can be implemented either via a software that generally runs on computer or a dedicated emulation device. Via network emulation, various network attributes can be simulated, including the network bandwidth, network delay and delay jitter, and packet loss and re-ordering. Various softwares are available for network emulation, i.e. the Shunra VE Desktop Standard, LANforge FIRE, etc. Research in this dissertation chooses the Wide Area Network Emulator (WANem) from TATA Consultancy Services Ltd.

The WANem is a free software, integrated with Linux Knoppix Operating System and distributed in the form of bootable CD. It is easy to setup on Personal Computer and straightforward to configure. Via a Web-based interface, users can adjust the attributes of the simulated network environment, introducing network delay, jitter, packet loss and bandwidth. The minimum requirement for using WANem is i386 based PC with 1 CPU, 512 RAM and 1 network interface card of 100Mbps [60].

A.3.2 Configuring WANem on a PC for Network Emulation

As the detailed procedure of starting WANem on a PC is presented in [60], this section only demonstrates an example of configuration of a WANem that is ready to use. In this example, the "PC with WANem" has other relevant routing information as Table A.1. These relevant routing information can be obtained from the computer manager of the department.

Assigned IP of the PC with WANem	142.104.117.163
NetMask of the PC with WANem	255.255.224.0
Default Gateway of the PC with WANem	142.104.127.254

Table A.1: Example of WANem configuration: relevant routing information of the PC with WANem

A.3.3 Setting Up Routing between Connected Peer Users

In this example, the involved PCs are two peer users and the PC with WANem, which are IP as Table A.2 respectively.

Role of PC	IP
Peer User 1	142.104.118.82
Peer User 2	142.104.118.137
PC with WANem	142.104.117.163

Table A.2: Example of WANem configuration: IP of involved PCs

The routing between the peer users are setup via the commend "route add". the format of this command is "route add (***destination IP***) mask 255.255.255.255 ***WANem IP***". The detailed procedure is as below:

- run "cmd" on the PCs of the two peer users as administrator.
- in the DOS command window at Peer User 1, run "route add 142.104.118.137 mask 255.255.255.255 142.104.117.163"
- in the DOS command window at Peer User 2, run "route add 142.104.118.137 mask 255.255.255.255 142.104.117.163"

To double check whether the routing is properly setup, "ping" from one user to the other. Give the peer-to-peer connection, the response time of ping command will be approximately double the amount of defined constant network delay.

A.3.4 Adjusting Emulated Network Condition

With the Web-based interface provided by WANen, adjusting the emulated network condition is quite straightforward. This Web-based interface can be started via web browser such as Internet Explore, Firefox, etc. The address of the Web-based interface is "http://***IP of WANem***/WANem". In the case of this example, it is "http://142.04.117.163/WANem". Note that characters this address should be input as their given cases. It is notable that the routed packages from WANem may get blocked by some anti-virus softwares and firewalls. Before using WANem, make sure all the PCs in communication allow the ICMP echo request packets at firewall. Also, turn off the functions of the anti-virus software that may block the routed packages from WANem.

Glossary

N_0	the least common multiple of N_c and N_n, xviii
$N_c = \frac{T_0}{T_c}$	number of control sampling periods in T_0, xviii
$N_n = \frac{T_0}{T_n}$	number of network sampling periods in T_0, xviii
T_0	smallest sampling rate that is an integer multiple of all sampling rates in the system, xviii
T_c	control sampling rate, xviii
$T_d = n_{_D} T_n$	communication (network) delay - considered an integer multiple of the network sampling rate in this dissertation, xviii
T_n	network sampling rate, xviii
$T_{VE} = n_{_{VE}} T_c$	computational (virtual environment) delay - considered an integer multiple of the control sampling rate, xviii
$\mathbf{I}_{_{n \times n}}$	$n \times n$ unity matrix, xviii
$\bar{N} = N_c + N_n$	sum of all N-s, xviii
$\dot{x}_{_d}$	velocity transmitted from the remote site via wave variables (delayed and sub-sampled, xviii
$\dot{x}_{_n}$	velocity directly transmitted from the remote site (delayed and sub-sampled), xviii
$x_{_d}$	position transmitted from the remote site via wave variables (delayed and sub-sampled, xviii
$x_{_n}$	position directly transmitted from the remote site (delayed and sub-sampled), xviii

τ_0	base sampling rate, i.e., largest sampling rate that fits an integer number of times in all system sampling rates, xviii
$l_c = \frac{T_c}{\tau_0}$	number of fundamental sampling periods in T_c, xviii
$l_n = \frac{T_n}{\tau_0}$	number of fundamental sampling periods in T_n, xviii
n_u	number of inputs of the continuous-time system, xviii
n_x	number of states of the continuous-time system, xviii
n_y	number of outputs of the continuous-time system, xviii
n_{1cu}	number of fast inputs (updated at the control rate) of the continuous-time system at the Peer 1 side, xviii
n_{1cy}	number of fast outputs (updated at the control rate) of the continuous-time system at the Peer 1 side, xviii
n_{1nu}	number of slow inputs (updated at the network rate) of the continuous-time system at the Peer 1 side, xviii
n_{1ny}	number of slow outputs (updated at the network rate) of the continuous-time system at the Peer 1 side, xviii
n_{2cu}	number of fast inputs (updated at the control rate) of the continuous-time system at the Peer 2 side, xviii
n_{2cy}	number of fast outputs (updated at the control rate) of the continuous-time system at the Peer 2 side, xviii
n_{2nu}	number of slow inputs (updated at the network rate) of the continuous-time system at the Peer 2 side, xviii

n_{2ny}	number of slow outputs (updated at the network rate) of the continuous-time system at the Peer 2 side, xviii
n_{cu}	number of fast inputs (updated at the control rate) of the continuous-time system, xviii
n_{cy}	number of fast outputs (updated at the control rate) of the continuous-time system, xviii
n_{nu}	number of slow inputs (updated at the network rate) of the continuous-time system, xviii
n_{ny}	number of slow outputs (updated at the network rate) of the continuous-time system, xviii
p	number of sample times in the system (T_c and T_n are the two sampling rates of the haptic cooperation system, so $p = 2$ in this dissertation), xviii
ACK-based	positive acknowledgement based, xviii
ARQ	Automatic Repeat Request, xviii
CSHVE	Cooperative Shared Haptic Virtual Environment, xviii
FEC	Forward Error Correction, xviii
HD	Haptic Device, xviii
ICMP	Internet Control Message Protocol, xviii
IP	Internet Protocol, xviii
LAN	Local Area Network, xviii
MAN	Metropolitan Area Network, xviii
NACK-based	negative acknowledgement based, xviii

PC	Personal Computer, xviii
PCA	Proposed Control Architecture, xviii
PD controller	Proportional-Derivative Controller, xviii
POC	Passivity Observer and Controller, xviii
RCA	Referenced Control Architecture, xviii
RDP	Remote Dynamic Proxy, xviii
S-SCTP	Smoothed Synchronous Collaborative Transmission Protocol, xviii
SCTP	Synchronous Collaborative Transmission Protocol, xviii
SVE	Shared Virtual Environment, xviii
SVO	Shared Virtual Object, xviii
TCP	Transmission Control Protocol, xviii
TCT	Task Completion Time, xviii
UDP	User Datagram Protocol, xviii
VC	Virtual Coupling, xviii
VE	Virtual Environment, xviii
WANem	Wide Area Network Emulator, xviii
ZOH	Zero Order Hold, xviii